Nitrone Cycloadditions Towards the Synthesis of the Core of the *Alstonia* and Tropane Alkaloids

Beth Louise Ritchie
Department of Chemistry
Project Supervisor: Professor Iain Coldham

May 2023

Thesis Submitted in Partial Fulfilment of the Requirements for the Degree of Doctor of Philosophy

Abstract

Alkaloids are naturally occurring organic compounds found in plants, containing at least one basic nitrogen atom. Many have known biological activity and, therefore, are regularly being isolated and studied. Work within the Coldham group has focused on developing a one-pot method to efficiently and stereoselectively build multiple-ring systems, commonly seen in alkaloids and other natural products. This has been applied to the synthesis of a variety of alkaloids, such as those from the *Aspidosperma* and *Daphniphyllum* genera.

This thesis explores routes through which this cascade chemistry can be applied to the synthesis of two alkaloid skeletons: that of ferrugine (compound **A**), a tropane alkaloid, and that of alstonoxine B (compound **B**), an alkaloid found in plants of the genus *Alstonia*.

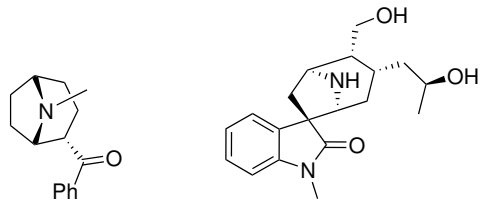

A **B**

Routes towards **A** focused predominantly on the application of vinyl sulfone chemistry popularised by Padwa, where the vinyl sulfone would act as a centre for cyclisation. This chemistry provided the desired oxime, but no cycloadducts were isolated on heating. Alternatively, an alkyl halide could be envisaged to act as an electrophile for cyclisaton. This would provide the first examples in the Coldham group of a secondary centre used in the cyclisation of the cascade chemistry. In one promising example, cascade precursor **D** was synthesised in just 3 steps from readily available epoxide **C**. Aldehyde **D** could now be tested in the one-pot procedure, which would afford cycloadduct **E**, and N–O bond cleavage could be attempted in order to form core structure **J**.

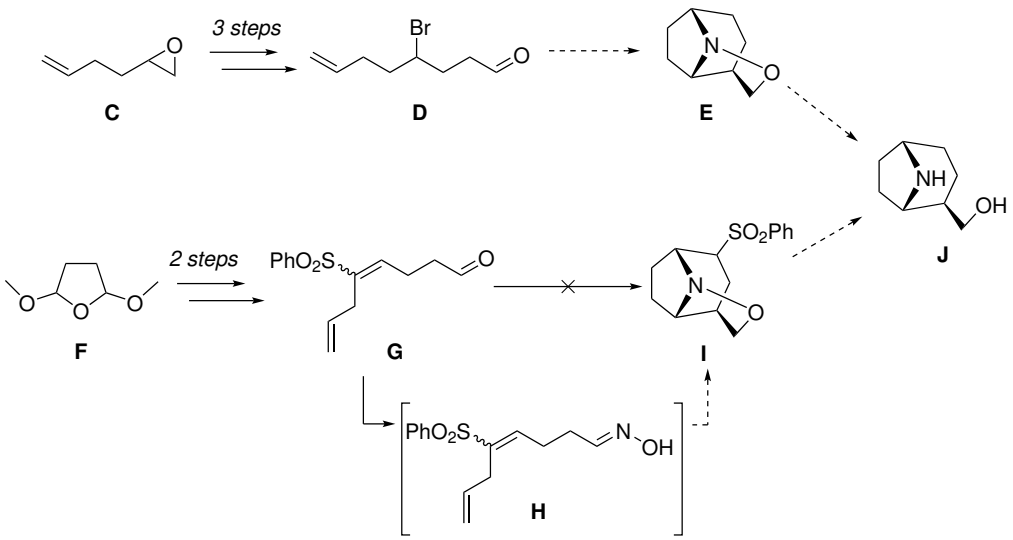

Various routes towards the synthesis of alstonoxine B (**B**) are also discussed. Initially, routes towards total synthesis were explored. However, when this proved difficult, efforts were focused on the application of the cascade chemistry to an oxindole core. This was performed successfully, generating cascade precursor **O** in 4 steps from readily available *N*-methylisatin, **K**. The cascade chemistry was performed with several external dipolarophiles, affording core structures in the general form of compound **P**. N–O bond cleavage was attempted but was unfortunately unsuccessful, and this requires further study.

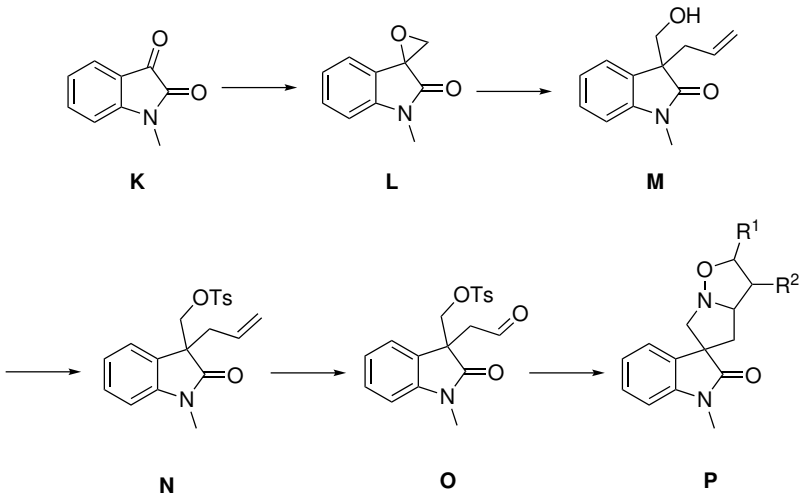

Acknowledgements

If there's one thing I've always been bad at, it's not waffling on. "Precis!" my Dad has always joked, usually after a few minutes of my rambling. This thesis won't, I hope, be an example of this, but perhaps I can indulge myself here, in the acknowledgements section.

The first thanks go to my supervisor, Professor Iain Coldham. Iain's supervision and help have been invaluable, and I am so grateful to have had a very present and involved supervisor. I'd also like to thank my independent advisor, Dr Ben Partridge, who has been an important source of support throughout.

I owe thanks to all of the Coldham group members I have worked with throughout my time in the department. Anthony Choi, thank you for helping me settle into the group and into the lab. Anjan Das, thank you for being an immensely kind and helpful postdoc. Jen - thank you for being an excellent co-worker, and an even more excellent friend. My PhD would have been so much harder without having you around to laugh with, vent to and eat noodles with! Thanks to my master's student, Richard Cox, for being a great supervisee, and for helping me so much with LaTeX - it's been such a huge help for my thesis.

I would also like to thank all of the departmental staff, with special mentions to a few. Nick and Sharon, for all of their help in stores and always being friendly faces. Khalid and Craig for all of their help with NMR, and all of the technicians past and present for keeping the department running! A special nod to Denise Richards and Louise Brown-Leng, for (at times, seemingly single-handedly) keeping the department afloat.

A special thanks to my thesis mentor, Lucy Urwin. I'm so glad I took part in the mentorship programme, and always really looked forward to chatting! You've been a great source of knowledge, advice and support. Thanks for helping me to learn how to say no - it may be the most valuable lesson I've learned!

My PhD experience has not gone the way I had first imagined. The sudden onset of a global pandemic massively affected my work, and I faced my own personal struggles along the way. It is therefore truer than ever to say that I couldn't have done this without the love and support of the amazing people in my life.

In Sheffield, I've made friends for life, without whom my experience would have been significantly more difficult. To our first friends in Sheffield, Freya and Sam, thank you for your friendship. For your lovely meals, our boozy evenings and your support throughout, I will be forever grateful. To Ellen and Luke, thank you for being my running buddies, and for always being there with a coffee, a smile and a hug on my roughest days.

Millie, your kindness, determination and hard work inspire me. I feel so lucky to be surrounded by strong women such as yourself. Alan, thank you for being such a kind and caring friend, both to myself and to Dan. Alice and Jack, thank you for many games nights and laughs throughout - Alice, thank you for introducing me to LaTeX - this thesis looks as good as it does because of you! Courtney, thank you for being a kind and understanding friend. I can't keep writing paragraphs for everyone, can I? So Anna, Jenny, Johnny, Neil, Reuben, Simon, Sophia, Xander - you're all amazing and I'm so glad I've got to know you all!

Outside of Sheffield, I'd like to thank Kathryn and Georgia, my two most treasured friends. You've always listened to, cared for and been supportive of me throughout. Kathryn, thanks for being someone I can always rely on. You're the Ant to my Dec, and I'd be lost without you. Georgia, my oldest friend, thanks for meeting a gobby five-year-old and sticking around! You're the funniest and most thoughtful friend I could ask for. No matter how far apart we are, I know I can always count on you both for anything.

There are some people I would like to thank who unfortunately cannot be here to share in this achievement; my grandparents. I am grateful of course to John and George, my wonderful grandfathers, but I would especially like to thank my Nana and Gran, Hilda and Joan. My Nana always believed in me. Even when she wasn't sure what exactly it was I was doing, she was proud, bragging to her friends "My granddaughter is going to university to do drugs!"... Don't go shouting that around the colliery! I'm interested in drug development, Nana! To my Gran, who unknowingly inspired me to start this whole journey - though it's been tough, if it takes me one step closer to helping people with life-limiting illnesses, it will all have been worth it. I hope I would have made you all proud.

Two of my biggest supporters have always been my parents, to whom I could write pages of thanks - but don't worry Dad, precis! I absolutely could not have done this without you. I'm so grateful to have parents I can turn to when things get tough, and know that I have your support in whatever I decide to do. Thanks for always believing in me, especially when I didn't believe in myself. You have supported me through every achievement (academic or otherwise) without ever pushing or expecting too much of me, and I owe all of this to you. Thanks for all of the laughs, hugs and baked goods posted to Sheffield to keep me going. Milo - thanks for all of those headbutts - maybe you knocked the sense into me!

My final thanks go to Dan, though I'm not sure there are enough words to fully express my gratitude. First of all, you moved to Sheffield so that I could do this PhD with you by my side. You've taken on so many

roles; chef, cleaner, chauffeur, coffee dealer, gym trainer, life coach, and the cheerleader always cheering me on. Most importantly, you've been the person I can't wait to get home to. You've been there through all of the Sunday Sads™, always offering support even when you've had a tough day, too. You've made me laugh. You've filled my evenings and weekends with fun and joy. You've provided unconditional love and support every single day, both while I worked in the lab and while I worked from home. I couldn't have done this without your tireless support, constant encouragement and unwavering belief in me. I am so grateful for everything you have done, and for the incredible person that you are. Who would have thought, all those years ago when you changed the title of my undergraduate lab's spreadsheet to "Daniel is the reason I get out of bed in the morning" that one day it would be true? Thank you for everything you have done for me; I love you unconditionally, and I can't wait to see what the future has in store.

Abbreviations

DABCO	1,4-diazabicyclo[2.2.2]octane
DMAP	4-dimethylaminopyridine
Ac	acetyl
Å	Angrstom(s)
Aq	aqueous
HMDS	bis(trimethylsilyl)amide
TEBAC	benzyltriethylammonium chloride
Triton B	benzyltrimethylammonium hydroxide
bpt	boiling point
c	concentration
℃	degrees Celcius
DFT	density functional theory
dr	diastereomeric ratio
DBE	dibromoethane
DCM	dichloromethane
DIBAL-H	diisobutylaluminium hydride
DMF	*N,N*-dimethyl formamide
DMSO	dimethyl sulfoxide
ee	enantiomeric excess
er	enantiomeric ratio
Eq.	equivalent(s)
Et	ethyl
FMO	frontier molecular orbital
g	gram(s)
Hz	hertz
HOMO	highest occupied molecular orbital

HPLC	high-performance liquid chromatography
HRMS	high-resolution mass spectrometry
HWE	Horner-Wadsworth-Emmons
h	hour(s)
IR	infrared
^{i}Pr	isopropyl
LCMS	liquid chromatography-mass spectrometry
lit.	literature
LDA	lithium diisopropylamide
LUMO	lowest unoccupied molecular orbital
LRMS	low-resolution mass spectrometry
m/z	mass to charge ratio
MHz	megahertz
mpt	melting point
Me	methyl
mg	milligram(s)
mL	millilitre(s)
min	minute(s)
M	molar
mol	mole(s)
M_w	molecular weight
nm	nanometre(s)
NBS	*N*-bromosuccinimide
n-Bu	*n*-butyl
$^{i}Pr_2NEt$	*N,N*-diisopropylethylamine
NMO	*N*-methylmorpholine *N*-oxide
NMR	nuclear magnetic resonance
Ph	phenyl
ppm	parts per million

Abbreviations

PCC	pyridinium chlorochromate
quant.	quantitative
R_f	retention factor
RSA	retrosynthetic analysis
RT	room temperature
SOMO	singly occupied molecular orbital
TBAB	tetra-*N*-butylammonium bromide
TBI	tetra-*N*-butylammonium iodide
Boc	*tert*-butoxycarbonyl
t-Bu	*tert*-butyl
tert	tertiary
THF	tetrahydrofuran
TLC	thin layer chromatography
Ts	tosyl
UV	ultraviolet

Contents

Chapter 1: Introduction

1.1 Introduction to cycloaddition reactions

In organic chemistry, a pericyclic reaction is a concerted reaction with a cyclic transition state, and more than one bond is made or broken in the cycle. There are three major types of reaction which fall into the pericyclic category: sigmatropic rearrangements, electrocyclic reactions and cycloaddition reactions. While sigmatropic rearrangements involve rearrangement of σ-bonds, electrocyclic reactions are characterised by either the conversion of a π-bond to a σ-bond or vice-versa, and can lead to ring opening or ring closing. Cycloaddition reactions are characterised by the formation of new σ-bonds at the expense of π-bonds. This is summarised in Figure 1.1.

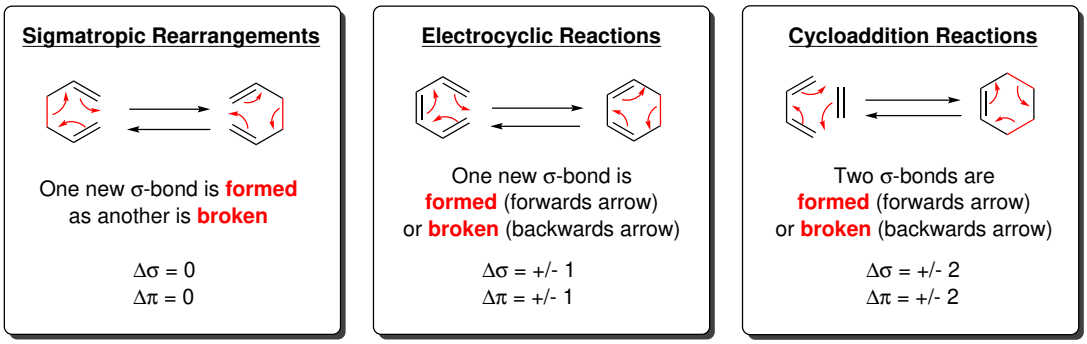

Figure 1.1: Summary of the three classes of pericyclic reactions

Cycloaddition reactions themselves come in a variety of forms, named according to the number of atoms involved in the cycloaddition reaction in each of the reacting components. For example, a [4 + 2] cycloaddition reaction (known more commonly as the Diels–Alder reaction) is thus named because it involves the reaction of a four-atom system (a diene) with one containing two atoms (such as an alkene, and known as the dienophile). This is classed as a cycloaddition, as new σ-bonds are formed at the expense of π-bonds, as can be seen in Scheme 1.1. It is pericyclic as it is concerted, as shown by the curly arrow mechanism, and involves ring formation.

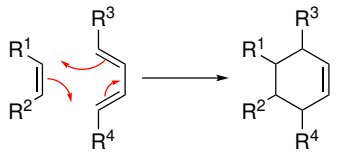

Scheme 1.1: [4 + 2] or "Diels–Alder" reaction mechanism

The [4 + 2] cycloaddition is not the only combination of components possible; which reactions are "allowed" is determined by the Woodward–Hoffmann rule, which states that for a thermal pericyclic reaction to be allowed, the total number of $(4q + 2)_s$ and $(4r)_a$ components must be odd". To explain this rule, the terms must be defined. Firstly, a component is a bond or an orbital which takes part in the pericyclic reaction. A (4q + 2) component is one with 4q + 2 π-electrons, where q is an integer, and a (4r) component is one with 4r π-electrons, where r is an integer. The 's' suffix denotes that the $(4q + 2)_s$ components must interact suprafacially (forming new bonds on the same face) while the $(4r)_a$ components must interact antarafacially (forming new bonds on opposite faces). Consider now the [4 + 2] reaction given in Scheme 1.1. Figure 1.2 shows how this reaction is described by the Woodward–Hoffmann theory.

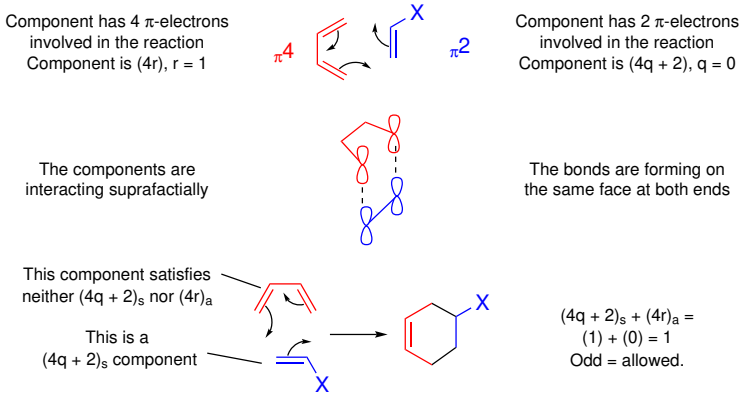

Figure 1.2: Rationalisation of [4 + 2] reaction using the Woodward–Hoffmann rule

Frontier molecular orbital (FMO) theory, which discusses the interaction between highest occupied molecular orbitals (HOMOs) and lowest unoccupied molecular orbitals (LUMOs) can be used to rationalise cycloaddition reactions. Related to the Woodward–Hoffmann rules, FMO theory shows how reactions occur based on the interaction of their FMOs. For Diels-Alder cycloaddition reactions, the FMOs are displayed in Figure 1.3. As the diagram shows, there are two ways that the FMOs can interact; the diene HOMO could interact with the dienophile LUMO (red dashed line, known as a type I reaction), or the dipolarophile's HOMO could interact with the LUMO of the dipole (blue dashed line, type III reaction). This is dependent on which

has the smaller energy difference. If the difference is small enough, there could be a combination of the two interactions, known as a type II reaction.[1]

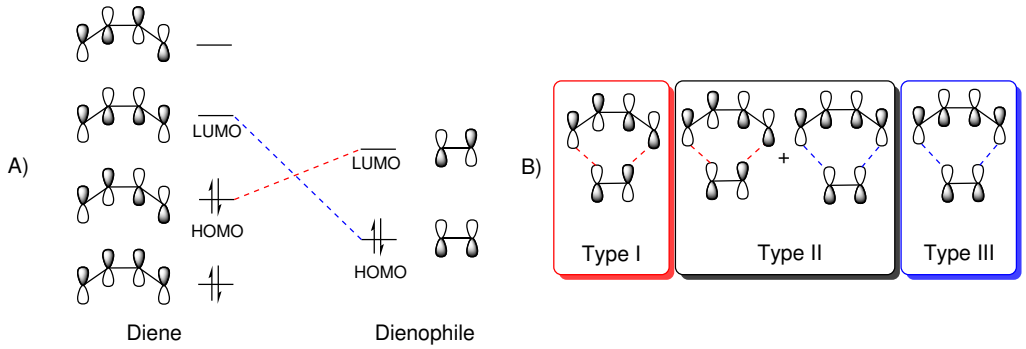

Figure 1.3: A) Orbital overlap diagram of frontier molecular orbitals for a [4 + 2] cycloaddition reaction B) Suprafacial interaction in type I, II and III Diels-Alder cycloaddition

A [3 + 2] reaction known as a 1,3-dipolar cycloaddition, given in Figure 1.4, is also allowed thermally according to this rule. [3 + 2] Cycloaddition reactions lead to the formation of five-membered rings. The three-atom component must be a dipole with a formal positive and negative charge spread over the component. This component is known as the 1,3-dipole, examples of which include azides, ozone, nitro compounds and nitrones.[2] The component with which the dipole reacts, known as the dipolarophile, can be any π-bond. The general form of this reaction is shown in Figure 1.4.

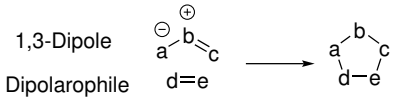

Figure 1.4: General scheme to show 1,3-dipolar cycloaddition

These [3 + 2] cycloaddition reactions are sometimes referred to as “Huisgen” 1,3-dipolar cycloadditions, after the man who discovered the general application of 1,3-dipoles. Individual examples were known as early as the nineteenth century, with Büchner describing the first 1,3-dipolar cycloaddition between diazoacetic esters with α,β-unsaturated esters.[3] However, the examples published by Huisgen in 1963 displayed the wide scope and generality of the reaction. He reported the successful cycloadditions of a variety of dipoles, some of which included nitrile ylides, azomethine ylides and nitro compounds.[4;5]

For some time, there was debate about the mechanism of these reactions. Huisgen’s in-depth study of 1,3-dipolar cycloadditions led him to believe that the reactions were concerted. Arguing against this, Firestone proposed a stepwise reaction which involved radical intermediates, based upon his own

experimental findings (Figure 1.5).[6] Huisgen, however, refuted this. In a following "reply" article, Huisgen stated that Firestone's attempt to account for the high level of specificity seen with a stepwise mechanism was energetically implausible.[5] It has since become widely accepted that the mechanism is in fact concerted, as Huisgen had reported.[7]

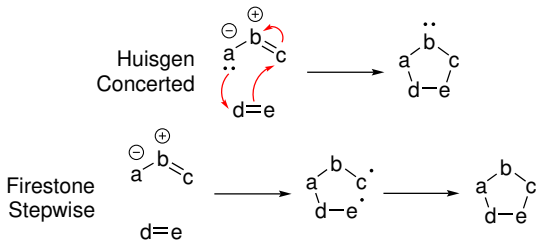

Figure 1.5: Concerted vs stepwise mechanisms for 1,3-dipolar cycloadditions

As with Diels-Alder cycloadditions, 1,3-dipolar cycloaddition reactions may also be considered using FMO theory. For 1,3-dipolar cycloaddition reactions, the FMOs are displayed in Figure 1.6, along with the Type I, II and III orbital interactions which are possible for this reaction.

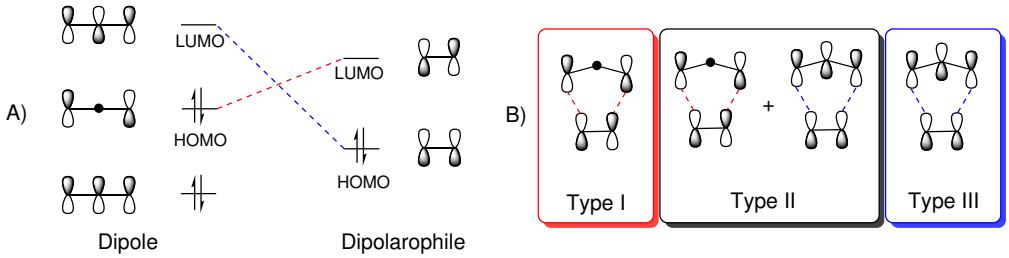

Figure 1.6: A) Orbital overlap diagram of frontier molecular orbitals for a [3 + 2] cycloaddition reaction B) Suprafacial interaction in type I, type II and type III dipolar cycloaddition

As well as FMO theory, dipolar cycloaddition reactions can be considered by the Woodward–Hoffmann rules (Figure 1.6); the reaction involves one two-electron component and one four-electron component, which interact suprafacially in both types I and III (Figure 1.6 B), so as with the Diels–Alder reaction, there is one $(4q + 2)_s$ component (q = 1) and no $(4r)_a$ components, meaning that the reaction is thermally allowed.

1.2 Nitrone cycloaddition reactions

Nitrones are one of numerous 1,3-dipoles reported by Huisgen in 1963. Nitrones have been used in the synthesis of various targets such as neocyanine dyes and in photographic plates.[8] One of their primary uses remains as 1,3-dipoles. There are a wide variety of routes to synthesise nitrones.[9] For example, a variety

of oxidation reactions can lead to nitrone formation, with arguably the most simple being the oxidation of secondary amines.[10] Examples of compounds that can be oxidised to form nitrones are shown in Figure 1.7, condensed from a 2019 review.[9]

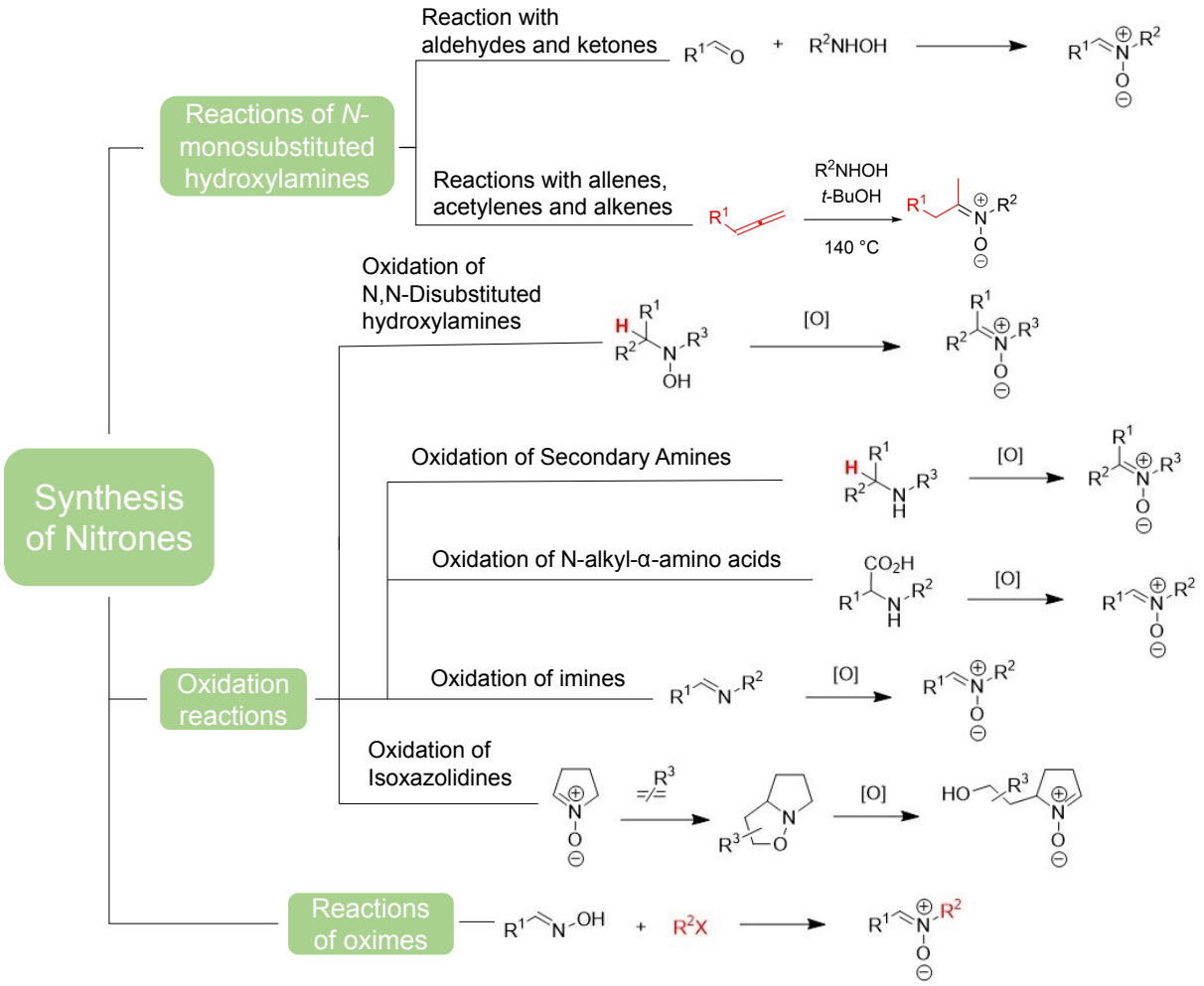

Figure 1.7: Mind map showing various routes to synthesise nitrones

Nitrones may be synthesised, amongst other methods, by the condensation of aldehydes and ketones with *N*-monosubstituted hydroxylamines (Figure 1.7, Scheme 1.2). Indeed, this has been used in the synthesis of complex polycyclic compounds, including alkaloids.[11;12] Though other methods provide alternative routes for nitrone synthesis, condensation is arguably the most versatile and commonly used method.

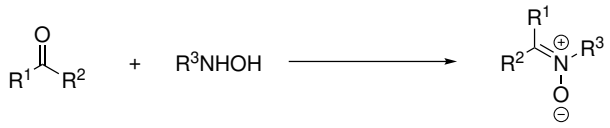

Scheme 1.2: General scheme for condensation of aldehydes/ketones with hydroxylamines

The reaction of nitrones with dipolarophiles generates 5-membered nitrogen-containing heterocycles (Scheme 1.3 A). Stereoselectivity arises when *cis* or *trans* dipolarophiles are used. In Scheme 1.3 B, when a *cis* alkene is used, the groups are *cis* in the heterocyclic product. A *trans* alkene gives a *trans* product, as in Scheme 1.3 C. The reaction is stereospecific, supporting the theory that the reaction is indeed concerted, owing to the suprafacial nature of the reaction. Diastereoisomers can arise when two or more stereocentres are generated during the reaction.

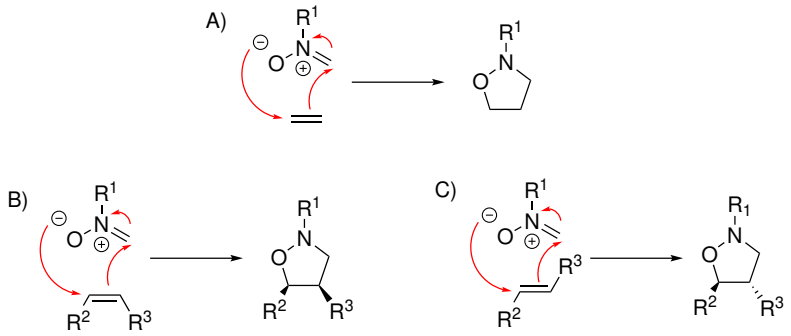

Scheme 1.3: A) Simple nitrone cycloaddition with alkene dipolarophile B) Example with cis selectivity C) Example with trans selectivity

When there is substitution present, there can be a preference for the *endo* or *exo* product. Scheme 1.4 shows an example Diels-Alder reaction with substituents present on the dienophile. When the reaction occurs, the substituents could be positioned beneath the diene, as in Scheme 1.4 A, or pointing away from the diene, as in Scheme 1.4 B. This affects the position of the substituents in the final product.

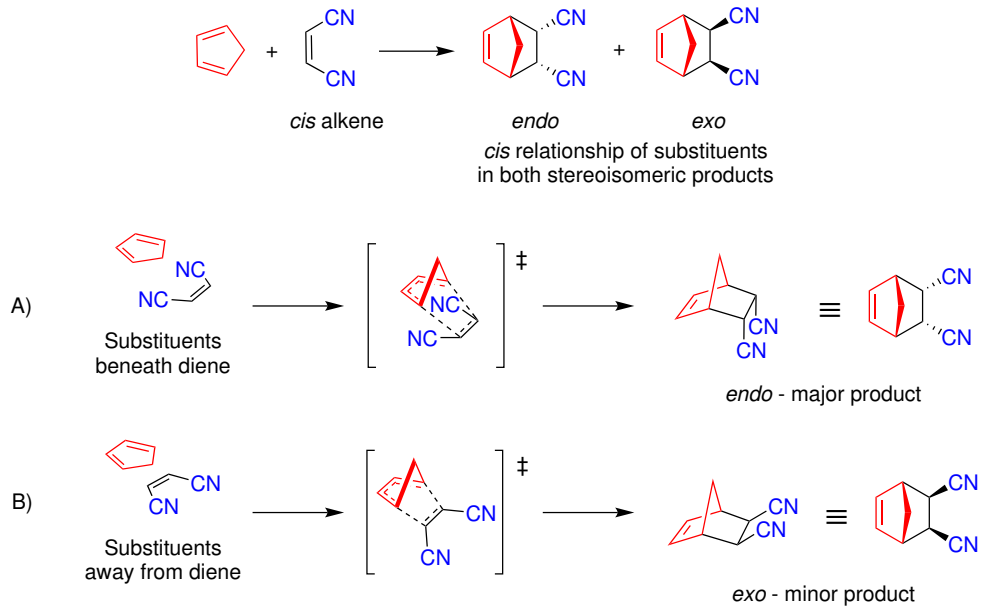

Scheme 1.4: Example of formation of A) endo and B) exo products in a Diels-Alder reaction

In the above example, the substituents are electron-withdrawing CN groups. The electron-withdrawing groups on the dienophile point towards the diene's π-electrons in Scheme 1.4 A. In 1965, Woodward and Hoffmann proposed that the reason for the so-called "*endo*" rule and the preference for the formation of the *endo* product was because of "secondary orbital interactions".[13] The theory stated that in a reaction such as that shown in Scheme 1.4 A, there were favourable interactions between the diene and the CN groups (or other substituents) on the dienophile. In reactions such as that shown in Scheme 1.4 B, however, as the substituents point away from the dienophile this interaction was absent, making the *exo* product less favoured. This theory has since been discredited.[14]

In Garcia's 2000 article, they argue that whilst it is logically impossible to prove something does not exist, there is insufficient evidence to support the existence of such interactions. They argue that other well-known mechanisms can be used in their place.[14]

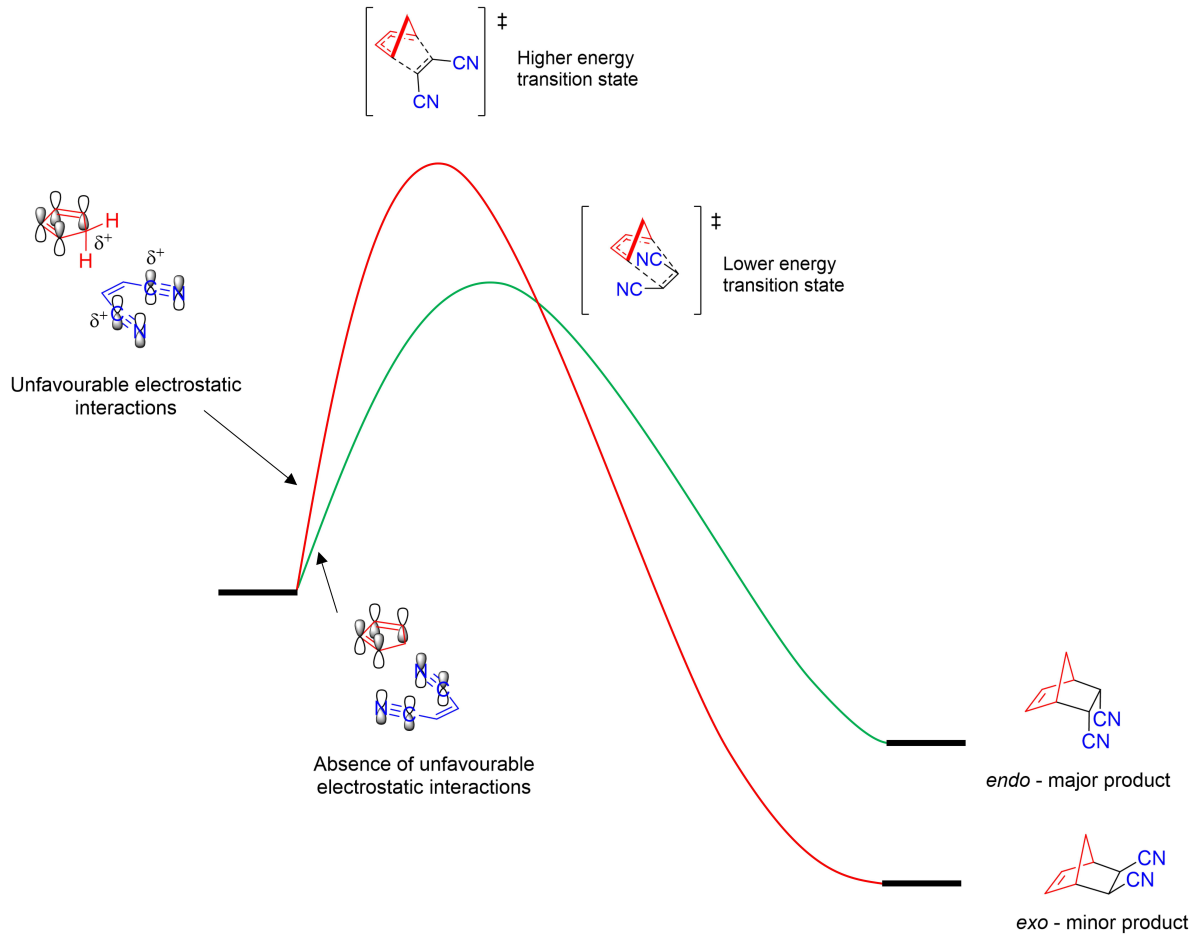

Figure 1.8: Graph showing energy differences in transition states and products during Diels-Alder reaction

As can be seen in Figure 1.8, there is an unfavourable electrostatic interaction for the *exo* transition state, encouraging the formation of the *endo* isomer. The *exo* product, though slower to form, is the more stable thermodynamic product, indicated by the lower energy for this product in Figure 1.8 – it has less steric hindrance/interactions. The *endo* product is the kinetic product; it forms fastest and is, therefore, the major product, but it is higher in energy and thus less stable than the alternative *exo* product. At low temperatures, the reaction can be treated as irreversible. Thus, the *endo* product, which has the lower energy transition state, is formed, and the reaction is under kinetic control. However, when temperatures are increased, the reaction can reverse, and the higher energy transition state of the *exo* isomer becomes accessible, thereby enabling the formation of the thermodynamic product.

In 1,3-dipolar cycloadditions, whilst there are examples of *endo*-selectivity,[15;16] there are also examples of *exo*-selectivity.[17;18] In some cases, this selectivity appears to be driven by the substrates used, whilst in other cases diastereoselectivity can be directed, for example through the use of a catalyst. When considering substrate-controlled diastereoselectivity, as with [4 + 2] cycloadditions, electronic interactions are still a factor. However, steric influences may come more into play in the 1,3-dipolar cycloaddition reaction.

Control of diastereoselectivity is possible using Lewis acid catalysis - the first example of this was thought to be in 1992, by Kanemasa and co-workers.[19] This publication described the first example of a Lewis acid catalyst exerting control over selectivity in such reactions, with an example of the best selectivity shown in Scheme 1.5. When Lewis acid $Ti(^{i}PrO)_2Cl_2$ is absent, the reaction had to be heated to 80 °C in order to complete, and whilst the yield obtained was a respectable 89%, the *endo* to *exo* ratio was 67:33. Addition of the Lewis acid not only enabled the reaction to be run at 0 °C, but it also hugely improved the diastereoselectivity - a ratio of > 99:1 *endo*:*exo* was obtained. The reaction is shown, in the presence of the Lewis acid, in Scheme 1.5. It is worth noting that whilst the addition of this Lewis acid catalyst to a non-chelating dipolarophile ((*E*)-3-penten-2-one) used for reference did increase the rate of reaction, diastereoselectivity was unchanged (dr = 73:27 in the absence of catalyst, 77:23 in the presence of catalyst). This indicates that chelation of the dipolarophile to the Lewis acid was indeed controlling selectivity. Diastereoselectivity in such reactions is summarised in a later review article by Kanemasa, where he discusses subsequent examples from his own group.[20]

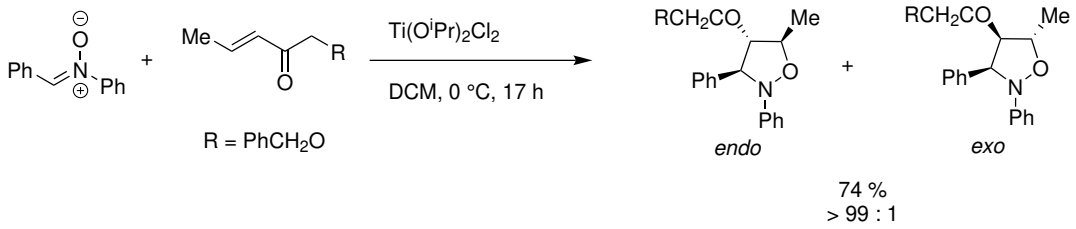

Scheme 1.5: Lewis acid catalysed 1,3-dipolar cycloaddition giving excellent endo-selectivity

As previously mentioned, nitrone dipoles lead to the formation of nitrogen-containing heterocycles. These are widely known in pharmaceuticals – according to a database of U.S. FDA-approved drugs in 2014, 59% of unique small-molecule drugs contained a nitrogen heterocycle.[21] Piperidine is found most commonly in this database, for example in antihistamines and local anaesthetics, but also in drugs for prostate cancer and antidepressants.[21] A chart detailing the most common ring size of nitrogen heterocycles in drugs, from this database, is shown in Figure 1.9. In the case of the more prevalent five- and six-membered heterocycles, the study decided to further split the analysis into aromatic and non-aromatic subsections. From this, it can be seen that there is a significant difference between the two, with 62% of five-membered nitrogen heterocycles being aromatic, compared to just 28% for six-membered rings. As this more detailed analysis has not been conducted for all other heterocycles in Figure 1.9, these are classified as “combined”, indicating a mixture of aromatic and non-aromatic structures.

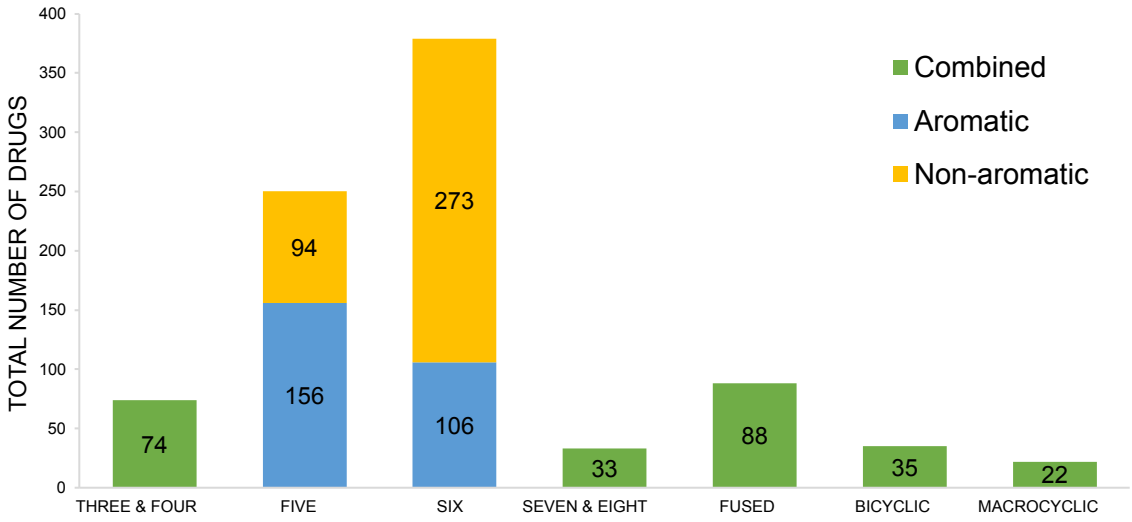

Figure 1.9: Prevalence of various structural types of nitrogen heterocycles in US FDA approved pharmaceuticals

1.3 Tandem Reactions

Tandem reactions are known by many names: domino reactions, cascade reactions, and one-pot reactions.[22] All are defined as "a process involving two or more consecutive reactions in which subsequent reactions result as a consequence of the functionality formed by bond formation or fragmentation in the previous step."[23] They offer an efficient way to perform a series of reactions in a single step. Their origins can be traced back to 1917, when Robinson achieved a biomimetic synthesis of tropinone, **1**.[24] Multiple reactions were performed in tandem, so that the natural product **1** was effectively synthesised in a single step. Firstly, succinaldehyde and methylamine underwent condensation, and the subsequently formed cyclic iminium reacted with starting material calcium acetone dicarboxylate in a Mannich reaction. Decarboxylation, Mannich cyclisation and a second decarboxylation followed, leading to the synthesis of **1** in an overall yield of 42%.[24;25]

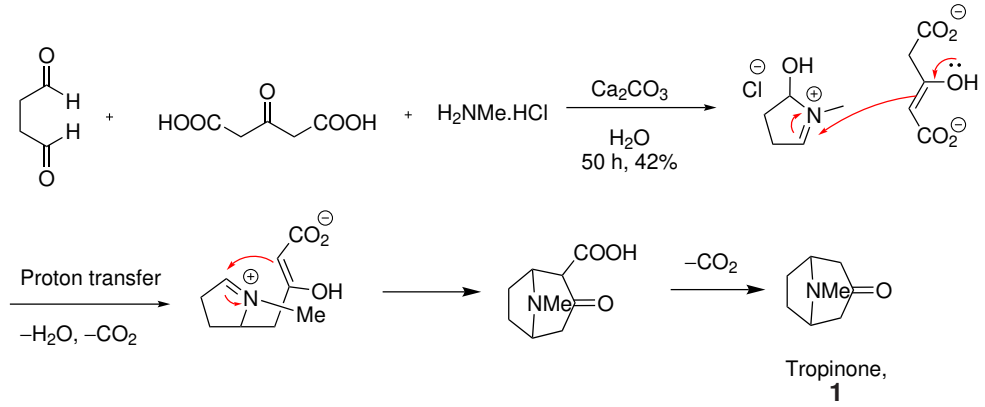

*Scheme 1.6: Tandem synthesis of tropinone, **1**, by Robinson*[24]

In recent years, as more evidence of the environmental impact that human activity is having on our planet comes to light, individuals and large organisations alike have moved to reduce this negative effect. As in many sectors, this is true also in science. Research needs to become more sustainable, and many researchers are utilising better practices in order to achieve this. Furthermore, as the availability of natural resources decreases, this puts yet more pressure on researchers to develop more environmentally friendly practices. In 1998, Anastas and Warner proposed 12 principles of Green Chemistry. These include "prevention" – better to prevent waste than treat it afterwards – atom economy and design for energy efficiency, amongst others.[26] There is also an emphasis on using renewables and catalysts, as saving resources is of great importance. Therefore, tandem reactions are an attractive method to better adhere

to the “Green Principles of Chemistry”. This is, in part, because tandem reactions do not require multiple workup or purification steps in between each step, reducing waste.[27]

1.4 Alkaloids

Alkaloids are naturally occurring organic compounds featuring at least one basic nitrogen atom. They are produced by plants and possess a wide range of biological activities. Due to their biological activities, plants containing alkaloids have been used in traditional medicine throughout the ages. The first recorded example of this dates back 4000 years; Assyrian clay tablets, written in cuneiform characters, describe the use of several alkaloid-containing plants.[28] Their medicinal use continued throughout the ages across a variety of cultures. Many modern medications are based on alkaloids. Quinine (**2**, Figure 1.10) is an alkaloid isolated from *Cinchona calisaya*. Commonly used as a flavour component in drinks such as tonic water, **2** has also found use as an anti-malarial.[29]

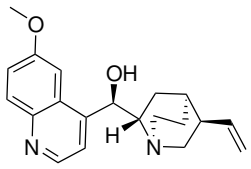

Quinine, **2**

*Figure 1.10: Structure of alkaloid **2***

The first individual alkaloid to be isolated was morphine (**3**, Scheme 1.7). This alkaloid was isolated in the early 19th century from poppy seeds.[30] Its first total synthesis was achieved in 1952, by Gates.[31]

Recently, a study reported a novel synthesis of thebainone A (**4**, Scheme 1.7), a known precursor for alkaloid **3**.[32] Alongside a Heck cyclisation, one crucial step of the synthesis of alkaloid **4** was an intramolecular nitrone cycloaddition to form the nitrogen-containing ring as shown in Scheme 1.7. High diastereoselectivity was obtained when this step was performed at low temperatures. This study reports the shortest total synthesis of compound **4**, and consequently offers a new synthesis route to alkaloid **3**.

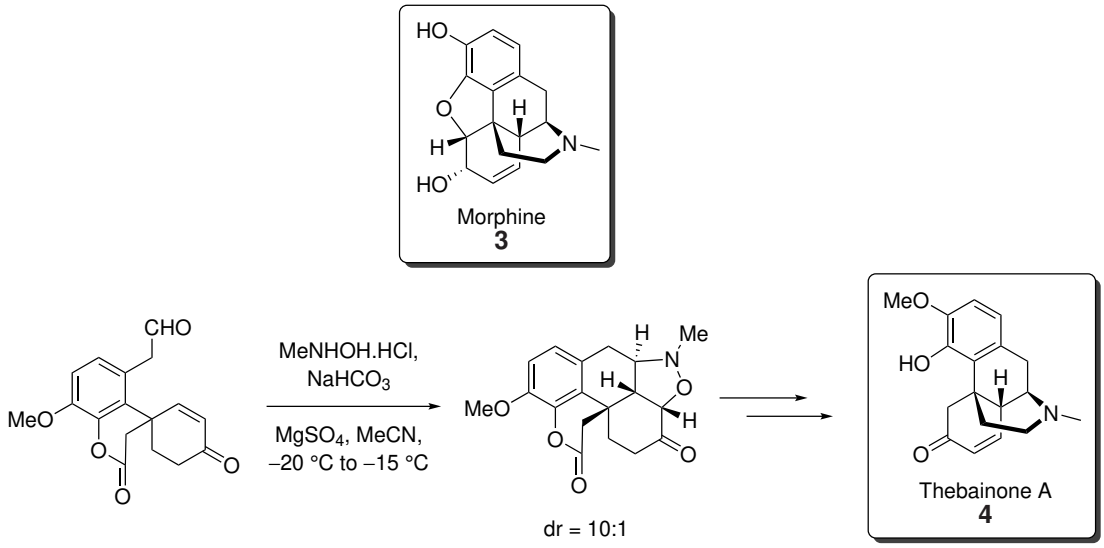

*Scheme 1.7: Structure of **3**, the first alkaloid to be isolated, and the key cycloaddition in the total synthesis to its precursor, alkaloid **4***

In work by the Stockman group, nitrones such as **5** were used to perform [3 + 2] cycloaddition reactions, and product **6** could then be further reacted to give natural product histrionicotoxin, **7** (Scheme 1.8).[33] Its role as a non-competitive inhibitor for certain acetylcholine receptors makes it useful in neurophysiological research. However, due to its low natural abundance, research into the total synthesis of the compound was desirable. Ultimately, the total synthesis developed by Stockman demonstrates one synthetic use of 1,3-dipolar cycloaddition reactions utilising nitrone dipoles. The group also reported the synthesis of a structural variant, (±)-histrionicotoxin 235 A.[34]

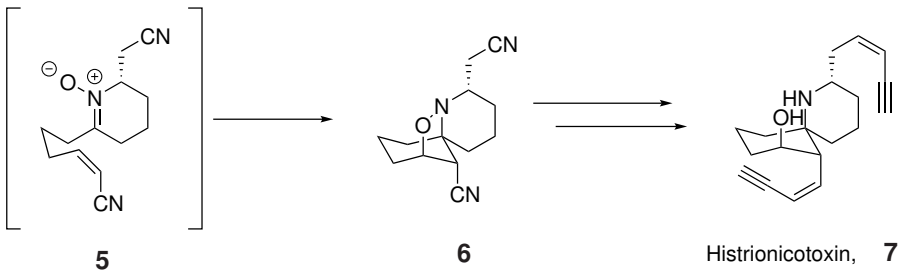

*Scheme 1.8: Nitrone 1,3-dipolar cycloaddition step as part of the total synthesis of natural product histrionicotoxin, **7***

Holmes and co-workers developed a synthetic route to histrionicotoxin 285 A, **8**. This route also utilised a nitrone dipolar cycloaddition reaction to form a similar tricyclic intermediate during the synthesis, as shown in Scheme 1.9[35]

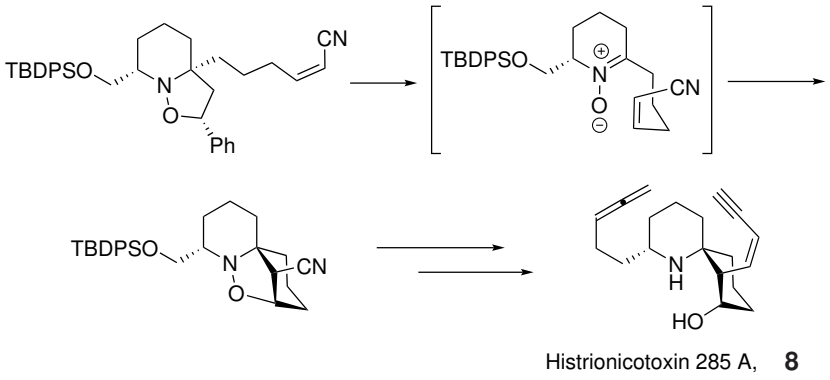

*Scheme 1.9: Synthesis of **8** using nitrone cycloaddition*

Several routes have been developed towards virosaine A (**9**) and B (**10**), alkaloids of the *Securinega* genus (Scheme 1.10). In 2013, Gademann and co-workers reported the first enantioselective total synthesis of **9**, featuring a key intramolecular 1,3-dipolar cycloaddition used to generate a complex ring system (Scheme 1.10, A).[35] In the same year, the first asymmetric total synthesis of alkaloid **10** was reported by Li and co-workers.[36] Li's group also reported a 1,3-dipolar cycloaddition as a key step in their synthesis (Scheme 1.10, B).

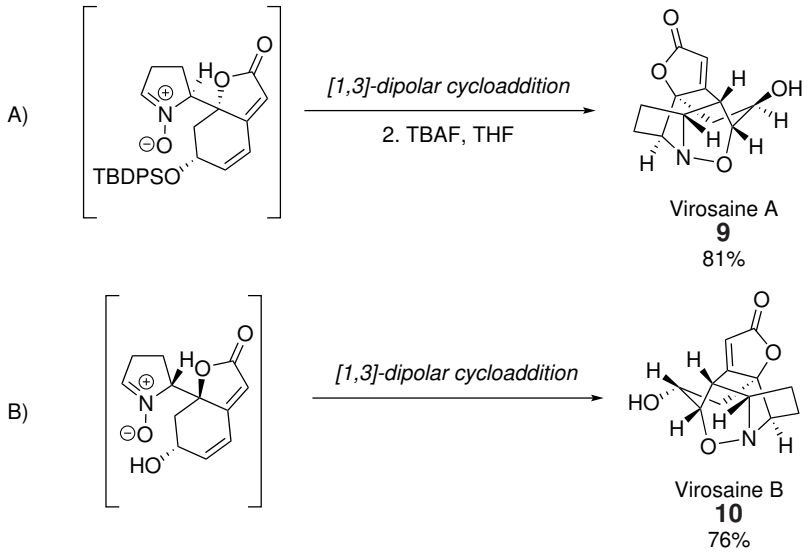

*Scheme 1.10: Key cycloaddition steps in the formation of alkaloids **9** and **10**.*

Both syntheses involved the use of another *Securinega* alkaloid within the synthesis - Gademann's synthesis of **9** involved oxidation and rearrangement of a bubbialidine core, whilst Li's synthesis of **10** required the use of allonorsecurinine. Both papers offered routes to synthesise these, however, and are therefore not reliant on extraction from plant matter. Then, in 2017, Hughes and Gleason reported the

synthesis of (–)-**9**, starting from readily available furan and 2-bromoacrolein.[37]

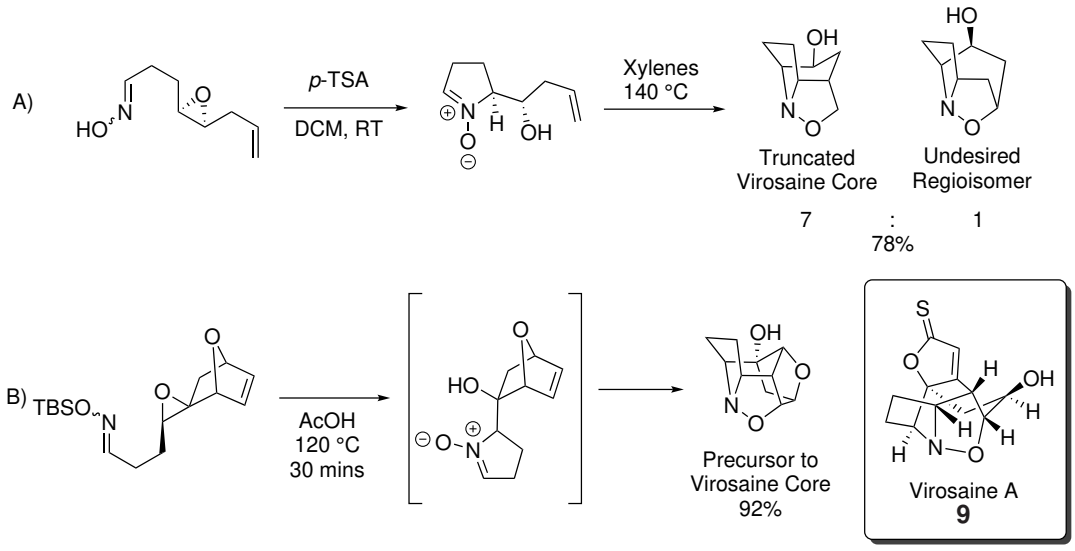

*Scheme 1.11: Use of nitrone cycloadditions in the synthesis of **9** in work by Gleason.*[37]

Their initially proposed route utilised a [3 + 2] cycloaddition reaction as a key synthetic step, which was shown to successfully lead to the synthesis of a truncated Virosaine core (alongside a regioisomeric product), as shown in Scheme 1.11 A.[38] This route utilised an epoxide opening to generate the nitrone. However, this route was unsuccessful in later steps, and a new route had to be proposed. This route also featured a [3 + 2] cycloaddition cascade (Scheme 1.11 B), which was instead used to form a precursor which was converted to compound **9** in 8 further steps.

This cascade chemistry provides close precedent to both the work previously undertaken within the Coldham group and the work which we propose to undertake as described in this thesis.

1.5 Previous work in the group

Research within the Coldham group has focussed heavily on the synthesis of polycyclic products over the past decade, utilising a novel cascade process developed within the group. This cascade process involves three steps which proceed in a one-pot process and has led to the preparation of a variety of natural products. The first step of this tandem procedure involves a condensation reaction. This is followed by cyclisation to afford a dipole, requiring a leaving group – primary alkyl halides have been used for this purpose throughout these studies. The newly formed dipole can then undergo a [3 + 2] dipolar cycloaddition reaction, reacting with either a tethered dipolarophile (intramolecular cycloaddition) or an

external dipolarophile (intermolecular cycloaddition).

Work within the group has touched upon the use of azomethine ylide dipoles, which led to the synthesis of three *Aspidosperma* alkaloids: aspidospermine **11**, aspidospermidine **12** and quebrachamine **13** (Figure 1.11).[39] This particular study used a tethered dipolarophile, thus enabling an intramolecular [3 + 2] dipolar cycloaddition.

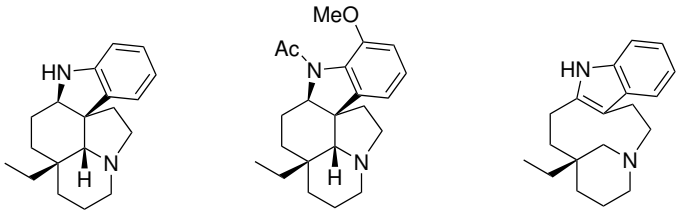

*Figure 1.11: Aspidosperma alkaloids **11**-**13** synthesised within the group*

Studies also included intermolecular cycloaddition reactions, and in 2009 a study from the group[40] reported the use of such a reaction to synthesise alkaloid **14**, (+)-crispine A, an alkaloid from *Carduus crispus*. Extracts of plants from this genus have been used in traditional Chinese medicine for the treatment of a variety of ailments, from the common cold to rheumatism.[41] This, too, utilised the one-pot procedure, and required a total of just 5 steps, as shown in Scheme 1.12.

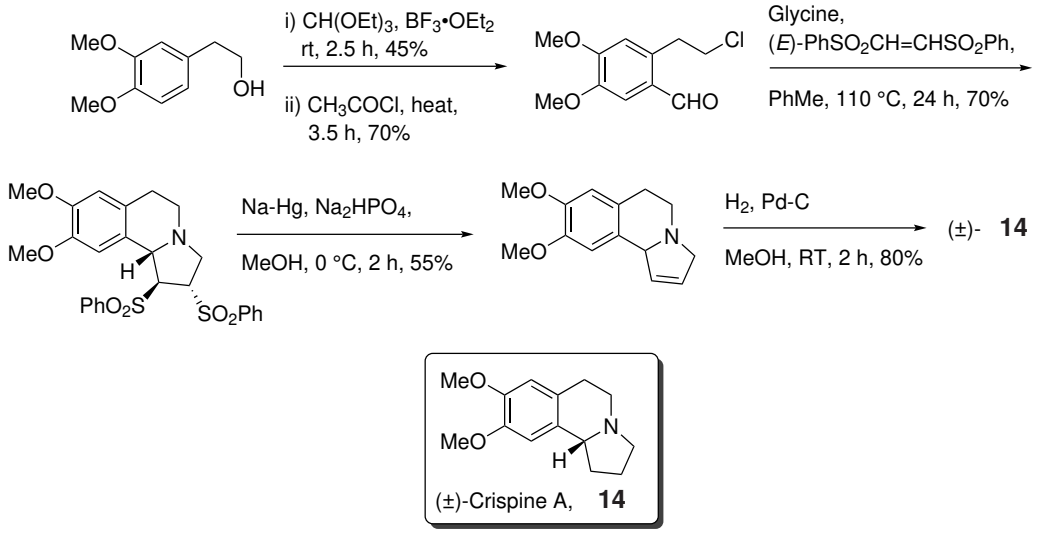

*Scheme 1.12: Synthesis route to **14**, using the one-pot condensation, cyclisation and cycloaddition procedure*

The scope of the reaction continued to grow, moving to study enolizable aldehydes which enabled

the synthesis of the natural product Myrioxazine A, **15**.[42] For synthesis of this alkaloid, aldehyde **16** was the starting material for the cascade process. A nitrone dipole was used in this work (Scheme 1.13), and this particular dipole became the focus of much work within the group. The cascade process resulted in the formation of a single diastereoisomer, displaying excellent stereoselectivity. It was thought that, since condensation is a fast and reversible process, this is the step which occurs first in the cascade.

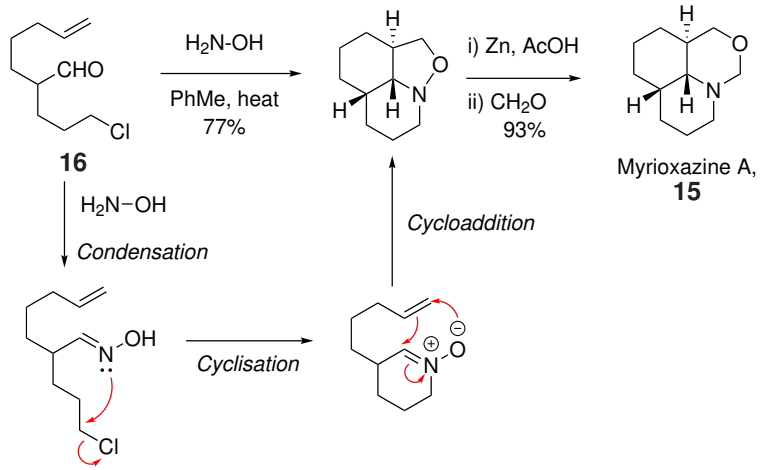

*Scheme 1.13: Synthesis of alkaloid **15** by cascade approach from aldehyde **16***

Synthesis of bridged compounds using nitrone dipoles also proved possible, leading to the synthesis of the bridged core ring system of the yuzurimine, daphnilactone B, and bukittinggine type *Daphniphyllum* alkaloids, **17**.[11;43] In this study, the condensation of an aldehyde, **18**, with a primary amine, most successfully hydroxylamine, initiated the one-pot procedure. Cyclisation then ensued, allowing the tethered dipolarophile to react with the nitrone dipole in an intramolecular cycloaddition reaction (Scheme 1.14) to afford cycloadduct **19**, which was then converted to core ring system **17** in four further steps. Discovering that the procedure could be used to form bridged systems meant that the synthesis of a variety of other alkaloids, such as those from *Alstonia*, looked promising.

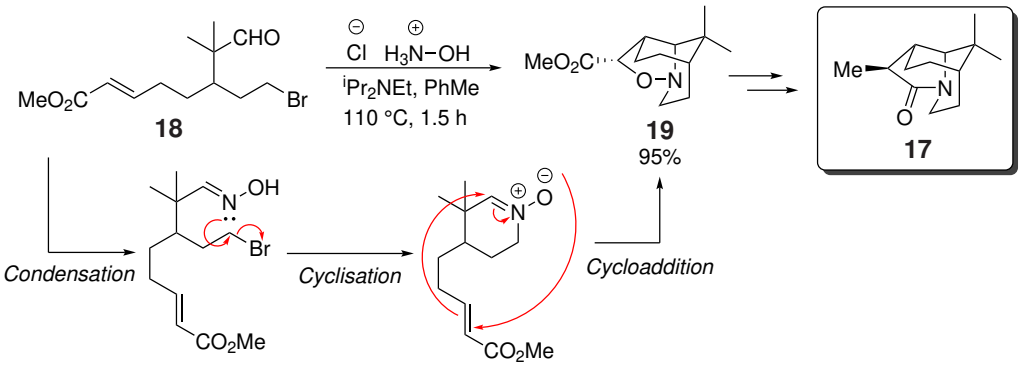

*Scheme 1.14: Example of key steps of tandem reaction forming bridged core structure **17**, seen in several Daphniphyllum alkaloids*

In the case in Scheme 1.14, the branch point between the alkene dipolarophile and the alkyl halide is β- to the aldehyde, leading to compounds with a one-carbon bridge. The research was then extended to compounds that would give a two-carbon bridge and hence access an isoquinuclidine ring system.[44] This would require the branch point to be γ- to the aldehyde and would provide a route to the *iboga* alkaloids. In the most recently published example of the nitrone cascade chemistry being applied to alkaloid synthesis, the study describes a formal synthesis of the natural product (±)-19-hydroxyibogamine, **20** (Scheme 1.15). The cascade process begins from aldehyde **21**, resulting in the formation of cycloadduct **22**. The study then describes several further steps towards the formal synthesis of **20**.

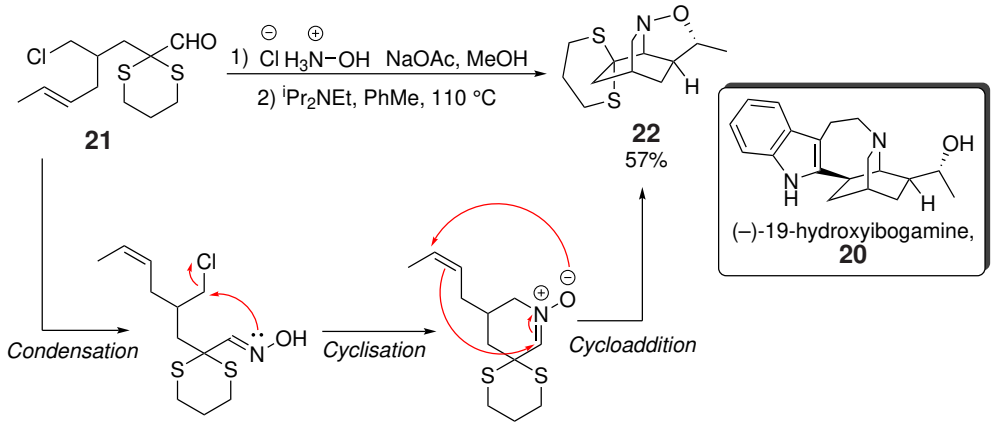

*Scheme 1.15: Example of key steps of tandem reaction in the formal synthesis of alkaloid **20***

It was also shown by the group that not only aldehydes but also ketones were suitable substrates for such cascade reactions.[12] The study showed that hydroxylamine could be condensed with ketones such as **23**, leading to the synthesis of spirocyclic compounds such as **24** (Scheme 1.16). The N–O bond of **24** could be reduced to afford spirocyclic amines, and diversity in both ring size and substitution was demonstrated.

However, while single regioisomers were obtained in cycloadditions to form 5-membered rings, mixtures were common during the formation of 6-membered rings.

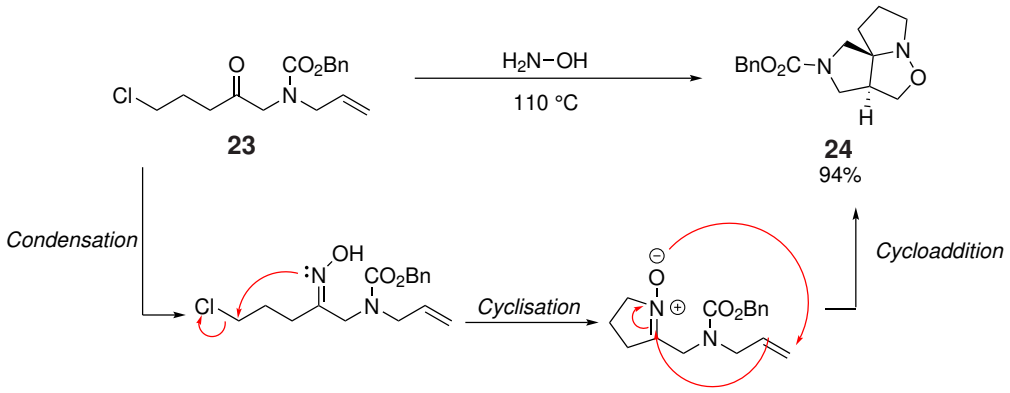

*Scheme 1.16: Example of key steps of tandem reaction forming spirocyclic compounds such as **24** using ketone precursors such as **23***

In 2019, work began on a proposed synthesis of tropane alkaloid ferrugine, **25**, utilising the cascade process. This procedure would require a secondary leaving group, and if successful this would be the first example of this cascade process being used on a secondary substrate within the group. It was initially decided to test this chemistry with a tosyloxy leaving group; halides had commonly been used for this purpose previously, but there was interest in trialling the chemistry in the presence of a different leaving group. The target compound chosen was aldehyde **26** which would be used to condense with hydroxylamine to promote the intramolecular cycloaddition.

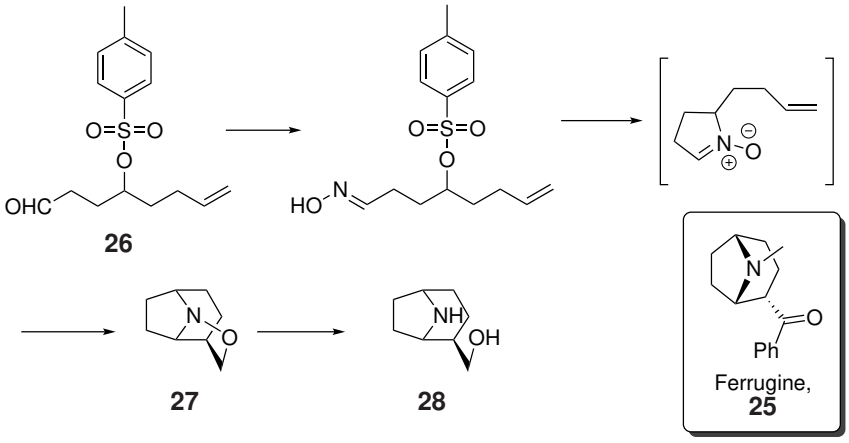

*Scheme 1.17: Planned route to **28**, core of ferrugine **25***

In initial work conducted by MChem student Hathway,[45] the desired aldehyde **26** was synthesised by a five-step procedure in moderate yield (Scheme 1.18) starting from readily available cyclooctadiene, **29**.

However, the subsequent tandem procedure (Scheme 1.17) was unsuccessful and cycloadduct **27** was not formed. The reason for this was not clear, but no aldehyde **26** was recovered.

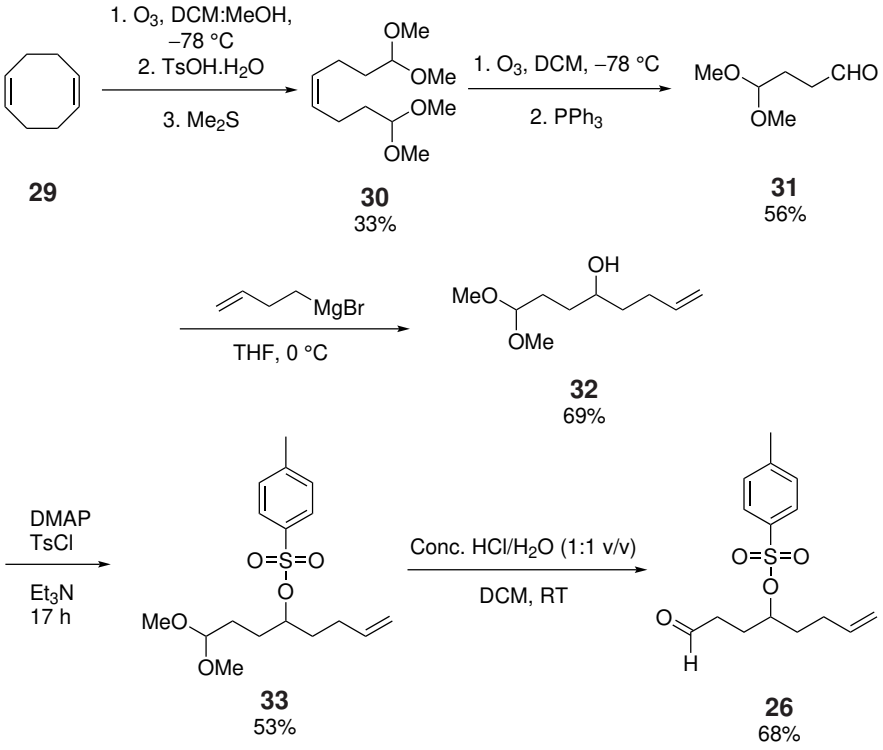

*Scheme 1.18: Synthesis route to aldehyde **26***

When the work was continued by MChem student Hennessy,[46] several changes were made in attempts to optimise the reaction. Firstly, the proposed leaving group was changed from an OTs group to a bromide. In addition, instead of using aldehyde **26**, the aldehyde to be used (**34**, Figure 1.12) would have a phenyl group pre-installed; if this proved successful, the route to **25** would be shorter.

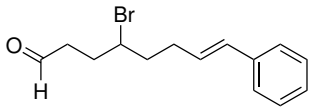

34

*Figure 1.12: Proposed aldehyde structure, **34**, for use in cascade reaction to synthesise core of **25***

However, synthesis of this new aldehyde **34** proved difficult; the Grignard reaction used successfully in the synthesis of alcohol **32** was unsuccessful in this case. Focus returned to the synthesis of an aldehyde without the pre-installed phenyl group, now only changing the leaving group to a bromide as opposed to a tosylate. This too proved difficult, as bromination of alcohol **32** was unsuccessful.

Chapter 2: Towards the Synthesis of Ferrugine

2.1 Introduction

2.1.1 Tropane Alkaloids

Tropane alkaloids are characterised by their 8-azabicyclo[3.2.1.]octane skeleton.[47] Tropane alkaloids have been isolated from a variety of plant families, including *Solanaceae*, *Erythroxylaceae*, *Convolvulaceae*, *Proteaceae*, *Rhizophoraceae*, *Brassicaceae*, and *Euphorbiaceae*.[47] Over 200 tropane alkaloids are known to occur naturally, and their synthesis is highly desirable due to their wide range of biological activities.

Tropane alkaloid atropine (**35**), for example, found use during the Gulf War as an antidote to nerve gas poisoning, but is also known to have cardiovascular and pulmonary effects, amongst other uses.[48] Found in deadly nightshade, or *Atropa belladonna*, **35** is known to be a poison. In spite of this fact, it has been used throughout history and continues to be used in modern medicine today. The name belladonna means beautiful lady; in the Middle Ages, the plant was used to enhance women's pupils, which was thought to make them more beautiful. This effect was proven by F. Runge in 1819, and relates to how the compound is used in ophthalmology today. As a muscarinic receptor antagonist,[49] **35** binds to muscarine receptors in the iris, and is used in certain treatments to dilate the pupils to relieve pain.[50]

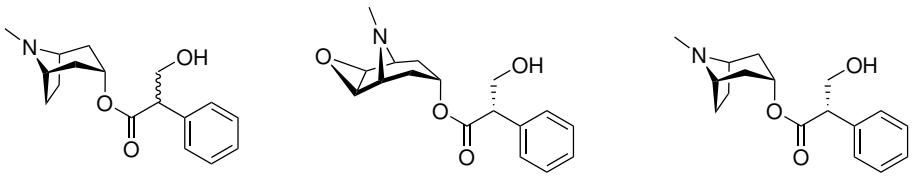

*Figure 2.1: Structures of three tropane alkaloids from nightshade; atropine **35**, scopolamine **36** and hyoscyamine **37***

Nightshade was informally known as one of several "hexing herbs", a nod to its historic association with witchcraft.[51] However, whilst tales of the berries causing one to "meet the devil in person" may not be rooted in fact, the truth remains that the plant is indeed deadly - its berries are poisonous and ingestion is fatal. It is rumoured that deadly nightshade was in fact used by Livia to poison her husband, Emperor Augustus,[52]

and thought to have been used by the original MacBeth to poison Duncan's troops.[53]

Deadly nightshade is also known to contain alkaloids scopolamine **36** and hyoscyamine **37**, and the use of the plant in traditional medicine dates back thousands of years. Studies into the properties of the plant increased from the 1600s onwards, with physicians finding medicinal benefits in spite of the fact that the plant was known to be poisonous. In 1803, Atropa was first described by Duncan, wherein the powdered leaves or roots of the plant were used in the treatment of conditions including epilepsy.[52]

Compounds **36** and **37** once again demonstrate the bioactivities so commonly seen with alkaloids, finding use in the treatment of neuromuscular disorders.[54] Whilst total synthesis would be desirable, often complex stereochemistries make this an onerous task which is not economically viable,[55] whilst extraction poses concerns for the supply. There was a shortage of scopolamine **36** in 2018-2019, which has since been resolved, but atropine **35** remains in shortage.[56;57] Biosynthesis could therefore provide a much-needed alternative. In one study by Srinivasan and co-workers,[58] medicinal tropane alkaloids **36** and **37** were produced by baker's yeast.

However, the most efficient and cost-effective method at present is still extraction from plant matter. It was discovered that *Dubosia* plants from Australia contain large quantities of alkaloids, with **36** making up 60% of these. When these plants are harvested, 10-15 tonnes of leaves are obtained per hectacre, and the plants can be harvested thrice annually. Therefore, these plants are the major source of **36** for the pharmaceutical industry.[54] In addition to the use of **36** in the treatment of neuromuscular disorders, derivatives of this alkaloid have found huge commercial uses. Scopolamine derivative scopolamine butylbromide (**38**) is an active pharmaceutical ingredient (API), sold under the brand name Buscopan, used for relief from irritable bowel syndrome and cramps. This puts large pressure on the demand for **36**.

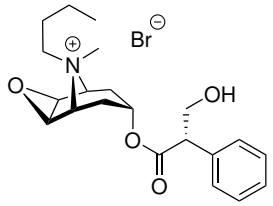

Scopolamine butylbromide
(Buscopan)
38

*Figure 2.2: Structure of Buscopan **38**, an API developed from tropane alkaloid **36***

One more commonly known tropane alkaloid is cocaine (**39**). Isolated from coca plants, cocaine is a stimulant; and also the second most frequently consumed illegal drug worldwide.[49] In the UK, illegal drugs are categorised based on the harm associated with their use. **39** is listed as a Class A drug, meaning it is deemed to be one of the most harmful illegal substances, so offences relating to its possession or distribution carry the harshest penalties.[59]

Cocaine's first reported usage was in Ecuador in 3000 BC, where the leaves of coca plants were chewed by tribesmen, which released the alkaloids - including **39**.[49]

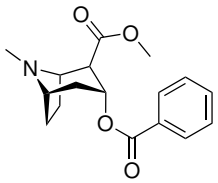

Cocaine
39

*Figure 2.3: Structure of alkaloid cocaine **39***

Cocaine, **39**, along with other tropane alkaloids such as **36** lead to hallucinations and psychoactive effects, dependent on the dose taken. The physiological effects of these drugs are, however, quite different in spite of their similar structures. Cocaine **39** inhibits the reuptake of neurotransmitters including dopamine, noradrenaline and serotonin by nerve cells. The accumulation of these neurotransmitters in synapses leads to extreme happiness and energy. Alternatively, scopolamine **36** acts as a muscarinic receptor antagonist, like **35**.[49]

There are many scientific studies surrounding **39**: its mode of action was determined in 1860,[60] followed shortly by the first chemical synthesis and structure determination in 1898. This first synthesis was developed by Richard Willstatter, who would go on to win the 1915 Nobel Prize in Chemistry for his work on plant pigments including chlorophyll.[61] Studies continued after **39** became an illegal substance under the 1920 Dangerous Drugs Act, but even after over 100 years of study, the biosynthetic pathway of cocaine remains incomplete, with particular issues surrounding the formation of the tropane skeleton. Studies to this end are still ongoing, with a 2022 article reporting a near-complete biosynthetic pathway.[62]

Whilst tropane alkaloids clearly have medicinal benefits, they are classed as 'plant toxins', but toxicity data is limited in this area, and there is a great deal of variation. For example, **35** is said to be toxic, and

consumption of just 100 mg can lead to death, but there have also been cases where a patient has survived a 500 mg dose. That being said, there is still more toxicity data available for **35** than for many other tropane alkaloids.[54]

The presence of tropane alkaloids in plants such as deadly nightshade and henbane can lead to contamination of cereal-based foods, which poses a concern to human health. In 2015, the Food Standards Agency in the UK conducted a study of cereal-based products, vegetables, oilseeds and teas, and flours.[63] They were analysed for the presence of tropane alkaloids, in order to assess the risks to human health if these alkaloids were found to be present. At low levels, tropane alkaloids were found in 18% of samples. It was concluded that this was comparable to the levels found in other countries tested, but unfortunately, it was also disclosed that toxicity information for tropane alkaloids (other than for **35** and **36**) remains very limited. This is one reason that methods for producing and testing tropane alkaloids are widely sought after.

2.1.2 Ferrugine

Ferrugine, **25**, is a tropane alkaloid, isolated from *Darlingia ferruginea*, a rainforest tree from Northern Queensland. Compound **25** is a nicotinic receptor antagonist, along with relative ferruginine, **40**. This means these alkaloids could be used in future treatments against Alzheimer's disease.[64] Reduced levels of the neurotransmitter acetylcholine have been implicated in the progression of the disease, and for this reason, acetylcholinesterase inhibitors are the predominant class of drugs used in the treatment of Alzheimer's disease symptoms. Nicotinic receptors are a class of acetylcholine receptors, and inhibition by **25** or **40** could aid treatment.[65]

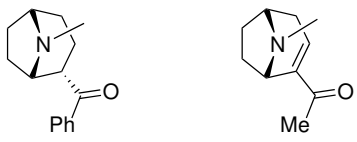

Ferrugine **25** Ferruginine **40**

*Figure 2.4: Structure of tropane alkaloid ferrugine, **25**, and relative ferruginine, **40***

2.1.3 Previous Syntheses of Ferrugine

Bick's synthesis

In 1979, Bick and co-workers reported the first total synthesis of **25**.[66] The approach used anhydroecgonine, from cocaine **39**,[67] using (–)**39** to produce anhydroecgonine **41** in an enantiomerically pure form. In the subsequent steps, shown in Scheme 2.1, ester hydrolysis, treatment with oxalyl chloride and reaction with diphenylcadmium formed (-)*ent*-**25** - the unnatural enantiomer.[68] This synthesis was completed in 23.6% overall yield from **41**.

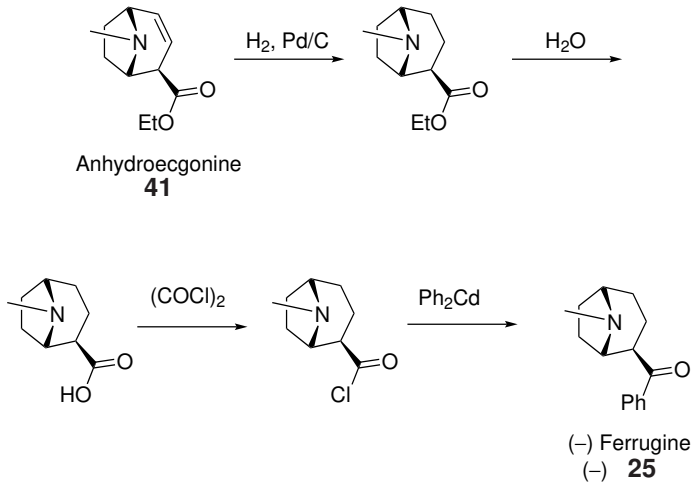

*Scheme 2.1: Final steps of Bick's pioneering synthesis of **25***

Throughout the 1990s and into the early 2000s, there was an uptick in synthetic efforts towards ferruginine **40**,[69–74] but efforts towards **25** remained limited. In fact, Bick's was the only synthesis reported until 2008, when Grainger's group began working towards the synthesis of **25**.[75]

Grainger's synthesis

Grainger and co-workers prepared an unsaturated [3.2.2] bridged bicyclic amide, which was converted through use of a one-pot procedure to **25**.

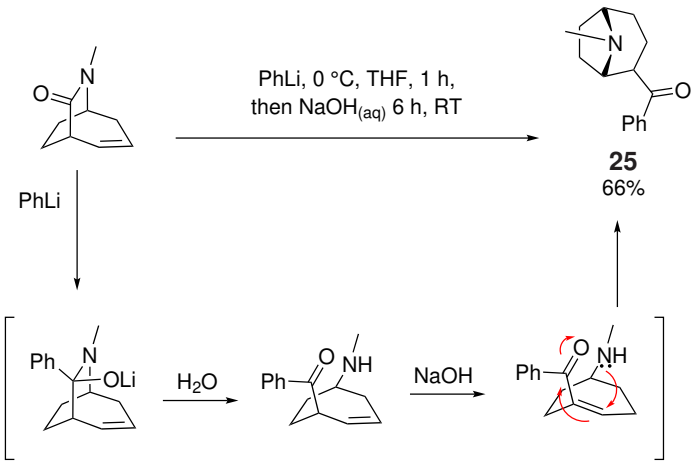

*Scheme 2.2: Final step of Grainger's synthesis of **25**, utilising a one-pot procedure*

The synthesis was completed in 6 steps, with the final step being the one-pot procedure, which is shown in Scheme 2.2. This tandem process is initiated through the use of PhLi, which undergoes nucleophilic attack. Aqueous workup affords an aminoketone, and in the presence of base, the alkene present becomes conjugated with the ketone moiety. This conjugation enables intramolecular conjugate addition to occur, thereby affording the desired alkaloid (±)**25** in 66% yield.

2.1.4 Vicario's Synthesis

More recently in 2021, Vicario's group published an alternative total synthesis of (±)-ferrugine.[76] This study applies a Brønsted acid-catalysed approach, utilising the ring opening of 1-aminocyclohept-4-ene-derived epoxides in the synthesis of tropane alkaloids. Whilst the approach had been applied to the synthesis of other alkaloids by the group,[77] including (+)-ferruginine, **40**, the 2021 paper further demonstrated the synthetic utility of this method as a tool for enantioselective synthesis by applying it to the synthesis of ferrugine, **25**.

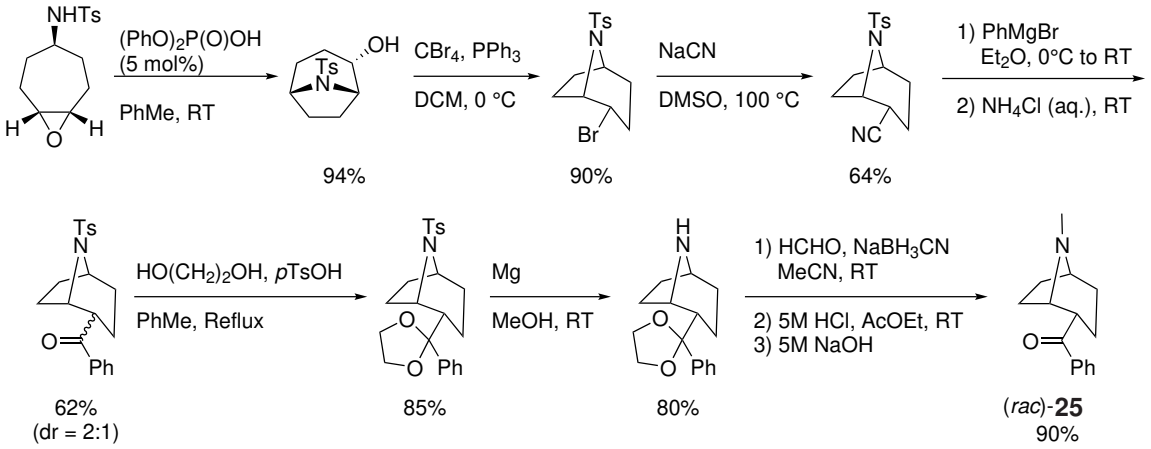

*Scheme 2.3: Total synthesis of racemic ferrugine, **25**, by Vicario et al.*

Though the study attempted an enantiopure synthesis of **25**, their attempts were unsuccessful, due to the tendency of intermediates in the synthesis to undergo racemisation, forming an achiral symmetric aziridinium intermediate. However, the complete synthesis of racemic **25** was demonstrated, with an 8-step linear sequence providing a good overall yield of 21%, as shown in Scheme 2.3. This route does not, however, appear to offer a more efficient synthesis than that proposed by Grainger.

2.1.5 One-pot procedures in natural product synthesis

Use of one-pot procedures such as that by Grainger[75] is popular in natural product synthesis. As discussed in section 1.5, this is the focus of much work in the Coldham group, making use of the condensation-cyclisation-cycloaddition cascade reaction.

This has focused predominantly on cascade chemistry where the cyclisation occurs through nucleophilic attack, leading to the loss of a leaving group. Predominantly, bromides and chlorides have been used for this purpose. However, there are other methods for such a cyclisation to occur. Research by Padwa and co-workers details the use of vinyl sulfones in one-pot cycloaddition reactions. In 1988, a paper detailed the first example of an oxime undergoing conjugate addition with a vinyl sulfone, followed by the subsequently formed nitrone performing a cycloaddition reaction with a second vinyl sulfone.[78] Related work has continued for almost 30 years, with vinyl sulfones used in tandem conjugate addition-cycloaddition reactions towards the synthesis of various natural products in Padwa's group.

Synthesis of 2,7,8-epi-perhydrohistrionicotoxin

An early example of the applicability of this cascade chemistry is in the total synthesis of 2,7,8-epi-perhydrohistrionicotoxin, **42**.[79] Amine **42** is a stereoisomer of spirocyclic alkaloid perhydrohistrionicotoxin **43**, the formal synthesis of which is also described in this paper. Derivatives of these alkaloids have garnered significant interest in the synthetic community, owing to their neurophysical properties. Padwa's study describes a multi-step route towards these compounds, which utilises the cascade chemistry as a key step (Scheme 2.4).

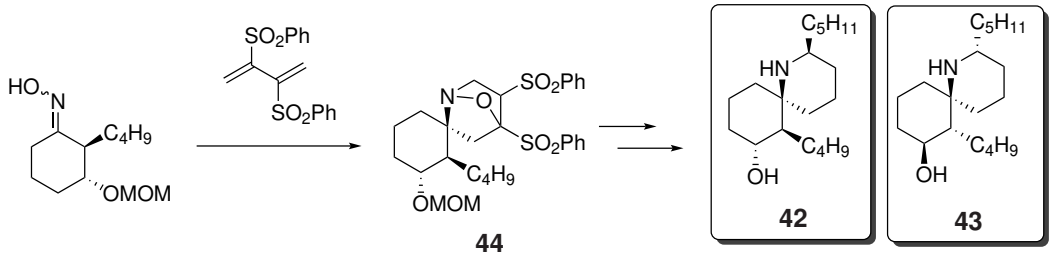

*Scheme 2.4: Cascade chemistry step utilised towards the total synthesis of **42**, and formal synthesis of **43***

In the total synthesis of **42**, the conjugate addition-cycloaddition cascade led to the formation of a key cycloadduct (**44**), which was converted to the desired **42** in subsequent steps.

Synthesis of a non-natural derivative such as **42** is desirable, as such derivatives have demonstrated use in the investigation into the mechanism of trans-synaptic transmission of neuromuscular impulses.[79]

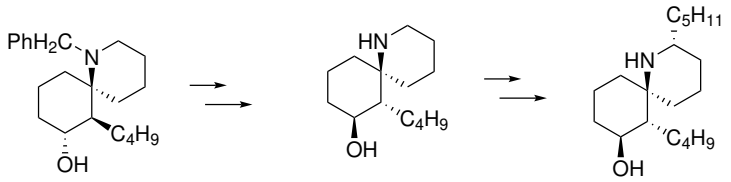

*Scheme 2.5: Intermediate formed by Padwa (**45**), which could be converted as shown by Corey to afford compound **43***

In the formal synthesis of perhydrohistrionicotoxin **43** described within the paper, the key step shown in Scheme 2.4 is still employed, preparing amine **45**. Intermediate **45** has been previously converted by Corey and co-workers to **43** *via* intermediate **46**, as shown in Scheme 2.5.[80–82]

Synthesis of Yohimbenone

A second example from the group was the synthesis of yohimbenone, **47**.[83] Amine **47** is an alkaloid from the rauwolifa class of indole alkaloids, a class which had again attracted attention due to the medicinal properties of its alkaloids. The synthetic method described in this paper is generally applicable to synthesis of yohimbene alkaloids, as well as structurally related ipecac alkaloids.

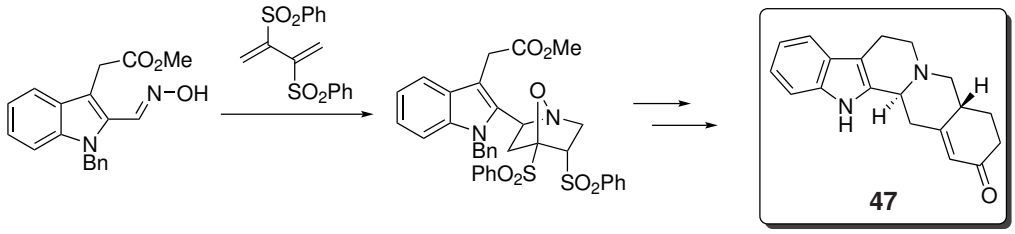

*Scheme 2.6: Cascade step employed towards the total synthesis of **47***

The route once again hinges on the key conjugate addition/dipolar cycloaddition cascade, forming a cycloadduct which was converted to **47** in four further steps; reductive cleavage, cyclisation, conjugate addition with subsequent sulfone reduction and Robinson annulation followed by functional group manipulation. The key cascade step is shown in Scheme 2.6.

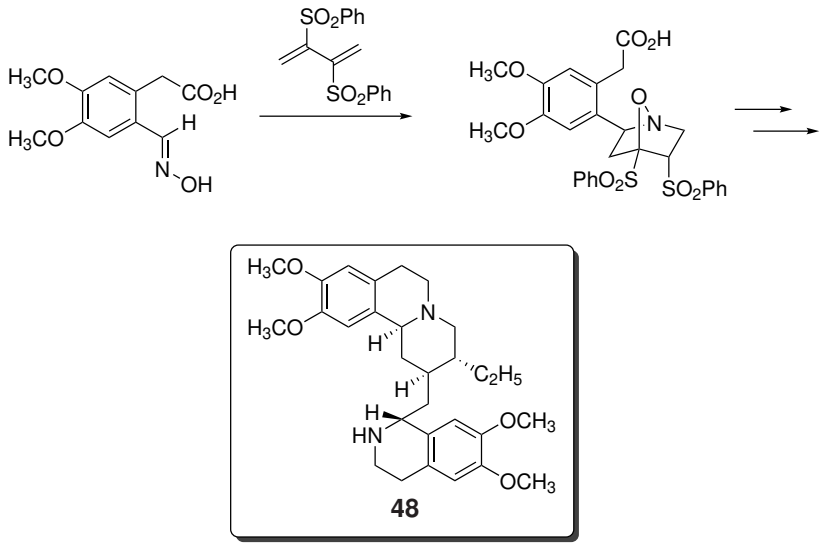

*Scheme 2.7: Cascade step employed towards the total synthesis of **48***

This paper also describes a formal synthesis of structurally related alkaloid emetine, **48**, which employs a similar cascade strategy, shown in Scheme 2.7. This forms a cycloadduct which was converted further in

the study to a key intermediate, and it had been shown by Takano and co-workers that this intermediate could then be converted to **48**.[84]

Synthesis of Cylindricine C

Marine alkaloid cylindricine C (**49**) was also synthesised through the use of this method.[85] The first step of this synthesis performs the cascade chemistry on an oxime with the bis(phenylsulfonyl)diene used previously. This is given in Scheme 2.8. The resulting cycloadduct was then converted in several steps to the desired alkaloid **49**.

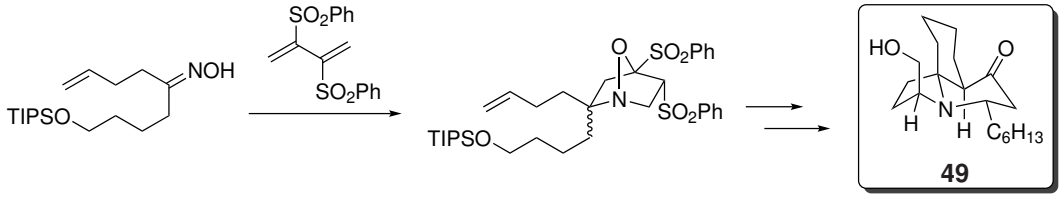

*Scheme 2.8: Cascade step employed towards the total synthesis of **49***

Synthesis of Halichlorine

A final example of this chemistry is given in the 2010 paper by Padwa and co-workers, reporting the synthesis of an advanced intermediate towards halichlorine, **50**.[86] Amine **50** is an alkaloid, shown to inhibit vascular cell adhesion, which has been isolated from species of marine sponge. In this 2010 study, the cascade conjugate addition/dipolar cycloaddition protocol provided the first step of this process, wherein an advanced halichlorine intermediate (**51**) is described. The cascade step is detailed below in Scheme 2.9.

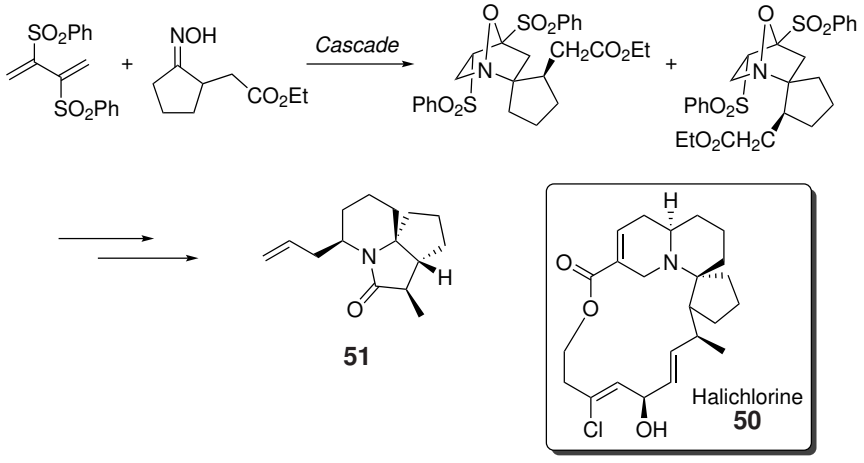

*Scheme 2.9: Route towards advanced intermediate of **50**, **51**, with key tandem reaction beginning the route*

Towards Ferrugine

As discussed in section 1.5, preliminary work in the Coldham group did attempt to use the cascade condensation-cyclisation-cycloaddition chemistry to synthesise ferrugine, **25**. Work by Hathway and Henessey focussed on a route towards a suitable precursor for this one-pot chemistry, which could ultimately yield **25**, but unfortunately were unable to develop a suitable route. Scheme 2.10 shows the precursor which was the most recent focus of synthetic efforts, though synthesis of this intermediate had not been successful.

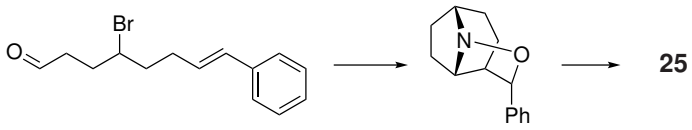

*Scheme 2.10: Desired precursor to cascade chemistry, with the view to synthesise **25***

2.2 Aims

Synthetic efforts were to be made towards the core structure of the tropane alkaloid Ferrugine, **25**. Though a limited number of examples of the synthesis of **25** do exist in the literature,[66;75] it was hoped that the Coldham group's one-pot condensation, cyclisation and cycloaddition cascade reaction could be used in an alternative synthetic route. Use of the cascade reaction would limit the number of steps required in the synthesis, and could therefore offer a more efficient route towards the synthesis of **25** or its core.

The synthesis of a ferrugine-like core through the use of the cascade process has long been a goal within the group, with previous master's students Hathway and Hennessey working towards this goal.[45;46] This work has since continued, both within this project and in that of another master's student, Cox, whose work will also be discussed within this chapter.[87]

New routes to this compound consider the work done by Padwa and co-workers, and explore the use of a vinyl sulfone in the cascade chemistry. It would also be desirable to install an internal dipolarophile within the cascade precursor molecule, thereby enabling intramolecular cycloaddition. Such a precursor would require synthesis, and various routes towards this goal are discussed herein, summarised in Scheme 2.11.

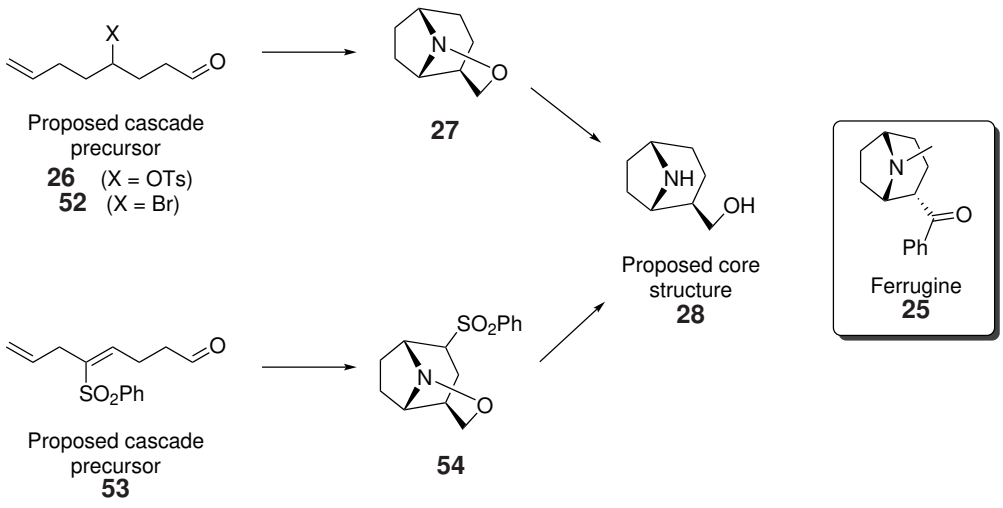

*Scheme 2.11: Proposed cascade precursors, which could be used in the synthesis of the core structure of **25***

2.3 Results and Discussion

2.3.1 Continuation of previous work

Initially, it was considered that the routes investigated previously, working from cyclooctadiene **29** (as discussed in sections 1.5 and 2.1.5)[45;46] could be adapted to incorporate Padwa's vinyl sulfone chemistry. The retrosynthetic analysis given in Scheme 2.12 shows this newly proposed route towards the core structure of **25**, compound **28**. The first two steps, featuring two subsequent ozonolysis reactions, replicate those performed previously in the group, affording aldehyde **31**. Instead of the Grignard reaction which previously led to problems in the synthesis, this aldehyde could then be employed in a Horner-Wadsworth-Emmons (HWE) reaction with a phenyl sulfonyl phosphonate, thereby installing the desired vinyl sulfone. Following deprotection of the acetal group, cascade chemistry could commence. With an internal dipolarophile installed, intramolecular cycloaddition to afford **54** would be possible. As in work by Padwa, the sulfone group could then be reduced, with concurrent N-O bond cleavage, to afford the desired core structure **28**.

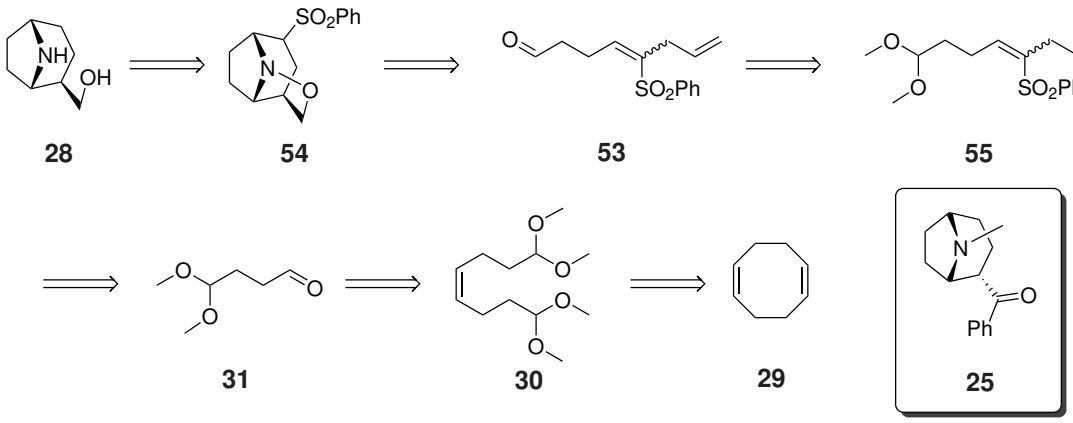

28 **54** **53** **55**

31 **30** **29** **25**

*Scheme 2.12: Proposed cascade precursors, which could be used in the synthesis of the core structure of **25***

To begin, the two ozonolysis steps were repeated. The first ozonolysis reaction was performed as detailed in Hennessey's MChem thesis (Scheme 2.13),[46] which in turn had been based on literature procedures.[88] The reaction was conducted in MeOH at –78 °C, with ozone bubbled through the solution for 2 h. The characteristic blue colour was not observed, but this is in line with what was seen in previous attempts, and is likely because there remains a second alkene present which has not been ozonolysed. After excess ozone was removed with argon, TsOH was added and the mixture was stirred at RT for a further 2 h.

Dimethyl sulfide was then added and the mixture was stirred overnight, before being concentrated under reduced pressure.

In earlier attempts, the product was taken forward following column chromatography, and subjected to the subsequent ozonolysis and HWE reactions, but poor results from these led to questions as to the purity of acetal **30**. It was discovered that, having followed the procedure detailed by Hennessey,[46] the basic aqueous workup present in the literature was not being performed. It is believed that, in the absence of this workup, remaining TsOH was acting to deprotect the acetal present. NMR spectra of **30** confirmed that all samples do exhibit aldehyde peaks, which supports this theory. In some cases, there appeared to be up to a 3:1 ratio (**30**:**56**) by mass, assuming deprotection of both aldehydes as opposed to partial deprotection (Scheme 2.13). It was believed that this impurity was causing issues in the subsequent steps.

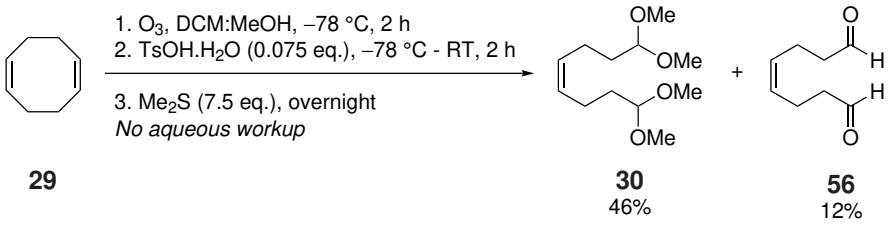

29 **30** 46% **56** 12%

*Scheme 2.13: Ozonolysis to afford compound **30**, with deprotected product **56** also being formed, likely due to the absence of an aqueous workup described in literature.*[88]

Therefore, the reaction was reattempted, this time including the aqueous workup, once again starting from 10 g of starting material, **29**. ^{1}H NMR analysis indicated an improved ratio of 93:7 **30**:**56**, by mass. This means that, of the 8.30 g of compound isolated, 7.72 g of the desired product **30** was obtained, though as part of an impure mixture. Though there was a reduced amount of side product **56**, the overall yield was actually lower than in the previous example, at only 36%, and this was still part of an impure mixture. Therefore, this would likely still affect the results of the following steps.

Next, it was considered that the aldehyde impurity could be removed by a reduction reaction. The goal was to reduce the aldehyde to a diol, **57**, which would likely be more easily removed, due to its significantly increased polarity compared with that of desired product **30**. Therefore, the mixture of the desired product **30** and aldehyde **56** was dissolved in MeOH, and $NaBH_4$ was added portion-wise, over 2 h at 0 °C. ^{1}H NMR analysis of the crude product showed, in addition to the peaks corresponding to **30**, an apparent quartet at 3.64 ppm, thought to correspond to the CH_2 groups neighbouring the OH groups in the alcohol product, **57**.

Following aqueous workup and column chromatography, none of diol **57** was isolated, and it was assumed to have been retained on the column due to the relatively low polarity of the solvent system used. However, pleasingly an extremely clean sample of **30** was obtained, though only in 19% overall yield from starting material **29**. With this in hand, the next step could be considered.

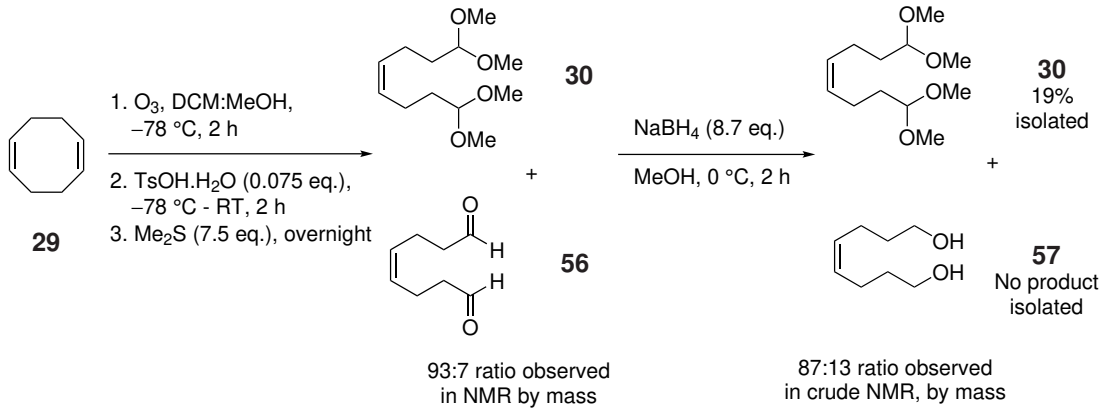

*Scheme 2.14: Ozonolysis and subsequent reduction of side product **56**, in order to purify mixture of **30***

The second ozonolysis step was next repeated.[45;46;88] Though examples using impure **30** afforded impure **31**, yields were improved when clean samples of **30** following reduction were used. The greatest yield obtained, 74%, was only marginally lower than the literature-reported yield of 79%, though this was obtained without the need for the additional reduction step.

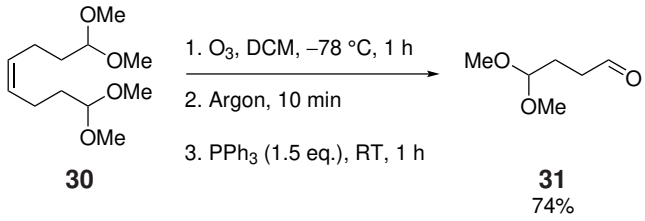

*Scheme 2.15: Ozonolysis reaction to afford compound **31***

To note, when impure **30** was being used, products from this reaction, too, were impure, with additional aldehyde peaks observed. It is likely that these correspond to dialdehyde **56** carried forwards from the first step. In earlier attempts, these impure samples were used in subsequent steps, though with less success.

Next, the HWE reaction was considered. In order to perform this reaction, a suitable phenyl sulfonyl phosphonate was needed, and required synthesis. Compound **58** was to be used for this purpose, enabling the installation of an internal dipolarophile alongside the desired vinylsulfone. This could be done in a single

step,[89] from readily available diethyl ((phenylsulfonyl)methyl)phosphonate (**59**) and allyl bromide **60**, as shown in Scheme 2.16.

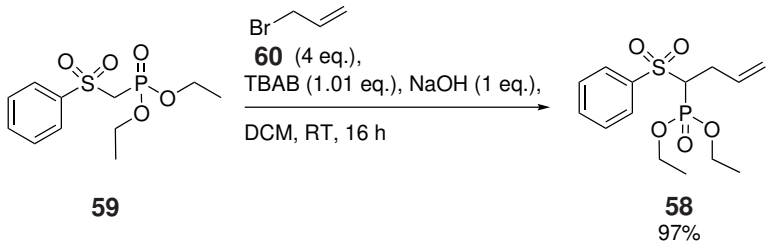

59 **58** 97%

*Scheme 2.16: Synthesis of phosphonate **58***

Phosphonate **58** was synthesised in 97% yield, and with the desired starting materials in hand, attention turned to the HWE reaction. In this reaction, NaOEt was to be used as the base, and this was synthesised prior to the reaction from Na metal refluxed in EtOH. This was found to be better than using the pre-made NaOEt available in the lab. Phosphonate **58** and aldehyde **31** were dissolved in EtOH at 0 °C, and the base was added, as a 1 M solution in EtOH. The mixture was warmed to RT and stirred overnight.

Initial attempts at the HWE reaction were undertaken prior to suitable purification of the starting materials, where it is believed that the aldehyde **56** was also present. These samples yielded unexpected results. Whilst LCMS analysis seemingly showed the desired mass ion, 2D NMR spectroscopy indicated that the main substance isolated from this reaction was not the expected product **55**. Based on the carbon-proton interactions observed by HSQC and HMBC, there may have been a mixture of products present, and it was considered that further purification of starting materials was required.

Thus, attention turned to producing clean samples of **30** and **31**, as discussed previously. When the reaction was performed using such clean samples, the desired product was obtained, in a mixture of *E* and *Z* isomers. It is expected that the NMR spectra of these will differ, particularly in the chemical shift of the proton of the vinyl sulfone alkene. This could therefore be used to calculate the ratio of the isomers present. Indeed, this method was used in DeLaPradilla's 2009 study, which found that in their sulfinyl-substituted alkenes, the chemical shift of the vinyl proton is around 0.7 ppm higher for the *E* isomer.[90] NMR prediction software within the MestReNova x64 program supported this conclusion, suggesting that in compound **55**, the chemical shift of the vinyl proton will be higher in the *E* isomer than in the *Z* isomer.

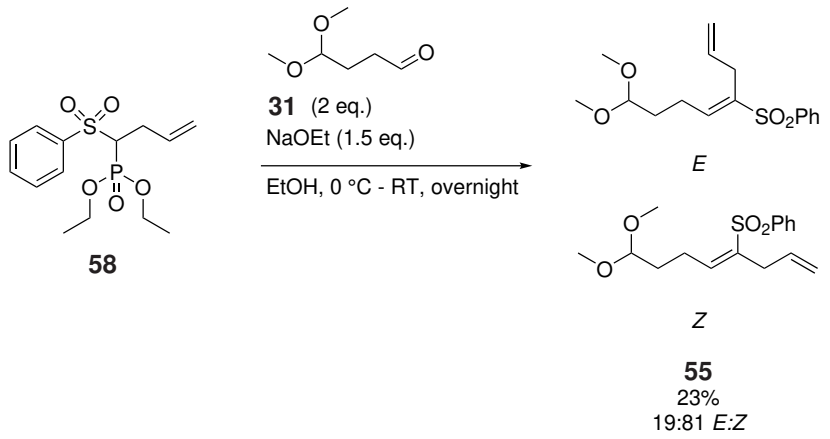

*Scheme 2.17: HWE reaction between **58** and **31***

In this particular case, the product was isolated as a mixture of *E*/*Z* isomers, as seen in Scheme 2.17, and it was concluded that the *Z* isomer was the major geometric isomer formed in this reaction, being produced in a 19:81 ratio (*E*:*Z*). This conclusion was based on the fact that the alkene peak at the higher chemical shift of 6.99 ppm was the minor isomer (integrating to 0.19H), whilst the major isomer was at the more upfield shift of 6.04 ppm, and integrated to 0.81H. The formation of the *Z* isomer is often less favourable due to an increase in steric clashes, and in simple HWE reactions, the stabilised ylide encourages the formation of the *E* isomer. However, as molecule complexity increases, the ratio of geometrical isomers is less predictable and is known to vary.[91] Therefore, this assignment was investigated further using NOESY analysis, focussing on the peaks at 6.99 (minor isomer, 0.19H) and 6.04 ppm (major isomer, 0.81H).

Irradiation of the peak at 6.04 ppm showed close-in-space contact between this proton (at the vinyl alkene in the major isomer) to the CH_2 group highlighted in Figure 2.5. Irradiation of the peak at 6.99 ppm did not indicate a close-in-space contact between the alkene proton and this CH_2 group. Considering the orientation of the groups in both isomers, as displayed in Figure 2.5, the proton sits closer to this CH_2 group in the *Z* isomer (2.89 and 2.67 Å) than in the *E* isomer (3.91 and 3.63 Å). This supports the assignment that the peak at 6.04 ppm corresponds to the *Z* isomer, thus confirming that the *Z* isomer is the major isomer formed in this case.

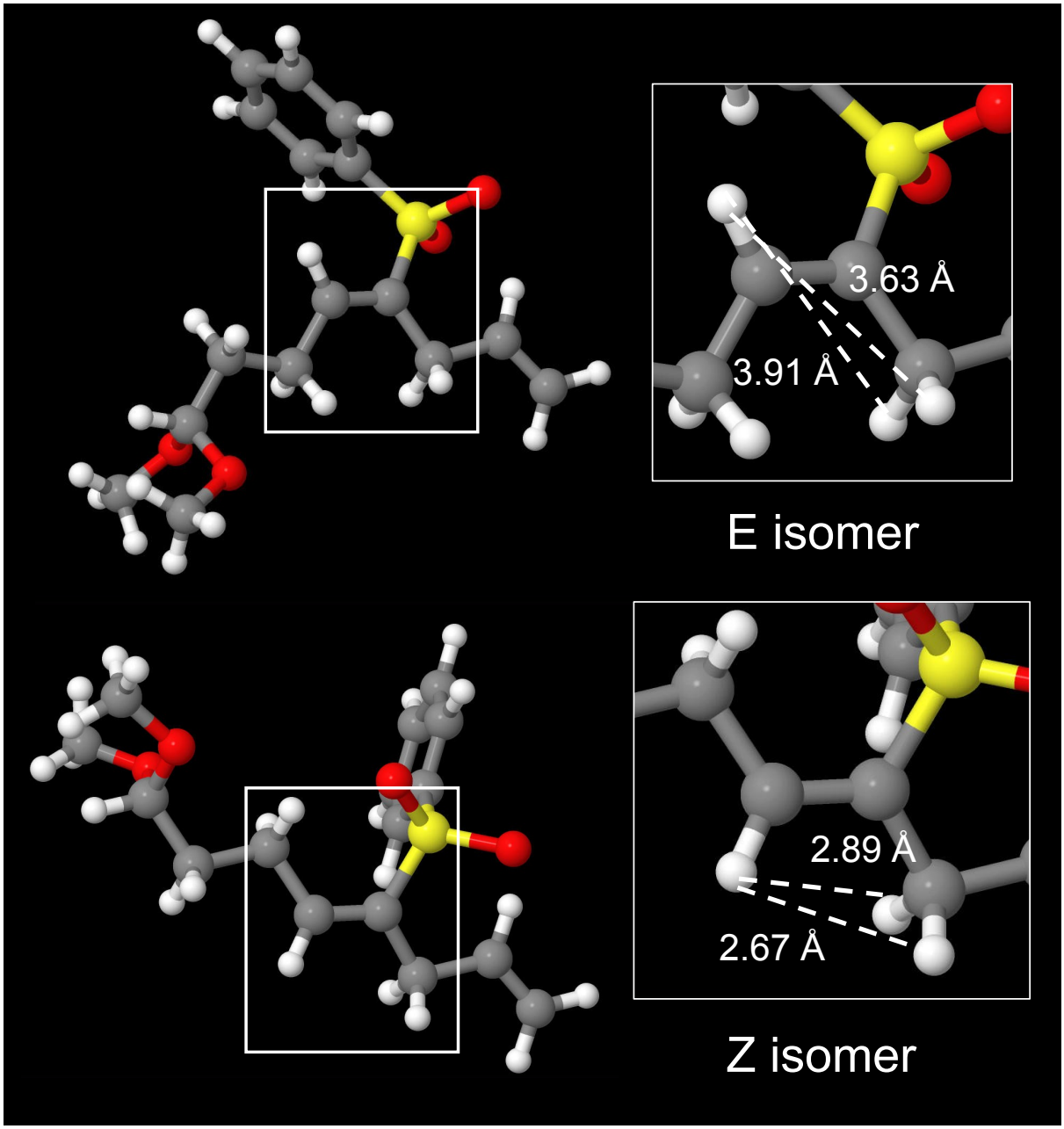

Figure 2.5: Conformations of E and Z isomers optimised using DFT, highlighting the difference in distance between the alkene protons in each isomer with the CH_2 group of interest

These structures were optimised with DFT and hybrid functional B3LYP, with the 6-311G(d,p) basis set, GD3BJ empirical dispersion functional and no solvent model was used. This optimisation was run by colleague Cox, with distances determined by myself within jmol software utilising these optimised structures.

Next, the acetal **55** needed to be deprotected, unveiling the aldehyde precursor to the cascade reaction. 6 M HCl was used for this reaction, which was performed on a relatively small scale of 150 mg. Compound **53** was isolated in a yield of around 45% (Scheme 2.18), but the sample remained impure following column

chromatography. Given the small masses involved, it was decided to prioritise trialling the cycloaddition cascade reaction on this 57 mg sample, rather than further purifying or fully characterising aldehyde **53** at this time.

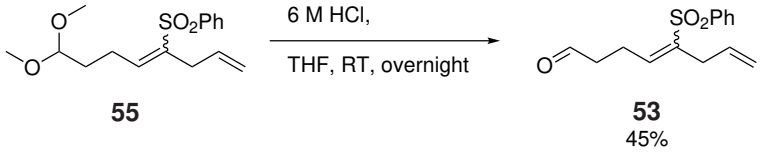

55 **53** 45%

*Scheme 2.18: Deprotection of acetal **55** to afford compound **53***

With the synthesis of precursor **53** complete, the cycloaddition reaction was next considered. Based on previous work in the group, conditions were proposed, and aldehyde **53** was dissolved in PhMe alongside hydroxylamine hydrochloride, $NH_2OH.HCl$. $^{i}Pr_2NEt$ was added to de-salt hydroxylamine, though more equivalents were added than was initially planned. The reaction was heated to reflux for 2 h. NMR analysis of the unpurified reaction mixture, unfortunately, did not indicate the formation of cycloadduct **54**, though it does not show starting material, either. The aldehyde peak is absent, but a broad singlet is observed at the more downfield chemical shift of 11.2 ppm. Whilst proton peaks are observed in the aromatic region, these are dwarfed by the other peaks observed, and alkene peaks were barely distinguishable from the noise. The identity of the product from this reaction was not able to be determined.

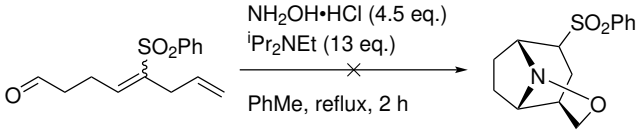

53 **54**

*Scheme 2.19: Initial attempt to syntesise **54** through use of condensation-cyclisation-cycloaddition cascade chemistry*

This route posed a variety of difficulties: purification of **30** following ozonolysis was difficult and subsequently low yielding; the HWE reaction too was disappointingly low yielding; initial attempts at cycloaddition proved fruitless. Therefore, alternative routes were considered at this time.

2.3.2 Alkylation with isobutyronitrile 61, and MeCN

Next, an alternative route to a similar target was considered. In this case, it was suggested that the presence of a gem-dimethyl would mimic useful substitution at this position, such as the oxindole ring of *Alstonia* alkaloids which will be discussed in Chapter 3. The retrosynthesis detailing the proposed route is given in Scheme 2.20.

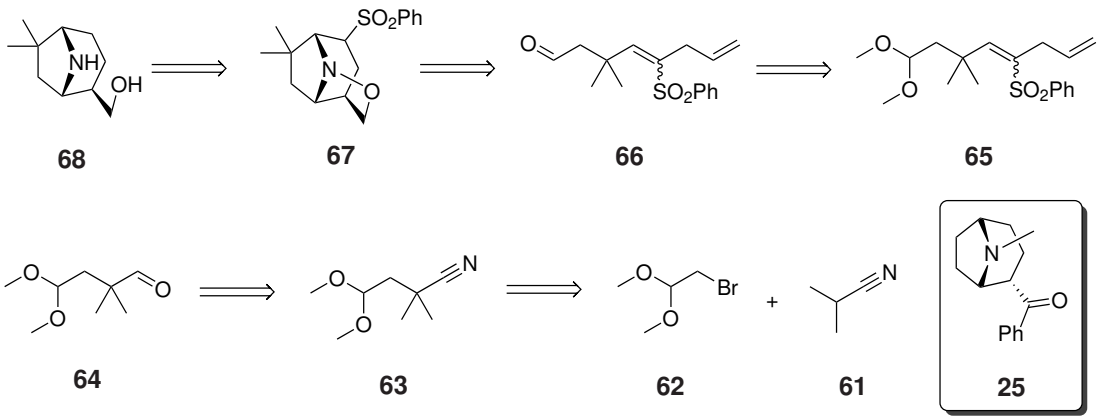

*Scheme 2.20: Retrosynthesis towards modified ferrugine core **68***

The first step of this route is an alkylation reaction between acetal **62** and nitrile **61**. Nitrile **63** has been synthesised in literature,[92] though not by the method used here. This alkylation was performed using LDA, synthesised *in situ* from *n*-BuLi, and was successful in 56% yield, as can be seen in Scheme 2.21.

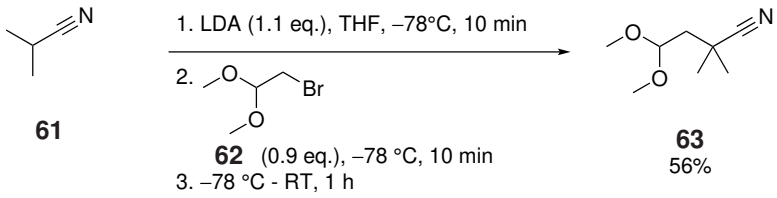

*Scheme 2.21: Alkylation reaction with LDA to afford compound **63***

Next, nitrile **63** was to be reduced to the desired aldehyde, **64**. This reaction was reported in literature,[92] performed using 1.1 M DIBAL-H in cyclohexanes. These conditions were replicated, and a yield of 44% was obtained, though some starting material remained (9% of the residue obtained from the column), co-eluting with **64**. Reduction in the polarity of the solvent system used for purification still did not enable suitable separation. Next, the equivalents of DIBAL-H used were increased from 1.1 (as in the literature) to 1.3 eq. Combined with the less polar conditions for purification, this led to the isolation of clean samples of **64**,

though in a lower yield of 33%. This brief optimisation is summarised in Table 2.1.

*Table 2.1: Results of varied conditions on yield and purity of samples of **64** following purification*

Entry	Eq. DIBAL-H	Yield of 64 /%	Amount of 63 present in NMR spectrum /%
1	1.1	44	9
2	1.3	33	-

The optimal conditions for this conversion appear to be those shown in Table 2.1 Entry 2, prioritising clean product over marginally improved yields. The next step is an HWE reaction and given the difficulties seen in section 2.3.1 when the impure product was used, 1.3 equivalents of DIBAL-H were used to ensure clean **64** was taken forward. The selected conditions are shown in Scheme 2.22.

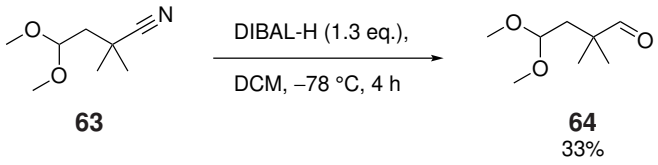

63 **64** 33%

*Scheme 2.22: Optimal conditions selected for the DIBAL-H reduction of **63** to afford compound **64***

Next, the HWE reaction could be considered. Given that the conditions used in the HWE reaction described in section 2.3.1 with structurally similar compound **31** were suitable for this conversion, the conditions were replicated in this reaction. Again, NaOEt was used as the base, and was prepared directly prior to use. The reaction was attempted several times.

During the first attempt, the majority of fractions following column chromatography were shown to contain aldehyde starting material **64** and phosphonate **58**. One 5 mg sample analysed by NMR spectroscopy appeared to contain a mixture of **65** and starting material **64** in a 1:0.13 ratio **65**:**64**, based on the presence of an additional peak in the alkene region, but this would still only mean a yield of less than 4% of the desired product **65**. The second attempt returned only starting materials. The reaction conditions are shown in Scheme 2.23.

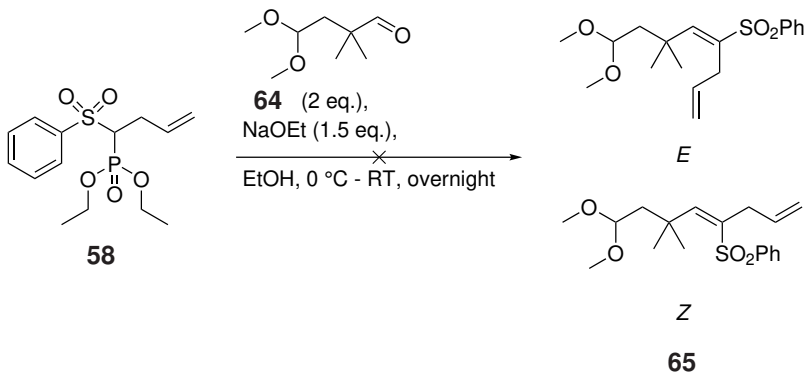

*Scheme 2.23: Unsuccessful HWE reaction between **58** and **64***

Given that, in the absence of the gem-dimethyl groups, this HWE reaction was successful, it is believed that this HWE reaction is stunted by hindrance caused by these additional groups. Therefore, it was assumed that this route was not viable with these methyl groups present. However, it was considered that this method could still offer an alternative route to aldehyde **31**, which may be more suitable than that proposed in section 2.3.1. This is briefly summarised in the modified retrosynthetic analysis given in Scheme 2.24.

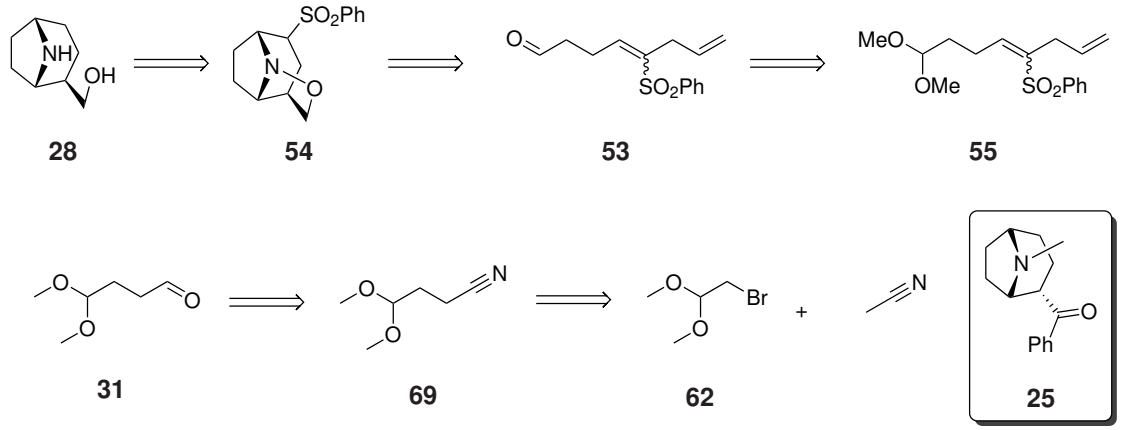

*Scheme 2.24: Retrosynthesis proposing new route towards core structure **28***

Therefore, the alkylation was repeated, using the previous conditions, but with MeCN as the alkylating agent as opposed to **61**, as shown in Scheme 2.25. Disappointingly, this was successful in yields of up to just 10%, with co-elution with starting materials difficult to eliminate, with a ratio of 1:0.45 **69**:**62**.

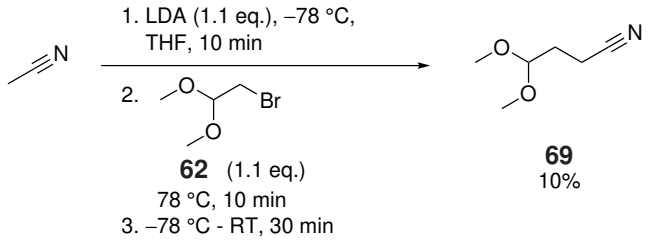

*Scheme 2.25: Alkylation of **62** with MeCN*

Nevertheless, DIBAL-H reduction of **69** was attempted, again using the optimal conditions determined for the structurally similar reduction of **63** (Scheme 2.22). The result, in this case, is given in Scheme 2.26.

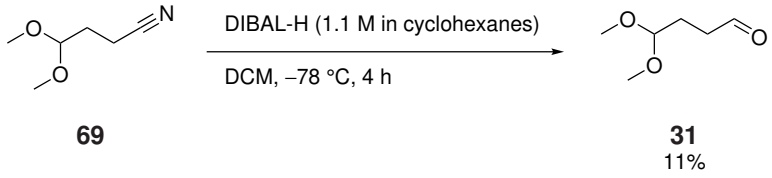

*Scheme 2.26: Reduction of **69** with DIBAL*

With just 11% yield, this clearly wasn't an improvement on the previous route towards **31** described in section 2.3.1. Therefore, a completely different route to cascade precursor **53** was proposed.

2.3.3 Oxidation of substituted alkene 72

The next suggested route is given by the retrosynthetic analysis shown in Scheme 2.27. The aldehyde target, cycloaddition precursor **53**, is the same as was proposed in the routes given in Scheme 2.12 and Scheme 2.24. However, instead of acetal deprotection unveiling the desired aldehyde prior to commencing the cascade reaction, it is proposed that the aldehyde would instead be formed by selective oxidation of one of three alkenes present in the molecule.[93–96]

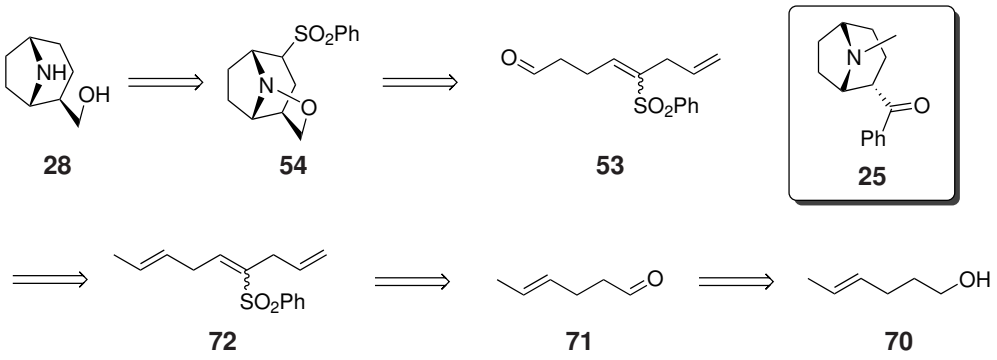

*Scheme 2.27: Newly proposed route towards the synthesis of the core structure of **25***

As in previous routes, the HWE reaction requires an aldehyde to react with phosphonate **58**. The aldehyde required, **71**, could be synthesised by oxidation of alcohol **70**. This has been shown in literature, with one procedure suggesting the use of Swern oxidation method.[97] This reaction was performed with consistent success, with yields of up to 59%, as is shown in Scheme 2.28.

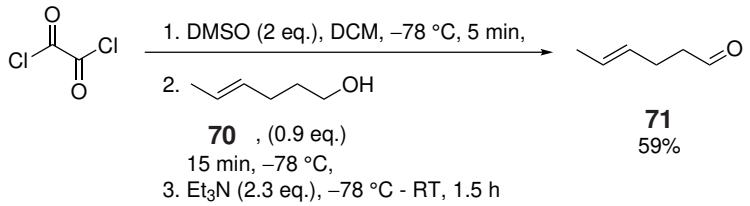

*Scheme 2.28: Swern oxidation of **70***

With aldehyde **71** in hand, the next step proposed was another HWE reaction. Once again, this would use phosphonate **58**, installing the vinyl sulfone. Conditions from previous HWE reactions were replicated, once again synthesising NaOEt prior to the reaction. The phosphonate **58** and aldehyde **71** were premixed, and the base was added dropwise at 0 ℃, as is shown in Scheme 2.29. A yield of 83% was obtained for the conversion, with an 81:19 ratio of geometrical isomers, where the major isomer was suggested to be the *E* isomer, based on the assignment of the alkene peaks in the NMR spectrum. Again, this was based on the fact that the major alkene peak (0.81H) came at a higher chemical shift of 6.99 ppm, compared to that of the minor (0.19H) at 6.02 ppm. The *E* isomer of this molecule is predicted to have a higher chemical shift value for the alkene peak, due to differences in the shielding of these atoms in each isomer.

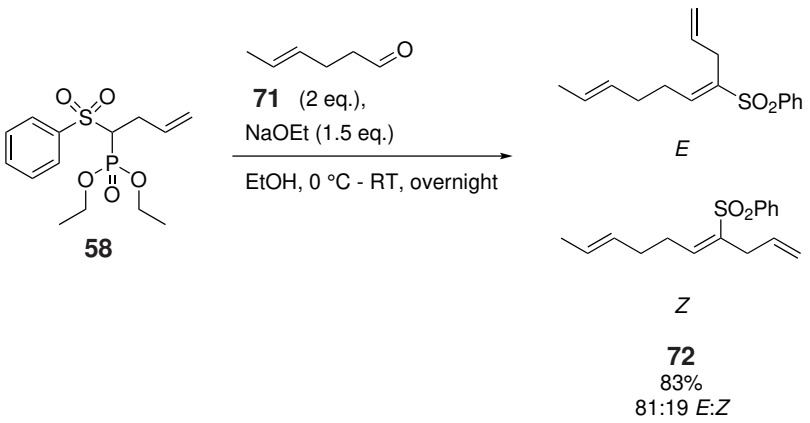

*Scheme 2.29: HWE reaction of aldehyde **71** with phosphonate **58**, affording an E/Z mixture of **72***

As the HWE reaction had appeared successful, the next step would be to selectively oxidise one of the alkenes to afford the desired aldehyde, **53**. With three alkenes present, this does at first appear a difficult task. The alkene of the vinyl sulfone is required in the cyclisation step, whilst the terminal alkene is required to act as the internal dipolarophile, and therefore both must remain intact after the conversion. The final alkene, however, must be converted to an aldehyde.

Each of the three alkenes is differently substituted, and as such they differ in their electron density at the π-bond. The terminal alkene is monosubstituted. Its electron density is impacted only by a relatively small positive inductive effect from its single alkyl substituent. The vinyl sulfone alkene is trisubstituted. Whilst increased substitution often increases the rate of oxidation, due to the increased positive inductive effect caused by multiple substituents, in this case, there is also a mesomeric effect in place. The sulfone group will withdraw electron density through resonance, making this alkene electron-poor, and therefore less attractive to oxidation than the terminal alkene. However, the target alkene should be the most electron-rich alkene in the molecule, due to greater positive inductive effects from the additional alkyl group combined with the absence of any negative mesomeric effects. It is therefore hoped that this property would allow this alkene to be distinguishable from the other alkenes, in line with known examples. Though there is no literature precedent for this exact conversion, it is well established that oxidation will take place preferentially at more substituted alkenes,[93–95] and that alkenes of vinyl sulfones are not oxidised in preference to alkenes present.[96]

The Lemieux–Johnson oxidation method was proposed, wherein an aldehyde will undergo oxidative cleavage, affording two aldehyde or ketone moieties. In this case, the proposed products would be the

desired aldehyde, **53**, and acetaldehyde.

The Lemieux-Johnson method involves two steps: dihydroxylation with osmium tetroxide, OsO_4, followed by cleavage of the diol formed with sodium periodate ($NaIO_4$), in a step known as the Malaprade reaction. These steps are shown in Scheme 2.30. It was hoped that being the most electron-rich alkene in the molecule would make the target alkene more reactive to oxidation in this reaction.

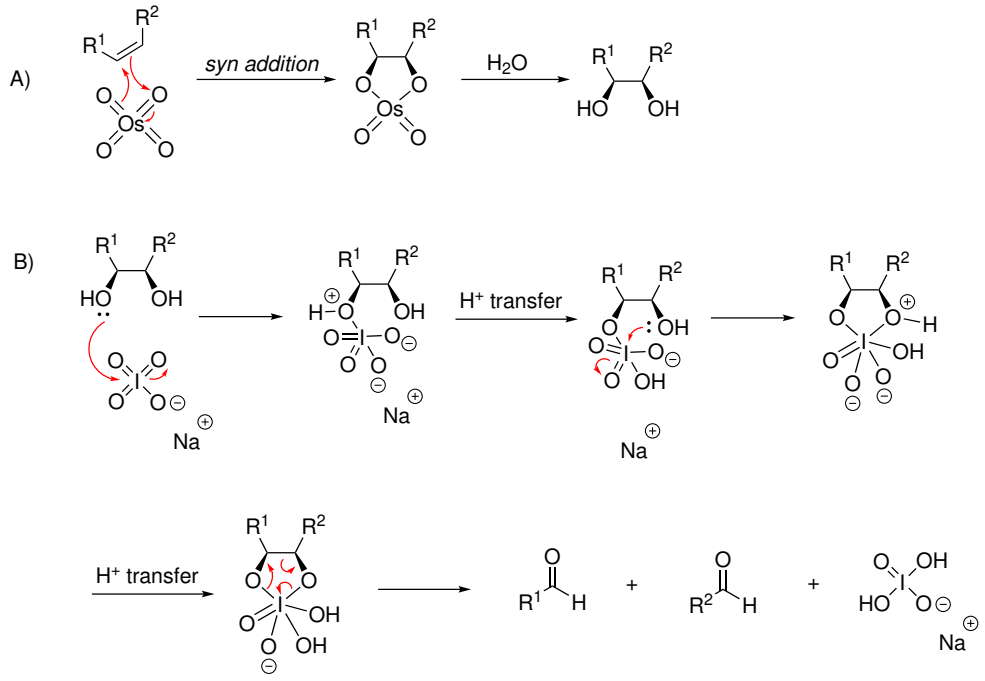

Scheme 2.30: General mechanism for the Lemieux-Johnson method: A) Dihydroxylation with osmium tetroxide B) Malaprade cleavage with periodate

Therefore, the reaction was attempted, as is summarised in Scheme 2.31. OsO_4 was added to a solution of **72**, along with *N*-methyl-morpholine-*N*-oxide (NMO). NMO is used to regenerate OsO_4 following the reaction, re-oxidising the Os(VI) formed back to Os(VIII). Its presence means that catalytic OsO_4 (in this case, 0.01 equivalents) can be used, which is beneficial due to both the toxicity and high cost of OsO_4. After the diol had been given time to form, a workup was performed with sodium sulfite, reducing the remaining osmium. The addition of $NaIO_4$ followed, initiating the Malaprade step.

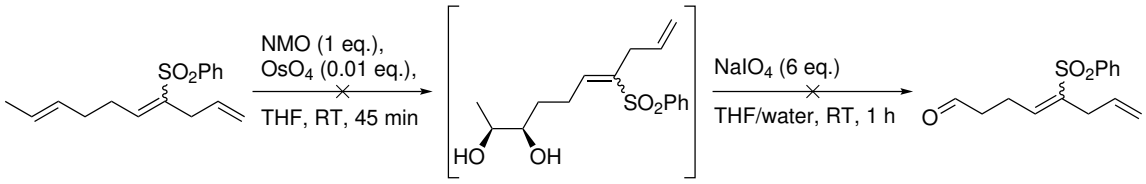

72 **73** **53**

*Scheme 2.31: Lemieux-Johnson reaction of **72***

Following a messy crude NMR spectrum, LCMS analysis was turned to in order to glean insight into the outcome of the reaction. There were several peaks present in the LCMS spectrum, with the major peaks corresponding to the sodium adduct of the starting material, **72**. Figure 2.6 shows the LCMS trace in red, and the blue line indicates the presence of mass ion 299.38, which corresponds to the MNa^+ of starting material **72**.

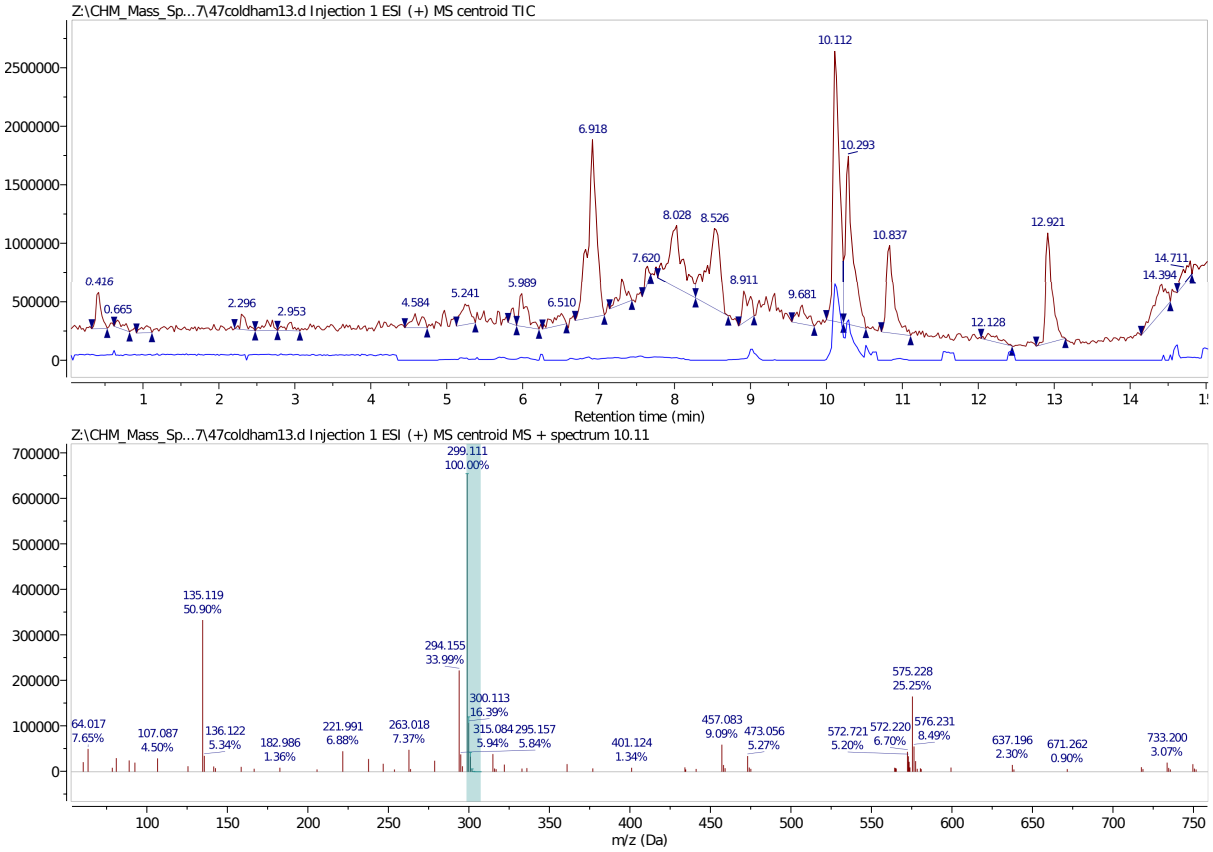

*Figure 2.6: LCMS data for the Lemieux-Johnson step. Above, the total LCMS trace (red) with trace corresponding to MNa^+ of **72** in blue, with the mass spectrum of the overall sample shown below*

The peaks at 10.1 and 10.3 min likely correspond to both geometrical isomers of **72**. As can be seen in the mass spectrum in Figure 2.6, the predominant mass ion present in the whole sample is that of the

sodium adduct of **72**, with m/z = 299.11. Whilst this indicates that the major component of the sample is starting material, clearly other compounds are present.

At the time the work was undertaken, LCMS analysis was performed by technical staff, and due to an apparent mix-up it was reported that there appeared to be none of the desired product **53** present. Since this time, MestReNova software was made available to researchers, meaning independent analysis of these old samples was now possible. Upon review at the time of writing, it appears that one of the minor peaks in the spectrum (at 8.03 min) may correspond to the mass ion for the sodium adduct of **53**, MNa^+ = 287.07. MestReNova's "molecule match" function did not identify this product as being present, which may have led to the initial conclusions being drawn, but the correct mass is indeed present. Figure 2.7 shows the peak at 8.03 min, and the corresponding mass spectrum observed at this time.

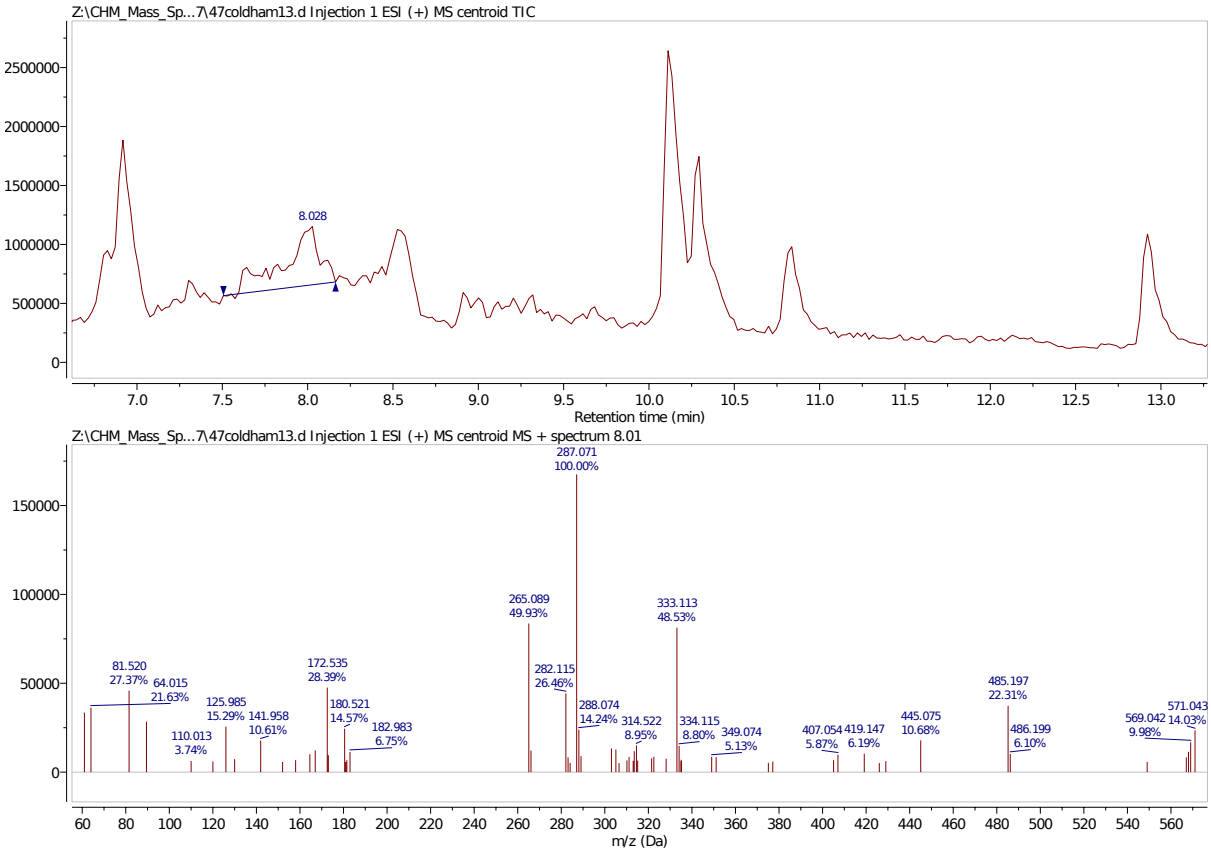

Figure 2.7: LCMS trace and mass spectrum corresponding to the peak at 8.03 min

The sample was unclean, but it was a crude sample which had not yet been subject to further purification, and it is unknown whether this product could have been isolated cleanly. This is an unfortunate oversight - the previous steps proffered reasonably good yields, especially compared to the previous route

to **53**, summarised in Scheme 2.12. Though the sample does appear to be composed predominantly of starting material **72**, it would have been good to attempt to isolate product **53**. Optimisation could have been performed if yield appeared to be low, in an attempt to convert the remaining starting material to product.

At this time, however, the presumed lack of success (combined with a reluctance to unnecessarily repeat reactions using toxic chemicals when positive results appeared unlikely) meant that other routes were pursued. This is a shame, as there is the possibility that, upon later reflection, this route may have offered an alternative method to synthesise the desired cascade precursor.

2.3.4 Use of succinaldehyde 74

The next route, detailed in Scheme 2.32, would begin with the synthesis of succinaldehyde, **74**, still targeting aldehyde **53** as the cascade precursor.

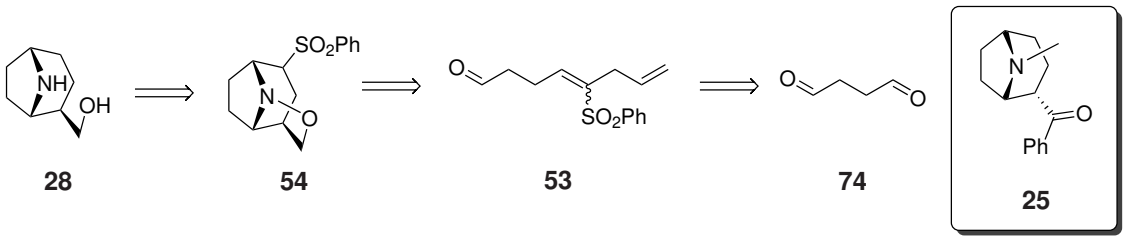

*Scheme 2.32: Retrosynthetic analysis of new route towards the synthesis of the core structure of **25***

Again, this route would utilise an HWE reaction with phosphonate **58**, but this time with a dialdehyde, **74**. Though there is a risk of di-addition in this case, it would mean that the aldehyde was already installed, therefore requiring no further conversions to reach the cascade precursor, as in previous examples.

To begin, succinaldehyde **74** required synthesis. As detailed in literature,[98] this could be done by hydrolysing dimethoxytetrahydrofuran **75**, simply stirring the heterocycle in HCl overnight.

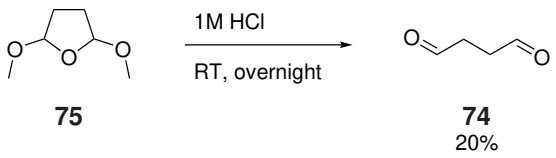

*Scheme 2.33: Synthesis of dialdehyde **74** by hydrolysis of **75***

Difficulties arose surrounding the purification of the dialdehyde **74**. Regardless of how long **75** was left

to stir in the acid, it appeared that starting material was always present in the crude material. Distillation was attempted to purify the mixture, but it appeared that the compounds had similar boiling points, and a mixture was usually still observed following distillation. It was decided that the mixture would be taken onto the next step. However, it was important to estimate the amount of **74** present in the mixture. If the whole mixture was simply assumed to be aldehyde, then the quantity of **58** used would be larger than necessary. This excess would increase the likelihood of di-addition, given that **74** is a dialdehyde. This was not a concern in previous HWE reactions, as there was only one aldehyde present in the starting material, but for this particular reaction, it was especially important for phosphonate **58** to be the limiting reagent. Thus, ^{1}H NMR spectroscopy was used to determine the ratio of **74** and **75** present in the mixtures. This was used to obtain a ratio of the masses of these compounds, and in turn the mass of each present in the sample could be determined. With this taken into account, yields for the synthesis of **74** were disappointingly low, often below 20%, but the HWE was nevertheless attempted with this material.

In previous HWE reactions, it had also not been as important to consider the order of addition of the compounds. However, once again the presence of the dialdehyde made this essential - if aldehyde were added to the deprotonated phosphonate, the likelihood of di-addition would be increased, as phosphonate **58** would initially be in a local excess during addition.

In earlier iterations of the reaction, di-addition was observed, but the above factors had not yet been taken into consideration. In one early example, the amount of aldehyde was not properly calculated, incorrectly assuming complete conversion. In actuality, however, conversion was not complete, and therefore instead of using the intended 1.4 equivalents of aldehyde, just 0.23 equivalents were actually used, thereby creating a large excess of **58**. Additionally, aldehyde **74** was added directly to the carbanion formed from the addition of NaH to **58**, as opposed to the other way around, serving to create an initially even larger excess. The result was that di-addition product **76** was isolated in 5% yield, alongside unreacted phosphonate **58**, as seen in Scheme 2.34. The desired HWE product **53** was not isolated in this instance.

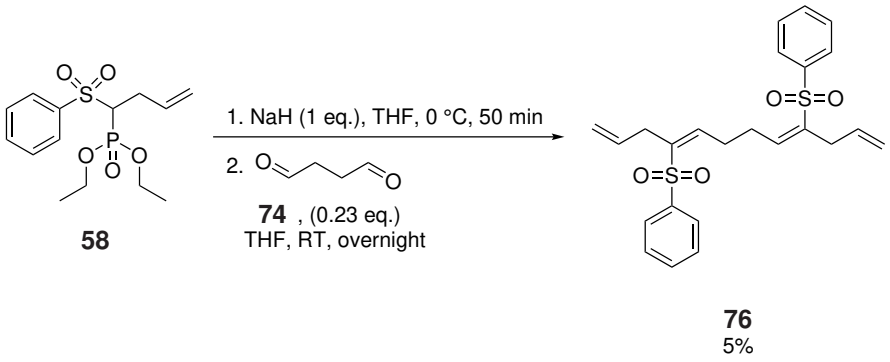

*Scheme 2.34: Attempted HWE reaction between dialdehyde **74** and phosphonate **58** under incorrect conditions, leading to di-addition product **76***

Therefore, in later attempts, the true amount of aldehyde was calculated. Also, base was first added to **58** to generate the phosphonate carbanion **77** as shown in Scheme 2.35, Reaction 1, and this mixture was then added slowly to a solution of **74** in THF, as shown in Scheme 2.35, Reaction 2. The HWE appeared to proceed, though with low yield, with no evidence of di-addition.

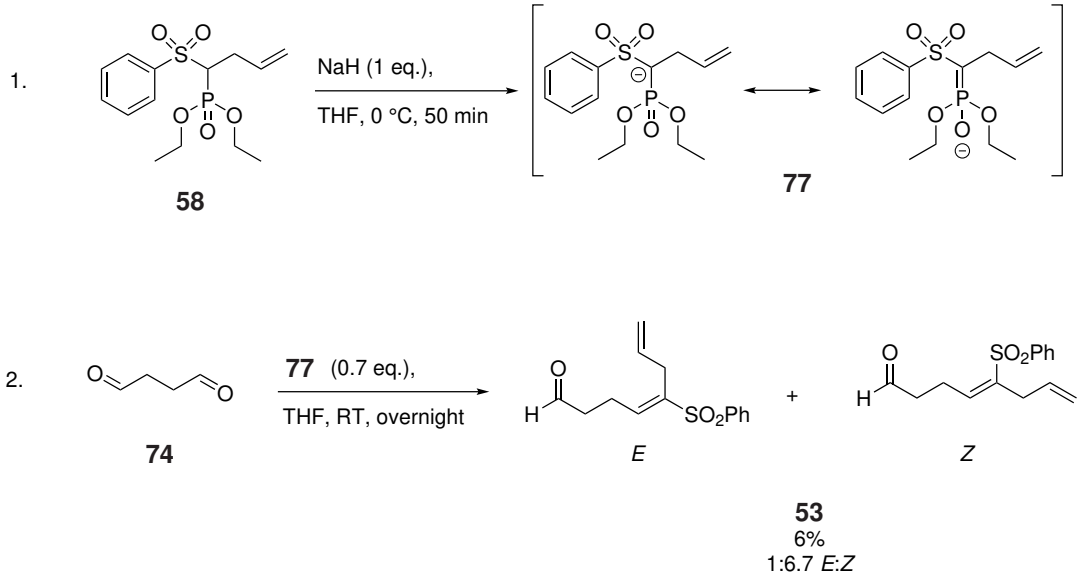

*Scheme 2.35: HWE reaction between dialdehyde **74** and phosphonate **58***

The yields here were low, so it was considered at this time whether a Wittig reaction could be used as opposed to the previously proposed HWE. Several examples of Wittig reactions using succinaldehyde have been reported in the literature, though all make use of phosphoranes as opposed to deprotonation of the Wittig salt to form a ylide.[99] Employing a Wittig reaction as opposed to the originally proposed HWE would mean that the vinyl sulfone would not be installed, and additionally this reaction would require the synthesis

of a Wittig salt, **78**. Several literature procedures were reported for the synthesis of **78**, and though the reaction was attempted in various solvents,[100] MeCN proffered the greatest yields for this conversion.[101] The reaction is summarised in Scheme 2.36.

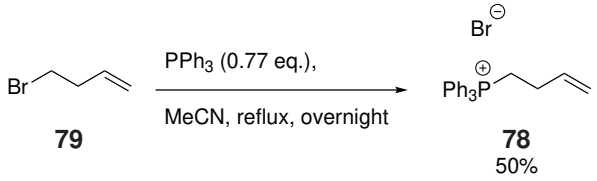

Scheme 2.36: Wittig salt synthesis

With Wittig salt **78** in hand, the reaction itself could be attempted. The reaction would again utilise succinaldehyde **74**, which was synthesised as above. The Wittig reaction was attempted as shown in Scheme 2.37.

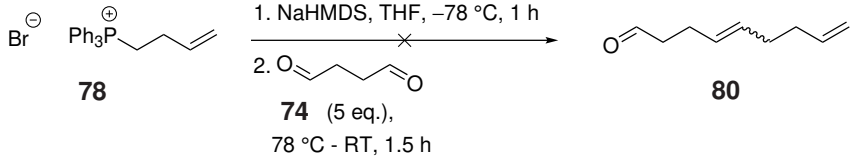

*Scheme 2.37: Wittig reaction with Wittig salt **78** and dialdehyde **74***

Unfortunately, the reaction was unsuccessful. Due to the time limitations of the project, it could not be reattempted, but further work was conducted on the HWE alternative.

Though low yields were obtained following the HWE reaction, it did lead to the synthesis of compound **53**, and this could therefore be taken forward in order to attempt the cascade reaction. The conditions used were based upon those used previously within the group, wherein aldehyde **53** was mixed with hydroxylamine hydrochloride and $^{i}Pr_2NEt$ in PhMe, and the mixture was heated to 60 °C until TLC indicated full conversion of the starting material.

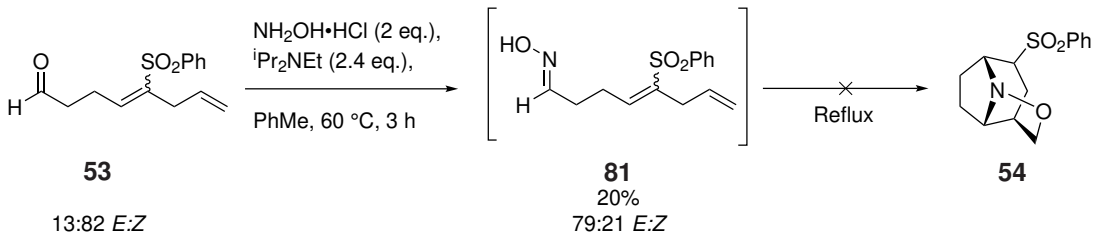

*Scheme 2.38: Attempted cascade reaction of **53**, where intermediate oxime **81** was isolated as opposed to the desired cycloadduct **54***

As can be seen in Scheme 2.38, though oxime **81** was formed when the reaction mixture was heated to 60 ℃, the cascade chemistry did not continue, with none of the cycloadduct **54** observed. It was considered that higher temperatures may encourage the cascade to proceed, so the oxime **81** was heated to reflux and stirred for 3.5 h. The TLC indicated that no further conversion had occurred at this time, and starting material **81** remained unchanged as determined by NMR analysis. It is worth noting here that the *E:Z* ratio of oxime **81** was determined to be 79:21, with the *E* isomer being the major product, again based on the fact that the *E* isomer will have a higher chemical shift at the vinyl proton. This is in contrast to the reported *E:Z* ratio of starting material (13:87), **53**, where *Z* was the major isomer. The oxime **81** was also heated to reflux in xylene, but even at this higher temperature, there still appeared to be no conversion.

In all of the examples from Padwa and co-workers, the cascade chemistry combined two steps - conjugate addition followed by cycloaddition. In these examples, as discussed in Section 2.1.5, an external 4-π component, 2,3-diphenylsulfonyl-1,3-butadiene, is used. In the work by Padwa, both steps involve addition at a vinyl sulfone. It is assumed that it is the cyclisation step of the Coldham cascade which is not working, as research suggests this is the reaction which follows condensation and oxime formation.

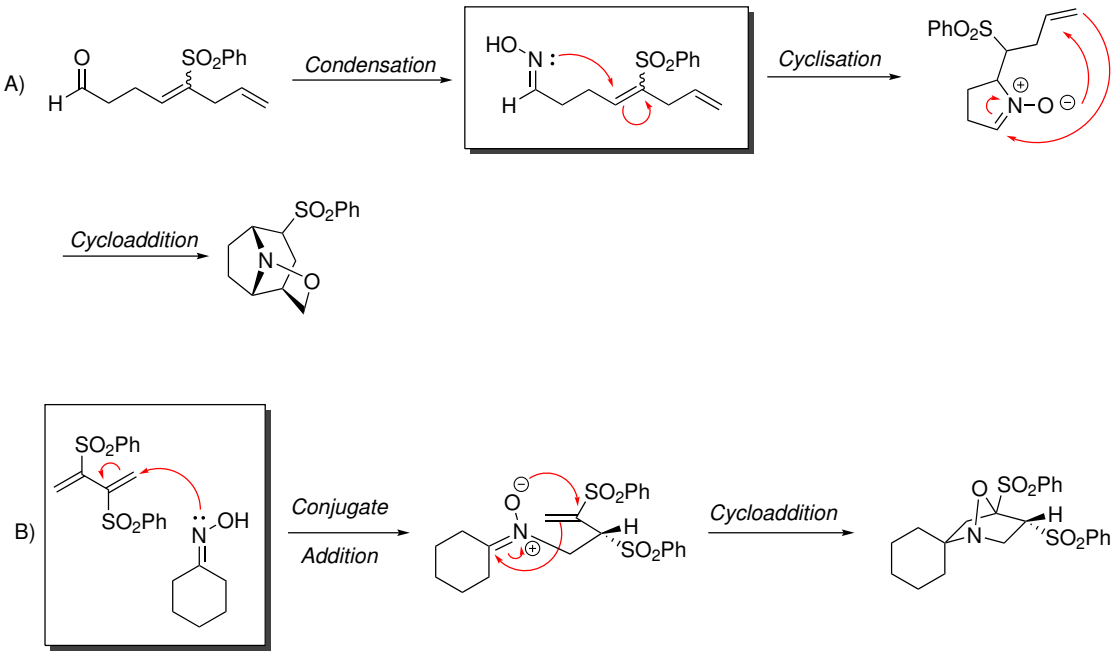

Scheme 2.39: Comparison of A) the cascade chemistry proposed here with B) the cascade chemistry from Padwa's group

There are therefore several key differences between these two cascade routes which could be preventing the reaction from proceeding. Therefore, comparing the cyclisation step of this work

(Scheme 2.39, Reaction A, with cyclisation step highlighted in box) with a generic example of Padwa's conjugate addition step (Scheme 2.39, Reaction B, with conjugate addition step highlighted in box):

1. The initial cyclisation is intramolecular, as opposed to intermolecular as in the conjugate addition steps in work by Padwa.

2. The alkene in this work is internal, as opposed to the terminal alkene used in Padwa's works.

3. The anion formed following conjugate addition in Padwa's work is allylic, whereas the anion formed in this work would not have any allylic character.

These facts lead to questions about the steric and electronic implications of the reaction proposed here. In intramolecular reactions, the reacting components are tethered together, and the conformation of the molecule may result in the two reacting components being brought closer together in space. When reactants are positioned in a conformation which allows easy access to a transition state, this is often known as a "near attack conformation", or NAC.[102] This conformation leads to large rate constants for the reaction, thereby increasing the rate of reaction compared to intermolecular reactions, where collisions of reactants are less likely. This may not be the case if steric hindrance makes such a conformation unfavourable, however. Here, it may be the case that the reaction is actually impeded by the more stable conformation holding reacting components apart from one another, to avoid steric clashes with the large phenyl group and with the more substituted (internal) alkene. The internal alkene is likely more difficult to access, thus making the reaction slower. The reduced entropic cost of an intra- rather than inter-molecular reaction does generally increase the rate of reaction; this is especially relevant in ring-forming reactions, when the entropy will naturally decrease upon ring formation, and there is an enthalpic cost due to strain. A ring is formed in the reaction proposed in this work, but this is not the case in Padwa's work, and therefore the energy barrier to reaction may be lower. These energetic factors may also have some influence on the outcome of this reaction. What is possibly even more significant is that in the work by Padwa, the anion formed following conjugate addition is allylic, thereby making it more stable than the anion formed in the work proposed here. This means that electronically, there is less drive for this reaction to proceed.

A retro-Cope reaction was considered at this time, as an alternative route to the nitrone.[103] Similar work was shown by Grigg in 1990.[104] In Grigg's paper, however, all of the examples of this chemistry given used starting materials with a quaternary centre next to the oxime, thereby preventing enamine formation. With

the absence of a quaternary centre in oxime **81** enabling enamine formation, it was thought that this route would likely be unsuccessful, too. Therefore, taking into account the time restraints of the project at this time, this route was not attempted.

Time constraints of the project meant that further work on this route was not pursued at this time, but future work may be considered. This is discussed in Section 2.4.

2.3.5 Towards ferrugine 25 utilising epoxide opening methods

Moving away from the idea of utilising vinyl sulfones in the synthesis of a ferrugine-like core, a new route is proposed, as shown in Scheme 2.40. The route suggests an alkylation reaction,[105] opening epoxide **82** with MeCN. This would install an alcohol group, along with nitrile functionality. The use of **82** means that an internal dipolarophile is preinstalled. The alcohol can be converted to a suitable leaving group, and Scheme 2.40 suggests the use of a tosyl group for this purpose. With a leaving group in place, it was proposed that the nitrile group could be reduced to an aldehyde *via* DIBAL-H reduction, affording cycloaddition precursor **26**. Cascade chemistry could then commence.

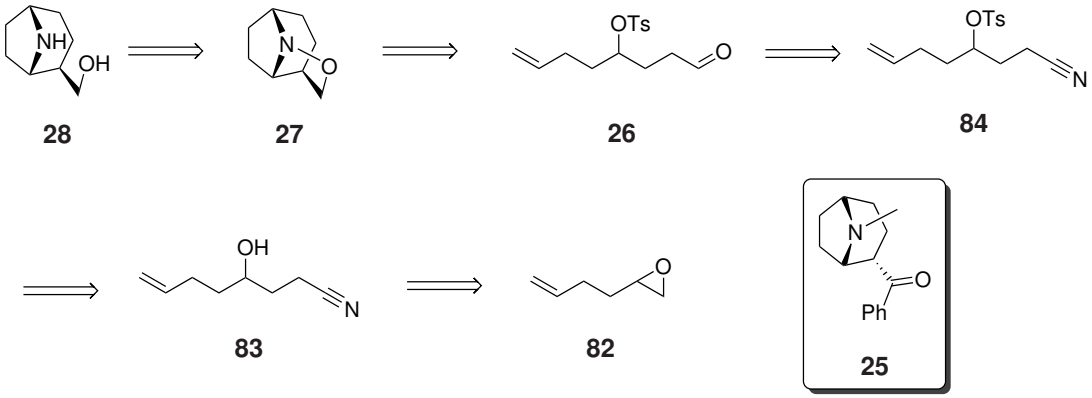

*Scheme 2.40: Retrosynthesis proposing new route to afford the desired cycloadduct **28***

The first step involves opening epoxide **82** with MeCN, thereby affording alcohol **83**. Applying conditions based on those seen in the literature,[105] the reaction was successful in 83% yield, as summarised in Scheme 2.41. This yield is calculated based on the epoxide acting as the limiting reagent, with an excess of acetonitrile used. This was done in order to avoid any anions of acetonitrile remaining unreacted, as there was the possibility of further deprotonation of the product, **83**, which may have led to double alkylation.

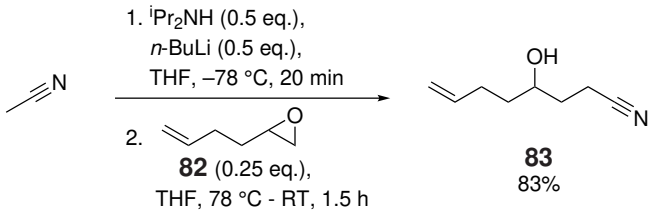

*Scheme 2.41: Epoxide opening of **82** with MeCN to afford **83***

The next step required the formation of a suitable leaving group, and in this case, a tosylate was proposed for this purpose. Tosylation was performed using TsCl, DMAP and Et_3N, and was successful in 56% yield, as summarised in Scheme 2.42.

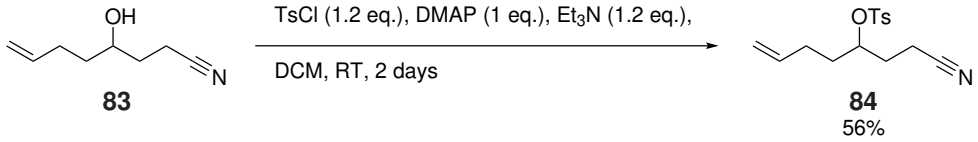

*Scheme 2.42: Tosylation of **83**, affording **84***

Next, it was proposed that the nitrile could be converted to an aldehyde, **26**, which would be able to act as the cascade precursor in this route. This conversion could be performed using reducing agent DIBAL-H. This was attempted but unfortunately proved unsuccessful. Though equivalencies of DIBAL-H were varied, and different bottles of DIBAL-H in different solvents were used (in case one of the older bottles was no longer active), the starting material was recovered, with no reaction observed in each instance. This is shown in Scheme 2.43.

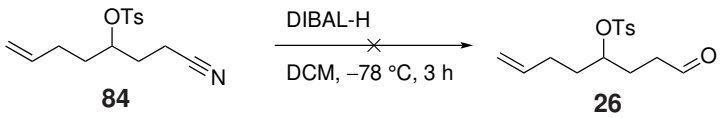

*Scheme 2.43: Attempted DIBAL-H reduction of **84** to afford cascade precursor **26***

Work on this chemistry was continued by master's student Cox,[87] whose work under my supervision towards this goal is discussed below, initially making attempts to optimise this DIBAL-H reduction reaction.

Work by Richard Cox

The aim of this master's project aligned closely with the aims discussed within Chapter 2, highlighted in Section 2.2. Therefore, the work conducted within this master's project is discussed herein.

The steps completed above were first repeated in this study, with similar success, as highlighted in Scheme 2.44.

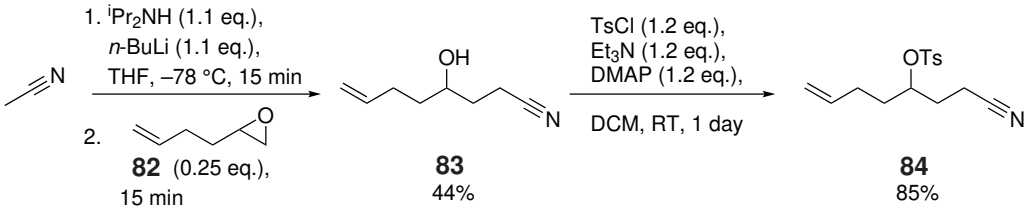

Scheme 2.44: Epoxide opening and subsequent tosylation as performed in masters' project by Cox

However, when attention was turned to the DIBAL-H reduction, there were still issues at this step. Initial attempts utilised a different workup, where a 15% LiOH solution was used to remove $Al(OH)_3$ salts formed after quenching, as opposed to the Rochelle salt method used in 2.3.4. This is a necessary step to remove emulsions formed by $Al(OH)_3$ which can make workup and purification more complex, but ultimately the reagent choice for this step will have no impact on the reaction itself, which will have already occurred (or not, as the case may be) and the DIBAL-H reagent will have been quenched. With none of the desired aldehyde **26** isolated, the reaction was repeated, this time using 2 equivalents of DIBAL-H, with the same outcome. This is not surprising, as the procedure was similar to the one used above which was also unsuccessful.

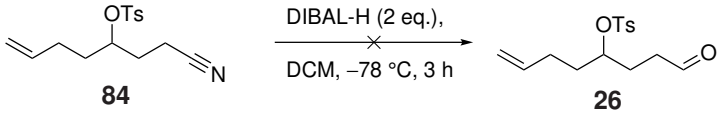

*Scheme 2.45: Attempted DIBAL-H reduction of **84** to afford cascade precursor **26***

A literature search at this time proposed an alternative reduction method,[106] wherein nitriles are reduced using sodium hydride and $ZnCl_2$. Though the article reported good yields for a range of nitriles, including α-quaternary nitriles, two attempts of this procedure yielded none of the desired product **26**.

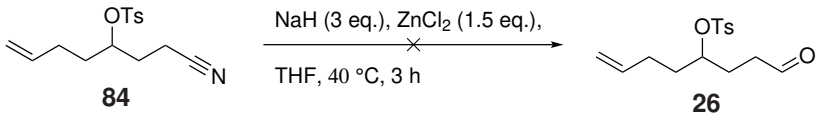

*Scheme 2.46: Attempted reduction of **84** with NaH/Zn to afford cascade precursor **26***

Alongside this work, it was also considered that the epoxide could be alkylated with isobutyronitrile **61**, once again introducing a gem-dimethyl group which would act to mimic the substitution of the oxindole group present in alkaloids of the *Alstonia* genus.

Epoxide ring-opening had been demonstrated in work by Larchevêque and Debal,[107] where epoxides were opened at the primary centre using a variety of nitriles, including isobutyronitrile **61**. The paper reports that different products may be isolated, depending on the workup used. It is possible to perform alkylation as was shown above with MeCN (as in Scheme 2.41 and Scheme 2.44), wherein compound **85** would be formed. This compound is formed when the reaction is worked up with a strong acid such as HCl. Alternatively, if workup is performed using a weaker acid like MeOH, a lactone product (**86**) is instead formed. The explanation for this is summarised in Scheme 2.47. A strong acid will protonate at site 1, which promotes ring opening of the carboximidate intermediate **87**, thereby forming **85**. Alternatively, a weaker acid such as MeOH protonates at site 2, promoting hydrolysis of the imino-ether to form the lactone **86**.

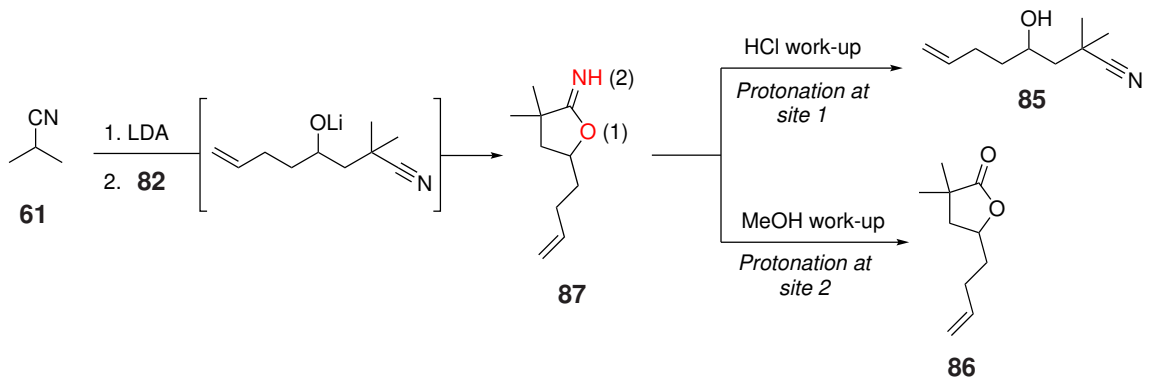

*Scheme 2.47: Different products of alkylation reaction based on workup conditions, promoting protonation at different sites in intermediate **87***

When this was investigated within this study, workup with HCl led to the formation of a range of side-products, leading to poor yields of around 30%. Alternatively, when MeOH was used in the workup, lactone **86** was formed in yields exceeding 90%.

First, compound **85** was taken, and tosylation was attempted on this compound, under a variety of

conditions (using Et_3N, pyridine and NaH as the base, and using both stoichiometric and catalytic DMAP) but unfortunately, none yielded the desired product. It was considered that this may be a steric issue, so mesylation was also attempted, hoping that the smaller size of this group may enable reaction. Unfortunately this method, too, proved unsuccessful. Therefore, it was considered that the lactol **86** produced by workup with MeOH could be used advantageously.

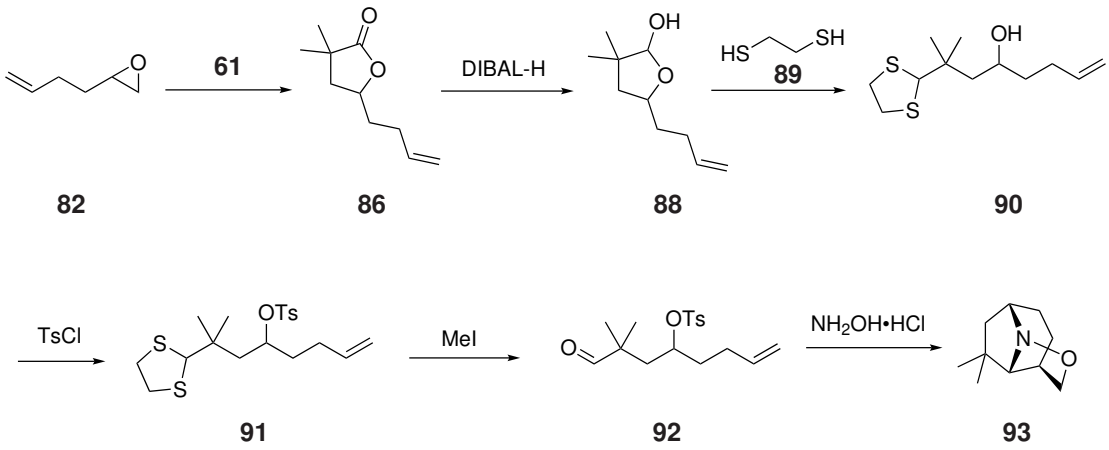

*Scheme 2.48: Alternative method, utilising the formation of lactone **86** by workup with weak acid*

The new route, proposed in Scheme 2.48, would first see lactone **86** converted to lactol **88** by DIBAL-H reduction. It was then proposed that 1,2-ethandithiol **89** could be used as a protecting group.[108] Alcohol **90** could then be tosylated and the dithiane deprotected, affording a cascade precursor, **92**.

DIBAL reduction was initially assumed to be a success, based on the presence of two shifts in the ^{1}H NMR spectrum, believed to correspond to the HC–O. The sample believed to contain lactol **88** was then taken crude onto the next step. Disappointingly, however, the subsequent dithiane formation appeared unsuccessful. At this time, closer inspection of analytical data suggested that carboximidate **87** had not been successfully hydrolysed to form lactone **86**. LCMS analysis showed that a compound with a mass of 322 gmol^{-1} was present, suggesting that dimerisation to afford compound **94** may have instead occurred.

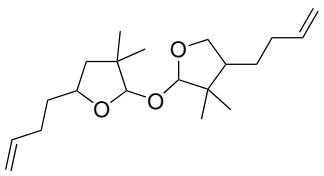

94

*Figure 2.8: Dimer **94**, whose presence was identified by LCMS following attempted tosylation*

Instead of pursuing these routes, previous ideas were reconsidered. Once again, MeCN was used to perform the epoxide opening of **82**, affording compound **83**. However, instead of tosylating as in previous work, it was instead considered that the alcohol could be converted to a bromide. This, too, is a suitable leaving group. Therefore, this reaction was performed, using NBS and PPh_3, successfully synthesising bromide **95** in 40% yield. Next, DIBAL-H reduction was again attempted, and in this case, proved successful. Aldehyde **52**, a potential cascade precursor, was synthesised in 32% yield. Both steps are summarised in Figure 2.9.

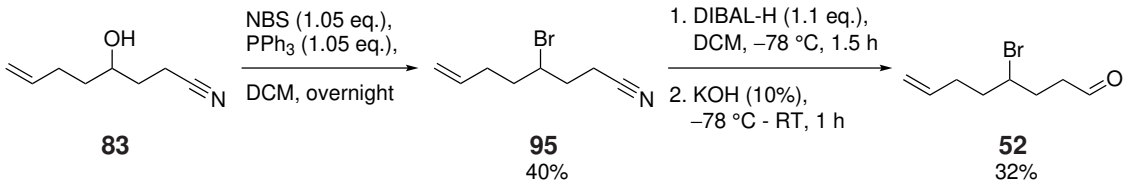

83 **95** 40% **52** 32%

*Figure 2.9: Bromination and DIBAL-H reduction to afford cascade precursor **52***

Unfortunately, the time constraints of the project meant that cascade chemistry was not able to be trialled on **52**, but this offers potential for future work.

2.4 Conclusions and Future Work

A variety of routes were considered in attempts to synthesise a cascade precursor, suitable for the synthesis of a ferrugine-like core. Many of the routes considered utilised vinyl sulfone chemistry, as popularised by Padwa and co-workers.[78;79;83;85] Whilst it proved possible to install the vinyl sulfone through HWE reactions, subsequent conversions of these HWE products often proved challenging.

When adapting chemistry performed previously in the group to include vinyl sulfone chemistry,[45;46] difficulty with purification led to low yields throughout the route. Though deprotection of the acetal group in **55** and subsequent cycloaddition were attempted, this proved unsuccessful and alternative routes were considered. The route is summarised in Scheme 2.49.

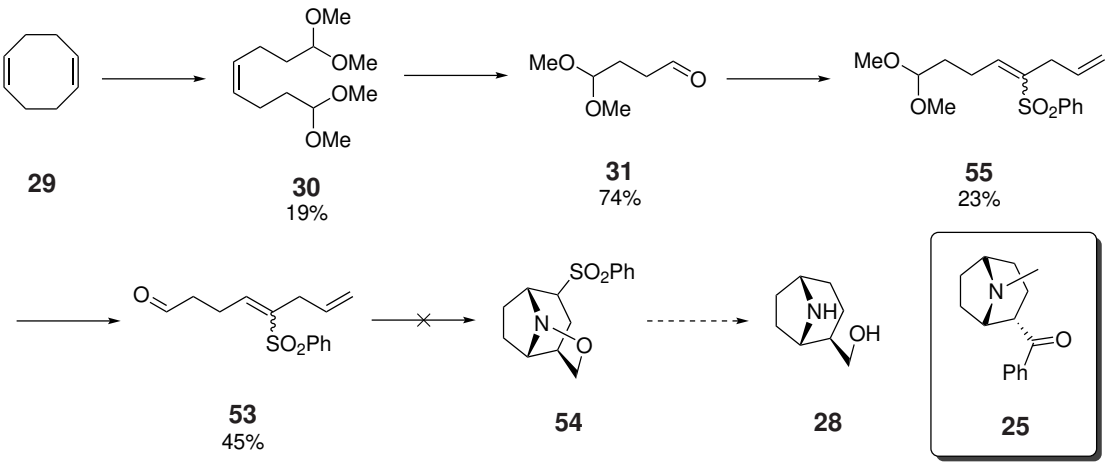

*Scheme 2.49: Overview of route towards **28**, core structure of Ferrugine **25** beginning from diene **29***

Though ultimately low yielding, it is possible that if these reactions were performed on larger scales, sufficient amounts of cascade precursor **53** could be produced to further trial the cascade chemistry, but ultimately this is not an efficient route to this compound. An alternative route was next considered, which would access a gem-dimethyl substituted analogue of **53**.

This route would involve alkylation using isobutyronitrile, synthesising a modified cascade precursor. Though it was proposed that the presence of the gem-dimethyl group would mimic substitution seen in *Alstonia* alkaloids, the steric implications of these groups appeared to prevent HWE reaction from proceeding. It was then considered that MeCN could be used as the alkylating agent, offering an alternative route to compound **55**, but this route also proved low yielding.

The use of a disubstituted alkene as an aldehyde precursor was briefly explored, but the oxidation step appeared unsuccessful at the time. However, due to issues surrounding LCMS analysis, this could be a topic for reinvestigation in future work.

In future work, this route could be reconsidered, now that it appears it may be viable. The osmium tetroxide reaction could be repeated, and the crude material purified in order to isolate compound **53**. Though conversion does appear to be low, optimisation could be attempted if this does appear to be a viable route.

In an alternative route, synthesis and characterisation of a vinyl-sulfone-containing cascade precursor, **53**, did prove possible, but attempts at cascade chemistry were unsuccessful. A summary of this work is shown in Scheme 2.50. The oxime intermediate, **81**, was isolated and characterised, but the subsequent intramolecular conjugate addition of the oxime onto the vinylsulfone followed by cycloaddition did not proceed.

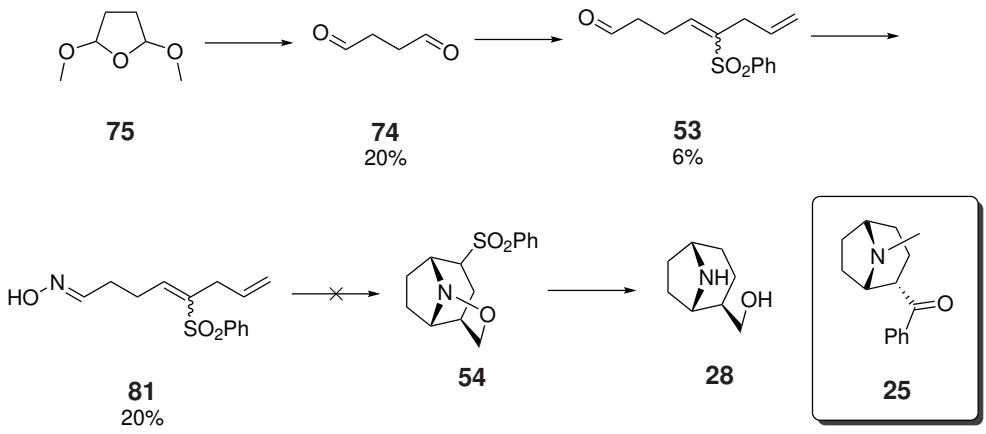

*Scheme 2.50: Overview of route towards **28**, the core structure of ferrugine **25**, from dialdehyde **74***

Had there been more time available, more in-depth studies could have been undertaken. Whilst temperature and solvent were varied, it may be the case that variation in other conditions, such as time or reagent equivalencies, may have enabled the reaction to progress further. If the reaction is not proceeding due to steric or electronic reasons, as proposed in section 2.3.4, changing such factors would likely have little effect. However, if the activation barrier is too high, it is possible that catalysts could be considered in order to lower the activation energy barrier. This could be explored in future work.

Attempts were also made to synthesise ferrugine-like cores in the absence of vinyl sulfones. The most

promising route, beginning within this work and continuing in work by master's student Cox,[87] did lead to the successful synthesis of a cascade precursor, **52**. This precursor has a bromide installed, which could act as a leaving group in the cyclisation step of the cascade chemistry, as seen in Figure 2.10.

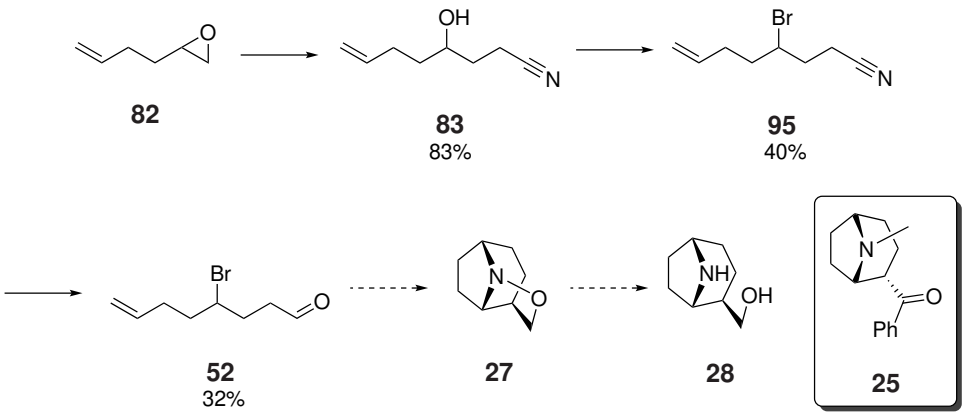

*Figure 2.10: Overview of route towards **28**, core structure of ferrugine **25** from using a bromide leaving group*

This is the key difference between **52** and **53**, and the difference in sterics and leaving group ability may well enable this reaction to proceed when its structurally related reaction could not. Further to this, the molecule still contains an alkene functionality, which can act as an internal dipolarophile in the subsequent intramolecular cycloaddition reaction.

Work on this route was stopped only due to the time constraints of the project - this is a route that should be explored in future work, as the route to the precursor looks promising. This would afford the first example of this cascade chemistry being successfully applied to a secondary leaving group.

Chapter 3: Towards the core of Alstonoxine B

3.1 Introduction

3.1.1 Alstonoxine B

Alstonia is a genus of evergreen trees, widely seen in tropical and subtropical regions of Africa, Central America, Southeast Asia, Polynesia and Australia. The majority are found in the Malesian region.[109] In this region, plants of the genus *Alstonia* have seen use in traditional medicine, with some species finding use in treatments for a wide variety of ailments, including coughs, ulcers, dysentery, fever, malaria, sore throats, toothache, rheumatism, and snake bites. *Alstonia angustifolia* is a genus of plant native to Indonesia, Malaysia, the Philippines and Vietnam. In Malaysia, a traditional treatment for fever involved externally applying the leaves of alstonia angustifolia to the area surrounding the spleen.[109] In addition to this, bark from this species of tree is used in the area to treat malaria. Studies attribute the medicinal qualities of many plants to the presence of alkaloids, an important secondary metabolite.[110] Within *Alstonia angustifolia*, there is a wealth of indole and oxindole alkaloids. If these alkaloids are responsible for the medicinal properties of their parent plants, there could be industrial and medicinal applications, should such compounds be isolated or synthesised on a large scale.

In 2014, Kam and co-workers reported the isolation of 20 new indole alkaloids, including alstofonidine **96**, macrogentine A **97**, and isoalstonoxine B **98**, shown in Figure 3.1.[111] Indole alkaloids were found to be the major secondary metabolites in a variety of plants, such as those of the genus *Alstonia*, and are known to have biological activity in humans. In Kam's study, a number of the alkaloids isolated displayed activity in reversing multidrug resistance in vincristine-resistant KB cells.

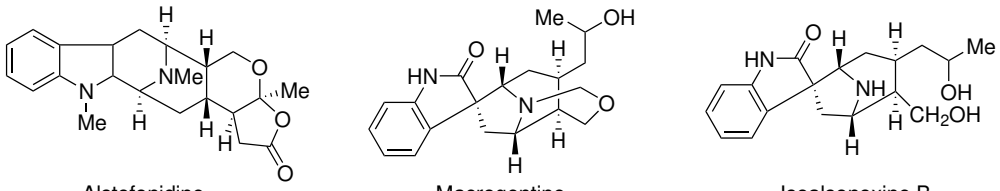

*Figure 3.1: Alkaloids **96**, **97** and **98** from Alstonia angustifolia, isolated by Kam and coworkers*[111]

In addition to their regular isolation, the total syntheses of several alkaloids from the species Alstonia angustifolia have been reported. In 2017, Cook and co-workers synthesised a number of oxindole alkaloids from *Alstonia angustifolia.*[112] Structures for four of the key alkaloids synthesised in this study, **99**-**100** are given in Figure 3.2. *tert*-Butyl hypochlorite-promoted oxidative rearrangement formed a key spiro[pyrrolidine-3,3'-oxindole] moiety, while stereocenters were established in >98% enantiomeric excess by an asymmetric Pictet–Spengler reaction. For compounds such as **99** and **101**, these key steps are shown in Scheme 3.1, starting from D-tryptophan.

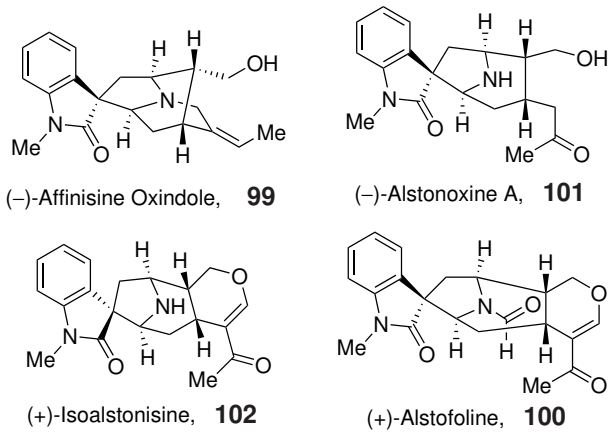

Figure 3.2: Some of the alkaloids synthesised by Cook[112]

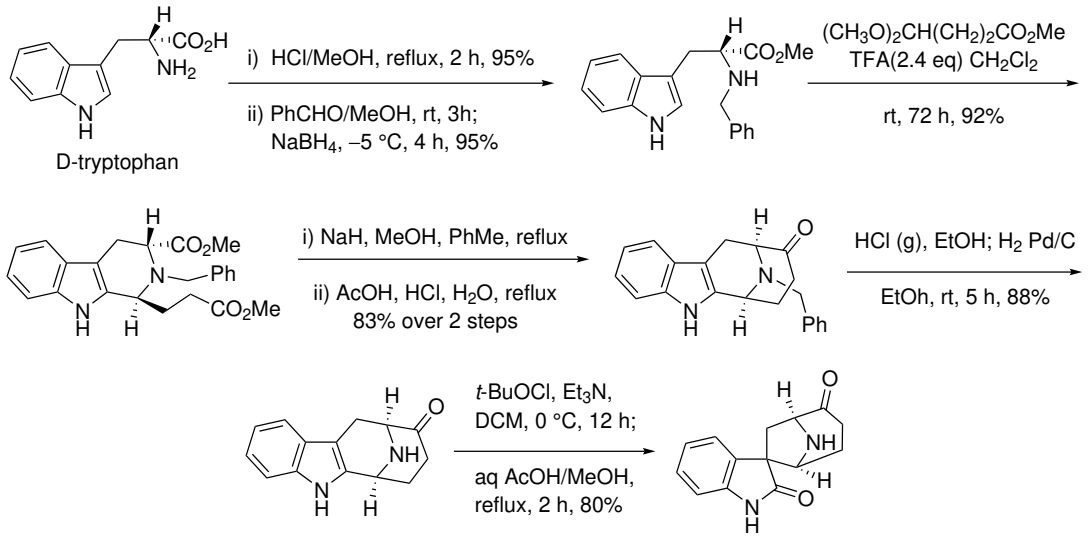

Scheme 3.1: Key steps from D-tryptophan

While some alkaloids from *Alstonia* have been shown to have biological activity, including antiprotozoal properties, the antimicrobial activity of most of these alkaloids remains unknown, due to limitations in the extraction process.

Large-scale extraction of important natural products from plants, such as for use in pharmaceuticals, can contribute to the reduction in the numbers of that particular plant. Take etoposide (**103**, Figure 3.3) for example, which is listed on the World Health Organisation's list of essential medicines.[113] Compound **103** is semi-synthesised from an extract of the Himalayan mayapple, a species which is now endangered. Consequently, alternative routes of production were considered. One study reported a biosynthetic route to the desired extract, which enabled a tobacco plant to produce the extract itself.[114]

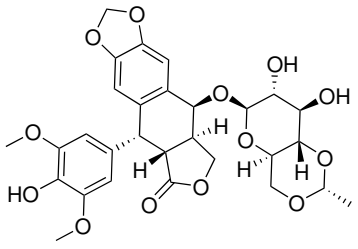

Figure 3.3: Structure of etoposide, ***103***

As extraction limits the amount of alkaloid available for testing, developing total synthesis routes is a desirable way to produce sufficient quantities of alkaloid to test for biological activity. For example, just

6 mg of the alkaloid **104**, macroxine (Figure 3.4) was isolated from 30 kg of dried leaves of *Alstonia macrophylla*.[115] With no reported syntheses for **104**, obtaining bioactivity data has not been possible. Were a large-scale synthesis route developed, however, the biological activity of **104** could be easily tested. Screening alkaloids from *Alstonia* for their biological activity could be particularly beneficial due to the use of these plants in traditional medicine. If the bioactivity of various alkaloids could be ascertained, this could help pinpoint the active ingredients that afford the plants their medicinal properties, leading to new treatments for ailments such as malaria.

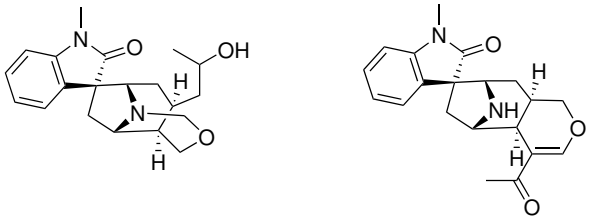

Macroxine, **104** Alstonisine, **105**

*Figure 3.4: Structure of **104** and **105**, Alstonia alkaloids*

Another *Alstonia* alkaloid, alstonisine (Figure 3.4, compound **105**) is a known antimalarial, displaying antiplasmodial activity against *Plasmodium falciparum* (IC_{50} = 7.6 μM),[116] one of the parasite species responsible for human malaria.

Alstonoxine B (**106**) is an oxindole alkaloid found in *Alstonia angustifolia*, and is shown in Scheme 3.2. Whilst its biological activity has never been tested, it is considered that **106**, like many other alkaloids found in this species, could have bioactivity against diseases such as malaria.

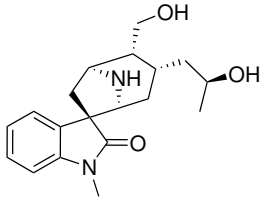

106

*Scheme 3.2: Alstonoxine B, compound **106***

3.1.2 Malaria

According to the World Health Organization (WHO), there were 247 million malaria cases in 84 endemic countries in 2021 alone.[117] This is an increase of 2 million cases compared to the previous year. In fact, the number of cases has been rising since 2016, with the largest annual increase observed in the year between 2019 and 2020. With the arrival of the COVID-19 pandemic, case numbers increased by 13 million in that year, attributed to disruptions during the pandemic.

Figure 3.5: Graph showing results from WHO surveys on disruptions to the diagnosis and treatment of malaria during the COVID-19 pandemic,[117] where no disruption = $<$ 5%, partial disruption = $<$ 50% and severe disruption = $\geq$ 50%.

In a report developed during the early stages of the pandemic, it was proposed that campaigns, continuous distributions of insecticide-treated nets, and access to effective malaria treatment were the main interventions likely to be disrupted as a direct result of the pandemic.[118] The WHO conducted surveys in order to determine the disruption in both the treatment and diagnosis of the disease during the pandemic.

Three rounds of surveys were conducted in five regions: the WHO African Region (AFR), the WHO Region of the Americas (AMR), the WHO Eastern Mediterranean Region (EMR) and the WHO South-East Asia Region (SEAR) and the WHO Western Pacific Region (WPR). The results of these surveys are shown in Figure 3.5. Although cases did rise significantly, results suggest that the worst-case scenario, predicted in the early stages of the pandemic, was avoided. Despite increasing case numbers, it was estimated by WHO that 2 billion malaria cases and 11.7 million malaria deaths were avoided between 2000 and 2021.

Malaria is caused by parasites of the *Plasmodium* genus, spread to humans by infected mosquitos known as vectors – living organisms with the ability to transmit parasites to humans and other animals. A mosquito can become infected by biting an infected human and will spread the parasite to everything it goes on to bite.[119]

Commonly, malaria is treated with combination therapies based around the drug artemisinin (**107**, Figure 3.6) and its semi-synthetic derivatives. Extracted from a herb traditionally used in Chinese medicine (*Artemisa annua*), **107** is recommended by WHO as the first line of treatment for uncomplicated malaria.[120] The combination therapy brings together two active ingredients with different mechanisms of action, because the use of **107** alone encourages the development of resistance.

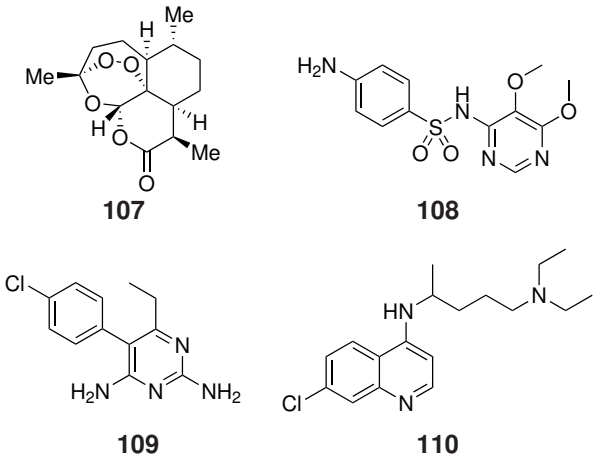

107 **108**

109 **110**

Figure 3.6: Structures of four previously common antimalarial drugs

Resistance to anti-malarial drugs is a developing problem. With the parasite already displaying resistance to previously common sulfadoxine/pyrimethamine **108**/**109**, often used in combination, and chloroquine **110** (Figure 3.6), resistance to **107** is now being closely studied.[121] With resistance emerging, studies are ongoing to map where resistance to **107** exists, in order to plan “containment and elimination

strategies".[122]

In the WHO African Region (AFR), treatments against malaria currently include combination treatments such as artemether-lumefantrine, amongst others.[117] Artemether, **111**, is an analogue derived from artemisinin, and is here given in combination with lumefantrine **112**, a drug only used in this specific combination therapy.

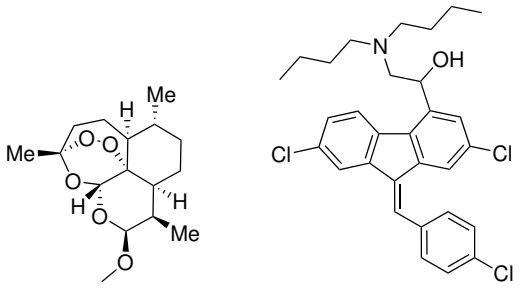

Artemether
111

Lumefantrine
112

*Figure 3.7: Structures of artemether (**111**) and lumefantrine (**112**), given in combination*

Most conducted tests indicate that all current first-line treatments show good efficacy against malaria. Polymorphisms in a gene known as PfKelch13 are under surveillance, as some have been linked to the partial resistance being seen in **107**.[117]

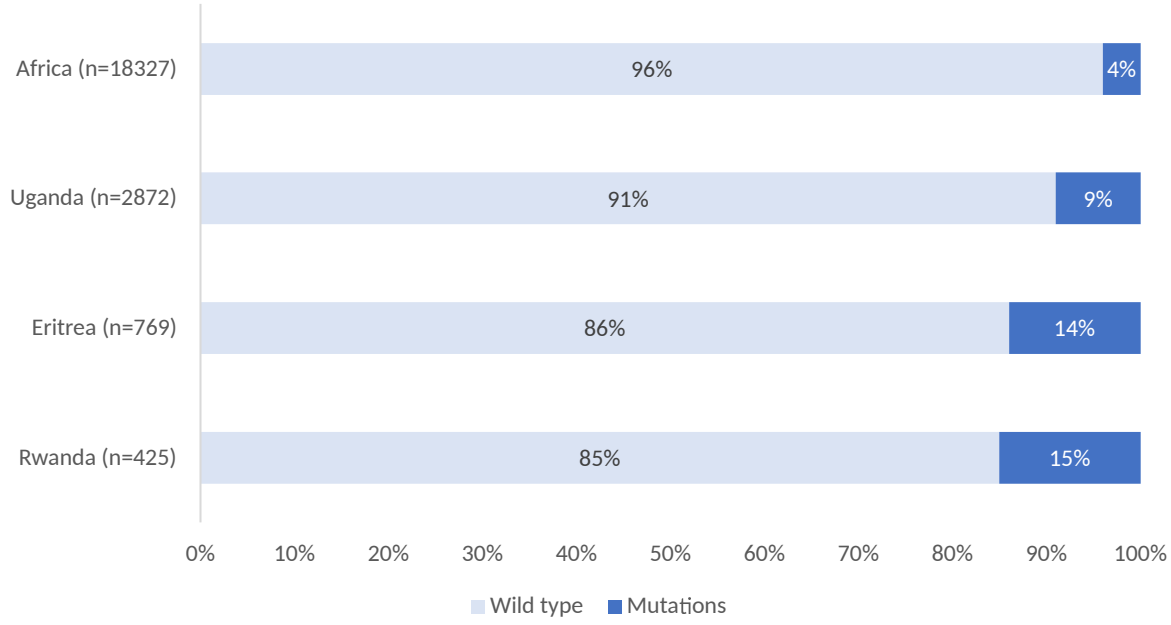

Figure 3.8: Countries in WHO AFR with >5% of parasites sampled with PfKelch13 mutations

With resistance emerging gradually against many anti-malarial treatments, the need to develop new treatment methods is ever-present. If plants of the genus *Alstonia* are used in traditional medicine to treat malaria, it seems reasonable to research synthetic routes to mass produce active ingredients as a new method of treatment. This includes alkaloids, such as oxindole alkaloids, which are present in this species.

3.1.3 Previous synthesis of oxindole alkaloids

The synthesis of several oxindole alkaloids has been reported. Horsfiline (**113**) is an oxindole alkaloid from the species *Horsfieldia superba*, a tree which grows in Southeast Asia. First isolated in 1991 by Bodo and co-workers,[123] several total syntheses of the alkaloid have been reported.

In 1992, Jones and co-workers reported a racemic synthesis of Horsfiline (**113**), employing a radical cyclisation approach.[124] Later, in 1994, Pellegrini *et al*[125] reported a stereoselective synthesis. With the absolute configuration of horsfiline unknown at the time of the synthetic effort, the group developed a route to synthesise both isomers. In 10 steps, both isomers were synthesised from L-tryptophan derivatives. This involved use of a chiral handle that was later removed. Diastereoselectivity was controlled during a rearrangement step, shown below in Scheme 3.3.

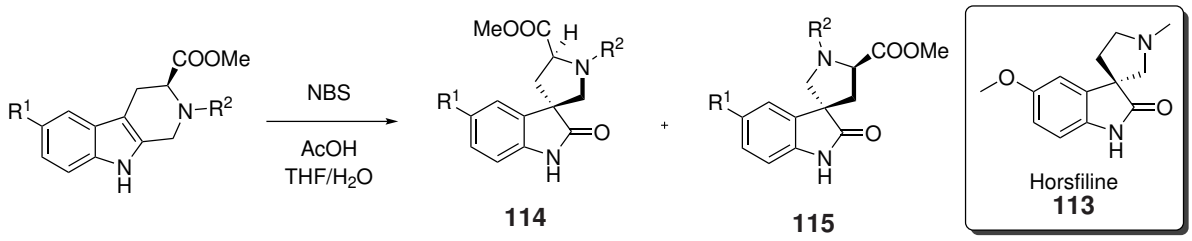

Scheme 3.3: Key rearrangement step in Pellegrini's horsfiline synthesis, enabling synthesis of both diastereoisomers

Following on from this, Fuji and co-workers developed their own methodology to synthesise chiral quaternary carbon centres, which was subsequently applied to the synthesis of (-)-**113** *via* asymmetric nitroolefination using chiral nitroenamine.[126] This step, shown in Scheme 3.4 proceeded with >99% ee. With the chiral quaternary centre in place, several other steps were performed, ultimately leading to the synthesis of (-)-**113**.

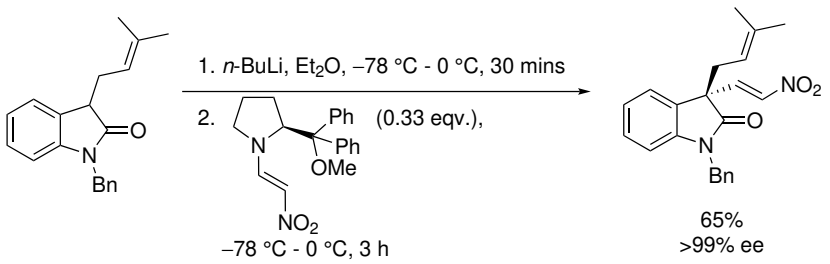

*Scheme 3.4: Asymmetric nitroolefination step in Fuki's synthesis of (-)-**113**, which enabled the installation of the quaternary centre in >99% ee*

The interest in the synthesis of oxindole alkaloids has continued this century. In 2013, Wanner and co-workers detailed the racemic synthesis of four spirocyclic oxindole alkaloids from the plant genus *Uncaria*, used in traditional Chinese and Japanese medicine.[127] Gou-Teng is a crude drug derived from *Uncaria*, and its medicinal activity is attributed to the presence of alkaloids within the plant, including those shown in Figure 3.9.

The structures of the alkaloids synthesised within this study are given in Figure 3.9. These alkaloids were obtained in racemic form, as no catalyst was available to achieve enantioselective spirocyclisation. The isomers were, however, readily separable.[127]

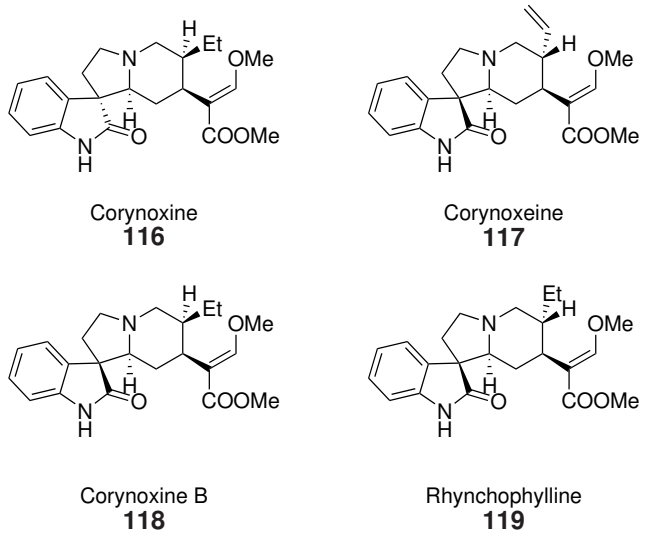

Figure 3.9: Structures of the four oxindole alkaloids synthesised in Wanner's 2013 study[127]

Alkaloids such as these have been linked to treatments for neurodegenerative diseases such as Parkinson's disease, the second most common neurodegenerative disorder after Alzheimer's disease.[128] The disease is characterised by the accumulation of protein aggregates, referred to as Lewy Bodies.

α-Synuclein, a major component of Lewy Bodies, is therefore known to be a causative factor of Parkinson's disease.[129] Evidence suggests that impairment of autophagy (the pathway by which dysfunctional organelles are broken down) may be involved with the accumulation of α-synuclein, and this impairment therefore likely has an important role in the pathogenesis and progression of the disease.[129]

Several studies have identified corynoxine B (**118**, Figure 3.9) as an inducer of neuronal autophagy, and thus could aid the breakdown of dysfunctional neurons.[129–131] Research suggests that **118** restores autophagy in cells which are overexpressing α-synuclein. Therefore, **118** may be a potential therapeutic target for Parkinson's disease. Other studies link corynoxine **116**[128] and isorhynchophylline[132] (an isomer of rhynchophilline **119**, Figure 3.9) with Parkinson's disease targets too.

However, with low brain permeability, the usefulness of such a therapeutic may be limited. Therefore, further studies were conducted, synthesising analogues of **118** with aims to develop a compound with improved brain permeability.[130] One compound developed in this study, CB6 **120** (Figure 3.10), showed improved brain permeability. The presence of the propyl group made **120** more hydrophobic than its precursor, and therefore increased permeability through the blood-brain barrier. A study done in mice indicated a much higher peak concentration of **120** in the brains compared with **118**, showing increased brain bioavailability.

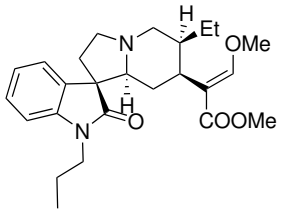

CB6
120

*Figure 3.10: CB6, the analogue of **118** with increased brain bioavailability*

An example of an *Alstonia* alkaloid synthesised using a dipolar cycloaddition reaction is Alsmaphorazine B, **121**. With its isolation reported in 2010 by Morita and co-workers,[133] Vanderwal and co-workers described the first synthesis of **121** in 2017.[134] The synthesis focussed on two key cycloaddition steps: a [4 + 2] cycloaddition, followed by a nitrone 1,3-dipolar cycloaddition. The latter of these steps is shown in Scheme 3.5.

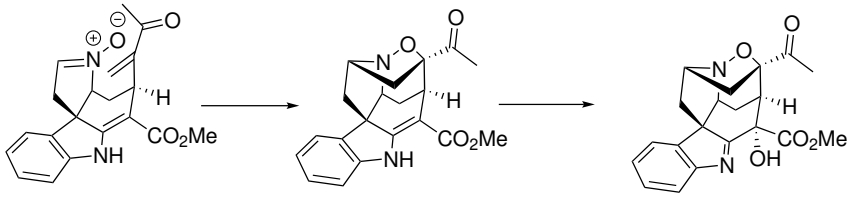

Alsmaphorazine B, **121**

*Scheme 3.5: 1,3-dipolar cycloaddition step in the synthesis of **121***

3.2 Aims

Synthetic efforts were to be made towards the core structure present in alkaloids from *Alstonia*, with the primary focus surrounding the core structure of oxindole alkaloid alstonoxine B, **106**. The cascade reaction involving condensation, cyclisation and cycloaddition (developed and used within the Coldham group to synthesise a variety of natural products) would be employed in these synthetic efforts. This could use both inter- or intramolecular cycloadditions, depending on the presence of an internal or external dipolarophile. Use of nitrone dipoles in such a reaction would allow the incorporation of a nitrogen and an oxygen atoms into the ring system, which would be useful in the synthesis of *Alstonia* alkaloids. The synthesis of such alkaloids could be particularly beneficial, as the use of these plants in traditional medicine could be an indication of further bioactivity.

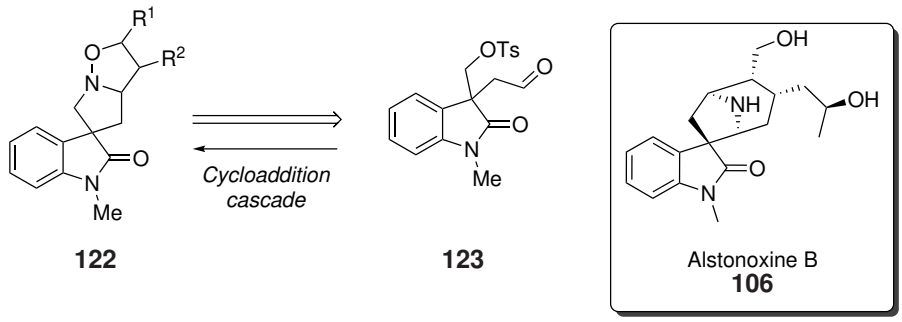

122 **123**

Scheme 3.6: Retrosynthesis of the core structure of oxindole alkaloids, employing cascade chemistry

As shown in the retrosynthesis given in Scheme 3.6, the aim would be to apply the cascade chemistry to aldehyde **123**, which would first require synthesis.

3.3 Initial routes towards the core structure of alstonoxine B

3.3.1 Retrosynthetic Analysis

The initially proposed route to access the core structure of Alstonoxine B, **106**, is given in Scheme 3.7.

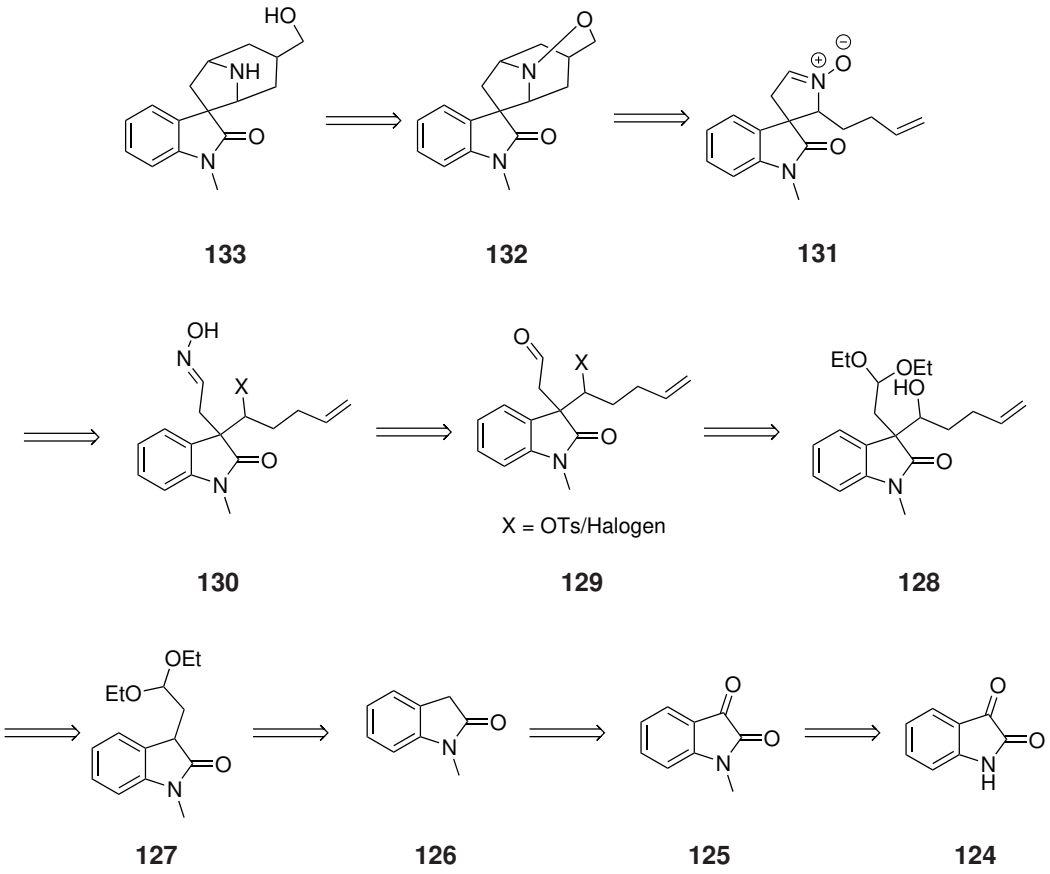

133 **132** **131**

130 **129** **128**

127 **126** **125** **124**

Scheme 3.7: Retrosynthesis detailing initially planned route

3.3.2 Synthesis of *N*-methyl oxindole 126

As suggested in the retrosynthesis given in Scheme 3.7, isatin **124** was first methylated to afford compound **125**, which was subsequently reduced to afford compound **126**. These procedures are known widely throughout the literature,[135–138] and afforded good yields, as shown in Scheme 3.8.

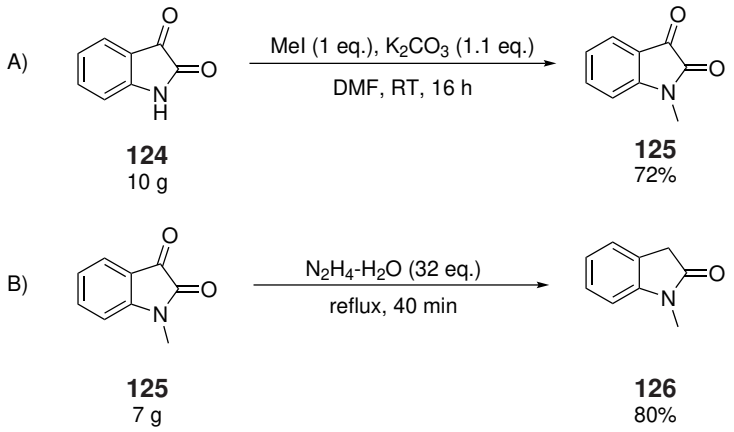

*Scheme 3.8: A) N-methylation of isatin **124** B) reduction of N-methyl isatin **125***

Although the synthetic route given in Scheme 3.8 afforded compound **126** in good yields, a shorter alternative route was found starting from readily available oxindole **134** (Scheme 3.9).[139] An initial attempt of this reaction used 1 equivalent of both NaH and Me_2SO_4, but following the workup a small amount of Me_2SO_4 remained, alongside unreacted starting material. Purification by recrystallisation and column chromatography was attempted, but the removal of these impurities proved difficult. It was therefore decided to increase the amount of base to 1.3 equivalents. This appeared to rectify the issue, allowing full conversion of the starting materials. Initially, it was considered that no further purification was required, as the product appeared clean by ^{1}H NMR spectroscopy. However, the orange solid formed was observed to change to a pink colour over the course of a day. Consequently, it was deemed necessary to purify by column chromatography. With an improved overall yield, this method was thus adopted.

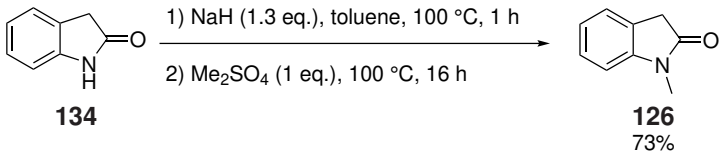

*Scheme 3.9: Shorter route to compound **126***

3.3.3 Alkylation of *N*-methyl oxindole 126

Having isolated compound **126**, the initial route proposed alkylation followed by an aldol reaction to install the required groups at the 3-position, thus forming the desired all-carbon quaternary centre. In order to form protected aldehyde **127**, an alkylation with LDA was attempted (Scheme 3.10), using bromoacetal **62** as an

alkylating agent. This would install an acetal group, which could be easily removed later in the synthesis, unveiling an aldehyde group with which to trial a cycloaddition. Though this step was attempted with both 1 and 4 equivalents of **126**, no product could be isolated. Following column chromatography of the crude product, only starting material **126** was isolated.

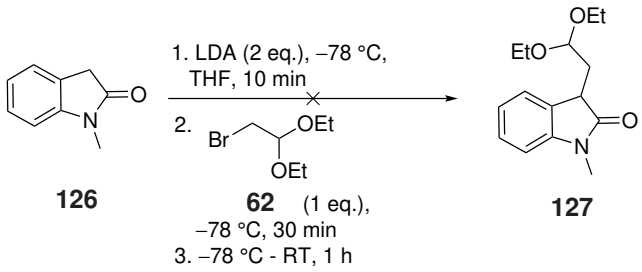

Scheme 3.10: Alkylation with deprotonation by LDA

Following this, a variety of alkylation methods were attempted. Synthesis of compound **127** had previously been reported,[140] using NaH to deprotonate **126** as opposed to LDA (Scheme 3.11).

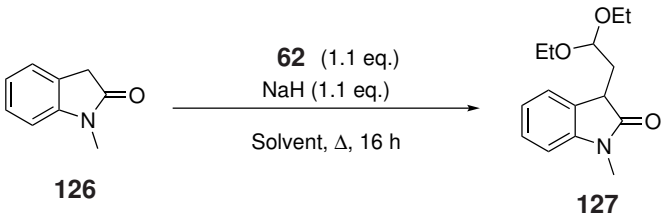

*Scheme 3.11: Alkylation of **126** with NaH*

A mixture of benzene and DMF was used as the solvent system within the literature procedure, but due to the carcinogenic properties of benzene, toluene was first investigated in its place. In comparison to the original reaction conditions, the reaction in toluene/DMF was heated to 100 °C rather than reflux. This precaution was taken due to toluene having a much higher boiling point than benzene (111 °C, compared with benzene's 80 °C[141]), with the hope that this would prevent decomposition of the product **127**. Following column chromatography, compound **127** was isolated in 10% yield. However, it appeared that some of compound **127** had also co-eluted with unreacted starting material **126**, which was present in a ratio of 0.59:1 **126**:**127** product according to ^{1}H NMR analysis. Given that some product was isolated, meaning that it had not decomposed on heating, it was next decided to heat the reaction at reflux overnight. However, once again some co-elution was seen, and the yield of pure acetal **127** still proved poor (14%). Following this, it was decided to trial the reaction in the original benzene/DMF solvent system, despite its associated

risks, in order to see if this proved more successful. This afforded just 7% of desired product **127**, while a further attempt conducted only in DMF returned just starting material **126**. The results of the solvent and temperature changes are summarised in Table 3.1.

Table 3.1: Results of varying temperature and solvent system for alkylation reaction

Entry	Solvent	Temperature /℃	Yield 127 /%
1	DMF/Toluene	100	10
2	DMF/Toluene	110	14
3	DMF/Benzene	90	7
4	DMF	110	-

The next attempt to optimise this reaction was a base screen. The reaction was repeated using the optimised conditions from Table 3.1 (Entry 2) with three different bases, using 1.1 equivalents of each. Results are summarised in Table 3.2.

Table 3.2: Results of base screen for alkylation reaction

Entry	Base	Yield 127 /%
1	NaH	28
2	NaHMDS	-
3	KO^tBu	26

The result for the repeated NaH reaction (Table 3.2, Entry 1) was surprising, as it appeared by NMR spectroscopy and high-resolution LCMS that during this attempt, some dialkylated product **135** had been formed (Scheme 3.12). Separation of the product **127** from dialkylated **135** proved simpler than separation of **127** from unreacted starting material **126** and afforded an improved yield of product **127** (28%).

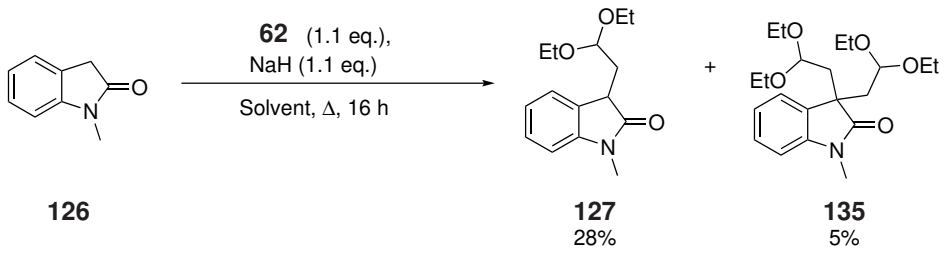

126 **127** 28% **135** 5%

*Scheme 3.12: Observed dialkylation of compound **126** to give compound **135** in Table 3.2, Entry 1*

While the use of NaHMDS afforded no product (Table 3.2, Entry 2), KO^{t}Bu did show promise with a yield of 26% of the clean product **127** (Table 3.2, Entry 3), though in addition to this product, it is thought that some product co-eluted with the deprotected aldehyde. The best yield, however, was afforded when NaH was used. Consequently, this was repeated on a larger scale (852 mg of **126**, compared with the previous 500 mg), increasing the equivalents of bromide present from 1.1 to 1.5. It was proposed that this would encourage the dialkylation seen in the previous NaH example, thus aiding separation and improving yield of **127**. Though dialkylated product **135** was indeed seen during this repeat, the yield of **127** was actually lower in this case (14%).

3.3.4 Synthesis of aldehyde 136

Whilst attempting to optimise this alkylation step, the next step was considered, wherein compound **127** would undergo an aldol reaction with aldehyde **136** to afford compound **128** (Scheme 3.13).

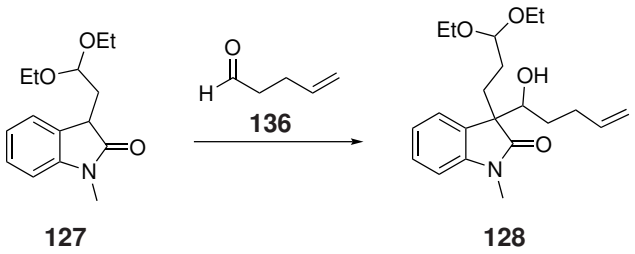

127 **128**

*Scheme 3.13: Proposed aldol step to give alcohol **128***

As aldehyde **136** was not widely available, it first needed to be synthesised (Scheme 3.14). It was proposed that this could be done by oxidising alcohol **137**, and three oxidation methods were trialled, beginning with PCC oxidation.[142] A relatively low yield of 20% of **136** was obtained (Table 3.3, Entry 1) using this method. It was thought that product **136** may be being lost during the process of filtration through Florasil, and so solid-supported chromium trioxide was next attempted, in order to remove the need for this filtration step. However, as seen in Table 3.3, Entry 2, no aldehyde **136** was isolated by this method. Some conversion to aldehyde **136** was seen by NMR spectroscopy (12%), but distillation proved unable to separate product from starting material **137**. Finally, Swern oxidation was attempted, as in Table 3.3 (Entry 3).[143;144] This is a popular method for such oxidations, so the relatively low yield of 12% was disappointing. Evaporation under reduced pressure was used to remove excess solvent and it is considered that some of

aldehyde **136** may have been lost during this procedure, which may account for a lower than anticipated yield. The reactions are summarised in Table 3.3.

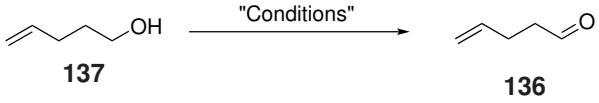

137 **136**

*Scheme 3.14: Three routes to oxidise alcohol **137** to aldehyde **136** - for conditions, see Table 3.3*

*Table 3.3: Oxidation methods for formation of aldehyde **136***

Entry	Conditions	Yield of 136 /%
1	PCC, DCM 3 h	20
2	CrO_3, DCM 3 h	No product isolated, 12% conversion by NMR
3	1. $(COCl)_2$, DMSO, DCM 15 min, –78 °C 2. Et_3N, 1.5 h	12

Marginally, the best yield was obtained from the PCC reaction (Table 3.3, Entry 1). Optimisation would be required, were any of these methods to be used on a large scale. For the aldol step, aldehyde **136** was to be added to compound **127**. However, whilst testing conditions for the synthesis of aldehyde **136**, the next step was trialled using commercially available acetaldehyde, to test the feasibility of this step.

3.3.5 Test Aldol Reaction

The first set of conditions trialled the use of LDA to perform the aldol reaction to afford compound **138**, shown in Scheme 3.15. Following column chromatography, LCMS analysis of fractions showed around 19% conversion to product **138**, but this was not isolated from the mixture, which also contained starting material **127**.

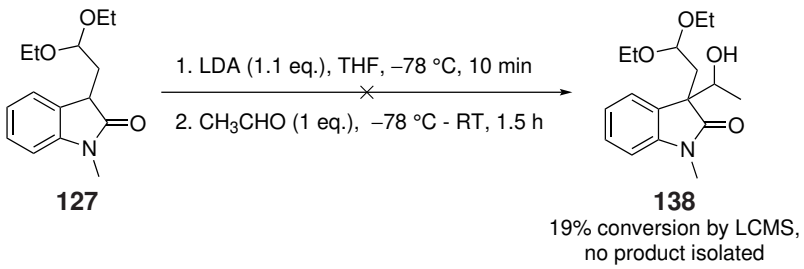

127 **138**
19% conversion by LCMS,
no product isolated

Scheme 3.15: Alkylation with LDA and CH_3CHO

A second attempt, based upon literature procedures,[145;146] used DABCO as the base in a direct aldol reaction, shown in Scheme 3.16 (reaction A). However, polymeric ethyl glyoxylate (the aldehyde used in the literature study) is more activated than either acetaldehyde or desired aldehyde **136**, owing to the presence of its more electron-withdrawing carbonyl group. Furthermore, catalysts such as $(DHQ)_2PHAL$ were used in the literature, enabling enantioselectivity. Nevertheless, the reaction was attempted with DABCO as the base, though in the absence of such ligands.

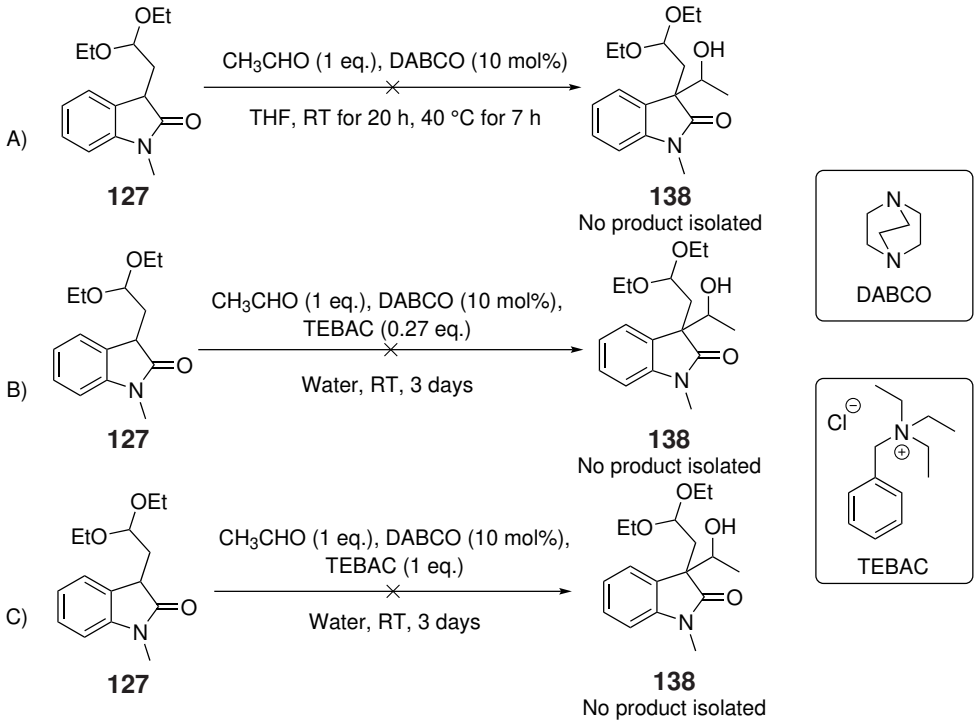

Scheme 3.16: Different routes for aldol reaction with CH_3CHO

The reaction was first attempted in THF (Scheme 3.16, Reaction A), but when only starting material **127** was visible by LCMS, the solvent was changed to water, and the reaction performed in the presence of phase transfer agent TEBAC,[146] as shown in Scheme 3.16 (Reaction B). When carrying out this procedure on a small scale to synthesise compound **138**, LCMS analysis of the crude product seemed to indicate that the desired product had been formed. This was due to a major peak being observed which corresponded to the MNa^+ of the desired product. However, upon scaling up this procedure only a small amount of conversion was seen by LCMS. Varying the equivalents of TEBAC (Scheme 3.16, Reaction C) showed no product by LCMS, so alternative routes were considered.

Reconsidering the route suggested in Scheme 3.7, while synthesis of oxindole was facile, the following

two steps to synthesise compound **128** were proving difficult. The first alkylation step to synthesise **127** afforded poor yields, as did the oxidation to afford the desired aldehyde **136**, which was to be added in the subsequent step. Furthermore, the addition of acetaldehyde in the test aldol reaction proved difficult, suggesting that similar reactions with the desired aldehyde **136** were unlikely to be successful. As a result, the route to compound **128** needed to be adapted.

3.3.6 Alternative Synthesis using Grignard Reagent 139

A new route, given in Scheme 3.17, was next considered. Following the formation of Grignard reagent **139**, it could be reacted with *N*-methyl isatin **125** to afford alcohol **140**. Subsequent Boc-protection, followed by hydrogenation, would then hopefully afford compound **127**.

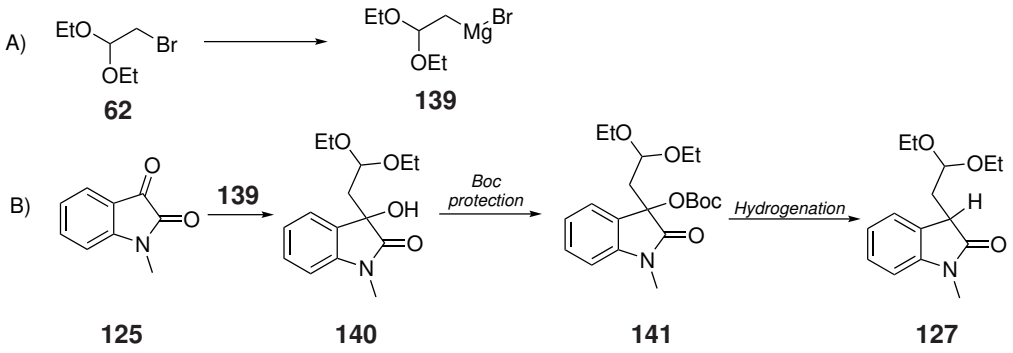

Scheme 3.17: Alternative route to alkylation, using Grignard procedure

While this general procedure exists in the literature,[147] at the time the work was conducted, a literature search did not return results on the synthesis of this particular Grignard reagent, **139**. Therefore, reaction conditions were proposed, using 1.1 equivalents of magnesium and 0.5 equivalents of dibromoethane (DBE), in diethyl ether. DBE was used to activate the magnesium, reacting with it to reveal a fresh magnesium surface which would then go on to react with the bromide present.

After attempting the Grignard formation and addition, the product was taken on crude to the Boc-protection step. When no product **141** was observed by ^{1}H NMR analysis, the Grignard formation was reattempted, with addition instead to acetophenone (Scheme 3.18), to test whether the Grignard reagent was being formed. As the expected product of the Grignard reaction (compound **142**) was not observed by LCMS, it was concluded that this Grignard reagent was not being formed. This was a surprising result, as

similar Grignard reagents have been made before,[148] but as mentioned previously there are no documented examples of this specific reagent. Consequently, this route was abandoned and alternatives were pursued.

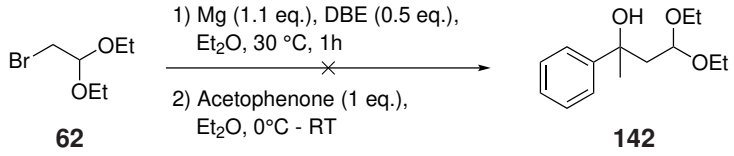

62 **142**

Scheme 3.18: Attempted Grignard addition to acetophenone to test Grignard formation

3.3.7 Acylation of *N*-methyl oxindole 126

It was next considered that, as opposed to alkylation of **126** occurring first, an acylation reaction could be performed prior to the alkylation, as shown in Scheme 3.19. Ideally, acylation would afford product **143**, before alkylation to form compound **144**. Literature suggested that this acylation should be possible, and even gave examples of subsequent alkylation.[149] It is important to mention that the literature study used acetic anhydride, thus installing a methyl ketone onto oxindole **126**. However, it was considered that other anhydrides, or possibly acid chlorides, could be used here to install different ketones onto the oxindole **126**. One difference with this route compared to the initial route proposed in Scheme 3.7 is that instead of forming alcohol **128** directly, ketone **144** is first formed, which must then be reduced to give desired alcohol **128**, adding an additional step to the synthesis.

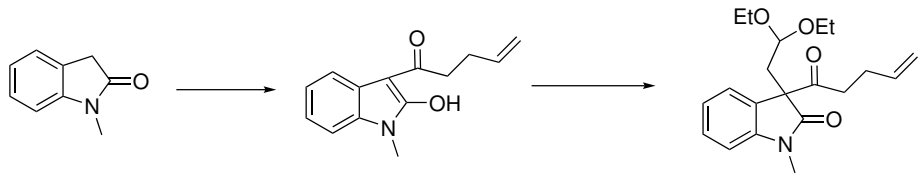

126 **143** **144**

Scheme 3.19: Proposed acylation reaction and subsequent alkylation

First, the reaction was trialled using acetic anhydride and acetyl chloride, as shown in Scheme 3.20. Though these would afford product **145** as opposed to desired product **143**, they are commercially available so did not require synthesis, and the subsequently formed compound **145** could be used to test the viability of the alkylation step. Though the use of acetic anhydride in this reaction was known in the literature, the use of acid chlorides had not been demonstrated, and therefore this would offer a comparison between the

two. These reactions indicated that the anhydride acted as a better acylating agent than the acid chloride, which afforded no product. This was somewhat expected, given the literature precedent.

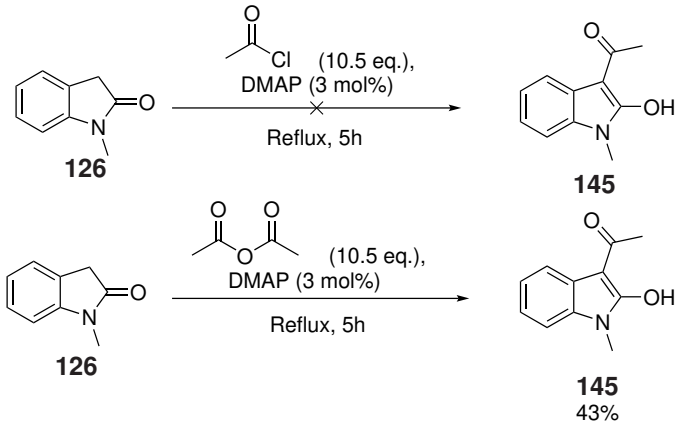

*Scheme 3.20: Acyl chloride vs anhydride as the acylating agent to give compound **145***

With compound **145** in hand, the alkylation step was then attempted using bromide **62** as the alkylating agent (Scheme 3.21).[149] Unfortunately, applying the reported reaction conditions used with other alkylating agents in the literature failed to give desired product **146** (Scheme 3.22, Table 3.6 Entry 1). This was a disappointing outcome, as the study reported successful results for this reaction with a variety of alkyl halides, reporting yields varying from 50–92%.

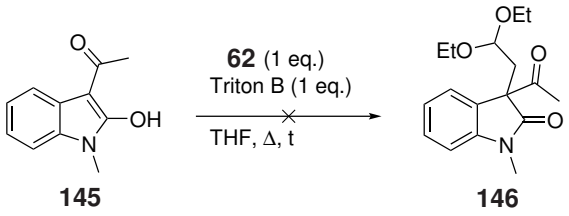

*Scheme 3.21: Alkylation of **145** with **62** to afford compound **146***

Whilst the majority of the alkylation reactions reported by Ortega-Martinez were run at room temperature, there was one reported example which was performed under reflux conditions. This was when using pentyl bromide, the only alkyl bromide used successfully as the electrophile in this study. Therefore, it was considered that increased temperatures may be required when using **62** as the alkylating agent. Additionally, in the study, the reaction was always run overnight, but it was considered that reaction time could also be varied, to see if this would allow for the synthesis of desired product **146**. Unfortunately, under all of the conditions tested, summarised in Table 3.6, only starting material was recovered.

Table 3.4: Results of varying conditions for alkylation following acylation

Entry	Temperature	Run Time	Yield 146 /%
1	RT	18 h	-
2	RT	72 h	-
3	40 ℃	18 h	-
4	Reflux then RT	7 h at reflux, 72 h at RT	-

In the literature,[149] the alkylation step is achieved using Triton B as the base, and this is what was originally used in this study. However, with no conversion seen, the reaction was next trialled using other bases. As can be seen in Table 3.5, none of the alternative bases led to the formation of any of the desired product **146**, even when trialled in different solvents. Instead, ^{1}H NMR spectroscopy showed mixtures containing only starting material **145** and bromide **62**. Consequently, it was considered that this route was not viable when using bromide **62** as the alkylating agent.

Table 3.5: Results of the base screen for alkylation following acylation

Reaction number	Solvent	Base	Yield 146 /%
1	THF	NaH	-
2		KOH	-
3		Na_2CO_3	-
4		Et_3N	-
5	MeCN	KOH	-
6		Na_2CO_3	-
7		Et_3N	-
8	Acetone	KOH	-
9		Na_2CO_3	-
10		Et_3N	-

One of the alkyl halides used in the literature procedure was allyl bromide, **60**. The reaction was next attempted with **60** in this study (as shown in Scheme 3.22), and the reaction was successful, as in the

literature, forming compound **147**. This suggested that bromide **62** may not be sufficiently activated to act as an alkylating agent.

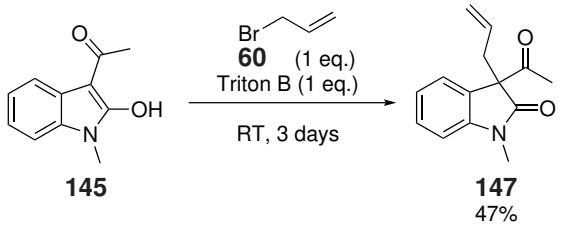

*Scheme 3.22: Successful alkylation using allyl bromide **60***

It was considered that this step may require an iodo- rather than 2-bromo-1,1-diethoxyethane in order to increase reactivity due to reduced bond strength (bond dissociation energy for C-Br = 280 kJ mol^{-1}, C-I = 209 kJ mol^{-1} at 273 K).[150] The literature study did report success with MeI as the alkylating agent, for example. Conversion of **62** could be performed *via* a Finkelstein reaction, which was first attempted *in-situ* using *tetra-n*-butylammonium iodide (TBI) (Scheme 3.23, Reaction A). However, ^{1}H NMR analysis showed that both starting materials **145** and **62** were isolated, with no conversion to the desired product **146**.

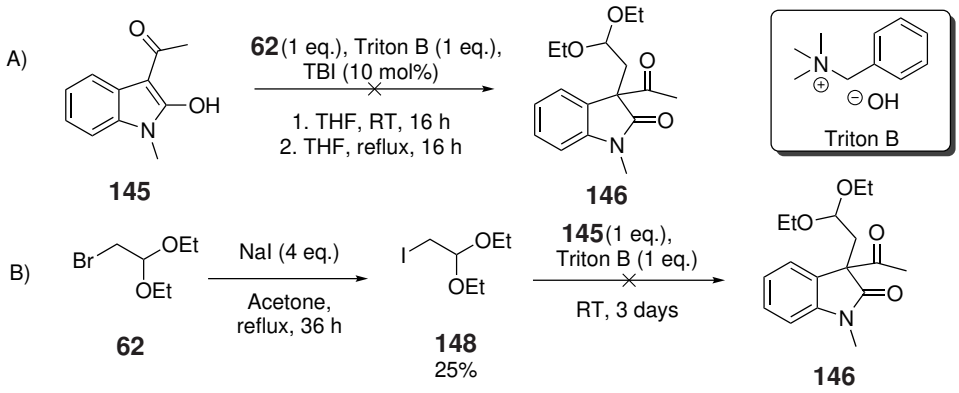

Scheme 3.23: A) In situ Finkelstein with TBI B) Traditional Finkelstein

Thus, a separate Finkelstein reaction was attempted prior to the alkylation step (Scheme 3.23, Reaction B), using sodium iodide in acetone. This resulted in the successful formation of 2-iodo-1,1-diethoxyethane **148** in 25% yield and 87% purity, containing 13% of bromide **62**. Iodide **148** was then used in the alkylation reaction, but once again there was no conversion to **146** observed, suggesting this reagent too may not be sufficiently reactive.

3.3.8 Changing Alkylating Agent

As bromide **62** was proving to be an unsuitable alkylating agent, alternatives were considered. The alkylating agent used must contain a group which could be easily converted to an aldehyde, but should be more activated than **62**. The study by Ortega-Martinez reported successful alkylations with a range of alkylating agents, providing insight into suitably activated electrophiles.[149] Based on these two key factors, two alternative alkylating agents were proposed.

Firstly, bromoacetonitrile **149** was considered, as the nitrile functional group could be converted to an aldehyde by DIBAL-H reduction. The conditions used in the literature were applied to compound **145** with electrophile **149** (Scheme 3.24, Reaction A). Following column chromatography, starting material **145** was recovered. One sample may have contained a mixture of starting material **145** and **150**, having co-eluted during purification in a 1:0.67 ratio. This was indicated by the presence of two doublets at 3.29 and 2.97 ppm, coupling to one another with a *J* value of 17.0 Hz. This could reasonably correspond to the diastereotopic CH_2 protons adjacent to the CN group, with the high coupling constant consistent with the geminal coupling of diastereotopic protons. This was not isolated cleanly, however, nor did it appear to be present in significant amounts.

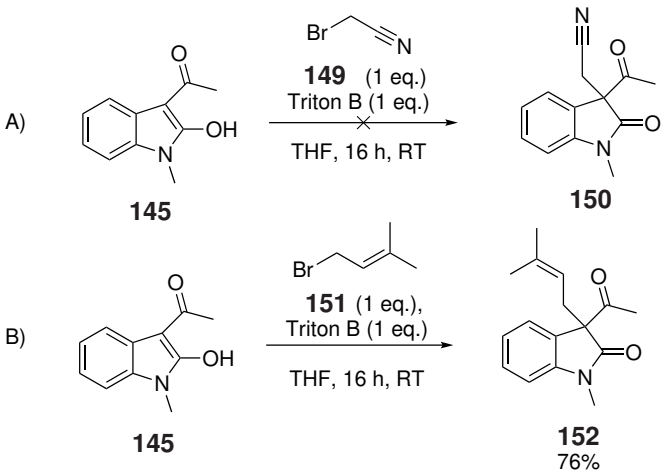

*Scheme 3.24: Alkylation with A) bromoacetonitrile **149** and B) prenyl bromide **151** under original literature conditions*[149]

Another alkylating agent to consider was prenyl bromide, **151**. As in the literature,[149] bromide **151** was shown to be sufficiently activated towards alkylation (Scheme 3.24, Reaction B), affording product **152** in 76% yield. It was now hoped that the more highly substituted alkene could later be selectively converted

to the desired aldehyde group by ozonolysis, followed by a reductive workup, in the presence of the less electron-rich terminal alkene. This alkene should remain intact following this conversion, enabling it to act as a dipolarophile during the cascade chemistry.

Thus, two alternative routes were proposed at this time to synthesise desired compound **153**. When comparing the two routes shown in Scheme 3.25, Route A appeared initially more beneficial, as compound **152** had already been successfully synthesised. It would be likely that the protons α- to the carbonyl group would be the most acidic in this molecule, and thus that deprotonation with LDA would occur at this position selectively, allowing the formation of compound **153**.

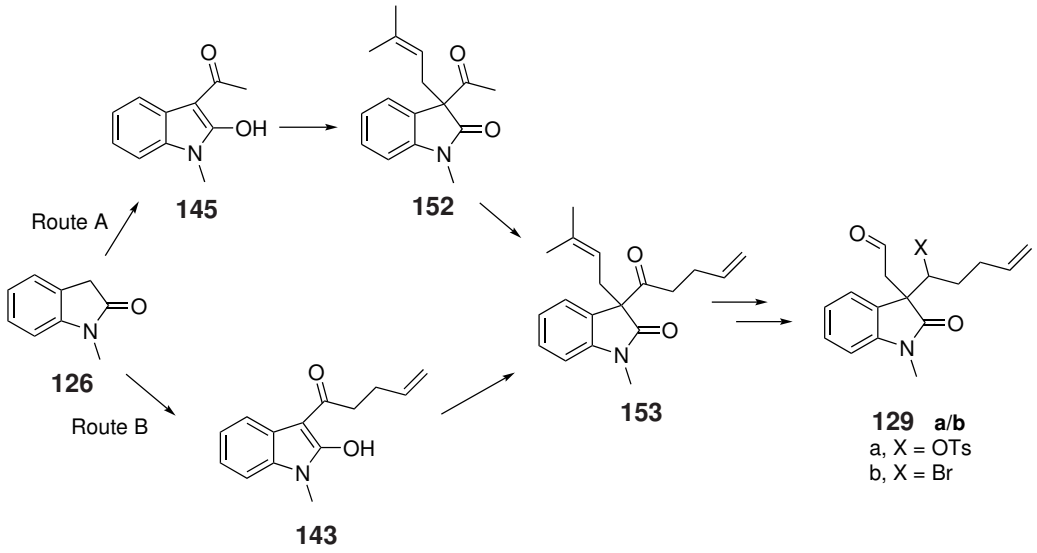

*Scheme 3.25: Two proposed routes to aldehyde **129***

In comparison, Route B (Scheme 3.25), though appearing shorter at first glance, required the added step to synthesise pentenoic anhydride, **154**, required in the acylation step. Acetic anhydride used in Route A, on the other hand, was readily available, and already proven to work in this reaction. Therefore, both routes had the same number of steps, and on paper, both seemed plausible. It was hoped that the compound produced by both routes, compound **153**, could be converted in several steps to afford compound **129**. Therefore, both routes were attempted.

It is worth noting here that compound **129** contains two stereocentres, and therefore two diastereoisomers may be synthesised. However, both diastereoisomers would lead to natural products, therefore the synthesis of either would be desirable. It may be possible, however, to exert some control over the stereoselectivity during the reduction of the ketone.

First considering Route A, the prenylation of **145** had already been shown to be successful (as shown in Scheme 3.24), so compound **152** was taken forward to the next step. The alkylation of **152** was attempted using 1.1 equivalents of LDA and allyl bromide **60** (Scheme 3.26), however LCMS analysis of the crude reaction mixture showed deacylation had occurred, and following the addition of allyl bromide compound **155** was instead formed. Deacylation is known to be possible in such compounds, as it was reported in the paper upon which the methods used here are based.[149] A potential way to avoid deacylation would be to use less harsh reaction conditions. However, at this time, Route B (Scheme 3.25) towards the synthesis of compound **129** was considered.

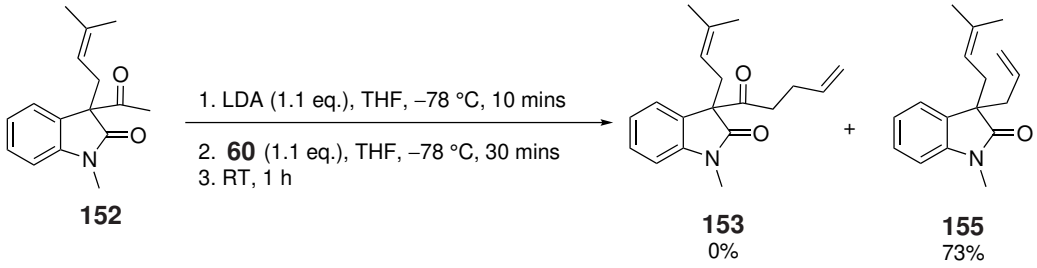

Scheme 3.26: Attempted alkylation with LDA, resulting in deacylation

As previously discussed, synthesis of pentenoic anhydride **154** would be required in Route B. This synthesis was facile, reacting pentenoic acid **156** with the coupling reagent DCC (Scheme 3.27).[151]

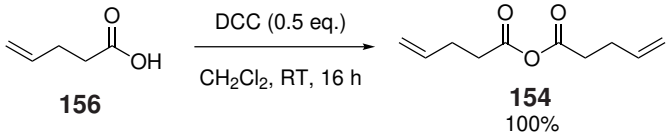

*Scheme 3.27: Synthesis of pentenoic anhydride **154***

With the anhydride in hand, the synthetic conditions used in the synthesis of compound **145** with acetic anhydride were repeated using anhydride **154** (Scheme 3.28). This meant that, when heating to 140 °C, anhydride **154** was not at reflux. Unlike acetic anhydride, which has a boiling point of 140 °C,[152] anhydride **154** has a significantly higher boiling point of 272 °C (literature, 78-81 °C/0.4 mmHg).[153] This also meant that while acetic anhydride was easily removed by concentration under reduced pressure following workup, this was not the case for anhydride **154**.

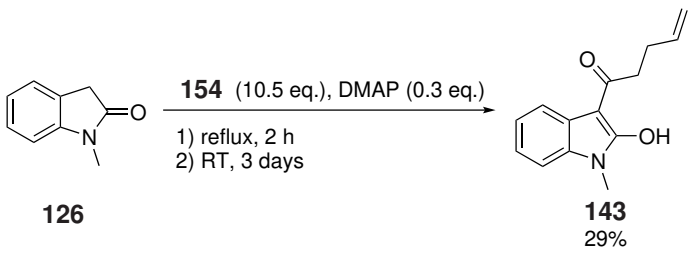

126 **143** 29%

*Scheme 3.28: Acylation to afford compound **143***

Consequently, when observing the crude reaction mixture by ^{1}H NMR, the possible product was obscured by the anhydride signals. Column chromatography was attempted at this time, but it is believed that the anhydride co-eluted with desired product **143**. Therefore, an alternative method for purification was required. Vacuum distillation was attempted, successfully reducing the presence of anhydride signals in the ^{1}H NMR spectrum of product **143**. However, it did not appear possible to remove all of the anhydride **154** in this way. Therefore, column chromatography was attempted following distillation, which proved successful.

When acetic anhydride was used during acylation, the anhydride acted as a solvent (using 10.5 equivalents). At first, this was replicated when using anhydride **154** (Table 3.6, Entry 1) which was successful in synthesising product **143**. However, it was decided that this large excess of anhydride should be reduced if possible, not only to simplify purification but also to reduce waste of the anhydride. Additionally, an optimum heating time for the reaction was to be determined. Therefore, tests were carried out to ascertain the best conditions for this reaction, shown in Table 3.6, entries 2-4. This table gives isolated yields, following purification by both column chromatography and distillation, in order to fully remove anhydride **154**.

Table 3.6: Optimisation of acylation conditions

Entry	Eq. of anhydride 85	Heating time /h	Yield 143 /%
1	10.5	2	48
2	7	2	39
3	5.6	5	35
4	5.6	2	33

While Table 3.6, Entry 1 does appear to offer the greater yield at this time, it does appear that reducing the equivalents of **154** reduces yield by only 9-15%. Therefore, it may be beneficial to reduce the number

of equivalents of anhydride, as **154** decomposes to **156** on distillation and therefore cannot be reused without repeating the synthesis. Therefore, too large an excess would be wasteful. Thus, 5.6 equivalents of anhydride were used in further experiments. Additionally, the marginal difference in yield between heating for 2 and 5 hours meant that, for the purpose of saving time, the reactions were heated for 2 hours going forward. Though these conditions do give the lowest yield presented in Table 3.6, as the difference is small, this was deemed the best compromise so as to reduce waste and save time.

The next step was to add prenyl bromide **151**; as this had been successfully achieved in Route A, it seemed reasonable to replicate the conditions used. Attempting the reaction first at room temperature overnight, column chromatography isolated the remaining starting material **143** co-eluted with desired product **153** in an approximate ratio of 1:1. Rather than attempting an additional purification, it was hoped that the yield could be increased by reacting the remaining starting material **143** further. Therefore, at this time, a further 1 equivalent of bromide **151** and Triton B were added to the reaction mixture which was then stirred at 40 ℃ overnight. Unfortunately, this appeared to cause deacylation, with bromide **151** adding twice in this case to afford compound **157** and apparently co-eluting with desired product **153**, as seen in Scheme 3.29.

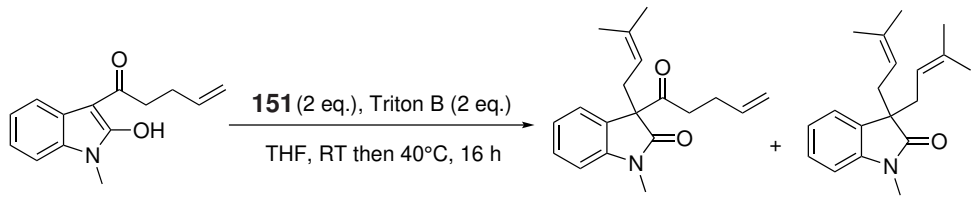

143 **153** **157**

Scheme 3.29: Attempted prenylation, resulting in deacylation and di-addition

Consequently, the reaction was repeated, using only a slight excess of 1.05 equivalents of both bromide **151** and Triton B, at room temperature, which proved a success (Scheme 3.30). It was therefore decided that Route B was likely to be the most successful route and was carried forward.

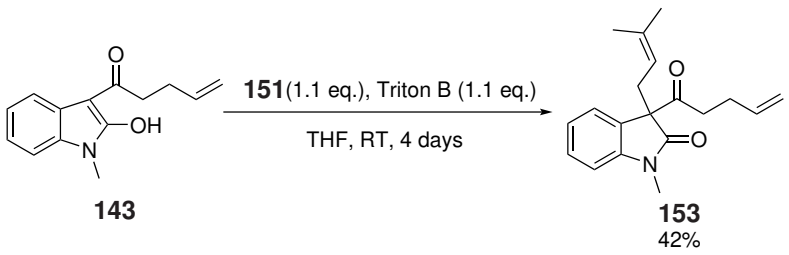

*Scheme 3.30: Successful prenylation of compound **143***

3.3.9 Reduction of 153

The next step in the route would be to reduce the ketone **153** to alcohol **158**, which would potentially afford diastereoisomers. Though stereoselective methods for such a reduction do exist, common reducing agents were first trialled to test the viability of the chemistry. It was decided, following a search of the literature, that several common reducing agents would be tested. First, $NaBH_4$ was trialled, reacting both at room temperature and at reflux overnight (Scheme 3.31). When conducted under reflux, LCMS of the crude reaction mixture indicated that the product had been formed but following column chromatography, ^{1}H NMR spectroscopy suggested that the product was no longer present. This could suggest that the product had formed but underwent a retro-aldol conversion on the column. It may be that crude **158** could have been trialled in the next step, or isolated using a different purification technique, but unfortunately, this was not attempted at the time. When performed at room temperature, LCMS analysis of the crude product showed only starting material.

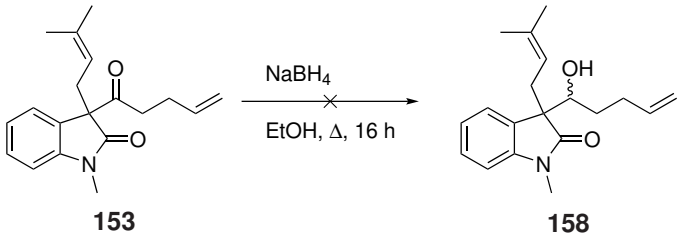

*Scheme 3.31: Reduction of **153** to give **158** using $NaBH_4$*

Following this, reduction with $LiAlH_4$ was considered. Being a stronger reducing agent, there was fear that the reaction may lead to the reduction of not only the ketone, but also of the amide functionality present in the molecule. Nevertheless, a literature search suggested that similar reactions, where amide groups were present, were performed with success. The reaction, shown in Scheme 3.32, was performed under reflux,

but unfortunately following purification by column chromatography none of the isolated fractions appeared to be distinguishable by NMR, as product or starting material. The impurity of the sample meant that a structure was not determined.

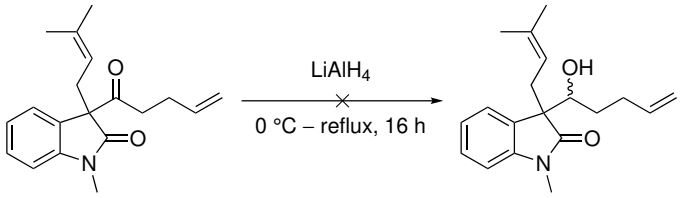

153 **158**

*Scheme 3.32: Reduction of **153** to give **158** using $LiAlH_4$*

A reducing agent used more commonly in the literature for such conversions is $BH_3.Me_2S$.[154] This required low temperatures, beginning at –30 °C and decreasing to –78 °C. The reaction, shown in Scheme 3.33, ultimately yielded no product as confirmed by LCMS, though starting material mass was also absent in the LCMS trace. The mass peaks observed were all of higher mass than both starting material and product, and the identity of this mixture is unknown. The reaction was repeated, with the same result both times.

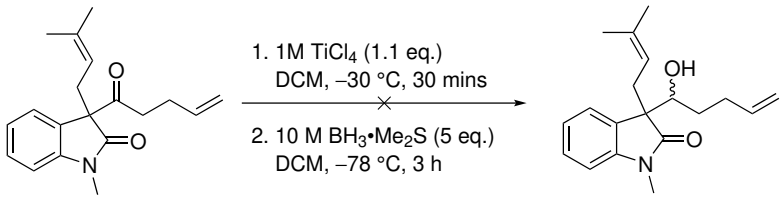

153 **158**

*Scheme 3.33: Reduction of **153** to give **158** using BH_3Me_2S*

In a final attempt at reducing compound **153**, the reaction was attempted using Me_2PhSiH, as shown in Scheme 3.34, again directed by literature precedent on less complex structures containing similar functionalities.[155] Though crude LCMS did indicate that some product may be present, following purification none of the desired alcohol **158** was isolated.

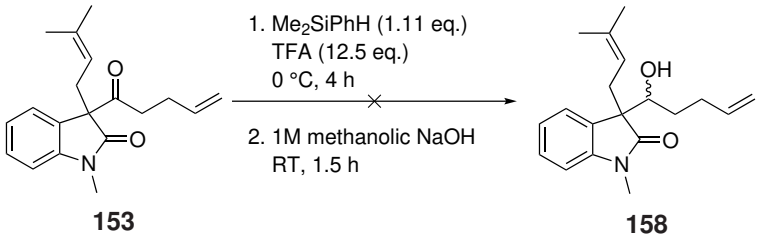

153 **158**

*Scheme 3.34: Reduction of **153** to give **158** using Me_2SiPh*

There are several instances in these attempts to reduce compound **153** where analysis of the crude material suggests that reduction may have occurred. However, no alcohol **158** was ever successfully isolated. It is considered that the alcohol may be decomposing on the silica column. Use of the crude alcohol without further purification was decided against, given how impure it appeared when analysed. Therefore, at this time an alternative synthetic route was considered, moving away completely from the route suggested in Scheme 3.7.

3.4 Asymmetric Synthesis *via* Epoxide 159

3.4.1 Retrosynthetic Analysis

A new route was proposed, as shown in the retrosynthetic analysis given in Scheme 3.35. This route was based on literature which showed that it was possible to convert *N*-methylisatin **125** to an epoxide, compound **159**, using a sulfur ylide.[156–158] The epoxide can then be opened using allyl BF_3K,[159] and it was considered that synthesis of a dimethyl allyl BF_3K would allow installation of the desired prenyl group. The epoxide opening would require not only the synthesis of the dimethyl allyl BF_3K, but also of a chiral BOX ligand,[159] which would enable selectivity in the reaction. Therefore, a single enantiomer of compound **160** could be formed selectively.

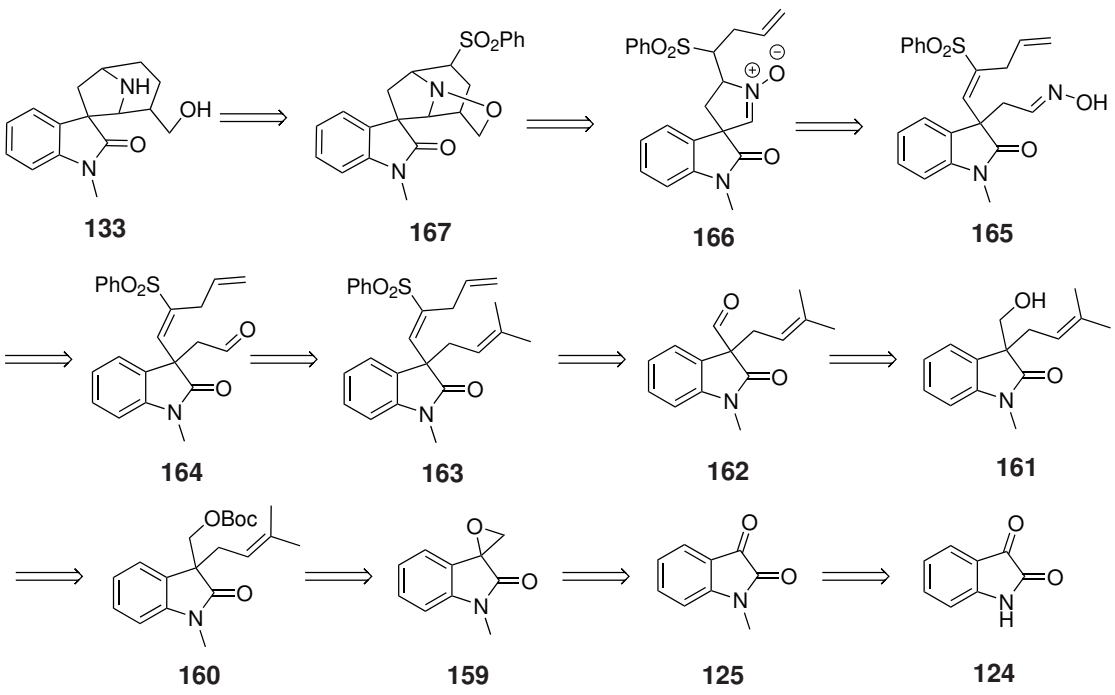

Scheme 3.35: Retrosynthesis detailing new route via epoxide

This route would require a later-stage installation of the internal dipolarophile, compared with previously proposed routes. This RSA (Scheme 3.35) suggests that this be installed through the use of an HWE reaction. For this, following Boc-cleavage of compound **160**, the alcohol would then need to be oxidised in order to install the necessary aldehyde functionality. It is proposed here that the aldehyde undergoes the HWE reaction with a phenylsulfonyl phosphonate, installing a sulfone functionality, as well as the internal dipolarophile. Padwa and co-workers have conducted extensive research surrounding vinyl sulfones and their use in cycloaddition reactions, with the work spanning decades, as discussed in 2.1.5.

3.4.2 Epoxidation of 125

N-Methylation was performed as in Section 3.3.2, resulting in the formation of compound **125**. A mixture of trimethyl sulfoxonium iodide and Cs_2CO_3 in MeCN was then stirred at 50 °C for 1 h, in order to generate the desired sulfur ylide. To the ylide was then added compound **125** in MeCN, thus generating epoxide **159**, as shown in Scheme 3.36. This was based upon literature precedent.[156;157]

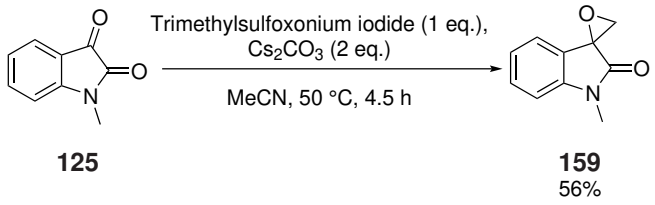

125 **159** 56%

*Scheme 3.36: Epoxide formation to afford compound **159** using trimethylsulfoxonium iodide*

Whilst this method was successful, issues arose surrounding the purification of the epoxide **159**. Purification by column chromatography appeared inefficient, with impurities co-eluting with the desired product in spite of different R_f values. It was considered that this could be due to the by-product of this reaction, dimethyl sulfoxide, causing co-elution of other components by solubilising them and dragging them through the silica more quickly than would ordinarily be expected. To counter this, an alternative was proposed. Literature suggested that in addition to trimethylsulfoxonium iodide, the epoxidation could be achieved using trimethylsulfonium iodide.[158] In this case, the by-product would be dimethyl sulfide, as opposed to dimethyl sulfoxide. Due to its lower boiling point of 38 °C,[160] dimethyl sulfide could far more easily be removed *in vacuo* compared to dimethyl sulfoxide, which has a boiling point of 189 °C.[161]

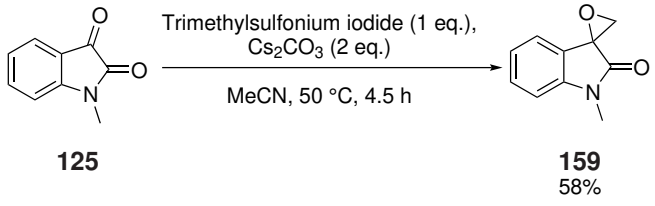

125 **159** 58%

*Scheme 3.37: Epoxide formation to afford compound **159** using trimethylsulfonium iodide*

Therefore, this route was attempted, as shown in Scheme 3.37 and did lead to an increased yield, but it was felt that further improvement could be made.

Firstly, it was observed that the fast addition of isatin **125** led to the formation of a red polymer-like compound in the solution, which slowed the reaction progress and complicated purification. When **125** was added dropwise over 40 minutes, this substance was absent. The speed of addition appeared to correlate to the colour of the solution observed, which varied from green and yellow to pink and purple across numerous attempts. The best yields were obtained when dropwise addition was used, reducing the formation of the red material in the solution.

Additionally, instead of purifying by column chromatography, a silica plug was trialled. This was a

vastly more efficient method and did provide suitable purification. Thus, both trimethylsulfonium iodide and trimethylsulfoxonium iodide were used in the epoxide synthesis with this new purification method. As can be seen in Table 3.7, yields have been greatly increased in both cases when using dropwise addition and a silica plug, though actually slightly higher when using trimethylsulfoxonium iodide. Whilst a silica plug may be considered a less efficient method of purification as compared to column chromatography, the products do appear to have improved purity when synthesised by this method, likely as a result of the dropwise addition, which appears to reduce the formation of impurities. This is therefore the route which was used going forward.

*Table 3.7: Varying yields of epoxide **159** when changing conditions*

Entry	Scale of **125** /g	Reagent	Purification method	Yield of **159** /%
1	7.00	Trimethylsulfonium iodide	Column	58
2	4.00	Trimethylsulfonium iodide	Silica Plug	85
3	1.00	Trimethylsulfoxonium iodide	Column	56
4	4.25	Trimethyl sulfoxonium iodide	Silica Plug	87

3.4.3 Testing the Route with Racemic Methods

Following the successful synthesis of epoxide **159**, the next step in the synthesis was to ring-open the epoxide to generate compound **160**. Literature reported that such a ring opening could be done asymmetrically,[159] by utilising a cobalt catalyst and a chiral ligand, known as a “BOX” ligand. The study reported the best combination of yield and enantiomeric excess (ee) when using the ligand **168**, given in Figure 3.11.

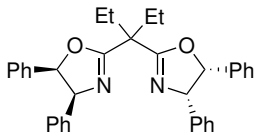

168

Figure 3.11: Best BOX ligand for asymmetric epoxide opening, as reported in literature[159]

However, prior to the synthesis of ligand **168**, the reaction was trialled in the absence of ligand, in an attempt to test whether this could provide an achiral route. Additionally, the reaction was attempted using

allyl BF_3K (**169**) first, as this was readily available, unlike the desired dimethyl allyl BF_3K salt (**170**) which required synthesis. The reaction is shown in Scheme 3.38.

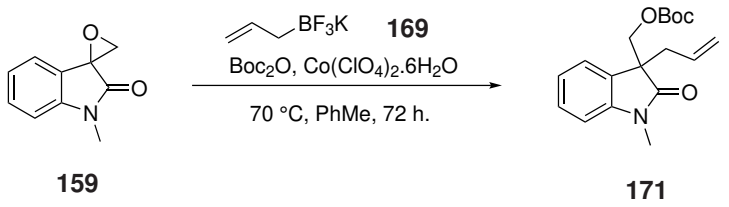

159 **171**

*Scheme 3.38: Conditions to synthesise compound **171***

This was attempted twice, once in the absence of both $Co(ClO_4)_2.6H_2O$ and ligand (Table 3.8, Entry 1), and then with $Co(ClO_4)_2.6H_2O$ present but the ligand absent (Table 3.8, Entry 2). In both cases, allyl BF_3K (**169**) and Boc_2O were added to epoxide **159**, either with or without $Co(ClO_4)_2.6H_2O$, and heated to 70 °C in PhMe for 72 h. No product was isolated from either iteration of this reaction, indicating that these conditions were not suitable for a racemic epoxide opening reaction.

Table 3.8: Results of tests on racemic epoxide opening reaction

Entry	Reactants present	Yield 171 /%
1	**159**, **169**, Boc_2O	Starting material recovered
2	**159**, **169**, Boc_2O, $Co(ClO_4)_2.6H_2O$	Crude LCMS showed trace product, not isolated

3.4.4 BOX ligand synthesis

While these tests were being performed, synthesis of ligand **168** was also underway. The route to the ligand required just two steps, the first[162] requiring reaction between (1*S*,2*R*)-(+)-2-amino-1,2-diphenylethanol (1*S*,2*R*)-**172** and diethyl malonimidate hydrochloride (**173**), as shown in Scheme 3.39. This would provide the ligand **168** as a single enantiomer, given the fixed stereochemistry within the amino alcohol starting material (**172**). This was successful in just 15% yield. Though ultimately successful, this reaction was consistently low yielding, in spite of literature reports of 81% yields.[162]

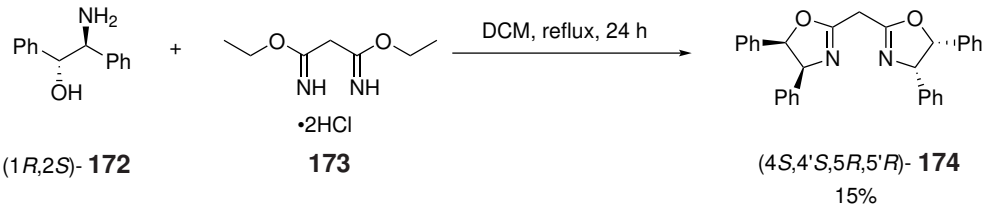

(1*R*,2*S*)- **172** **173** (4*S*,4'*S*,5*R*,5'*R*)- **174** 15%

*Scheme 3.39: First step to synthesise BOX ligand (4S,4'S,5R,5'R)-**168**, via intermediate (4S,4'S,5R,5'R)-**174***

A different procedure was therefore considered, wherein the reactants (1*R*,2*S*)-**172** and **173** were mixed and stirred at reflux for 1 h, at which time Et_3N was added dropwise and the mixture was heated for a further 3.5 h. This procedure was attempted in DCE, suggested in the alternative literature procedure (Scheme 3.40).[163]

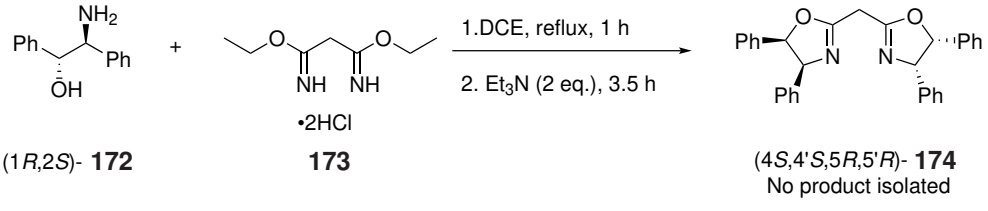

(1*R*,2*S*)- **172** **173** (4*S*,4'*S*,5*R*,5'*R*)- **174** No product isolated

*Scheme 3.40: First step to synthesise BOX ligand (4S,4'S,5R,5'R)-**168**, via intermediate (4S,4'S,5R,5'R)-**174**, using alternative method*

NMR and LCMS analysis showed a large amount of amino alcohol (1R,2S)-**172** present following the reaction. A minor peak in the LCMS did correspond to the m/z of product, but this was in very small quantities and was not isolated.

Therefore, the original procedure was used despite its low yield. The second step involved alkylating compound (4*S*,4'*S*,5*R*,5'*R*)-**174**,[164] and literature reported this conversion being performed using EtI. At first, the reaction was tested using EtBr (Table 3.9, Entry 1). Then EtBr with TBI was used, as seen in Table 3.9, Entry 2, to encourage conversion of EtBr to EtI *in situ*, before ultimately testing with EtI (Table 3.9, Entry 3), which was found to be the most successful. The selected conditions are shown in Scheme 3.41.

Table 3.9: Results of alkylation with various alkylating agents

Entry	Alkylating Agent	Yield 168 /%
1	EtBr	-
2	EtBr (+ TBI)	66
3	EtI	81

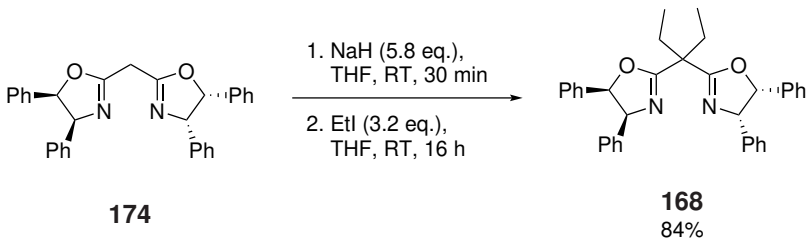

174 **168** 84%

*Scheme 3.41: Synthesis of BOX ligand (4S,4'S,5R,5'R)-**168**, via intermediate (4S,4'S,5R,5'R)-**174***

The opposite enantiomer of (4*S*,4'*S*,5*R*,5'*R*)-**168**, (4*R*,4'*R*,5*S*,5'*S*)-**168** was also synthesised, using the above procedures but starting from (1*S*,2*R*)-**172**.

3.4.5 Racemic Ligand Synthesis

It was also considered that, although the reactions proved unsuccessful in the absence of BOX ligand as seen in 3.4.3, it may still be possible to do the reaction racemically in the presence of an achiral ligand. As the BOX ligand synthesis was consistently low yielding and was a bottleneck in the synthesis, synthesis of an achiral ligand, if higher yielding, may provide an easy way to test the validity of the chemistry on larger scales.

The achiral ligand used, **175**, was based upon the BOX ligands seen in literature,[156] but without any chiral centres present. Scheme 3.42 shows the proposed route to achiral ligand **175**.

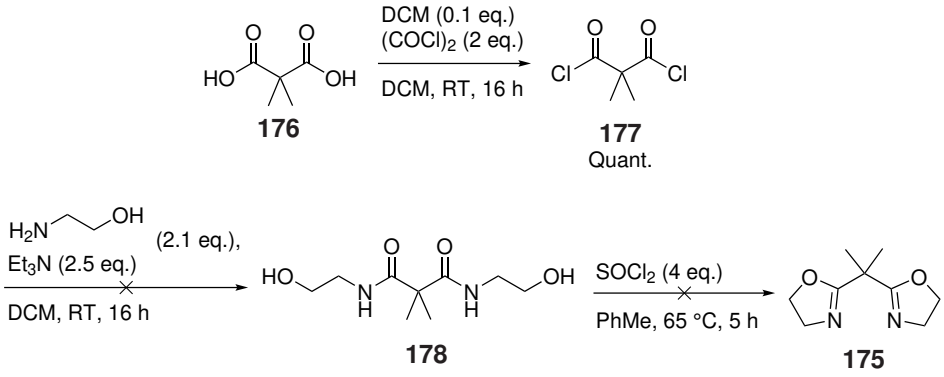

176 **177** Quant. **178** **175**

*Scheme 3.42: Route to achiral ligand, **175***

The first step took readily available dimethyl malonyl diacid, **176**, and converted this into the corresponding dichloride, **177**. Then, according to literature,[165] the dichloride **177** was added to an amino alcohol – in this case, ethanolamine - resulting in the formation of compound **178**. Literature procedures took

this crude, without analysis, onto the subsequent step, suggesting that this compound would subsequently cyclise in the presence of thionyl chloride to afford the desired ligand, **175**. However, this was not observed. Upon further analysis of the crude **178**, it appeared that this compound was not forming, hence the failure of the cyclisation step. At this time, in spite of its low yield, the next steps were instead trialled using BOX ligand.

3.4.6 Epoxide opening with allyl boron trifluoride salt 169

With ligand **168** successfully synthesised, albeit in low yields, attention turned to the asymmetric epoxide opening, using ligand **168**, $Co(ClO_4)_2.6H_2O$, and readily available allyl BF_3K, **169**. Whilst synthesis of desired dimethyl allyl BF_3K **170** was underway, attempting this procedure, though known in the literature, was an opportunity to test and optimise these conditions.

First, the epoxide opening step was trialled. Initially, ligand **168** and 10 mol% of $Co(ClO_4)_2.6H_2O$ were mixed together in PhMe for 30 min at room temperature, as suggested in the literature. Following this, the mixture was transferred into a second toluene mixture containing **159**, **169** and Boc_2O. Unfortunately, it was thought that some catalyst and/or ligand was not successfully transferred, thus reducing the amount present in the reaction mixture. As in Table 3.10 Entry 1, while crude LCMS suggested a small amount of product, the majority of the reaction mixture was unreacted epoxide **159**. When purification was attempted, no product was isolated.

*Table 3.10: Conditions tested for asymmetric epoxide opening of **159***

Entry	Conditions	Yield 171 /%
1	10 mol% $Co(ClO_4)_2.6H_2O$ Mixing prior to addition to **159**	Product seen in crude LCMS, but no product isolated
2	20 mol% $Co(ClO_4)_2.6H_2O$ Simultaneous addition of all reagents	83

It was thought that increasing the mol% of cobalt from 10% to 20% may increase the yield of the product. It was also considered that a different method for mixing the reagents was required, as the ineffectual transfer of the cobalt/ligand mixture into the reaction flask may be contributing to the poor conversion to **171**. In the

second attempt (Table 3.10, Entry 2), 20 mol% of cobalt catalyst was used, and all reagents were added simultaneously. There was therefore no premixing of the cobalt catalyst and BOX ligand prior to addition, thus preventing ineffectual transfer to the reaction flask. This deviates from the literature procedure, and it was considered that this may lead to coordination problems. Pleasingly, however, the procedure proved a success, obtaining compound (*R*)-**171** in 81% yield. Following chiral HPLC, the er of this compound was determined to be 84:16 (see appendix). This determination was made based on the synthesis of the opposite enantiomer, enabling comparison. The successful method is summarised in Scheme 3.43.

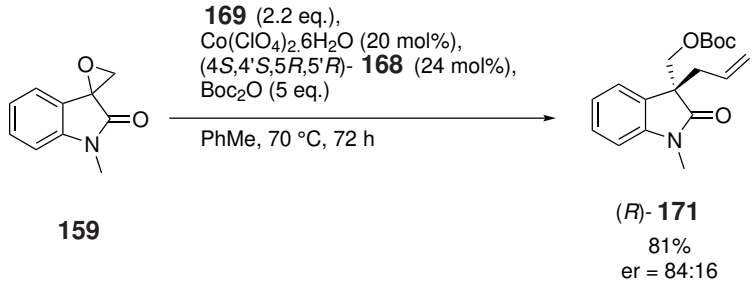

*Scheme 3.43: Epoxide opening to afford (R)-**171***

With this compound in hand, the next step was the removal of the Boc-protecting group to afford compound (*R*)-**179**, revealing an alcohol group which could then be converted to a suitable leaving group such as a tosylate (compound (*R*)-**180**). The Boc-deprotection was successful in 64% yield, and the subsequent tosylation was achieved in 58% yield. These steps are summarised in Scheme 3.44.

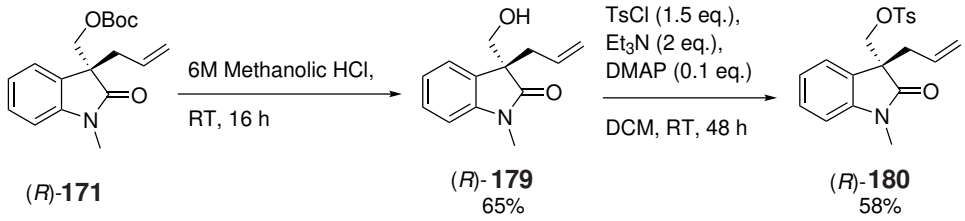

*Scheme 3.44: Deprotection of (R)-**171**, and subsequent tosylation, affording (R)-**180***

The procedure was also attempted with the opposite enantiomer BOX ligand, (4*R*,4'*R*,5*S*,5'*S*)-**181**, and polarimetry confirmed that (*S*)-**171** was indeed formed, in 86% and with an er of 77:23 (see appendix). This is shown in Scheme 3.45.

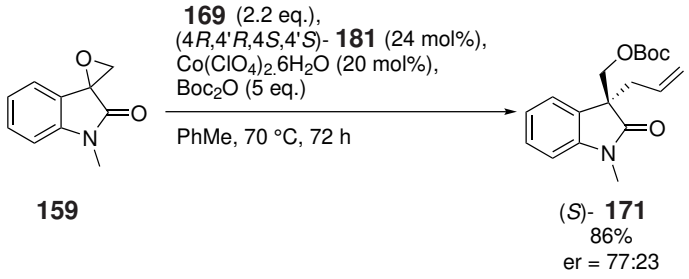

Scheme 3.45: Epoxide opening yielding opposite enantiomer products when using opposite enantiomer of BOX ligand, ***181***

Subsequent deprotection was performed with similar success (Scheme 3.46), with one sample shown to have an er of 83:17, as determined by chiral HPLC (see appendix). However, (*S*)-**179** was not subjected to further transformations at this time.

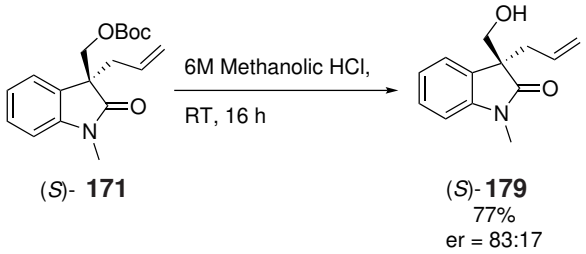

Scheme 3.46: Epoxide opening and deprotection, yielding opposite enantiomer products when using opposite enantiomer of BOX ligand, ***181***

3.4.7 Epoxide opening with dimethyl allyl boron trifluoride salt 170

Following the success of the epoxide opening with boron salt **169** affording compound **171**, attention turned to performing the reaction with the desired BF_3K salt, **170**. According to literature, **170** could be synthesised in two steps from readily available prenyl bromide, **151** (Scheme 3.47).

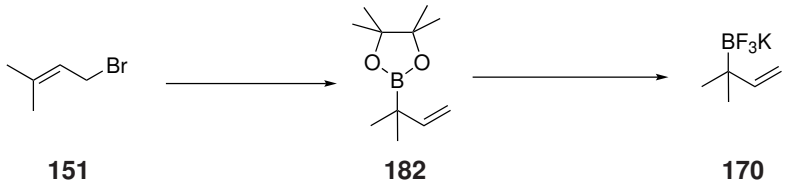

Scheme 3.47: Proposed two-step synthesis to access BF_3K salt ***170***

As seen in Scheme 3.48, the first step required the formation of a boron pinacol ester from bromide **151**. This was achieved using magnesium, generating a Grignard reagent with which HBpin reacts to afford

compound **182**.[166] NMR spectroscopy showed clean product, and thus, assuming quantitative yield the material was taken on crude to the next step.

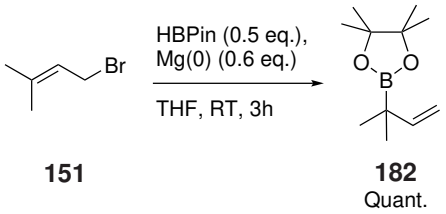

151 **182** Quant.

*Scheme 3.48: Conversion to pinacol ester **182***

Literature precedent showed many examples of boron pinacol esters being converted to BF_3K salts using KF.[167] The procedure did not, however, appear to yield any product by NMR or LCMS analysis.

A literature search also suggested a second method, converting the pinacol ester using KHF_2, another popular method for such conversions.[168] This procedure was proven to be a success, as shown in Scheme 3.49.

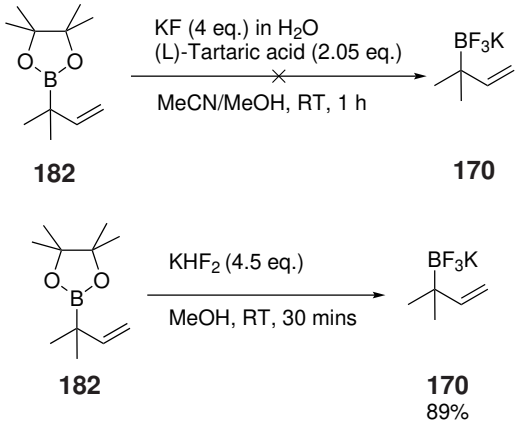

182 **170**

182 **170** 89%

*Scheme 3.49: Attempts to synthesise BF_3K salt **170***

Several methods of purification were attempted in order to remove the pinacol by-product, as if the product was impure the subsequent ring opening step proved difficult. Firstly, the procedure suggested that the crude product be concentrated, and then redissolved in 60% MeOH in water. This process was to be repeated until the pinacol peak (1.12 ppm) was no longer present. However, this was time-consuming and not always successful after multiple repeats. Therefore, after repeating this redissolution procedure three times, the crude mixture was then dissolved in acetone. Impurities precipitated out, and the mixture was filtered. The filtrate was then dissolved in ice-cold Et_2O. Any remaining pinacol was dissolved, and the

product could be filtered off as a white powder. This proved to be much cleaner than when these additional steps were absent, where a yellow gum was produced.

With compound **58** synthesised as in section 2.3.1, and with the desired starting materials in hand, the epoxide opening reaction could now be considered. It was determined that, as opposed to forming the desired compound, **160**, isomer (*R*)-**183** had instead been synthesised, in 34%. This is shown in Scheme 3.50.

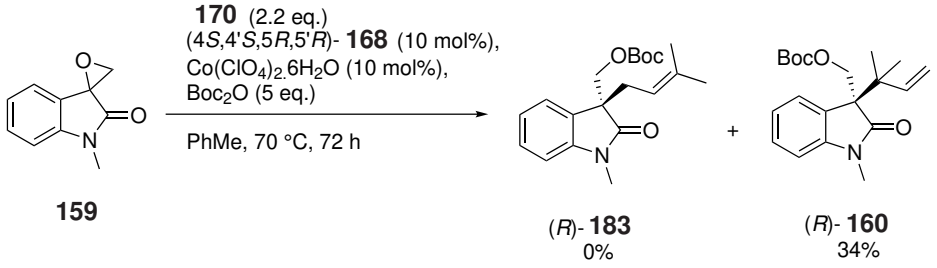

*Scheme 3.50: Epoxide opening with newly synthesised dimethyl allyl BF_3K salt **170**, which was expected to form compound **160**, but was shown to form compound **183***

The NMR spectrum indicated the presence of a terminal alkene, with the =CH peak showing characteristic *cis* and *trans* couplings at 11 and 18 Hz, respectively. The prenyl boron compound **170** had unexpectedly added exclusively at the γ-carbon, instead leading to the formation of **183** as opposed to **160**. There is literature precedent which supports this, with work by Hepburn also observing this reverse prenylation with prenyl boron compound **170**.[169] This work demonstrated that the same products were formed when the isomer of **170**, **184** was used, also. In Hepburn's work, these results were used to support the determination of the structure of the allylrhodium species which was leading to allylation, as shown in Scheme 3.51. It is assumed therefore that this is also the case in the work detailed herein.

Despite forming the wrong isomer during the prenylation, the subsequent reactions were performed as if **160** had in fact been formed, in order to test these steps. Therefore next, as with compound **171**, Boc-deprotection was required. The deprotection reaction, performed in methanolic HCl as previously, was anticipated for afford compound **161**, but instead afforded compound **185** in 99% yield, as shown in Scheme 3.52. An alkene would now be required, which could act as an internal dipolarophile in the cascade reaction. Though it was first proposed that this alkene be installed *via* a Grignard reaction, literature precedent guided the decision to install the alkene *via* an HWE reaction. This would first require the oxidation of the alcohol to its respective aldehyde, compound **162**, though this would of course not be the product

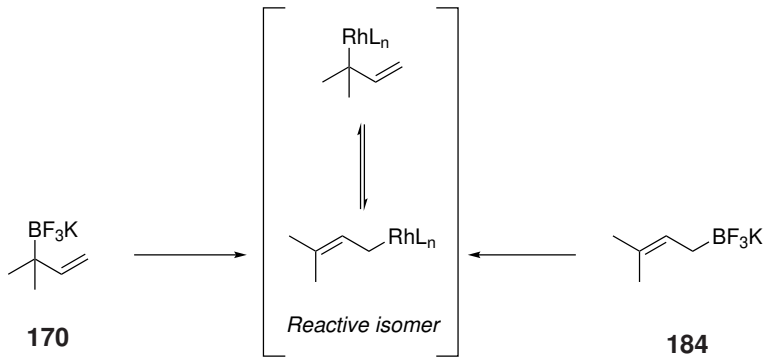

*Scheme 3.51: Work by Hepburn[169] showed that both prenyl boron compound **170** and its isomer **184** added at the α position, thereby leading to reverse prenylation, and this led to the determination of the structure of the reactive allylrhodium species used in Hepburn's work*

formed in this case - **186** would be the expected product now. This oxidation was attempted using the Swern oxidation method.

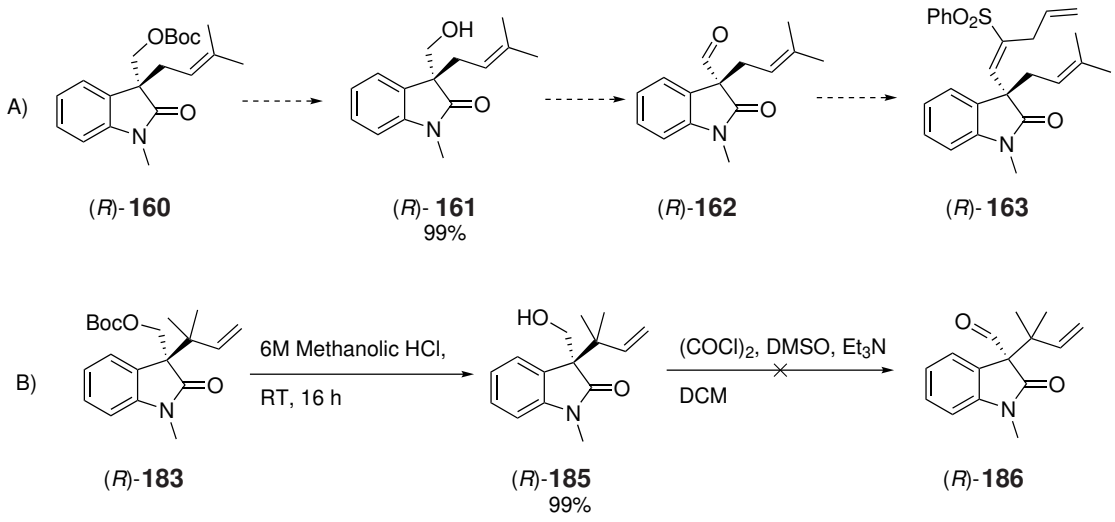

*Scheme 3.52: A) The planned subsequent steps B) The steps actually undertaken, due to the unexpected formation of **183***

The reaction was attempted several times. There was an indication that small amounts of product may have formed; analysis of some samples by LCMS indicated the desired mass ion was present, whilst NMR spectroscopy of unpurified samples did contain aldehyde peaks. This proved difficult to isolate, however, and other routes were once again considered. Now that it is understood that **160** was not formed, even if the Swern oxidation had been successful, the product formed (**186**) would not have been a desirable compound for the synthesis of the desired core structure in any case.

3.5 Racemic Synthesis *via* Epoxide

3.5.1 Retrosynthetic Analysis

Instead of trying to adapt the preexisting method to make it racemic, as in sections 3.4.3 or 3.4.5, a new route was proposed, based on racemic epoxide opening methods reported in the literature. The retrosynthetic analysis utilising this is given in Scheme 3.53. The racemic epoxide opening method means that this route negates the need for an asymmetric ligand, such as BOX ligand **168**, or even an achiral ligand such as **175**. Additionally, this epoxide opening method does not require Boc-protection of the alcohol during the epoxide opening step. Thus, instead of forming protected compound **171**, which subsequently requires deprotection, alcohol **179** is instead formed directly, reducing the number of steps to reach desired aldehyde **123**, prior to commencing the cascade chemistry. This is a simplified route, which would not see the installation of an internal dipolarophile. As such, cascade chemistry could be tested on nitrone **187** to test the applicability of this chemistry on an oxindole core, but this would be an intermolecular cycloaddition, as opposed to the originally proposed intramolecular cycloaddition.

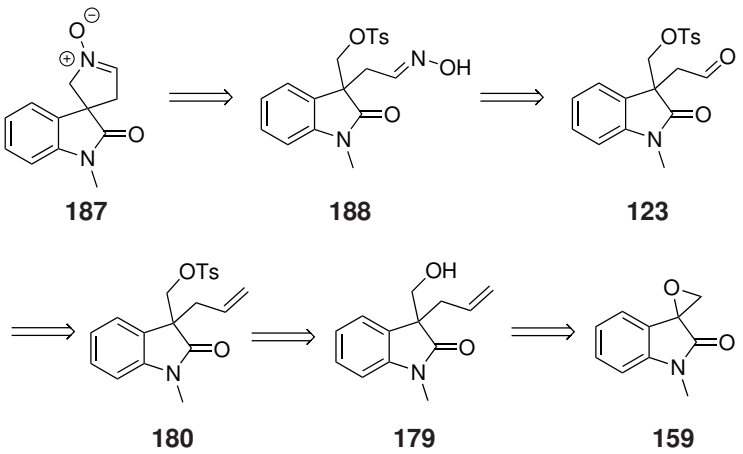

*Scheme 3.53: Retrosynthetic analysis to synthesise nitrone **187**, utilising racemic epoxide opening method*

3.5.2 Racemic Epoxide Opening

Epoxide **159** was again synthesised as in Section 3.4.2, but instead of being opened asymmetrically using ligand **168**, the intention was to open the epoxide to afford racemic alcohol **179**. A search of the literature identified two methods to achieve this conversion, both using allyltrimethylsilane, **189**. Both methods were

attempted.

The first method,[170] described by Sharma, suggested that the optimal reagent for this conversion was BF_3OEt_2. Whilst a number of conditions were varied, the article reported the best yields in DCM at 0 ℃, with the reaction running for 2 h. Most significantly, the maximum yield of 75% was obtained when 2 equivalents of BF_3OEt_2 were used. However, when 20 mol% of this Lewis acid was used, it was reported that formation of a spiro-annulated product, **190** was instead favoured.

The conditions for both of these reactions were repeated, and are summarised in both Scheme 3.54 and Table 3.11. Any **190** formed could, as detailed in the paper, be converted into desired product **179** by simply reacting further with 2 equivalents of **189**. This too was tested, and 50% yield was obtained from this conversion (Scheme 3.54).

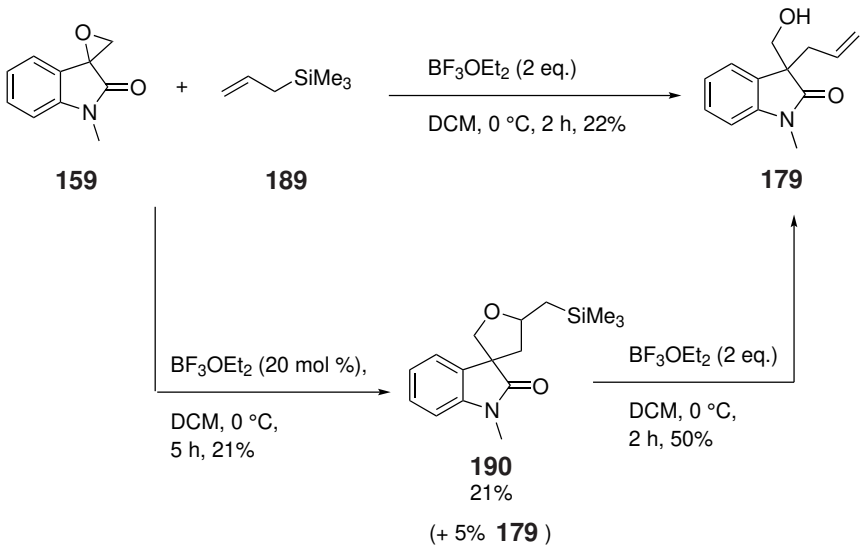

*Scheme 3.54: Epoxide opening using BF_3OEt_2, resulting in the formation of either **179** as desired, or undersirable **190***

In the alternative method, by Hajra *et al*,[171] scandium triflate is reported as the optimal Lewis acid catalyst, using MeCN as the solvent. The reaction, run at 0 ℃ for 1 h, used 10 mol% $Sc(OTf)_3$, and this was not varied throughout the study. Formation of **190** was reported, being formed in greatest yield when DCE was used as the reaction solvent, whilst still using the scandium catalyst. The optimal conditions were again repeated. As can be seen in Table 3.11, a 32% yield of the desired compound **179** was obtained, with no byproduct **190** formed in these conditions.

Table 3.11: Comparison of conditions for racemic epoxide opening

Entry	Conditions	Yield 179 /%	Yield 190 /%
1	BF_3OEt_2 (2 eq.), **189**, DCM, 0 ℃ - RT, 2 h	22	-
2	BF_3OEt_2 (20 mol%), **189**, DCM, 0 ℃, 30 min	5	21
3	$Sc(OTf)_3$ (10 mol%), **189**, MeCN, 0 ℃, 2 h	32	-

Both Sharma and Hajra propose that the reaction occurs through a Hosomi-Sakurai-type allylation, as shown in Scheme 3.55. It was proposed that the allylation proceeds through direct addition of the allyl group to the intermediate, following C-Si bond cleavage, whereas annulation occurs as a result of the β-silicon effect. It is clear from both studies that which product is formed in preference depends on various factors, including Lewis acid, stoicheometry of Lewis acid and solvent used.

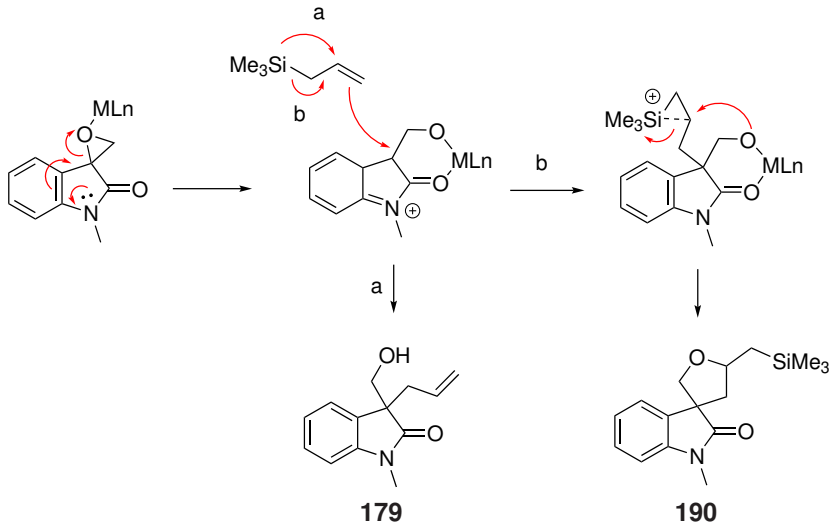

*Scheme 3.55: Proposed mechanism for epoxide opening, resulting in the formation of either **179** or **190***

Upon comparison of the results given in Table 3.11, the method where $Sc(OTf)_3$ was employed as the Lewis acid appeared to give the highest yield and was therefore used as the epoxide opening method in subsequent reactions.

3.5.3 Subsequent conversions to afford aldehyde 123

In contrast to the asymmetric method described in Section 3.4 which produced Boc-protected compound requiring deprotection, the free alcohol **179** produced from this epoxide opening was taken straight on to tosylation. The compound was tosylated using the conditions described in 3.4, resulting in a yield of 79%, as shown in Scheme 3.56.

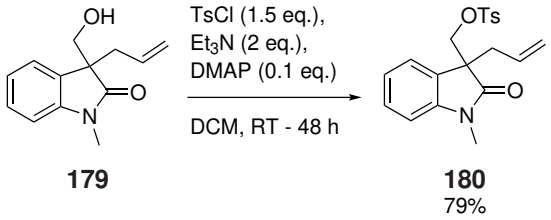

*Scheme 3.56: Tosylation to afford compound **180***

With the tosylated compound **180**, ozonolysis could be considered. This would afford compound **123**, the first example in this study where an aldehyde has been prepared which is suitable to trial cascade chemistry. This, too, was done using the procedure detailed in the paper by Hajra *et al.*[171] As shown in Scheme 3.57, this was achieved in a yield of 42%. Whilst lower yielding than was reported in literature (84%), the reaction was successful and the aldehyde **123** was ready to trial cycloaddition cascade reactions.

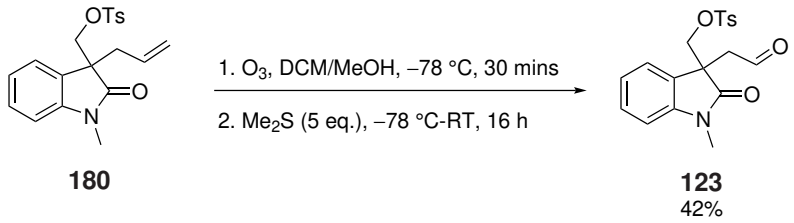

*Scheme 3.57: Ozonolysis to afford compound **123***

3.5.4 Intermolecular Cycloaddition Cascade Reactions

With aldehyde **123** in hand, it was now possible to test the cascade chemistry. Using hydroxylamine hydrochloride, oxime **188** could be formed. With the tosyl group acting as a leaving group, the oxime may then cyclise and form a nitrone (**187**). As there is no pre-installed alkene to act as an internal dipolarophile in compound **123**, an external dipolarophile must be added at this stage.

Oxime formation

Within the Coldham group, conditions had been developed for the synthesis and isolation of oximes, prior to cyclisation and cycloaddition. This involved reaction with hydroxylamine hydrochloride, using sodium acetate as the base, in MeOH, as in previous studies such as the synthesis of 19-hydroxyibogamine.[44]

These conditions were applied to aldehyde **123**. Whilst NMR spectroscopy showed complete loss of the aldehyde peak as expected, the integration of the aromatic region suggested the loss of the tosyl group, too. This led to the conclusion that, following formation of oxime **188**, subsequent cyclisation had occurred, affording compound **191**. However, in spite of the conversion seen by NMR, this compound was not isolated following column chromatography.

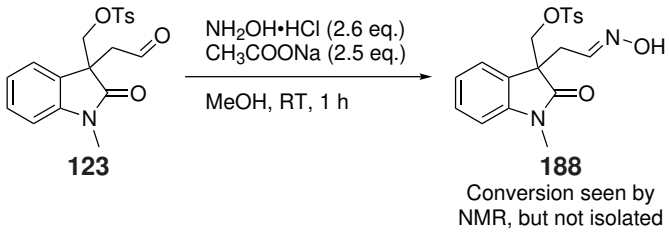

123 **188**
Conversion seen by NMR, but not isolated

*Scheme 3.58: Ozonolysis to afford compound **123***

Whilst this route may be viable if optimised, it was decided at this stage to also trial the complete cycloaddition cascade.

***N*-methylmaleimide 191 as external dipolarophile**

Dipolarophile *N*-methylmaleimide **192** has been used as an external dipolarophile in previous studies within the Coldham group.[40;172] It was proposed that **192** could be used as an external dipolarophile in the cycloaddition cascade of **123**, as shown in Scheme 3.59.

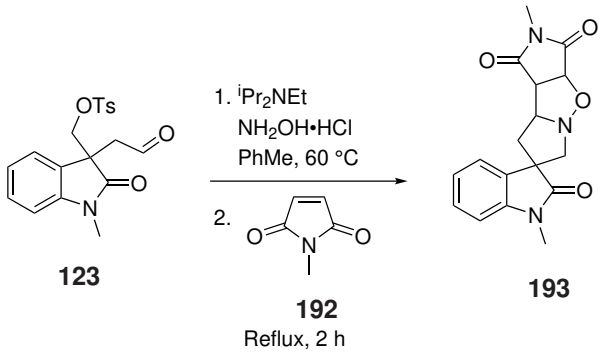

Scheme 3.59: General scheme of cascade reaction with N-methylmaleimide as an external dipolarophile

The reaction was first trialled using the conditions seen in the literature (Entry 1, Table 3.12), and then variations in hydroxylamine equivalencies and solvent were also tested (Entries 2-4, Table 3.12), in an attempt to optimise the reaction. In all entries shown in Table 3.12, the reaction time was determined by the point at which TLC indicated complete reaction, and is, therefore, variable between entries.

Table 3.12: Comparison of conditions for cycloaddition cascade with dipolarophile N-methylmaleimide

Entry	Eq. $NH_2OH.HCl$	Solvent	Reaction time	Outcome
1	1.3	PhMe	3 h at 60 °C (before addition of **192**) then overnight at reflux	64% of **193** isolated as diastereomeric mixtures
2	2.0	PhMe	2 h at 60 °C (before addition of **192**) then 3 h at reflux	62% of **193** with a single diastereoisomer isolated cleanly in 8%
3	2.3	PhMe	1 h at 60 °C (before addition of **192**) then 2 h at reflux	60% of **193** isolated as diastereomeric mixtures
4	2.3	Xylene	5 h at 60 °C (before addition of **192**) then 1.5 h at reflux	No reaction

Marginally, the best yield appears to have been obtained when the literature conditions were replicated (Table 3.12, Entry 1). However, in Table 3.12 Entry 2, a single isomer was isolated in an 8% yield following column chromatography, as part of a 62% overall yield, with the other samples containing mixtures of diastereoisomers. This proved difficult to replicate in all other samples, though the same column conditions were used. Therefore, the products obtained from this reaction were used to determine the isomer ratio, and the structure of the major isomer was able to be determined. This is shown in Scheme 3.60. Although these conditions led to a slightly lower yield than those in Table 3.12 Entry 1, with the clean isolation of a single isomer these conditions were selected for future work.

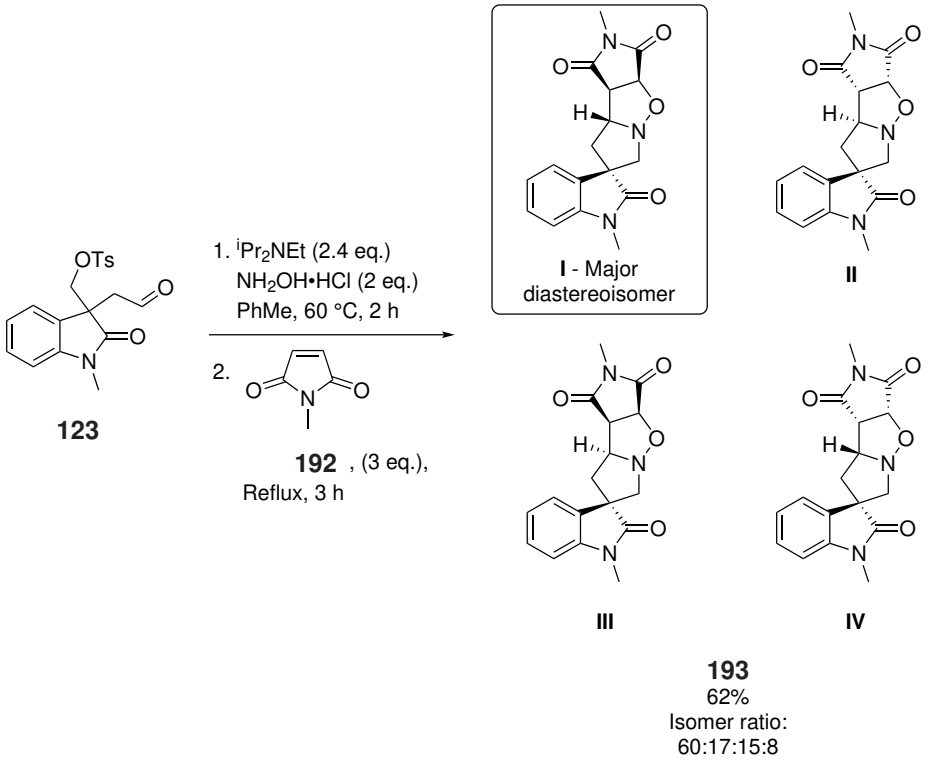

Scheme 3.60: Cascade reaction with N-methylmaleimide as an external dipolarophile

Four diastereoisomers were determined to be present, based upon the proton NMR spectra of products isolated by column chromatography. This ratio was determined from the ^{1}H NMR spectra by integrating the peaks corresponding OC–H. The peak values are detailed in Table 3.13.

*Table 3.13: Details of the peaks in the proton NMR spectra of the isomers of **193** used to determine the isomer ratio*

Peak /ppm	Relative Integration	Multiplicity	J value /Hz
5.07	0.60	d	7.5
5.04	0.08	d	8.0
5.03	0.15	d	7.5
5.00	0.17	d	8.0

The structure of the major isomer was determined to be that given in Figure 3.12, isomer I in Scheme 3.60. This isomer was cleanly separated from the mixture. Unfortunately, while a variety of solvent systems were tested, it didn't prove possible to crystallise this compound in order to obtain a crystal structure. Therefore, 2D NOESY NMR analysis was used in order to determine the structure.

Table 3.14: Correlations highlighted by NOE analysis

Irradiated Peak (and assignment)	Peaks showing space close-in-space contact
5.1 ppm (H^f)	3.7 ppm (H^e)
4.24 ppm (H^d)	7.23 ppm (H^a)
	3.7 ppm (H^e)
	3.44 ppm (H^g)
	2.25 ppm (H^b)
3.88 ppm (H^h)	3.44 ppm (H^g)
3.7 ppm (H^e)	5.1 ppm (H^f)
	2.56 ppm (H^c)
3.44 ppm (H^g)	7.23 ppm (H^a) (weak correlation)
	3.88 ppm (H^h)
2.56 ppm (H^c)	5.1 ppm (H^f) (weak correlation)
	4.24 ppm (H^d) (weak correlation)
	3.7 ppm (H^e)
	2.25 ppm (H^b)
2.25 ppm (H^b)	7.23 ppm (H^a) (weak correlation)
	4.24 ppm (H^d)
	2.56 ppm (H^c)

The NOE analysis highlighted several close-in-space correlations, detailed in Table 3.14. The 3-dimensional explanation of this is shown in Figure 3.13. When protons b, d and g were irradiated, each showed a close-in-space relationship with the benzene ring proton at 7.23 ppm (H^a). This indicates that protons b, d and g must be on the same face of the molecule, but that this must position them close to the aromatic proton, H^a. This led to the assignment of the stereochemistry at the oxindole chiral centre. When H^e was irradiated, it was shown to be close in space to H^f, but not to H^d. This indicates that proton e and f are positioned on the same face of the molecule, but it is likely that this is on the opposite face to proton d, helping to assign the stereochemistry at the remaining chiral centres.

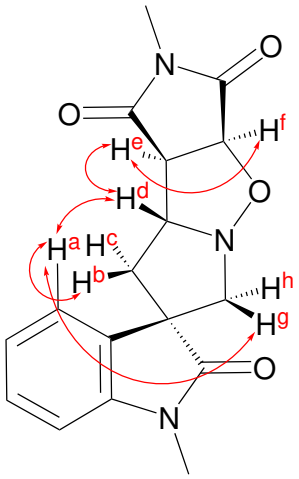

Figure 3.12: Structure of the major isomer, as determined by 2D NOESY NMR analysis, with key correlations shown by red arrows

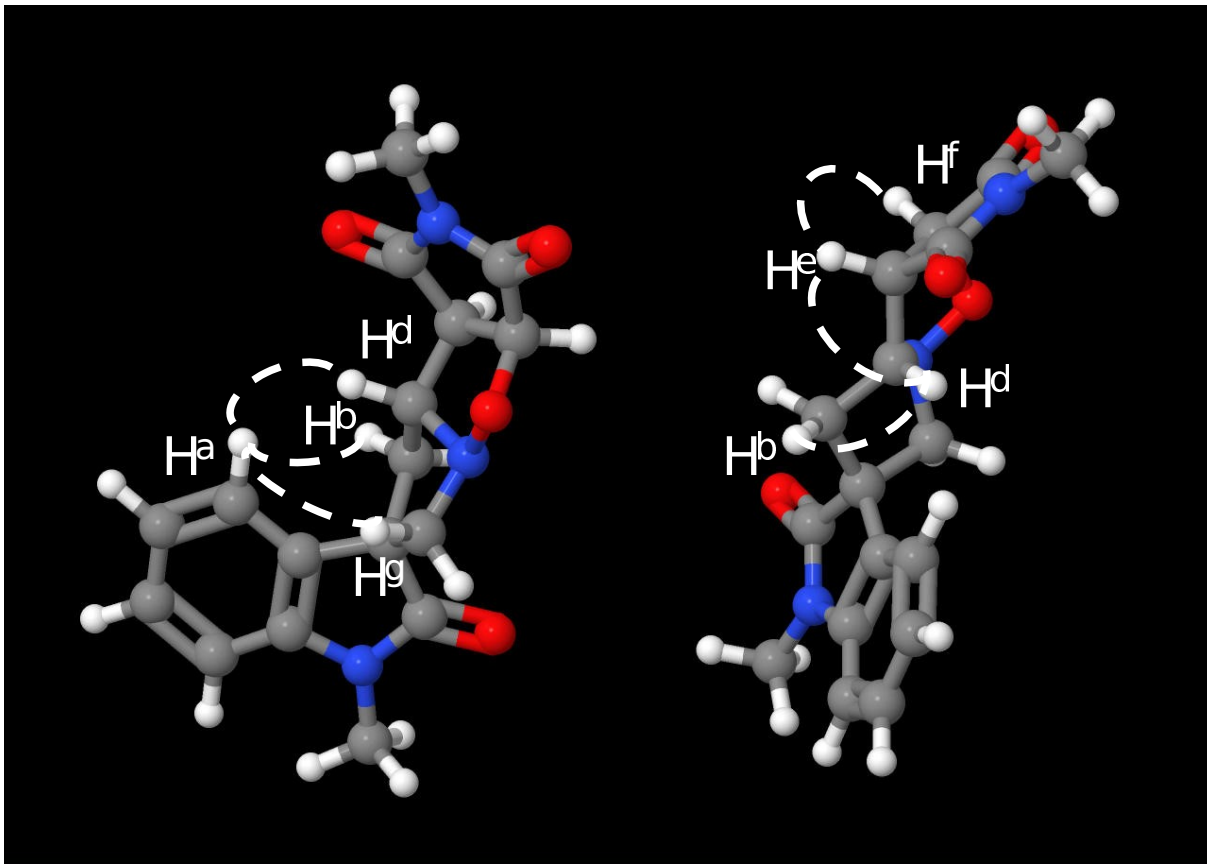

Figure 3.13: 3-dimensional model of the structure of the major isomer, as determined by 2D NOESY NMR analysis, with key correlations shown by dotted white lines

N-phenylmaleimide 193 as external dipolarophile

Following the success of the cascade reaction using **192**, the next dipolarophile tested was *N*-phenylmaleimide **194**, using the optimised conditions determined in Table 3.12. Again, this dipolarophile had been used in nitrone cycloadditions in the group previously.[172]

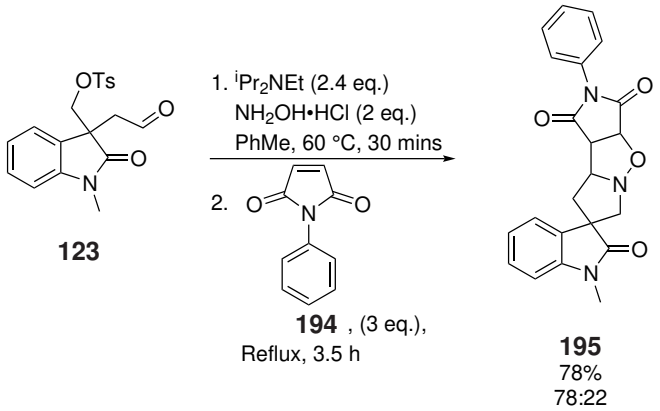

Scheme 3.61: Cascade reaction with N-phenylmaleimide as an external dipolarophile

Using the best conditions from earlier, a mixture of isomers of heterocycle **195** was isolated in 78% yield. Further purification attempts were made with the view to separate these diastereoisomers, but unfortunately, these proved futile. So, too, did purification by recrystallisation. Therefore, the diastereomeric ratio of the mixture was determined. Only two isomers were detected, present in a ratio of 78:22, again determined by integration of the OC–H peaks, shown in Table 3.15.

*Table 3.15: Details of the peaks in the proton NMR spectra of the isomers of **195** used to determine the isomer ratio*

Peak /ppm	Relative Integration	Multiplicity	J value /Hz
5.21	0.78	d	7.5
5.15	0.22	d	8.0

Dimethyl fumarate 195 as external dipolarophile

Next, dimethyl fumarate **196** was used as the external dipolarophile.[172] Alkene **196** is the *E*-isomer of dimethyl but-2-enedioate, and it is expected that the ester groups installed will therefore have a *trans* relationship, due to the concerted, suprafacial nature of dipolar cycloaddition reactions.

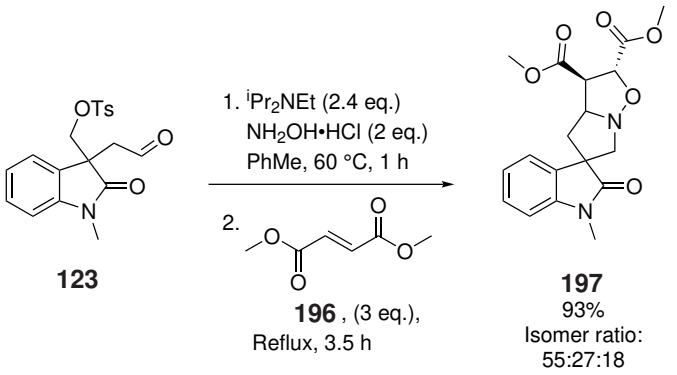

Scheme 3.62: Cascade reaction with dimethyl fumarate as an external dipolarophile

A mixture of diastereoisomers of **197** was isolated in 93% yield. Integration of the OC–H peaks is given in Table 3.16, and these were used to determine the ratio of diastereoisomers, which was 55:27:18.

*Table 3.16: Details of the peaks in the proton NMR spectra of the isomers of **197** used to determine the isomer ratio*

Peak /ppm	Relative Integration	Multiplicity	J value /Hz
5.22	0.55	d	5.0
5.09	0.18	d	6.0
5.06	0.27	d	8.0

Once again, the cycloadduct proved difficult to recrystallise, though various conditions were trialled. Given that the isomers were not separated, no structure was determined for any of the diastereoisomers formed. However, the ester groups are assumed to have a *trans* relationship, based on the geometry of the alkene in starting material **196**.

Dimethyl maleate 197 as external dipolarophile

Next, dimethyl maleate **198**, the stereoisomer of **196**, was used as the dipolarophile. The expectation here was that, using the *Z*-alkene starting material, the ester groups would now be *cis* in the products formed.

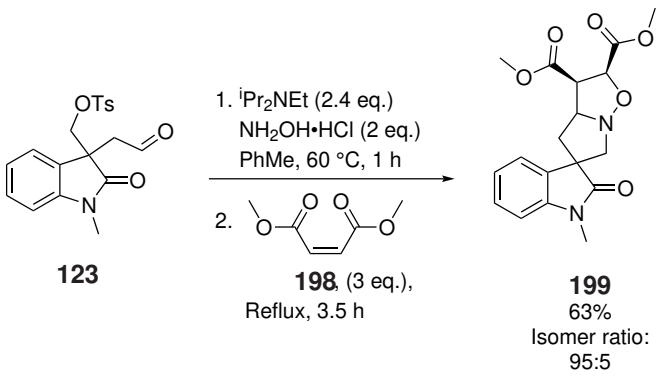

Scheme 3.63: Cascade reaction with dimethyl maleate as an external dipolarophile

A mixture of diastereoisomers was isolated in 63%, with a 95:5 ratio of isomers. Once again, integration of the OC–H peaks was used to determine the ratio of diastereoisomers, with details given in Table 3.17.

*Table 3.17: Details of the peaks in the proton NMR spectra of the isomers of **199** used to determine the isomer ratio*

Peak /ppm	Relative Integration	Multiplicity	J value /Hz
5.14	0.95	d	8.5
5.09	0.05	d	6.0

In this case, the structure of the major diastereoisomer was determined to be that which is given in Scheme 3.64. As was expected based on previous work, attempts at recrystallisation proved futile, and therefore 2D NOESY NMR spectroscopy was used to garner structural information, which is shown in Table 3.18.

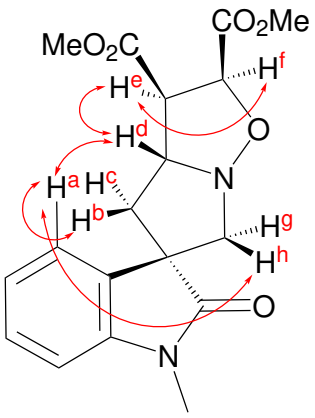

*Scheme 3.64: Structure of the major diastereoisomer of **199**, as determined by NOE analysis*

As predicted based on the configuration of the groups in the starting material, **198**, the ester groups

retained their *cis* relationship, showing clear close-in-space correlations in the NOE NMR spectrum. This and other correlations shown by NOESY analysis are shown in Table 3.18.

Table 3.18: Correlations highlighted by NOE analysis

Irradiated Peak (and assignment)	**Peaks showing close-in-space contact**
7.43 ppm (H^a)	4.48 ppm (H^d)
	3.44 ppm ($H^{g/h}$)
	2.32 ppm (H^b)
5.14 ppm (H^f)	4.05 ppm (H^e)
	3.44 ppm ($H^{g/h}$)
	2.45 ppm (H^c)
4.48 ppm (H^d)	7.46 ppm (H^a) (weak correlation)
	4.05 ppm (H^e)
	2.45 ppm (H^c)
	2.32 ppm (H^b)
4.05 ppm (H^e)	5.14 ppm (H^f)
	4.48 ppm (H^d)
	3.44 ppm ($H^{g/h}$)
	2.45 ppm (H^c)

The 3-dimensional structure determined on the basis of these correlations is further explained by the model in Figure 3.14. Proton d at the N-C chiral centre showed a close-in-space correlation with proton e, but not to proton f, as in the previous case with cycloadduct **193**. This once again led to the determination that whilst protons e and f had a *cis* relationship, H^d sat on the opposite side of the molecule.

Once again, the correlation between the aromatic proton at 7.46 ppm (H^a) with nearby protons c and g/h was used to determine the configuration at the spirocyclic ring junction, with the correlation between H^c and H^d indicating that these too both sit on the same face of the molecule.

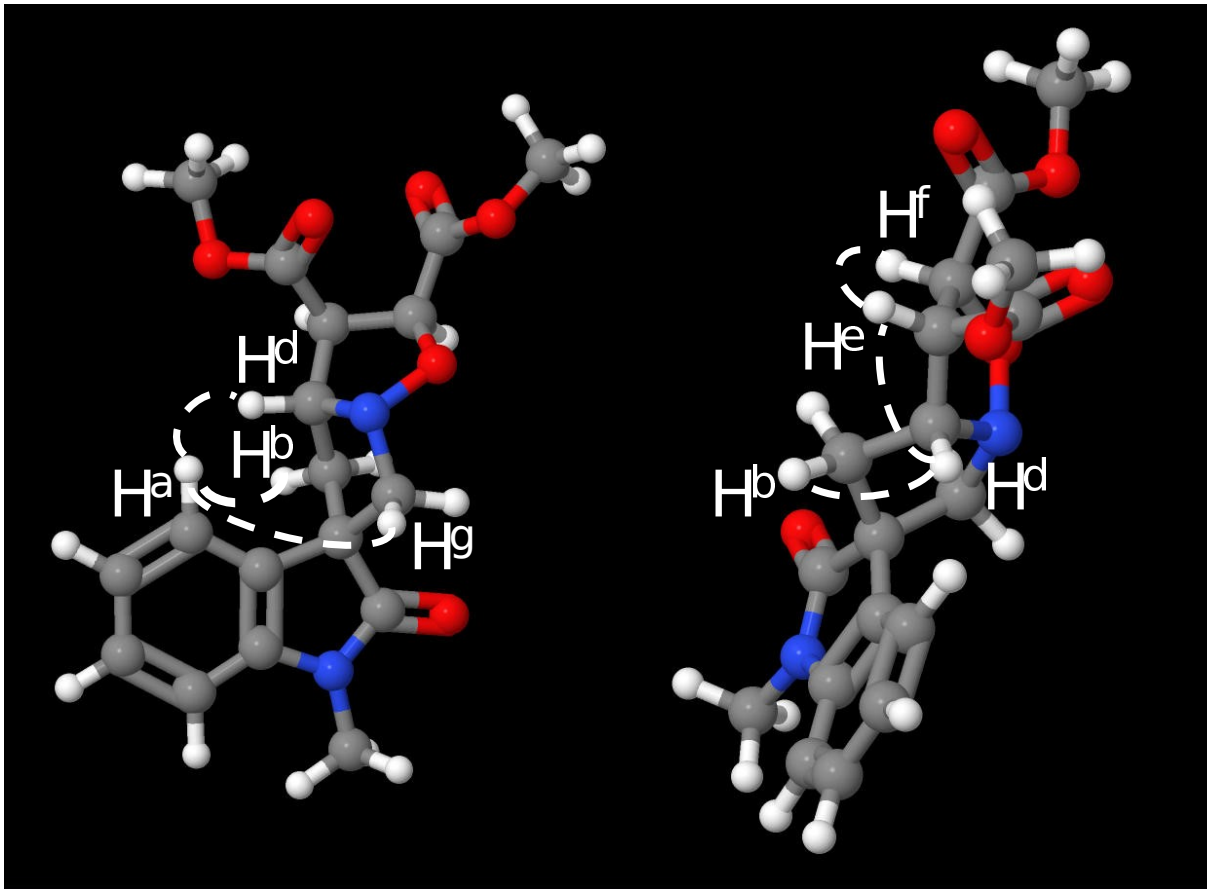

*Figure 3.14: 3-dimensional model of the structure of the major isomer of **199**, as determined by 2D NOESY NMR analysis, with key correlations shown by dotted white lines*

The major diastereoisomers of both **193** and **199** were determined by NOE analysis. Both were shown to have the same relationship between protons E and D (Figure 3.15), with these protons positioned on opposite faces. This suggests that the formation of the *endo*-product is favoured in this reaction.

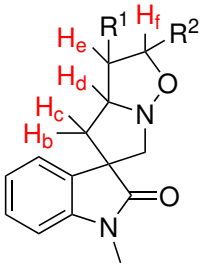

Figure 3.15: General structure of cycloadducts, highlighting labelling of protons

Having determined the structure of the major diastereoisomers of cycloadducts **193** and **199**, the coupling constants for these products could be used, alongside the Karplus equation (3.1), to infer stereochemical information about the major configuration of the other cycloadducts. In each cycloadduct

(**193**, **195**, **197** and **199**), proton H_d may couple to protons H_b, H_c and H_e.

$$J(\theta) = ACos^2\theta + BCos\theta + C \tag{3.1}$$

As can be seen in Table 3.19, the coupling for proton H_d differs between cycloadducts, and this may be used to draw conclusions about the relationship between protons D and E.

Table 3.19: Analysis of coupling constants and their implications on the configuration of diastereoisomers.

Compound	**H_d shift /ppm**	**Multiplicity**	**Coupling to H_e /Hz**	**Proposed dihedral angle, θ /°**
193	4.25	ddd	1.5	90
195	4.34	dd	-	90
197	4.40	dt	7	120
199	4.48	td	8	120

First considering structurally related cycloadducts **193** and **195**, the data suggest that the major isomer has the same structure in both cases. In **193**, H_d couples to H_e with a *J* value of 1.5 Hz, which suggests that the dihedral angle, θ, is close to 90 degrees. In compound **195**, H_d does not show coupling to H_e, which would suggest that θ = 90°. This suggests the same relative configuration at these centres, and therefore that the major product in this case is also the *endo* product.

Compounds **197** and **199** show larger coupling constants of 7 and 8 Hz, respectively. This suggests that the dihedral angle between H_d and H_e is either around 45 or 120 degrees. In the case of **199**, NOE has shown that H_d and H_e are on opposite faces. Whilst both 45 and 120 degrees may both be plausible in this configuration, a 120-degree angle is more likely, considering ring strain.

In the case of compound **197**, it is expected that the ester groups originating from the dipolarophile will have a *trans* relationship, owing to the concerted and suprafacial nature of cycloaddition reactions. If H_d and H_e were *cis* in this case, the dihedral angle would likely be 0, leading to a much larger *J* value than the 8 Hz observed. Once again, a coupling constant of 8 Hz would likely imply that in the major diastereoisomer of **197**, θ = 120°.

These coupling constants would suggest that, in all four cycloadducts, protons H_d and H_e are positioned on opposite faces of the molecule, thereby suggesting that in all four reactions, the *endo* product is favoured. Further NOE analysis or X-ray crystal structures on all products would assist further in confirming these assignments, and would also enable the stereochemistry at the oxindole stereocentre to be assigned.

3.5.5 N-O Bond cleavage

Next, the cleavage of the N-O bond was considered. This has been performed in several works by the Coldham group,[12;44;172] as well as in related work by Padwa and co-workers.[85;83;79] In the Coldham group, the reduction has been performed by zinc in acetic acid, which has predominantly been performed at 70 °C.

In simplified cases such as that detailed in a 2019 paper from the Coldham group,[44] cleavage of the N-O bond leads to the formation of an amino alcohol. In the 2019 paper, the formation of this amino alcohol allowed for further functionalisation which ultimately led to the formal synthesis of 19-hydroxyibogamine, **20** (Scheme 3.65).

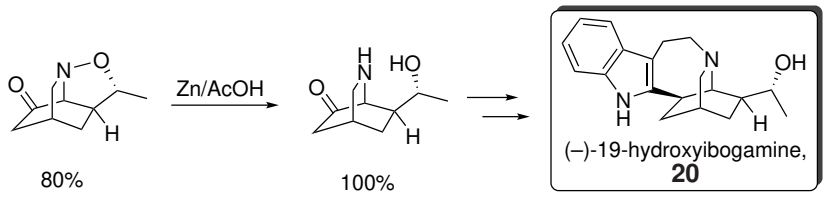

*Scheme 3.65: N-O bond cleavage with Zn/AcOH in synthesis of **20**[44]*

In a 2017 paper from the group, whilst some reported examples of N-O cleavage did lead to the formation of amino alcohols, some more complex examples did not.[12] As shown in Scheme 3.66, in cases where an ester is present in an appropriate position within the molecule, the amine formed can cyclise onto the ester to give the lactam product.

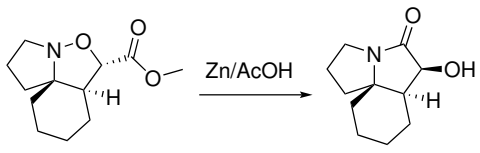

Scheme 3.66: Example of N-O bond cleavage with Zn/AcOH followed by lactamisation from the Coldham group[12]

Therefore, compounds **197** and **199** were interesting candidates for the N-O bond cleavage, with

the expectation that the Zn reduction to form **200** would be followed by subsequent cyclisation to afford the lactam, **201**. The reaction was first trialled using conditions proposed in Coldham group literature, to synthesise lactam **201**, as shown in Scheme 3.67.[12]

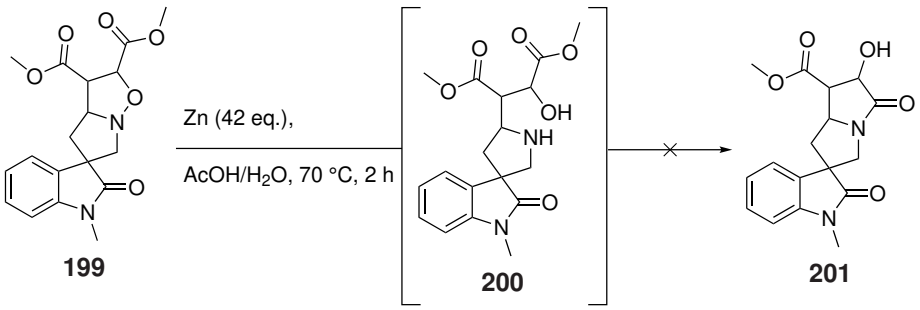

Scheme 3.67: Attempted N-O bond cleavage with Zn/AcOH

Due to a calculation error, in this particular example, 42 equivalents of zinc were used, as opposed to the necessary 4.2 equivalents. Nevertheless, it was expected that the reaction would still progress, but after 2 hours the TLC remained unchanged. It was considered that sonication could be used here, as opposed to heating. This was next trialled on a new sample of **197**, using 4.2 equivalents of Zn (Scheme 3.68).

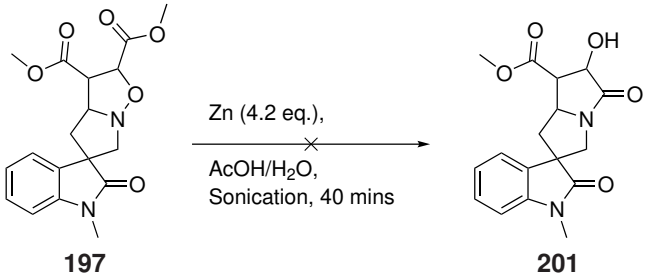

Scheme 3.68: Attempted N-O bond cleavage with Zn/AcOH, using sonication

In this case, a new spot did seem to emerge by TLC, and therefore the reaction was worked up and purified by column chromatography. The proton NMR spectrum appeared messy and difficult to interpret, so an LCMS was also run on a sample obtained from the purification. The LCMS trace appeared relatively clean, showing a clear major peak, the mass of which corresponded to the starting material mass +2. This does not align with the peak representing starting material **197**, or the expected lactam product **201**.

This mass could correspond, however, to the amino alcohol product **200**. As it was not possible to interpret the NMR, the reaction was then repeated. The conditions above were repeated on two occasions, but following column chromatography only starting material was recovered, as seen by NMR spectroscopy

and LCMS analysis.

This did however highlight that the LCMS spectrum of recovered starting material was indeed different to the LCMS spectrum seen after the previous reduction attempt, with the starting material ion (m/z 361.1) being observed at 6.90 min, whilst the previous peak (m/z 363.2) was observed at 5.36 min. It is therefore still possible that this did contain amino alcohol, as this would afford the m/z observed, but this could not be fully characterised. However, it seems unlikely that this would not cyclise to form the lactam as in other iterations, and the result could not be replicated in later attempts.

It was therefore concluded that the N-O bond cleavage and subsequent lactamisation did not appear to occur under the provided conditions.

3.6 Conclusions and future work

To summarise, though the work detailed within this chapter has shifted focus significantly throughout the course of the project, intermolecular cycloaddition with several dipolarophiles on an oxindole core proved a success. This validates the use of the cascade condensation, cyclisation and cycloaddition reaction on oxindole cores such as those found in alkaloids from plants of the *Alstonia* genus. At this time, no route has been found to install an internal dipolarophile and allow for intramolecular cycloaddition, which would enable access to larger core structures.

Within this work, a racemic route was found that enabled the formation of the desired aldehyde, **123**, in just 4 steps. The aldehyde was then reacted with several dipolarophiles; *N*-methylmaleimide, *N*-phenylmaleimide, dimethyl maleate and dimethyl fumarate. The ratio of diastereoiomers formed in each of these reactions was determined, and the structure of two of the major isomers was determined through 2D NOESY NMR analysis.

In the future, the route detailed in section 3.4 could be revisited. In spite of consistently low yields, BOX ligand **168** can be synthesised, and used as shown herein as a ligand in the asymmetric epoxide opening reaction. Though er was determined to be 84:16, which is lower than reported in the literature, the asymmetrically formed compound could be deprotected and tosylated, as in Scheme 3.44. Assuming that ozonolysis of this compound would be successful, as was the case with the racemic version, the cycloadditions detailed in section 3.5.4 could be performed on enantioenriched compound instead.

To prove a broad scope for this reaction, the cascade chemistry could be performed with a wider range of dipolarophiles. Cleavage of the N-O bond by zinc reduction is still desirable, and with more time this reaction could be reattempted, varying conditions to see if the reaction is possible. The LCMS result that indicated that the amino alcohol may have formed has not been validated, as supporting data was not obtained, but could be a promising indication that the reaction may be possible.

In the early stages of this work, it was hoped that the oxindole cores synthesised could be tested for biological activity, in collaboration with Keele University. This would still be a desirable outcome, given the use of plants containing oxindole alkaloids in the traditional treatment of malaria, and the commonality of biological activities in alkaloids. Future work should aim towards building a library of analogues through variation of dipolarophiles, which could then be submitted to such tests.

Chapter 4: Experimental

4.1 General Reagent Information

All reagents were obtained from commercial suppliers. Unless otherwise stated, these were used without further purification. Solvents were obtained from commercial suppliers or, in the case of dry solvents, from a Grubbs dry solvent system (model SPS-200 or SPS-400) when not purchased from commercial suppliers.

4.2 General Analytical Information

Thin layer chromatography (TLC) performed on Merck silica gel 60 F_{254} plates, visualised either by UV irradiation at 254 nm or by staining with an alkaline $KMnO_4$ dip. Flash column chromatography was carried out on Geduran silica gel (40-63 micron mesh). Petrol refers to petroleum ether, b.p. 40–60 °C. Unless otherwise stated, ^{1}H proton NMR spectra were recorded on a Bruker AC400 spectrometer (400 MHz), with experiments performed at room temperature in deuterated chloroform, deuterated acetonitrile or hexadeuterodimethyl-sulfoxide. All chemical shifts are expressed in parts-per-million (ppm) with respect to residual solvent peaks. Coupling constants (*J*), given in Hz, are quoted to the nearest 0.5 Hz. Multiplicity is indicated by the following abbreviations (s = singlet, d = doublet, t = triplet, q = quartet, quin = quintet, sep = septet, m = multiplet, br = broad). ^{13}C NMR were recorded on the above instrument at 101 MHz. ^{31}P NMR were recorded on the above instrument at 162 MHz. Low and high resolution (accurate mass) mass spectra were recorded on a Micromass Autospec for Electron Impact (EI) and on an Elmer Spectrum RX Fourier Transform IR System. Absorption maxima are given in cm^{-1}. Infrared (IR) spectra were recorded on a Perkin-Elmer Spectrum RX Fourier Transform IR System. Melting points were recorded using a Gallenkamp hot stage and were uncorrected. Specific rotations were calculated from optical rotations recorded on an AA-10 automatic polarimeter. Resolution between enantiomers was achieved using a Beckman system fitted with a Daicel ChiralPak AD-H column (250 nm x 4.60 mm i.d.) as the stationary phase with a mixture of *n*-hexane:isopropanol as the mobile phase at the flow rates specified, at ambient temperature, with detection by UV absorbance at 254 nm.

4.2.1 Experimental Procedures and Data

(*Z*)-1,1,8,8-Tetramethoxyoct-4-ene (30)

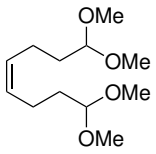

Cyclooctadiene **29** (10.0 g, 92.4 mmol) was dissolved in DCM (100 mL) and MeOH (100 mL), then cooled to –78 °C. Ozone was bubbled through the solution for 2 h, then excess ozone was removed by bubbling argon gas through the solution for 10 min. Next, $TsOH.H_2O$ (1.32 g, 6.93 mmol) was added. The mixture was warmed to RT and stirred for a further 2 h, prior to addition of dimethyl sulfide (51.3 mL, 693 mmol). The reaction mixture was stirred at RT for 16 h, then concentrated under reduced pressure. The residue was dissolved in DCM (30 mL), washed with $NaHCO_3$ (30 mL), dried ($MgSO_4$), filtered and concentrated under reduced pressure. The residue was purified by column chromatography on silica gel, eluting with EtOAc–petrol (1:9 to 1:4), affording 12.6 g of an impure oil.

As the oil was still impure, a reduction reaction was performed in order to remove deprotected aldehyde **56**. The residue was dissolved in MeOH (200 mL) at 0 °C, and $NaBH_4$ (600 mg, 15.9 mmol) was added. The mixture was stirred at 0 °C for 30 min. When TLC indicated the reaction was incomplete, a further 3 batches of $NaBH_4$ (3 × 600 mg, 15.9 mmol) were added over 1.5 h, at which time TLC indicated the reaction had gone to completion. The reaction mixture was concentrated under reduced pressure. The residue was redissolved in EtOAc (30 mL), washed with water (30 mL) and brine (30 mL), dried ($MgSO_4$), filtered and concentrated under reduced pressure. The residue was purified by column chromatography on silica gel, eluting with EtOAc–petrol (1:4) to afford compound **30** (4.07 g, 19%) as a colourless oil; $\mathbf{R_f}$ 0.67 [EtOAc–petrol (1:1)]; ^{1}**H NMR** (400 MHz, $CDCl_3$) δ 5.44–5.32 (2H, m, 2 × =CH), 4.36 (2H, t, *J* = 6.0 Hz, 2 × CH), 3.31 (12H, s, 4 × CH_3), 2.10 (4H, td, *J* = 8.0, 6.0 Hz, 2 × CH_2), 1.69–1.59 (4H, m, 2 × CH_2); ^{13}**C NMR** (101 MHz, $CDCl_3$) δ 129.5 (2 × =CH), 104.1 (2 × CH), 52.8 (4 × CH_3), 32.5 (2 × CH_2), 22.5 (2 × CH_2). Spectroscopic data in accordance with literature values.[88]

4,4-Dimethoxybutanal (31)

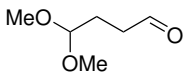

Compound **30** (4.07 g, 17.5 mmol) was dissolved in DCM (100 mL), and cooled to –78 °C. Ozone was bubbled through the solution for 1 h. Argon was then bubbled through the solution for 10 min, before PPh_3 (6.89 g, 26.3 mmol) was added. The mixture was then warmed to RT and stirred for 1 h, before being concentrated under reduced pressure. The residue was purified by distillation under reduced pressure (vapour temperature 62 °C under house vacuum) to give aldehyde **31** (1.71 g, 74%) as a colourless oil; $\mathbf{R_f}$ 0.52 [EtOAc–hexane (1:1)]; **^{1}H NMR** (400 MHz, $CDCl_3$) δ 9.76 (1H, t, *J* = 1.5 Hz, O=C–H), 4.37 (1H, t, *J* = 5.5 Hz, CH), 3.32 (6H, s, 2 × CH_3), 2.50 (2H, td, *J* = 7.0, 1.5 Hz, CH_2), 1.93 (2H, td, *J* = 7.0, 5.5 Hz, CH_2); **^{13}C NMR** (101 MHz, $CDCl_3$) δ 201.8 (C=O), 103.9 (CH), 53.5 (CH_3), 39.0 (CH_2), 25.5 (CH_2). Spectroscopic data in accordance with literature values.[88]

Alternatively, compound **31** was also synthesised *via* the following method:

To **69** (3.10 g, 19.7 mmol) dissolved in DCM (105 mL) at –78 °C, DIBAL-H (23.3 mL, 1.1 M in cyclohexanes) was added, and the mixture was stirred at –78 °C for 4 h. The mixture was allowed to warm to RT, then quenched with NH_4Cl (30 mL) and Rochelle salt (30 mL) and stirred vigorously for 1 h. The mixture was extracted with DCM (3 × 20 mL) and the combined organic layers were washed with brine (10 mL), dried ($MgSO_4$), filtered and concentrated under reduced pressure. The residue was purified by column chromatography on silica gel, eluting with EtOAc–hexane (1:4) to afford compound **31** (168 mg, 33%) as a colourless oil. Data as above.

5-(Phenylsulfonyl)octa-4,7-dienal (E/Z mixture) (53)

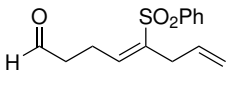

Z

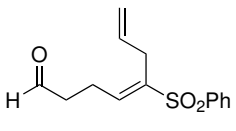

E

Dimethoxytetrahydrofuran **75** (10.0 g, 75.7 mmol) was added to HCl (37.8 mL, 1 M, 37.8 mmol) and stirred at RT for 3 days. The pH was adjusted to approximately pH 7 with $NaHCO_3$ (3.10 g). The organic

product was extracted with EtOAc (3 × 20 mL), and the combined organic layers were washed with brine (20 mL), dried ($MgSO_4$), filtered and concentrated under reduced pressure to afford a crude mixture of succinaldehyde **74** and starting material **75** (1.27 g, 17% yield of **74** as determined from NMR spectroscopy, as part of a mixture of **74**:**75** in a 1:1 ratio) as a colourless oil; **^{1}H NMR** (400 MHz, $CDCl_3$) δ 9.82 (2H, s, C(=O)H), 2.81 (4H, s, 2 × CH_2). Spectroscopic data in accordance with literature values,[173] taken crude to the next step.

Phosphonate **58** (3.43 g, 10.3 mmol) and NaH (411 mg, 17.1 mmol, 60% in mineral oil) were stirred in THF (15 mL) at 0 ℃ for 50 min. The mixture was added to aldehyde **74** (1.27 g, 13.8 mmol) in THF (15 mL) and stirred at RT overnight. The reaction was quenched with MeOH, then the mixture was concentrated under reduced pressure. The residue was purified by column chromatography on silica gel, eluting with EtOAc–hexane (1:4) to afford compound **53** (225 mg, 6%) as a yellow oil, as a mixture of isomers (ratio 13:87 E:Z); **R_f** = 0.61, 0.45 [EtOAc–petrol (1:1)]; **FT-IR** ν_{max} (film)/cm^{-1} 2951, 2722 (C–H), 1714 (C=O), 1640, 1613, 1494, 1470, 1446, 1378, 1353, 1303 (S=O), 1175, 1147, 1122, 1084, 1033, 1010, 982, 818, 754; **^{1}H NMR** (400 MHz, $CDCl_3$) δ 9.77 (1H, t, *J* = 1.0 Hz, C(=O)H), 7.95–7.88 (2H, m, 2 × ArH), 7.67–7.59 (1H, m, ArH), 7.59–7.53 (2H, m, 2 × ArH), 6.98 (0.13H, t, *J* = 7.5 Hz, =CH^E), 6.04 (0.87H, tt, *J* = 8.0, 1.5 Hz, =CH^Z), 5.64 (0.87H, ddt, *J* = 17.0, 10.0, 6.5 Hz, =CH^Z), 5.56–5.41 (0.13H, m, =CH^E), 5.09 (1H, dtd, *J* = 10.0, 2.5, 1.5 Hz, =CH), 5.04 (0.87H, dtd, *J* = 17.0, 3.0, 1.5 Hz, =CH^Z), 5.02 (0.13H, dd, *J* = 17.0, 1.5 Hz, =CH^E), 3.06–2.94 (3.74H, m, 2 × $CH_2{}^Z$ and $CH_2{}^E$), 2.92–2.78 (0.26H, m, $CH_2{}^E$), 2.63 (1.73H, td, *J* = 7.0, 1.5 Hz, $CH_2{}^Z$), 2.35 (0.26H, q, *J* = 7.5 Hz, $CH_2{}^E$); **^{13}C NMR** (101 MHz, $CDCl_3$, one quaternary carbon peak not observed) δ 200.8 (CHO), 141.4 (=CH), 133.8 (ArC–H/=CH), 133.6 (ArC–H/=CH), 129.4 (2 × ArC–H), 127.7 (2 × ArC–H), 118.6 (=CH_2), 117.0 (C$^{E/Z}$), 116.8 (C$^{E/Z}$), 43.3 ($CH_2{}^Z$), 36.8 ($CH_2{}^Z$), 30.6 ($CH_2{}^E$), 28.1 ($CH_2{}^E$), 27.2 ($CH_2{}^E$), 21.5 ($CH_2{}^{E/Z}$); **HRMS** m/z (ES) Found: MH$^+$, 265.0893. $C_{14}H_{16}O_3S$ requires MH$^+$ 265.0896; **LRMS** m/z (ES) 265 (100%, MH$^+$).

The *E*:*Z* ratio was determined from the ^{1}H NMR spectra by comparing the integration of the peaks for =CH at 6.98 (0.13H, t, *J* = 7.5 Hz, =CH) and 6.04 (0.87H, tt, *J* = 8.0, 1.5 Hz, =CH). The major isomer is assumed to be E based on the prior determination that the E isomer alkene peak appears at a more downfield shift.

((8,8-Dimethoxyocta-1,4-dien-4-yl)sulfonyl)benzene (E/Z mixture) (55)

Z E

To Na metal (285 mg, 12.4 mmol), EtOH (12.3 mL) was slowly added *via* a pressure equalising dropping funnel, and the mixture was heated to reflux and stirred for 10 min. The mixture was added to a mixture of phosphonate **58** (2.15 g, 6.47 mmol) and aldehyde **31** (1.71 g, 12.9 mmol) in EtOH (8 mL) at 0 ℃ and stirred at RT overnight. The reaction mixture was then concentrated under reduced pressure. Water (100 mL) was added, and the organic product was extracted with Et_2O (3 × 100 mL). The combined organic layers were dried ($MgSO_4$), filtered and concentrated under reduced pressure. The residue was purified by chromatography on silica gel, eluting with EtOAc–hexane (1:9) to afford compound **55** (471 mg, 23%) as a yellow oil as a mixture of geometrical isomers (0.19:0.81 E:Z); $\mathbf{R_f}$ 0.63 [EtOAc–petrol (1:1)]; **^{1}H NMR** (400 MHz, $CDCl_3$) δ 7.90–7.79 (2H, m, 2 × ArH), 7.65–7.56 (1H, m, ArH), 7.55–7.49 (2H, m, 2 × ArH), 6.99 (0.19H, t, *J* = 6.5 Hz, $=CH^E$), 6.04 (0.81H, tt, *J* = 8.0, 1.5 Hz, $=CH^Z$), 5.73–5.56 (1H, m, =CH), 5.09–4.98 (2H, m, $=CH_2$), 4.32 (0.81H, t, *J* = 5.5 Hz, CH^Z), 4.18 (0.19H, t, *J* = 5.5 Hz, CH^E), 3.30 (2.42H, s, 2 × $CH_3{}^Z$), 3.29 (2.42H, s, 2 × $CH_3{}^Z$), 3.24 (0.58H, s, $CH_3{}^E$), 3.22 (0.58H, s, $CH_3{}^E$), 3.07–2.98 (1.62H, m, $CH_2{}^Z$), 2.77-2.65 (1.62H, m, $CH_2{}^Z$), 2.32–2.19 (0.38H, m, $CH_2{}^E$), 1.82–1.72 (0.38H, m, $CH_2{}^E$), 1.69–1.59 (2H, m, CH_2); **^{13}C NMR** (101 MHz, $CDCl_3$) δ 143.3 ($=CH^Z$), 142.7 ($=CH^E$), 141.3 (ArC), 139.3 (=C), 133.7 (=CH), 133.3 (ArC–H), 128.9 (2 × ArC–H), 127.5 (2 × ArC–H), 118.2 ($=CH_2$), 104.3 (CH^E), 104.0 (CH^Z), 53.1 (2 × $CH_3{}^Z$), 52.8 (2 × $CH_3{}^E$), 36.8 ($CH_2{}^Z$), 36.2 ($CH_2{}^E$), 32.1 ($CH_2{}^Z$), 27.6 ($CH_2{}^E$), 24.1 ($CH_2{}^{E+Z}$); **HRMS** m/z (ES) Found: MNa^+ 333.1110, $C_{16}H_{20}O_2SNa$ requires MNa^+ 333.1131; **LRMS** m/z (ES) 333 (100%, MNa^+).

The *E*:*Z* ratio was determined from the ^{1}H NMR spectra by comparing the integration of the peaks for =CH at 6.99 (0.19H, t, *J* = 6.5 Hz, =CH), 6.04 (0.81H, tt, *J* = 8.0, 1.5 Hz, =CH). NOESY analysis of this compound indicated the peak at 6.99 ppm was of the E isomer (showing no close-in-space correlations) and the peak at 6.04 ppm the Z (showing close-in-space correlation to CH_2 at 3.07-2.98 ppm). NMR assignments are supported by HSQC.

Diethyl[1-(phenylsulfonyl)-3-butenyl]phosphonate (58)

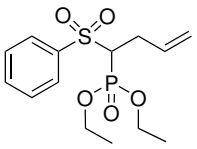

Compound **59** (10.0 g, 34.2 mmol) and allyl bromide **60** (11.8 mL, 137 mmol) were dissolved in DCM (120 mL). TBAB (11.1 g, 34.6 mmol) dissolved in aq. NaOH (68 mL, 0.5 M) was added and the biphasic mixture was stirred at RT overnight. The organic layer was separated and the aqueous layer was washed with DCM (50 mL). The organic layers were combined and concentrated under reduced pressure. The residue was then shaken with Et_2O (100 mL), filtered and concentrated under reduced pressure. The residue was purified by column chromatography on silica gel, eluting with EtOAc–petrol (13:7) to afford compound **58** (7.86 g, 95%) as a yellow oil; $\mathbf{R_f}$ 0.20 [EtOAc–hexane (1:1)]; **^{1}H NMR** (400 MHz, $CDCl_3$) δ 8.02–7.95 (2H, m, 2 × ArH), 7.71–7.62 (1H, m, ArH), 7.61–7.51 (2H, m, 2 × ArH), 5.86 (1H, ddt, J = 17.0, 10.0, 7.0 Hz, =CH), 5.12–5.01 (2H, m, $=CH_2$), 4.23–4.05 (4H, m, 2 × CH_2), 3.56 (1H, ddd, J = 19.0, 6.5, 5.5 Hz, CH), 2.93–2.69 (2H, m, CH_2), 1.29 (6H, td, J = 7.0, 3.0 Hz, 2 × CH_3); **^{13}C NMR** (101 MHz, $CDCl_3$) δ 139.0 (ArC), 134.1 (ArC–H), 134.0 (d, $J_{C,P}$ = 6.0 Hz, =CH), 129.5 (2 × ArC–H), 129.0 (2 × ArC–H), 118.0 ($=CH_2$), 63.7 (d, $J_{C,P}$ = 137.0 Hz, CH), 63.5 (d, $J_{C,P}$ = 6.5 Hz, CH_2), 63.4 (d, $J_{C,P}$ = 7.0 Hz, CH_2), 30.4 (d, $J_{C,P}$ = 3.0 Hz, CH_2), 16.4 (d, $J_{C,P}$ = 6 Hz, 2 × CH_3, J = 6.0 Hz); ^{31}P NMR (162 MHz, $CDCl_3$) δ 15.8–15.2 (m). Spectroscopic data in accordance with literature values.[174]

4,4-Dimethoxy-2,2-dimethylbutanenitrile (63)

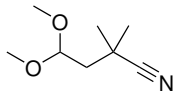

At –78 °C, *n*-BuLi (3.18 mL, 7.96 mmol, 2.5 M in cycloheane) was added to ^{i}Pr$_2$NEt (1.22 mL, 8.68 mmol) in THF (7 mL). The mixture was stirred for 10 min, prior to the addition of isobutyronitrile **61** (649 μL, 7.24 mmol). The mixture was stirred for a further 10 min, at which time 2-bromo-1,1-diethoxyethane **62** (941 μL, 7.96 mmol) was added. The mixture was stirred at –78 °C for a further 10 min, then warmed to RT over 40 min. The mixture was quenched with NH_4Cl (20 mL), and the organic product was extracted with Et_2O (2 × 10 mL). The combined organic layers were dried ($MgSO_4$), filtered and concentrated

under reduced pressure. The residue was purified by column chromatography on silica gel, eluting with EtOAc–petrol (1:5) to afford compound **63** (574 mg, 50%) as a yellow oil; $\mathbf{R_f}$ 0.67 [EtOAc–petrol (1:1)]; **^{1}H NMR** (400 MHz, $CDCl_3$) δ 4.60 (1H, t, *J* = 5.5 Hz, CH), 3.36 (6H, s, 2 × CH_3), 1.83 (2H, d, *J* = 5.5 Hz, CH_2), 1.39 (6H, s, 2 × CH_3); **^{13}C NMR** (101 MHz, $CDCl_3$) δ 124.8 (CN), 102.4 (CH), 53.3 (2 × O-CH_3), 43.1 (CH_2), 30.1 (C), 27.6 (CH_3). Spectroscopic data in accordance with literature values.[92]

4,4-Dimethoxy-2,2-dimethylbutanal (64)

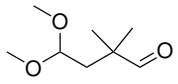

To compound **63** (500 mg, 3.65 mmol) in dry DCM (20 mL) at –78 °C was added DIBAL-H (3.76 mL, 4.14 mmol, 1.10 M in cyclohexanes) dropwise. The mixture was stirred for 4 h at –78 °C, then warmed to RT. The mixture was quenched with NH_4Cl (10 mL) and saturated aq. Rochelle salt (10 mL) and then stirred vigorously for 1 h. The mixture was extracted with DCM (3 × 20 mL) and the combined organic layers were washed with brine (10 mL), dried ($MgSO_4$), filtered and concentrated under reduced pressure. The residue was purified by column chromatography on silica gel, eluting with EtOAc–Hexane (1:4) to afford compound **64** (168 mg, 33%) as a colourless oil; $\mathbf{R_f}$ 0.24 [EtOAc–petrol 1:9]; **^{1}H NMR** (400 MHz, $CDCl_3$) δ 9.39 (1H, s, C(=O)H), 4.35 (1H, t, *J* = 6.0 Hz, CH), 3.30 (6H, s, 2 × CH_3), 1.84 (2H, d, *J* = 6.0 Hz, CH_2), 1.07 (6H, s, 2 × CH_3); **^{13}C NMR** (101 MHz, $CDCl_3$) δ 204.8 (C(=O)H), 102.8 (CH), 53.8 (2 × CH_3), 44.0 (C), 41.7 (CH_2), 22.0 (2 × CH_3). Spectroscopic data in accordance with literature values.[92]

4,4-Dimethoxybutanenitrile (69)

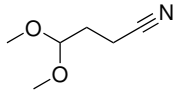

At –78 °C, *n*-BuLi (12.8 mL, 31.9 mmol, 2.5 M in hexane) was added to ^{i}Pr_2NEt (4.88 mL, 34.8 mmol) in THF (27 mL). The mixture was stirred for 10 min, prior to the addition of MeCN (1.55 mL, 29.0 mmol). The mixture was stirred for a further 10 min, at which time 2-bromo-1,1-diethoxyethane **62** (3.77 mL, 31.9 mmol) was added. The mixture was stirred at –78 °C for a further 10 min, then warmed to RT over 40 min. The mixture was quenched with saturated aq. NH_4Cl (20 mL), and the organic product was extracted with EtOAc (2 × 10 mL). The combined organic layers were dried ($MgSO_4$), filtered and concentrated under reduced

pressure. The residue was purified by column chromatography on silica gel, eluting with EtOAc–petrol (1:9, to 1:5, to 2:3) to afford compound **69** (619 mg, 17%) as a yellow oil; **^{1}H NMR** (400 MHz, $CDCl_3$) δ 4.45 (1H, t, J = 5.5 Hz, CH), 3.38 (6H, s, 2 × CH_3), 2.41 (2H, t, J = 7.5 Hz, CH_2), 1.98–1.92 (2H, m, CH_2); **^{13}C NMR** (101 MHz, $CDCl_3$) δ 121.5 (C), 102.4 (CH), 54.0 (CH_3), 28.7 (CH_2), 12.6 (CH_2). Spectroscopic data in accordance with literature data.[175]

4-Hexenal (71)

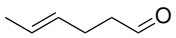

To oxalyl chloride (2.80 mL, 32.6 mmol) in DCM (15 mL) was added a solution of DMSO (4.63 mL, 65.2 mmol) in DCM (15 mL) at –78 °C. The mixture was stirred for 5 min, at which time a solution of alcohol **70** (3.60 mL, 29.7 mmol) in DCM (15 mL) was added. The mixture was stirred for a further 15 min, at which time Et_3N (10.3 mL, 74.1 mmol) was added. The reaction mixture was allowed to warm to RT and stirred for 1.5 h. The mixture was quenched with water (40 mL), and the organic product was extracted with DCM (10 mL). The organic layer was washed with brine (30 mL), aq. HCl (30 mL, 2 M), aq. Na_2CO_3 (30 mL) and water (30 mL). The combined organic layers were dried ($MgSO_4$) and filtered, then the mixture was purified by vacuum distillation (vapour temperature 26 °C under house vacuum) to afford compound **71** (1.72 g, 59%) as colourless oil; **^{1}H NMR** (400 MHz, $CDCl_3$) δ 9.78 (1H, t, J = 1.5 Hz, C(=O)H), 5.58–5.36 (2H, m, 2 × =CH), 2.51 (2H, tdd, J = 7.0, 1.5, 1.0 Hz, CH_2), 2.45–2.29 (2H, m, CH_2), 1.66 (3H, dd, J = 6.0, 1.0 Hz, CH_3); **^{13}C NMR** (101 MHz, $CDCl_3$) δ 202.6 (CHO), 130.3 (=CH), 125.6 (=CH), 43.6 (CH_2), 26.7 (CH_2), 18.1 (CH_3). Spectroscopic data in accordance with literature values.[97]

((Deca-1,4,8-trien-4-yl)sulfonyl)benzene (E/Z mixture) (72)

Z E

To Na metal (500 mg, 21.7 mmol) was slowly added EtOH (21.7 mL) *via* a pressure equalising dropping funnel and the mixture was heated to reflux for 10 min, before being allowed to cool to RT. To a mixture of phosphonate **58** (1.38 g, 4.15 mmol) and 4-hexenal **71** (815 mg, 8.30 mmol) in EtOH (4.2 mL) at 0 °C,

the mixture was added dropwise. The mixture was warmed to RT and stirred overnight. The residue was purified by column chromatography on silica gel, eluting with EtOAc–petrol (1:4) to afford compound **72** (1.01 g, 83%) as a yellow oil, as a mixture of geometrical isomers (81:19 E:Z); $\mathbf{R_f}$ 0.85 [EtOAc–petrol (1:1)]; **^{1}H NMR** (400 MHz, $CDCl_3$) δ 7.92–7.84 (2H, m, 2 × ArH), 7.59–7.55 (1H, m, ArH), 7.55–7.46 (2H, m, 2 × ArH), 6.99 (0.81H, t, J = 7.5 Hz, $=CH^E$), 6.02 (0.19H, t, J = 7.0 Hz, $=CH^Z$), 5.66 (1H, ddt, J = 17.0, 10.0, 7.0 Hz, =CH), 5.42–5.29 (1H, m, =CH), 5.28–5.17 (1H, m, =CH), 5.04–4.97 (0.38H, m, $=CH_2{}^Z$), 4.92–4.82 (1.62H, m, $=CH_2{}^E$), 3.06 (0.38H, dq, J = 7.0, 1.5 Hz, $CH_2{}^Z$), 3.02 (1.62H, dt, J = 7.0, 1.5 Hz, $CH_2{}^E$), 2.27–2.20 (1.62H, m, $CH_2{}^E$), 2.20–2.11 (1.62H, m, $CH_2{}^E$), 2.09–2.03 (0.38H, m, $CH_2{}^Z$), 2.03–1.97 (0.38H, m, $CH_2{}^Z$), 1.60 (3H, d, J = 6.5 Hz, CH_3); **^{13}C NMR** (101 MHz, $CDCl_3$) δ 139.1 (=CH), 138.8 (ArC^Z) 137.5 (ArC^E), 133.6 (=CH), 133.3 (ArC–H), 129.4 (2 × ArC–H), 128.9 (2 × ArC–H), 127.8 ($=CH^{E\text{ or }Z}$), 126.8 ($=CH^{E\text{ or }Z}$), 122.1 (=CH), 118.3 ($=CH_2$), 116.6 (C), 35.5 (CH_2), 31.8 ($CH_2{}^E$), 31.3 ($CH_2{}^Z$), 30.6 ($CH_2{}^Z$), 28.5 ($CH_2{}^E$), 18.0 (CH_3); **HRMS** m/z (ES) Found: MNa^+ 299.1101, $C_{16}H_{20}O_2SNa$ requires MNa^+ 299.1076; **LRMS** m/z (ES) 299 (100%, MNa^+).

The *E*:*Z* ratio was determined from the ^{1}H NMR spectra by comparing the integration of the peaks for =CH at 6.99 ppm (0.81H, t, J = 7.5 Hz, $=CH^E$), 6.02 ppm (0.19H, t, J = 7.0 Hz, $=CH^Z$). The major isomer is assumed to be E based on the prior determination that the E isomer alkene peak appears at a more downfield shift.

But-3-enyltriphenylphosphonium bromide (78)

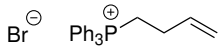

To a solution of 4-bromo-1-butene **79** (3.00 mL, 29.6 mmol) in MeCN (75 mL) was added PPh_3 (5.98 g, 22.8 mmol) and the mixture was refluxed overnight. After being cooled to RT, the mixture was concentrated under reduced pressure. The precipitate was collected by filtration, washed with EtOAc (4 x 50 mL), and dried to afford compound **78** (5.79 g, 50%) as an amorphous white solid; $\mathbf{R_f}$ = 0.61 [EtOAc–petrol (1:1)]; **^{1}H NMR** (400 MHz, $CDCl_3$) δ 7.93–7.66 (15H, m, 15 × ArH), 6.03 (1H, ddt, J = 17.0, 10.0, 6.5 Hz, =CH), 5.10–4.97 (2H, m, =CH), 4.09–3.97 (2H, m, CH_2), 2.53–2.39 (2H, m, CH_2); **^{13}C NMR** (101 MHz, $CDCl_3$) δ 135.1 (d, $J_{C,P}$ = 3.0 Hz, CH), 134.0 (d, $J_{C,P}$ = 10.0 Hz, CH), 133.9 (d, $J_{C,P}$ = 20.0 Hz, CH), 130.6 (d, $J_{C,P}$ = 12.5 Hz, CH), 118.5 (d, $J_{C,P}$ = 85.5 Hz, C), 117.5 (CH_2), 26.9 (d, $J_{C,P}$ = 3.5 Hz, CH_2), 22.6 (d, $J_{C,P}$ = 49.0

Hz, CH_2). Spectroscopic data in accordance with literature values.[100]

5-(Phenylsulfonyl)octa-4,7-dienal oxime (81)

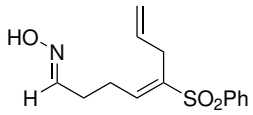

Compound **53** (458 mg, 1.73 mmol) and hydroxylamine hydrochloride (241 mg, 3.47 mmol) were dissolved in PhMe (12 mL). $^{i}Pr_2NEt$ (0.724 mL, 4.16 mmol) was added and the mixture was heated to 60 °C and stirred for 3 h. The solution was concentrated under reduced pressure, and purified by column chromatography on silica gel, eluting with EtOAc–hexane (1:4 to 3:7), to afford compound **81** (124 mg, 20%) as a mixture of geometrical isomers (79:21 E:Z). A single isomer (E) was isolated (27 mg) as a yellow gum, and a mixture of both *E* and *Z* isomers was isolated (97 mg) as a white gum.

Data for the single E isomer: $\mathbf{R_f}$ = 0.60 [EtOAc–petrol (1:1)]; **FT-IR** ν_{max} (film)/cm^{-1} 3259 (O–H), 2910, 1640 (C=N), 1613 (C=C), 1446, 1291 (S=O), 1177, 1146, 1084, 1011, 998, 922, 730; **^{1}H NMR** (400 MHz, $CDCl_3$) δ 7.92–7.81 (2H, m, ArH), 7.67–7.59 (1H, m, ArH), 7.59–7.49 (2H, m, ArH), 7.39 (1H, t, *J* = 6.0 Hz, C(=N)H), 6.03 (1H, t, *J* = 7.5 Hz, =CH), 5.66 (1H, ddt, *J* = 17.0, 10.0, 6.5 Hz, =CH), 5.09 (1H, dtd, *J* = 10.0, 2.5, 1.5 Hz, =CH), 5.05 (1H, dtd, *J* = 17.0, 2.5, 1.5 Hz), 3.05 (2H, dt, *J* = 6.5, 1.5, CH_2), 2.91 (2H, q, *J* = 7.5 Hz, CH_2), 2.32 (2H, td, *J* = 7.5, 6.0 Hz, CH_2); **^{13}C NMR** (101 MHz, $CDCl_3$) δ 150.7 (C=N), 141.8 (=CH), 141.0 (C), 140.4 (C), 133.6 (=CH), 129.3 (2 × ArC—-H), 127.9 (2 × ArC—-H), 118.5 (=CH_2), 36.9 (CH_2), 29.1 (CH_2), 25.5 (CH_2); **HRMS** m/z (ES) Found: MH^+ 280.1007, $C_{14}H_{17}NO_3S$ requires MH^+ 280.1002; **LRMS** m/z (ES) 280 (100%, MH^+).

4-Hydroxyoct-7-enenitrile (83)

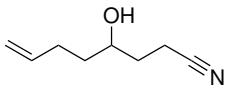

At –78 °C, to $^{i}Pr_2NEt$ (1.51 mL, 10.2 mmol) in THF (10 mL) was added *n*-BuLi (4.25 mL, 10.2 mmol, 2.4 M in hexane). After 10 min, MeCN (962 μL, 20.4 mmol) was added and the mixture was stirred for 20 min. Epoxide **82** (636 μL, 5.10 mmol) was added, and the mixture was stirred at –78 °C for a further 30 min. The mixture was then allowed to warm to RT over 1 h. NH_4Cl (10 mL) was added, and the mixture

was extracted with Et_2O (3 × 5 mL), dried ($MgSO_4$), filtered and concentrated under reduced pressure. The residue was purified by column chromatography on silica gel, eluting with EtOAc–petrol (1:4) to afford compound **83** (530 mg, 83%) as a colourless oil; $\mathbf{R_f}$ 0.82 [EtOAc–petrol (1:1)]; **^{1}H NMR** (400 MHz, $CDCl_3$) δ 5.83 (1H, ddt, *J* = 17.0, 10.0, 6.5 Hz, =CH), 5.08 (1H, ddd, *J* = 17.0, 1.5, 1.5 Hz, =CH), 5.01 (1H, ddd, *J* = 10.0, 1.5, 1.5 Hz, =CH), 3.82–3.70 (1H, m, CH), 2.57–2.46 (2H, m, CH_2), 2.29–2.09 (2H, m, CH_2), 1.91–1.78 (1H, m, CH), 1.77–1.66 (1H, m, CH), 1.65–1.61 (1H, m, CH); **^{13}C NMR** (101 MHz, $CDCl_3$) δ 138.0 (=CH), 120.0 (C), 115.7 (CH_2), 69.8 (CH), 36.5 (CH_2), 32.7 (CH_2), 30.1 (CH_2), 13.8 (CH_2). Spectroscopic data in accordance with literature values.[105]

1-Cyanohept-6-en-3-yl benzenesulfonate (84)

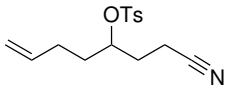

To compound **83** (633 mg, 5.06 mmol), TsCl (596 mg, 6.07 mmol) and DMAP (324 mg, 5.06 mmol) in DCM (30 mL) was added Et_3N (846 μL, 6.07 mmol), and the mixture was stirred at RT for 2 days. The mixture was quenched with $NaHCO_3$ (20 mL), extracted with DCM (3 × 10 mL), dried ($MgSO_4$), filtered and concentrated under reduced pressure. The residue was purified by column chromatography on silica gel, eluting with EtOAc–petrol (1:4) to afford compound **84** (791 mg, 56%) as a yellow oil; $\mathbf{R_f}$ 0.56 [EtOAc–petrol (1:1)]; **FT-IR** ν_{max} (film)/cm^{-1} 2931 (C-C), 2249 (CN), 1642 (C=C), 1598, 1495, 1446, 1356 (S=O), 1307, 1293, 1189, 1173, 1121, 1097, 1019, 998, 892, 838, 815, 736; **^{1}H NMR** (400 MHz, $CDCl_3$) δ 7.85–7.77 (2H, m, 2 × ArH), 7.37 (2H, d, *J* = 8.0 Hz, 2 × ArH), 5.66 (1H, ddt, *J* = 17.0, 10.5, 6.5 Hz, =CH), 5.03–4.91 (2H, m, =CH_2), 4.64 (1H, qd, *J* = 6.5, 4.0 Hz, CH), 2.46 (3H, s, CH_3), 2.44–2.22 (2H, m, CH_2), 2.07–1.86 (4H, m, 2 × CH_2), 1.82–1.59 (2H, m, CH_2); **^{13}C NMR** (101 MHz, $CDCl_3$) δ 145.4 (ArC), 136.5 (=CH), 133.8 (ArC), 131.3 (2 × ArC–H), 127.9 (2 × ArC–H), 118.9 (CN), 116.1 (=CH_2), 80.5 (CH), 33.4 (CH_2), 30.3 (CH_2), 28.9 (CH_2), 21.8 (CH_3), 13.4 (CH_2); **HRMS** m/z (ES) Found: MNH_4^+ 311.1422, $C_{15}H_{19}NO_3S$ requires MNH_4^+ 311.1424; **LRMS** m/z (ES) 311 (100%, MNH_4^+).

(1-Methyl-2-oxo-3-(2-oxoethyl)indolin-3-yl)methyl-4-methylbenzenesulfonate (123)

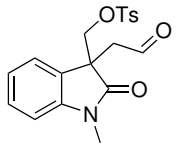

Compound **180** (1.30 g, 3.74 mmol) was dissolved in DCM (22 mL) and MeOH (22 mL), then cooled to –78 °C. Ozone was bubbled through the solution for 1 h, then excess ozone was removed by bubbling argon gas through the solution for 5 min. Dimethyl sulfide (51.3 mL, 693 mmol) was added, and the mixture was warmed to RT and stirred for 16 h, then concentrated under reduced pressure. The residue was purified by column chromatography on silica gel, eluting with EtOAc–petrol (1:1) then recrystallised from *n*-hexane/DCM to afford compound **123** (562 mg, 40%) as white crystals; **mpt** 94–96 °C (lit. does not report mpt); $\mathbf{R_f}$ 0.35 [EtOAc–petrol (1:1)]; **FT-IR** ν_{max} (film)/cm^{-1} 2942, 1712 (2 × C=O), 1614, 1581, 1495, 1472, 1260 (S=O), 1190, 1177, 1122, 1096, 1064, 1019, 815, 785, 755; **^{1}H NMR** (400 MHz, $CDCl_3$) δ 9.44 (1H, t, *J* = 1.0 Hz, C(=O)H), 7.69–7.62 (2H, m, 2 × ArH), 7.36–7.28 (3H, m, 3 × ArH), 7.20 (1H, dd, *J* = 7.5, 1.0 Hz, ArH), 7.02 (1H, td, *J* = 7.5, 1.0 Hz, ArH), 6.86 (1H, d, *J* = 7.5 Hz, ArH), 4.27 (1H, d, *J* = 9.5 Hz, CH), 3.97 (1H, d, *J* = 9.5 Hz, CH), 3.23 (3H, s, CH_3), 3.17 (1H, dd, *J* = 18.0, 1.0 Hz, CH), 2.99 (1H, dd, *J* = 18.0. 1.0 Hz, CH), 2.44 (3H, s, CH_3); **^{13}C NMR** (101 MHz, $CDCl_3$) δ 196.7 (C=O), 174.9 (C=O), 145.0 (C), 143.6 (C), 132.0 (C), 129.8 (2 × ArC—-H), 129.0 (ArC–H), 127.8 (2 × ArC—-H), 127.6 (C), 124.0 (Ar-CH), 123.7 (ArC–H), 108.4 (ArC–H), 72.0 (O-CH_2), 48.4 (C), 46.2 (CH_2), 26.4 (CH_3), 21.5 (CH_3). Spectroscopic data in accordance with literature values.[171]

N-Methyl isatin (125)

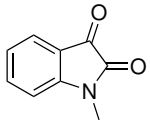

To a stirred solution of isatin **124** (10 g, 68 mmol) in DMF (136 mL) was added methyl iodide (4.2 mL, 68 mmol), followed by potassium carbonate (10 g, 75 mmol). The mixture was left to stir at RT for 16 h. The mixture was diluted with Et_2O (600 mL) and water (300 mL). The organic layer was separated, dried ($MgSO_4$), filtered and concentrated under reduced pressure to afford *N*-methyl isatin **125** (8.1 g, 72%) as an orange amorphous solid; **mpt** 122–124 °C (lit.[176] 130–133 °C); $\mathbf{R_f}$ 0.45 [EtOAc–petrol (1:1)]; ^{1}H NMR

(400 MHz, $CDCl_3$) δ 7.64–7.55 (2H, m, 2 × ArH), 7.13 (1H, t, *J* = 7.5 Hz, ArH), 6.89 (1H, d, *J* = 7.5 Hz, ArH), 3.25 (3H, s, CH_3); ^{13}C NMR (101 MHz, $CDCl_3$) δ 183.3 (C=O), 158.2 (C=O), 151.4 (ArC), 138.4 (ArC–H), 125.3 (ArC–H), 123.8 (ArC–H), 117.4 (ArC), 109.9 (ArC–H), 26.2 (CH_3). Spectroscopic data in accordance with literature values.[177]

1-Methyl-2-oxindole (126)

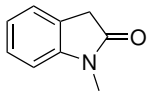

N-Methylisatin **125** (1.6 g, 10 mmol) and hydrazine monohydrate (10.0 mL, 320 mmol) were refluxed for 40 min. The reaction mixture was poured onto cold water (20 mL), extracted using EtOAc (3 × 20 mL), washed with water (3 × 20 mL), dried ($MgSO_4$) and filtered. The solvent was evaportated and the product was recrystallised from *n*-hexane/DCM to afford oxindole **126** (1.3 g, 86%) as an orange amorphous solid; **mpt** 58–62 °C (lit.[178] 85–88 °C); $\mathbf{R_f}$ 0.63 [petrol–EtOAc (1:1)]; **^{1}H NMR** (400 MHz, $CDCl_3$) δ 7.32–7.22 (2H, m, 2 × ArH), 7.04 (1H, t, *J* = 7.5 Hz, ArH), 6.82 (1H, d, *J* = 7.5 Hz, ArH), 3.52 (2H, s, CH_2), 3.21 (3H, s, CH_3); **^{13}C NMR** (101 MHz, $CDCl_3$) δ 175.1 (C=O), 145.2 (ArC), 127.8 (ArC–H), 124.5 (ArC), 124.3 (ArC–H), 122.3 (ArC–H), 108.0 (ArC–H), 35.7 (CH_2), 26.1 (CH_3). Spectroscopic data in accordance with literature values.[137]

3-(2,2-Diethoxyethyl)-1-methyl-1,3-dihydro-*2H*-indol-2-one (127)

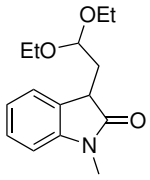

To NaH (90 mg, 3.7 mmol) in DMF (2.4 mL), a solution of oxindole **126** (500 mg, 3.40 mmol) in PhMe (5.4 mL) was added gradually. The reaction mixture was stirred at RT for 45 min before a solution of 2-bromo-1,1-diethoxyethane **62** (0.57 mL, 3.7 mmol) in PhMe (0.6 mL) was added dropwise. The mixture was stirred at RT for 45 min, then refluxed for 16 h. After cooling to RT, the mixture was poured onto ice-water and diluted with Et_2O (30 mL). The organic layer was separated, and the aqueous layer was washed with Et_2O (30 mL). The combined organic layers were washed with water (2 × 30 mL), dried ($MgSO_4$), filtered and

concentrated under reduced pressure. The residue was purified by column chromatography on silica gel, eluting with EtOAc–petrol (1:9 to 1:4) to give acetal **127** (128 mg, 14%) as a yellow oil; $\mathbf{R_f}$ 0.47 [EtOAc-petrol (1:1)]; **FT-IR** ν_{max} (film)/cm^{-1} 2975 (C–H), 2931 (C–H), 2884 (C–H), 1710 (C=O), 1611, 1496, 1473, 1376, 1347, 1128, 1092, 1060, 1024, 933; **^{1}H NMR** (400 MHz, $CDCl_3$) δ 7.34–7.24 (2H, m, 2 × ArH), 7.04 (1H, t, *J* = 7.5 Hz, ArH), 6.81 (1H, d, *J* = 7.5 Hz, ArH), 4.84 (1H, t, *J* = 6.0 Hz, CH), 3.75–3.61 (2H, m, 2 × CH), 3.56 (1H, t, *J* = 6.0 Hz, CH), 3.53–3.39 (2H, m, 2 × CH), 3.20 (3H, s, CH_3), 2.20 (2H, t, *J* = 6.0 Hz, CH_2), 1.16 (3H, t, *J* = 7.0 Hz, CH_3), 1.15 (3H, t, *J* = 7.0 Hz, CH_3); **^{13}C NMR** (101 MHz, $CDCl_3$) δ 177.8 (C=O), 144.3 (ArC), 128.8 (ArC), 127.9 (ArC–H), 124.1 (ArC–H), 122.2 (ArC–H), 107.9 (ArC–H), 100.3 (CH), 62.3 (CH_2), 61.1 (CH_2), 42.0 (CH), 34.3 (CH_2), 26.2 (CH_3), 15.4 (CH_3), 15.2 (CH_3); **HRMS** m/z (ES) Found: MNa^+, 286.1426. $C_{15}H_{21}NO_3Na$ requires MNa^+ 286.1414; **LRMS** m/z (ES) 286 (100%, MNa^+).

3,3-Bis(2,2-diethoxyethyl)-1-methyl-1,3-dihydro-*2H*-indol-2-one (135)

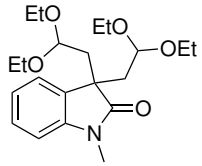

To NaH (90 mg, 3.7 mmol) in DMF (2.4 mL), a solution of oxindole **126** (500 mg, 3.40 mmol) in PhMe (5.4 mL) was added portion-wise. The mixture was stirred at RT for 1 h, prior to the dropwise addition of a solution of 2-bromo-1,1-diethoxyethane **62** (0.57 mL, 3.7 mmol) in PhMe (0.6 mL). The mixture was then stirred for 1 h, then heated to 110 °C for 19 h. After cooling to RT, the mixture was poured onto ice-water and diluted with Et_2O (30 mL). The organic layer was separated, and the aqueous layer was washed with Et_2O (30 mL). The combined organic layers were washed with water (2 × 30 mL), dried ($MgSO_4$), filtered and concentrated under reduced pressure. The residue was purified by column chromatography on silica gel, eluting with EtOAc–petrol (1:9) gave the oxindole **127** (248 mg, 28%) as an orange gum and the oxindole **135** (48 mg, 5%) as a yellow gum; Data for oxindole **127** as above; Data for **135**: $\mathbf{R_f}$ 0.88 [EtOAc–petrol (1:1)]; **FT-IR** ν_{max} (film)/cm^{-1} 2971 (C–H), 2930 (C–H), 2898 (C–H), 1716 (C=O), 1612, 1495, 1471, 1375, 1350, 1119, 1058, 1001, 753; **^{1}H NMR** (400 MHz, $CDCl_3$) δ 7.27–7.20 (1H, m, ArH), 7.20–7.14 (1H, m, ArH), 7.05–6.98 (1H, m, ArH), 6.78 (1H, d, *J* = 8.0 Hz, ArH), 4.19–4.09 (2H, m, 2 × CH), 3.47–3.34 (4H, m, 4 × CH), 3.27–3.15 (5H, m, 2 × CH and 1 × CH_3), 3.14–3.02 (2H, m, 2 × CH), 2.38 (2H, dd, *J* = 14.0, 7.5 Hz, 2 × CH), 2.02 (2H, dd, *J* = 14.0, 4.5 Hz, 2 × CH), 1.03–0.94 (12H, m, 4 × CH_3); **^{13}C NMR** (101 MHz, $CDCl_3$)

δ 179.2 (C=O), 144.2 (ArC), 131.0 (ArC), 128.0 (ArC–H), 123.6 (ArC–H), 122.0 (ArC–H), 107.8 (ArC–H), 99.5 (2 × CH), 61.1 (2 × O-CH_2), 60.4 (2 × O-CH_2), 47.7 (C), 41.4 (2 × CH_2), 26.3 (CH_3), 15.2 (2 × CH_3), 15.0 (2 × CH_3); **HRMS** m/z (ES) Found: MNa^+, 402.2266. $C_{21}H_{33}NO_5Na$ requires MNa^+ 402.2251; **LRMS** m/z (ES) 402 (100%, MNa^+).

Pent-4-enal (136)

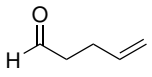

DMSO (5.4 mL, 77 mmol) in DCM (18 mL) was added dropwise to a solution of oxalyl chloride (3.3 mL, 38 mmol) in DCM (70 mL) at –78 °C under argon. The mixture was stirred for 5 min before the addition of a solution of alcohol **137** (3.4 mL, 35 mmol) in DCM (18 mL). The mixture was stirred for 15 min, at which time Et_3N (24 mL, 170 mmol) was added and the mixture was warmed to RT. After 1.5 h, the mixture was diluted with water (200 mL) and the layers were separated. The aqueous layer was extracted with DCM (2 × 200 mL). The combined organic layers were washed with brine (2 × 150 mL) and aq. HCl (2 × 150 mL, 1 M), then dried ($MgSO_4$) and filtered. The solvent was removed by distillation at atmospheric pressure to give pent-4-enal **136** (1.2 g, 41%) as a colourless liquid; $\mathbf{R_f}$: no spots visible under development conditions; **^{1}H NMR** (400 MHz, $CDCl_3$) δ 9.80 (1H, t, J = 1.5 Hz, CH), 5.93–5.73 (1H, m, =CH), 5.20–4.94 (2H, m, =CH_2), 2.67–2.48 (2H, m, CH_2), 2.48–2.33 (2H, m, CH_2). Spectroscopic data in accordance with literature values.[11]

1-(2-Hydroxy-1-methyl-*1H*-indol-3-yl)pent-4-en-1-one (143)

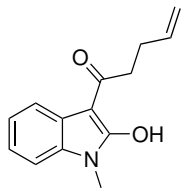

Oxindole **126** (500 mg, 3.40 mmol) and DMAP (125 mg, 1.02 mmol) were dissolved in pentenoic anhydride **154** (3.5 mL). The mixture was heated at 140 °C for 2 h, then stirred at RT for 3 days. The mixture was diluted with MeOH (8 mL) and cooled to 0 °C. KOH (2.0 g, 36 mmol) in MeOH (12 mL) was added and the mixture was stirred at RT for 22 h. After cooling the mixture to 0 °C the pH of the mixture was adjusted

to pH 1 with aq. HCl (12 M) and diluted with water (14 mL). The layers were separated, and the aqueous layer was extracted with EtOAc (3 × 20 mL). The combined organic layers were washed with water (3 × 10 mL), dried ($MgSO_4$), filtered and concentrated under reduced pressure. The residue was purified by column chromatography on silica gel, eluting with EtOAc–petrol (1:9). The product was then repurified by vacuum distillation, and further purified by column chromatography on silica gel, eluting with EtOAc–petrol (1:19) to afford enol **143** (225 mg, 29%) as a yellow liquid; $\mathbf{R_f}$ 0.66 [petrol–EtOAc (1:1)]; **FT-IR** ν_{max} (film)/cm^{-1} 3076 (O–H), 3056, 2977 (C–H), 2932 (C–H), 1651 (C=O), 1608, 1491, 1467, 1433, 1416, 1378,1300, 1262, 1209, 1186, 1145, 1079, 979, 947, 913, 890, 781; **^{1}H NMR** (400 MHz, $CDCl_3$) δ 13.82 (1H, br s, O–H), 7.37 (1H, d, *J* = 7.5 Hz, ArH), 7.23 (1H, t, *J* = 7.5 Hz, ArH), 7.11 (1H, t, *J* = 7.5 Hz, ArH), 6.96 (1H, d, *J* = 7.5 Hz, ArH), 5.93 (1H, ddt, *J* = 17.0, 10.0, 6.5 Hz, CH), 5.15 (1H, dd, *J* = 17.0, 1.0 Hz, =CH), 5.05 (1H, dd, *J* = 10.0, 1.0 Hz, =CH), 3.36 (3H, s, CH_3), 2.89–2.83 (2H, m, CH_2), 2.56 (2H, q, *J* = 6.5 Hz, CH_2); **^{13}C NMR** (101 MHz, $CDCl_3$) δ 175.9 (C=O), 171.4 (=COH), 139.0 (ArC), 136.7 (=CH), 125.4 (ArC–H), 122.3 (ArC–H), 122.0 (ArC), 119.9 (ArC–H), 116.1 (=CH_2), 108.6 (ArC–H), 101.6 (C), 33.3 (CH_2, 30.0 (CH_2), 25.9 (CH_3).

1-(2-Hydroxy-1-methyl-*1H*-indol-3-yl)ethan-1-one (145)

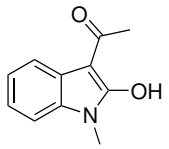

Oxindole **126** (1.0 g, 6.8 mmol) and DMAP (261 mg, 2.14 mmol) were dissolved in acetic anhydride (6.74 mL, 71 mmol) and refluxed for 5 h. The reaction mixture was diluted with MeOH (16 mL) and was cooled to 0 °C. KOH (4.0 g, 71 mmol) in MeOH (24 mL) was added and the reaction mixture was stirred at RT for 1 day. After cooling the mixture to 0 °C the pH of the mixture was adjusted to pH 1 with aq. HCl (12 M) and diluted with water (14 mL). The layers were separated, and the aqueous layer was extracted with EtOAc (3 × 20 mL). The combined organic layers were washed with water (3 × 10 mL), dried ($MgSO_4$), filtered and concentrated under reduced pressure. The residue was purified by column chromatography on silica gel, eluting with EtOAc–petrol (1:9). The product was then repurified by vacuum distillation, and further purified by column chromatography on silica gel, eluting with EtOAc–petrol (1:9) to afford the enol **145** (546 mg, 43%) as an amorphous purple solid; **mpt** 106–107 °C (lit.[179] 107–108 °C); $\mathbf{R_f}$ 0.75 [EtOAc–petrol (1:1)]; **^{1}H NMR** (400 MHz, $CDCl_3$) δ 13.65 (1H, br s, OH), 7.37 (1H, d, *J* = 7.5 Hz, ArH), 7.25–7.18 (1H, m, ArH), 7.14–7.07

(1H, m, ArH), 6.95 (1H, d, J = 7.5 Hz, ArH), 3.34 (3H, s, CH_3), 2.45 (3H, s, CH_3); **^{13}C NMR** (101 MHz, $CDCl_3$) δ 172.9 (C=O), 171.1 (ArC), 138.9 (ArC), 125.2 (ArC–H), 122.2 (ArC), 122.1 (ArC–H), 119.7 (ArC–H), 108.4 (CH), 101.8 (C), 25.7 (CH_3), 20.3 (CH_3). Spectroscopic data in accordance with literature values.[180]

3-Acetyl-1-methyl-3-(prop-2-en-1-yl)-1,3-dihydro-*2H*-indol-2-one (147)

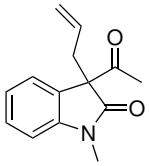

To a mixture of enol **145** (150 mg, 0.79 mmol) and allyl bromide **60** (0.07 mL, 0.8 mmol) in THF (5 mL) was added Triton B (0.36 mL, 0.79 mmol) and the mixture was stirred at RT for 3 days. The mixture was concentrated under reduced pressure and the residue was dissolved in water (10 mL). The layers were separated and the aqueous layer was extracted with EtOAc (3 × 10 mL). The combined organic layers were washed with water (2 × 10 mL) and dried ($MgSO_4$), filtered and concentrated under reduced pressure. The residue was purified by column chromatography on silica gel, eluting with EtOAc–petrol (1:9), then recrystallised from *n*-hexane/DCM, to afford dicarbonyl **147** (86 mg, 47%) as colourless gum; **R_f** 0.59 [EtOAc–petrol (1:1)]; **^{1}H NMR** (400 MHz, $CDCl_3$) δ 7.39–7.32 (1H, m, ArH), 7.18 (1H, d, J = 7.5 Hz, ArH), 7.13–7.07 (1H, m, ArH), 6.89 (1H, d, J = 7.5 Hz, ArH), 5.38–5.23 (1H, m, =CH), 5.05–4.96 (1H, m, =CH), 4.91–4.86 (1H, m, =CH), 3.27 (3H, s, CH_3), 3.03–2.78 (2H, m, 2 × CH), 1.99 (3H, s, CH_3); **^{13}C NMR** (101 MHz, $CDCl_3$) δ 200.8 (C=O), 174.6 (C=O), 144.3 (ArC), 131.5 (=CH), 129.3 (ArC–H), 127.0 (ArC), 124.2 (ArC–H), 123.3 (ArC–H), 119.6 (CH_2), 108.6 (Ar–CH), 66.5 (C), 37.6 (CH_2), 26.7 (CH_3), 24.0 (CH_3). Spectroscopic data in accordance with literature values.[149]

3-Acetyl-1-methyl-3-(3-methylbut-2-en-1-yl)-1,3-dihydro-*2H*-indol-2-one (152)

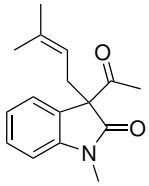

To a mixture of enol **145** (50 mg, 0.26 mmol) and prenyl bromide **151** (0.03 mL, 0.3 mmol) in THF (2 mL) was added Triton B (48 μL, 0.26 mmol) and the mixture was stirred at RT for 1 day. The reaction mixture

was diluted with water (5 mL), and the layers were separated. The aqueous layer was extracted with EtOAc (3 × 2 mL), then the combined organic layers were washed with water (3 × 2 mL), then dried ($MgSO_4$), filtered and concentrated under reduced pressure. The residue was purified by column chromatography on silica gel, eluting with EtOAc–petrol (1:4), to afford dicarbonyl **152** (46 mg, 76%) as an orange gum; $\mathbf{R_f}$ 0.69 [EtOAc–petrol (1:1)]; **FT-IR** ν_{max} (film)/cm^{-1} 3056 (C–H), 2967 (C–H), 2917 (C–H), 1704 (C=O), 1609 (C=C), 1491, 1470, 1372, 1343, 1306, 1254, 1194, 1179, 1127, 1086, 1020, 980, 922, 840, 751, 695, 579, 542, 520, 485, 455; **^{1}H NMR** (400 MHz, $CDCl_3$) δ 7.32 (1H, t, *J* = 7.5 Hz, ArH), 7.16 (1H, d, *J* = 7.5 Hz, ArH), 7.06 (1H, t, *J* = 7.5 Hz, ArH), 6.87 (1H, d, *J* = 7.5 Hz, ArH), 4.63 (1H, t, *J* = 7.5 Hz, =CH), 3.25 (3H, s, CH_3), 2.95–2.70 (2H, m, CH_2), 1.98 (3H, s, CH_3), 1.49 (3H, s, CH_3), 1.47 (3H, s, CH_3); **^{13}C NMR** (101 MHz, $CDCl_3$) δ 201.4 (C=O), 175.0 (C=O), 144.3 (ArC), 136.1 (ArC), 129.1 (=CH), 127.5 (C), 124.2 (ArC–H), 123.1 (ArC–H), 116.7 (ArC–H), 108.4 (ArC–H), 66.5 (C), 32.2 (CH_2), 26.7 (CH_3), 26.6 (CH_3), 25.9 (CH_3), 18.12 (CH_3); **HRMS** m/z (ES) Found: MNa^+, 280.1320, $C_{16}H_{19}NO_2Na$, requires MNa^+ 280.1308; **LRMS** m/z (ES) 280 (100%, MNa^+).

1-Methyl-3-(3-methylbut-2-en-1-yl)-3-(pent-4-enoyl)-1,3-dihydro-*2H*-indol-2-one (153)

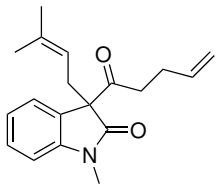

To a mixture of enol **143** (371 mg, 1.62 mmol) and prenyl bromide **151** (0.2 mL, 2 mmol) in THF (12 mL) was added Triton B (0.3 mL, 2 mmol) and the mixture was stirred at RT for 4 days. The reaction mixture was diluted with water (10 mL) and the organic product was extracted with EtOAc (3 × 10 mL). The combined organic layers were washed with water (10 mL), dried ($MgSO_4$), filtered and concentrated under reduced pressure. The residue was purified by column chromatography on silica gel, eluting with EtOAc–petrol (1:19) to give the dicarbonyl **153** (201 mg, 42%) as a purple oil; $\mathbf{R_f}$ 0.75 [EtOAc–petrol (1:1)]; **FT-IR** ν_{max} (film)/cm^{-1} 2913, (C–H) 1705 (C=O), 1608 (C=C), 1491, 1469, 1372, 1344, 1305, 1253, 1124, 1085, 1019, 996, 913; **^{1}H NMR** (400 MHz, $CDCl_3$) δ 7.37–7.29 (1H, m, ArH), 7.17 (1H, d, *J* = 7.5 Hz, ArH), 7.07 (1H, t, *J* = 7.5 Hz, ArH), 6.87 (1H, d, *J* = 7.5 Hz, ArH), 5.70–5.55 (1H, m, =CH), 4.92–4.87 (1H, m, =CH), 4.87–4.84 (1H, m,

=CH), 4.64 (1H, t, *J* = 7.5 Hz, =CH), 3.26 (3H, s, CH_3), 2.96–2.79 (2H, m, 2 × CH), 2.62–2.49 (1H, m, CH), 2.31–2.08 (3H, m, 3 × CH), 1.50 (3H, s, CH_3), 1.49 (3H, s, CH_3); **^{13}C NMR** (101 MHz, $CDCl_3$) δ 203.0 (C=O), 175.3 (C=O), 144.6 (ArC), 137.1 (ArC–H), 136.3 (ArC), 129.3 (ArC–H), 127.8 (C), 124.5 (ArC–H), 123.3 (ArC–H), 116.9 (CH), 115.6 (CH_2), 108.6 (CH), 66.4 (C), 38.5 (CH_2), 32.7 (CH_2), 27.6 (CH_2), 26.8 (CH_3), 26.1 (CH_3), 18.3 (CH_3); **HRMS** m/z (ES) Found: MH^+, 298.1805. $C_{19}H_{24}NO_2$ requires MH^+ 298.1802; **LRMS** m/z (ES) 298 (100%, MH^+).

Pent-4-enoic anhydride (154)

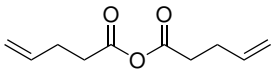

To a solution of 4-pentenoic acid **156** (16.3 mL, 160 mmol) in dry DCM (272 mL) was added a solution of *N,N*-dicyclohexylcarbodiimide (16.5 g, 79.9 mmol) in dry DCM (128 mL) over a period of 1 h. The mixture was allowed to stir for an additional 16 h at RT. The mixture was filtered, and the solvent was evaporated under reduced pressure. The residue was suspended in petrol (60 mL) and cooled to 0 °C for 16 h. The precipitated material was filtered off and washed with petrol (20 mL). The solvent was removed under reduced pressure to give pent-4-enoic anhydride **154** (14.6 g, quant. yield) as an orange liquid; **R_f** 0.82, [EtOAc–petrol (1:1)]; **FT-IR** ν_{max} (film)/cm^{-1} 3081 (C–H), 2981 (C–H), 2925 (C–H), 2857 (C–H), 1817 (C=O), 1748 (C=O), 1642 (C=C), 1519, 1439, 1413, 1355, 1268, 1224, 1116, 1036, 1000, 914, 842, 785, 633, 556, 466; **^{1}H NMR** (400 MHz, $CDCl_3$) δ 5.90–5.74 (2H, m, CH), 5.13–4.97 (4H, m, 2 × CH_2), 2.60–2.34 (8H, m, 4 × CH_2); **^{13}C NMR** (101 MHz, $CDCl_3$) δ 168.8 (C=O), 135.9 (CH), 116.3 (CH_2), 34.7 (CH_2), 28.2 (CH_2). Spectroscopic data in accordance with literature values.[181]

3-Allyl-1-methyl-3-(3-methylbut-2-en-1-yl)indolin-2-one (155)

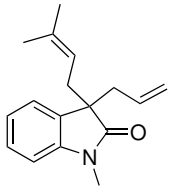

To a solution of ^{i}Pr$_2$NEt (165 μL, 1.18 mmol) in THF (0.5 mL) was added *n*-BuLi (513 μL, 1.18 mmol, 2.3 M in hexane) at –78 °C. The mixture was stirred for 10 min, at which time a solution of **152** (276 mg, 1.07

mmol) in THF (1 mL) was added and the mixture was stirred for a further 10 min. Then, bromide **60** (102 μL, 1.18 mmol) was added and the mixture was stirred at –78 °C for a further 30 min, before being allowed to warm to RT over 1 h. The mixture was quenched with NH_4Cl (3 mL), and the organic product was extracted with EtOAc (3 × 5 mL). The combined organic layers were washed with water (5 mL), dried ($MgSO_4$), filtered and concentrated under reduced pressure. The residue was purified by column chromatography, eluting with EtOAc–petrol (1:4) to afford compound **155** (201 mg, 73%) as a yellow oil; $\mathbf{R_f}$ 0.63 [EtOAc–petrol (1:1)]; **^{1}H NMR** (400 MHz, $CDCl_3$) δ 7.28–7.22 (1H, m, ArH), 7.21–7.15 (1H, m, ArH), 7.04 (1H, td, *J* = 7.5, 1.0 Hz, ArH), 6.80 (1H, d, *J* = 7.5 Hz, ArH), 5.37 (1H, ddt, *J* = 17.0, 10.0, 7.5 Hz, =CH), 4.97 (1H, ddt, *J* = 17.0, 2.0, 1.5 Hz, =CH), 4.86 (1H, ddt, *J* = 10.0, 2.0, 1.0 Hz, =CH), 4.82–4.74 (1H, m, =CH), 2.57 (2H, ddd, *J* = 7.5, 1.5, 1.0 Hz, CH_2), 2.50 (2H, d, *J* = 7.5 Hz, CH_2), 1.55 (3H, s, CH_3), 1.51 (3H, s, CH_3); **HRMS** m/z (ES) Found: $MH^{+\cdot}$ 256.1758. $C_{17}H_{21}NO$ requires MH^+ 256.1657; **LRMS** m/z (ES) 256 (100%, MH^+).

1-Methylspiro[indoline-3,2'oxiran]-2-one (159)

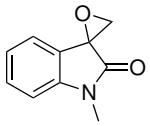

A mixture of trimethylsulfoxonium iodide (11.0 g, 50.1 mmol) and Cs_2CO_3 (17.2 g, 52.7 mmol) in dry MeCN (20 mL) was heated to 50 °C and stirred for 1 h. *N*-methyl isatin **125** (4.25 g, 26.4 mmol) in MeCN (40 mL) was added dropwise over 40 min, at which time the temperature was increased to 65 °C and the mixture was stirred for 1 h. The reaction mixture was filtered through celite and purified through a silica pad, then concentrated under reduced pressure to afford epoxide **159** (8.03 g, 87%) as a red amorphous solid; **mpt** 84–85 °C (literature does not report melting point); $\mathbf{R_f}$ 0.5 [EtOAc–petrol (1:1)]; **^{1}H NMR** (400 MHz, $CDCl_3$) δ 7.39 (1H, td, *J* = 7.5, 2.0 Hz, ArH), 7.15–7.04 (2H, m, ArH), 6.93 (1H, d, *J* = 7.5 Hz, CH), 3.59 (1H, d, *J* = 6.5 Hz, CH), 3.44 (1H, d, *J* = 6.5 Hz, CH), 3.28 (3H, s, CH_3); **^{13}C NMR** (101 MHz, $CDCl_3$) δ 171.8 (C), 145.1 (C), 130.4 (CH), 122.9 (CH), 122.7 (C), 122.1 (CH), 108.9 (CH), 56.4 (C), 54.1 (CH_2), 26.7 (CH_3). Spectroscopic data in accordance with literature values.[158]

(4*S*,4'*S*,5*R*,5'*R*)-2,2'-(Pentane-3,3-diyl)bis(4,5-diphenyl-4,5-dihydrooxazole) (168)

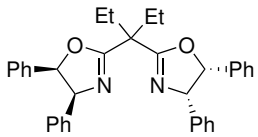
Et
Et
O
O
Ph
N
N
Ph
Ph
Ph

Compound **174** (3.19 g, 5.44 mmol) and NaH (723 mg, 31.4 mmol) were dissolved in THF (25 mL) and stirred for 30 min at RT. Then, EtI (1.38 mL, 17.2 mmol) was added, and the mixture was stirred at RT for a further 24 h. The reaction was quenched with water (20 mL), and the organic product was extracted with EtOAc (3 × 10 mL), dried ($MgSO_4$), filtered and concentrated under reduced pressure. The residue was purified by column chromatography on silica gel, eluting with EtOAc–petrol (3:17 to 1:1) to give ligand **168** (2.78 g, 99%) as a white amorphous solid; **mpt** 85–87 °C (lit.[164] 86–87 °C); $\mathbf{R_f}$ 0.46 [EtOAc–petrol (1:1)]; **^{1}H NMR** (400 MHz, $CDCl_3$) δ 7.10–6.84 (20H, m, 20 × ArH), 5.95 (2H, d, *J* = 10.0 Hz, 2 × CH), 5.60 (2H, d, *J* = 10.0 Hz, 2 × CH), 2.46 (2H, dq, *J* = 15.0, 7.5 Hz, CH_2), 2.31 (2H, dq, *J* = 15.0, 7.5 Hz, CH_2), 1.14 (6H, t, *J* = 7.5 Hz, 2 × CH_3); **^{13}C NMR** (101 MHz, $CDCl_3$) δ 169.1 (C), 137.6 (ArC), 136.2 (ArC), 128.1 (ArC–H), 127.7 (ArC–H), 127.7 (ArC–H), 127.5 (ArC–H), 127.1 (ArC–H), 126.8 (ArC–H), 86.2 (CH), 73.9 (CH), 47.7 (C), 26.0 (2 × CH_2), 8.9 (2 × CH_3); $[\alpha]^{19}_D$ = –403 (1.0, $CHCl_3$). Spectroscopic data in accordance with literature values.[164]

Potassium trifluoro(2-methylbut-3-en-2-yl)borate (170)

To compound **182** (6.13 g, 31.3 mmol) in MeOH (200 mL) was added a solution of KHF_2 (11.0 g, 140 mmol) in water (31.3 mL). The mixture was stirred for 30 min, then concentrated under reduced pressure. The residue was redissolved in 60% MeOH in water (12 mL), then reconcentrated (the process of dissolution and concentration was repeated 4 times). The residue was then dissolved in acetone and the impurities were filtered off. The residue was then suspended in cold Et_2O, and filtered to afford compound **170** (1.86 g, 33%) as an amorphous white solid; $\mathbf{R_f}$ 0.24 [EtOAc–petrol (1:1)] **^{1}H NMR** (400 MHz, CD_3CN) δ 6.09–5.98 (1H, m, =CH), 4.63–4.53 (2H, m, =CH), 0.79 (6H, s, 2 × CH_3); **^{13}C NMR** (101 MHz, CD_3CN, quaternary C not observed) δ 110.6 (=CH), 105.2 (=CH_2), 23.7 (CH_3). Spectroscopic data in accordance with literature values.[169]

(*R*)-(3-Allyl-1-methyl-2-oxoindolin-3-yl)methyl *tert*-butyl carbonate ((*R*)-171)

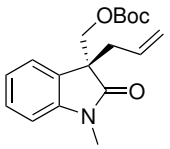

Compound **159** (1.00 g, 5.71 mmol), allyl BF_3K **169** (1.96 g, 13.4 mmol), $Co(ClO_4)_2.6H_2O$ (460 mg, 1.26 mmol), **168** (837 mg, 1.63 mmol) and Boc_2O (2.78 g, 12.7 mmol) were dissolved in PhMe (80 mL), heated to 70 °C and stirred for 3 days. The mixture was then concentrated under reduced pressure. The residue was purified by column chromatography on silica gel, eluting with EtOAc–hexane (1:4) to afford carbamate (*R*)-**171** (1.56 g, 86%) as a red gum; $\mathbf{R_f}$ 0.65 [EtOAc–petrol (1:1)]; **^{1}H NMR** (400 MHz, $CDCl_3$) δ 7.31–7.29 (1H, m, ArH), 7.29–7.26 (1H, m, ArH), 7.06 (1H, td, *J* = 7.5, 1.0 Hz, Ar-H), 6.83 (1H, dd, *J* = 8.0, 1.0 Hz, Ar-H), 5.48–5.33 (1H, m, =CH), 5.02 (1H, dq , *J* = 17.0, 1.5 Hz, =CH), 4.93 (2H, ddt, *J* = 10.0, 1.5, 1.0 Hz, =CH), 4.48 (1H, d, *J* = 10.5 Hz, 2 × CH), 4.25 (1H, d, *J* = 10.5 Hz, 2 × CH), 3.21 (3H, s, CH_3), 2.67–2.52 (2H, m, CH_2), 1.34 (9H, s, 3 × CH_3); **^{13}C NMR** (101 MHz, $CDCl_3$) δ 176.9 (C=O), 153.2 (C=O), 144.2 (ArC), 131.3 (=CH), 129.1 (ArC), 128.6 (ArC–H), 124.2 (ArC–H), 122.5 (ArC–H), 119.5 (=CH_2), 108.2 (ArH), 82.4 (C), 69.1 (CH_2), 52.7 (C), 38.3 (CH_2), 27.8 (CH_3), 26.4 (CH_3); **HPLC** [Daicel Chiralpak AD-H, hexane/^{i}PrOH = 90/10, 240 nm, 0.8 mL/min. t_{R1} = 7.5 min (minor), t_{R2} = 10.3 min (major), ee = 68% (see appendix); $\mathbf{[\alpha]^{22}_D}$ = +13.8 (1.1, $CHCl_3$). Spectroscopic data in accordance with literature values.[159]

(*S*)-(3-Allyl-1-methyl-2-oxoindolin-3-yl)methyl *tert*-butyl carbonate ((*S*)-171)

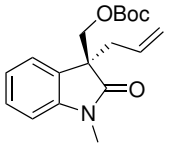

Compound **159** (1.00 g, 5.71 mmol), allyl BF_3K **169** (1.96 g, 13.4 mmol), $Co(ClO_4)_2.6H_2O$ (460 mg, 1.26 mmol), ligand **181** (837 mg, 1.63 mmol) and Boc_2O (2.78 g, 12.7 mmol) were dissolved in PhMe (80 mL), heated to 70 °C and stirred for 3 days. The mixture was then concentrated under reduced pressure. The residue was purified by column chromatography on silica gel, eluting with EtOAc–hexane (1:4) to afford (*S*)-**171** (1.56 g, 86%) as a red gum; $\mathbf{R_f}$ 0.65 [EtOAc–petrol (1:1)]; **^{1}H NMR** (400 MHz, $CDCl_3$) δ 7.30 (1H, td, *J* = 4.0, 1.0 Hz, ArH), 7.27 (1H, dd, *J* = 4.0, 1.0 Hz, ArH), 7.08 (1H, td, *J* = 8.0, 1.0 Hz, Ar-H), 6.86 (1H, dd, *J*

= 8.0, 1.0 Hz, Ar-H), 5.42 (1H, ddt, *J* = 17.0, 10.0, 7.5 Hz, =CH), 5.04 (1H, dq, *J* = 17.0, 1.5 Hz, $=CH_2$), 4.95 (ddt, *J* = 10.0, 1.5, 1.0 Hz, =CH), 4.51 (1H, d, *J* = 10.5 Hz, CH), 4.28 (1H, d, *J* = 10.5 Hz, CH), 3.23 (3H, s, CH_3), 2.70–2.53 (2H, m, CH_2), 1.37 (9H, s, 3 × CH_3); **^{13}C NMR** (101 MHz, $CDCl_3$) δ 176.9 (C=O), 153.2 (C=O), 144.2 (ArC), 131.3 (=CH), 129.1 (ArC), 128.6 (ArC–H), 124.2 (ArC–H), 122.5 (ArC–H), 119.5 (CH_2), 108.2 (ArH), 82.4 (C), 69.1 (CH_2), 52.7 (C), 38.3 (CH_2), 27.8 (CH_3), 26.4 (CH_3); **HPLC** [Daicel Chiralpak AD-H, hexane/^{i}PrOH = 90/10, 240 nm, 0.8 mL/min, t_{R1} = 7.4 min (major), t_{R2} = 10.1 min (minor); ee = 53% (see appendix); **[α]$^{22}_{D}$** = –11 (1.0, $CHCl_3$).

(4*S*,4'*S*,5*R*,5'*R*)-2,2'-Methylenebis[4,5-dihydro-4,5-diphenyloxazole] (174)

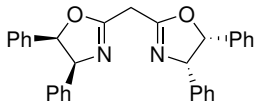

A mixture of diethyl malonimidate dihydrochloride **173** (3.71 g, 23.5 mmol) and (1*R*,2*S*)-**172** (10.0 g, 46.9 mmol) in DCM (100 mL) was refluxed for 20 h. The mixture was diluted with water (100 mL) and the layers were separated. The organic layer was dried ($MgSO_4$), filtered and concentrated under reduced pressure. The residue was purified by column chromatography on silica gel, eluting with DCM–MeOH (49:1 to 19:1), and recrystallised from *n*-hexane/DCM, to afford compound **174** (5.07 g, 37%) as white needles; **mpt** 184–185 °C (literature does not report melting point); **R_f** 0.88 [MeOH–DCM 1:9]; **^{1}H NMR** (400 MHz, $CDCl_3$) δ 7.12–6.90 (20H, m, 20 × ArH), 5.99 (2H, d, *J* = 10.0 Hz, 2 × CH), 5.65 (2H, d, *J* = 10.0 Hz, 2 × CH), 3.90 (2H, s, CH_2); **^{13}C NMR** (101 MHz, $CDCl_3$) δ 163.3 (C), 137.5 (ArC), 136.2 (ArC), 128.0 (ArC–H), 127.8 (ArC–H), 127.8 (ArC–H), 127.6 (ArC–H), 127.1 (ArC–H), 126.7 (ArC–H), 86.4 (CH), 74.3 (CH), 29.3 (CH_2). Spectroscopic data in accordance with literature values.[162]

2,2-Dimethylmalonyl dichloride (177)

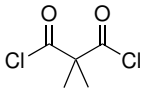

To a solution of dimethyl malonyl diacid **176** (2.64 g, 20.0 mmol) in DCM (8 mL) at 0 °C was added oxalyl chloride (3.43 mL, 40.0 mmol) dropwise, then DMF (155 μL, 2.00 mmol) was added. The mixture was warmed to RT and left to stir overnight. The mixture purified by vacuum distillation (vapour temperature

77 ℃, under house vacuum) to afford compound **177** (897 mg, 26%) as a colourless liquid; $\mathbf{R_f}$ 0.28 [EtOAc–petrol (1:1)]; **^{1}H NMR** (400 MHz, $CDCl_3$) δ 1.68 (6H, s, 2 × CH_3). Spectroscopic data in accordance with literature values.[182]

(*S*)-3-Allyl-3-(hydroxymethyl)-1-methylindolin-2-one ((*S*)-179)

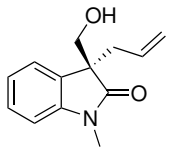

Carbamate (*R*)-**171** (1.78 g, 5.60 mmol) was dissolved in methanolic HCl (6 M, 180 mL), and stirred overnight at RT. The mixture was quenched with $NaHCO_3$ (50 mL), and the organic product was extracted with EtOAc (2 × 50 mL). The combined organic layers were dried ($MgSO_4$), filtered and concentrated under reduced pressure to give (*S*)-**179** (942 mg, 77%) as an orange gum; $\mathbf{R_f}$ 0.18 [EtOAc–petrol (1:1)]; **^{1}H NMR** (400 MHz, $CDCl_3$) δ 7.31 (1H, td, *J* = 7.5, 1.0 Hz, Ar-H), 7.23 (1H, dd, *J* = 7.5, 1.0 Hz, Ar-H), 7.13–7.05 (1H, m, Ar-H), 6.87 (1H, d, *J* = 7.5 Hz, Ar-H), 5.46 (1H, ddt, *J* = 17.0, 10.0, 7.5 Hz, =CH), 5.03 (1H, dd, *J* = 17.0, 2.0 Hz, $=CH_2$), 4.94 (1H, dd, *J* = 10.0, 2.0 Hz, $=CH_2$), 3.91 (1H, d, *J* = 11.0 Hz, CH), 3.76 (1H, d, *J* = 11.0 Hz, CH), 3.22 (3H, s, CH_3), 2.69 (1H, dd, *J* = 13.5, 7.5 Hz, CH), 2.63 (1H, dd, *J* = 13.5, 7.5 Hz, CH), 2.36 (1H, br s, O–H); **^{13}C NMR** (101 MHz, $CDCl_3$) δ 179.1 (C=O), 144.2 (ArC), 132.0 (=CH), 129.6 (ArC), 128.6 (ArC–H), 123.5 (ArC–H), 122.8 (ArC–H), 119.2 ($=CH_2$), 108.4 (ArC–H), 66.6 (CH_2), 54.2 (C), 37.5 (CH_2), 26.3 (CH_3); **HPLC** [Daicel Chiralpak AD-H, hexane/^{i}PrOH = 90/10, 240 nm, 0.8 mL/min, t_{R1} = 9.8 min (minor), t_{R2} = 10.9 min (major)]; ee = 66% (see appendix); $\mathbf{[\alpha]^{22}_D}$ = –4 (1.0, $CHCl_3$). Spectroscopic data in accordance with literature values.[159]

(*R*)-3-Allyl-3-(hydroxymethyl)-1-methylindolin-2-one ((*R*)-179)

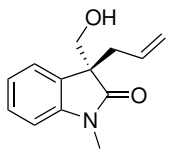

Carbamate (*R*)-**171** (1.56 g, 4.92 mmol) was dissolved in methanolic HCl (6 M, 146 mL) and stirred at RT for 16 h. The reaction mixture was quenched with $NaHCO_3$ (50 mL), and the organic product was extracted with EtOAc (2 × 50 mL). The combined organic layers were dried ($MgSO_4$), filtered and

concentrated under reduced pressure. The residue was purified by column chromatography on silica gel, eluting with EtOAc–petrol (1:1), then further purified again by column chromatography on silica gel, eluting with EtOAc–petrol (4:1) to give (*R*)-**179** (272 mg, 25%) as a yellow gum. Data as shown above, with the exception of $[\alpha]^{23}_{D}$ = +1.4 (1.0, $CHCl_3$). HPLC not performed.

3-Allyl-3-(hydroxymethyl)-1-methylindolin-2-one (179)

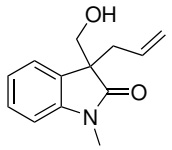

To epoxide **159** (6.00 g, 34.2 mmol) and trimethylallylsilane (16.3 mL, 103 mmol) in dry MeCN (190 mL) at 0 °C was added $Sc(OTf)_3$ (1.69 g, 3.43 mmol) in dry MeCN (10 mL), and the mixture was stirred for 4 h at 0 °C. The reaction was quenched with $NaHCO_3$ (100 mL), and the organic product was extracted with EtOAc (2 × 50 mL). The combined organic layers were washed with brine (100 mL), dried (Na_2SO_4), filtered and concentrated under reduced pressure. The residue was purified by column chromatography on silica gel, eluting with EtOAc–petrol (1:2) to afford compound **179** (2.04 g, 27%) as an orange solid; **mpt** 68–70 °C (lit.[138] 74 °C). Other spectroscopic data as shown above, and in accordance with literature values.[138]

(*R*)-(3-Allyl-1-methyl-2-oxoindolin-3-yl)methyl 4-methylbenzenesulfonate ((*R*)-180)

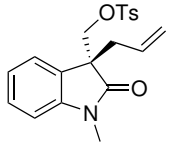

To (*R*)-**179** (272 mg, 1.25 mmol), TsCl (358 mg, 1.88 mmol) and DMAP (46 mg, 0.38 mmol) in DCM (15 mL) was added Et_3N (523 μL, 3.76 mmol) and stirred at RT for 4 days. The reaction was quenched with $NaHCO_3$ (15 mL), and the layers were separated. The organic layer was dried ($MgSO_4$), filtered and concentrated under reduced pressure. The residue was purified by column chromatography on silica gel, eluting with EtOAc–petrol (1:4), to afford (*R*)-**180** (309 mg, 54%) as an amorphous yellow solid; **mpt** 64–66 °C; $\mathbf{R_f}$ 0.57 [EtOAc–petrol (1:1)]; **FT-IR** ν_{max} (film)/cm^{-1} 2943 (C-H), 1708 (C=O), 1647 (C=C), 1611, 1599, 1494, 1468, 1455, 1425, 1359 (S=O), 1314, 1292, 1258, 1178, 1119, 1023, 976, 936, 885, 831, 816, 776, 752; **^{1}H NMR** (400 MHz, $CDCl_3$) δ 7.66–7.59 (2H, m, 2 × ArH), 7.33–7.27 (3H, m, ArH), 7.19 (1H, dd,

J = 7.5, 1.0 Hz, ArH), 7.04 (1H, td, *J* = 7.5, 1.0 Hz, ArH), 6.81 (1H, d, *J* = 7.5 Hz, ArH), 5.38–5.25 (1H, m, =CH), 4.97 (1H, dq, *J* = 17.0, 1.5 Hz, =CH), 4.90 (1H, dd, *J* = 10.0, 1.5 Hz, =CH), 4.27 (1H, d, *J* = 9.5 Hz, CH), 4.13 (1H, d, *J* = 9.5 Hz, CH), 3.16 (3H, s, CH_3), 2.61–2.45 (2H, m, CH_2), 2.44 (3H, s, CH_3); **^{13}C NMR** (101 MHz, $CDCl_3$, one quaternary C not observed) δ 207.1 (C=O), 145.1 (ArC), 134.5 (ArC), 130.7 (ArH/=CH), 130.0 (2 × ArH), 128.9 (ArH/=CH), 128.4 (ArC), 128.1 (2 × ArH), 124.1 (ArH), 122.9 (ArH), 119.9 (=CH_2), 108.3 (ArH), 72.2 (CH_2–O), 60.5 (C), 38.0 (CH_2), 31.1 (CH_3), 26.4 (CH_3); **HRMS** m/z (ES) Found: MH^+, 372.1281, $C_{20}H_{21}NO_4S$ requires MH^+ 372.1264; **LRMS** m/z (ES) 372 (100%, MH^+). HPLC and specific rotation data not measured.

(4*R*,4'*R*,5*S*,5'*S*)-2,2'-(Pentane-3,3-diyl)bis(4,5-diphenyl-4,5-dihydrooxazole) (181)

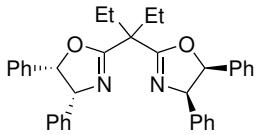

Compound **202** (4.90 g, 8.37 mmol) and NaH (1.11 g, 48.3 mmol) were dissolved in THF (40 mL) and stirred for 30 min at RT. Then, EtI (2.12 mL, 26.4 mmol) was added, and the mixture was stirred at RT for a further 24 h. The mixture was quenched with water (30 mL), and the organic product was extracted with EtOAc (3 × 10 mL). The combined organic layers were dried ($MgSO_4$), filtered and concentrated under reduced pressure. The residue was purified by column chromatography on silica gel, eluting with EtOAc–petrol (3:17 to 1:1) to afford compound **181** (3.28 g, 76%) as an amorphous white solid; **mpt** 83–86 °C (lit.[159] 91–93 °C); **R_f** 0.56 [EtOAc–petrol (1:1)]; **^{1}H NMR** (400 MHz, $CDCl_3$) δ 7.08–6.88 (20H, m, 20 × Ar-H), 5.95 (2H, d, *J* = 10.0 Hz, 2 × CH), 5.60 (2H, d, *J* = 10.0 Hz, 2 × CH), 2.46 (2H, dq, *J* = 15.0, 7.5 Hz, 2 × CH), 2.31 (2H, dq, *J* = 15.0, 7.5 Hz, 2 × CH), 1.14 (6H, t, *J* = 7.5 Hz, 2 × CH_3); **^{13}C NMR** (101 MHz, $CDCl_3$) δ 169.1 (C=N), 137.6 (ArC), 136.2 (ArC), 128.1 (ArC–H), 127.7 (ArC–H), 127.7 (ArC–H), 127.5 (ArC–H), 127.1 (ArC–H), 126.8 (ArC–H), 86.2 (2 × CH), 73.9 (2 × CH), 47.7 (C), 26.0 (2 × CH_2), 8.9 (2 × CH_3); $[\alpha]^{21}_D$ = +403 (1.0, $CHCl_3$). Spectroscopic data in accordance with literature values.[159]

(*R*)-*tert*-Butyl((1-methyl-3-(2-methylbut-3-en-2-yl)-2-oxoindolin-3-yl)methyl) carbonate ((*R*)-183)

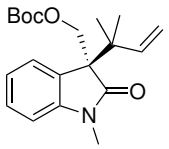

Compound **159** (500 mg, 2.85 mmol), boron salt **170** (844 mg, 4.80 mmol), $Co(ClO_4)_2.6H_2O$ (230 mg, 628 μmol), ligand **168** (353 mg, 0.685 mmol) and Boc_2O (1.90 g, 8.85 mmol) were dissolved in PhMe (40 mL), heated to 70 °C and stirred for 3 days. The mixture was concentrated under reduced pressure, and the residue was purified by column chromatography on silica gel twice, eluting with EtOAc–hexane (1:5.7 to 1:9) to afford carbamate (*R*)-**183** (279 g, 31%) as a pale pink amorphous solid; $\mathbf{R_f}$ 0.88 [EtOAc–petrol (1:1)]; **^{1}H NMR** (400 MHz, $CDCl_3$) δ 7.28 (2H, d, *J* = 7.5 Hz, 2 × ArH), 7.00 (1H, td, *J* = 7.5, 1.0 Hz, ArH), 6.83–6.78 (1H, m, ArH), 6.07 (1H, dd, *J* = 17.5, 11.0 Hz, =CH), 5.10 (1H, dd, *J* = 11.0, 1.0 Hz, CH), 5.00 (1H, dd, *J* = 17.5, 1.0 Hz, CH), 4.73 (1H, d, *J* = 10.5 Hz, CH), 4.48 (1H, d, *J* = 10.5 Hz, CH), 3.19 (3H, s, CH_3), 1.24 (9H, s, 3 × CH_3), 1.14 (3H, s, CH_3), 1.03 (3H, s, CH_3); **^{13}C NMR** (101 MHz, $CDCl_3$, 5 quaternary carbon peaks not observed) δ 204.4 (C=O), 177.3 (C=O), 143.0 (=CH), 128.4 (ArC–H), 126.1 (ArC–H), 121.6 (ArC–H), 114.1 (=CH_2), 107.7 (ArC–H), 67.2 (CH_2), 27.7 (3 × CH_3), 26.2 (CH_3), 22.7 (CH_3), 22.2 (CH_3); **HRMS** m/z (ES) Found: MNa^+ 368.1832, $C_{20}H_{27}NO_4Na$ requires MNa^+ 368.1832; **LRMS** m/z (ES) 368 (100%, MNa^+); $\mathbf{[\alpha]^{22}_D}$ = –4 (1.0, $CHCl_3$).

(*R*)-3-(Hydroxymethyl)-1-methyl-3-(2-methylbut-3-en-2-yl)indolin-2-one ((*R*)-185)

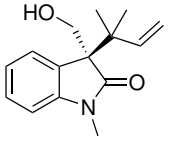

Compound **183** (201 mg, 0.582 mmol) was dissolved in methanolic HCl (11.6 mL, 6.00 M) and stirred overnight at RT. The mixture was quenched with $NaHCO_3$ (10 mL), extracted with EtOAc (3 × 5 mL), dried ($MgSO_4$), filtered and concentrated under reduced pressure, to afford (*R*)-**185** (138 mg, 97%) as an amorphous orange solid; $\mathbf{R_f}$ 0.20 [EtOAc–petrol (1:1)]; **^{1}H NMR** (400 MHz, $CDCl_3$) δ 7.31 (2H, dd, *J* = 7.5, 1.0 Hz, ArH), 7.10–7.01 (1H, m, ArH), 6.87–6.80 (1H, m, ArH), 6.06 (1H, dd, *J* = 17.5, 11.0 Hz, =CH),

5.07 (1H, dd, *J* = 11.0, 1.0 Hz, =CH), 4.98 (1H, dd, *J* = 17.5, 1.0 Hz, =CH), 4.22 (1H, d, *J* = 11.0 Hz, CH), 3.97 (1H, d, *J* = 11.0 Hz, CH), 3.20 (3H, s, CH_3), 1.16 (3H, s, CH_3), 1.01 (3H, s, CH_3); **^{13}C NMR** (101 MHz, $CDCl_3$) δ 178.3 (C=O), 145.4 (C), 143.6 (=CH), 128.8 (ArC), 128.6 (ArC–H), 125.2 (ArC–H), 121.9 (ArC–H), 113.6 (=CH_2), 108.0 (ArC–H), 64.0 (CH_2), 60.4 (C), 41.2 (C), 26.2 (CH_3), 22.9 (CH_3), 22.5 (CH_3); **HRMS** m/z (ES) Found: MH^+ 246.1500, $C_{15}H_{19}NO_2$ requires MH^+ 246.1489; **LRMS** m/z (ES) 246 (100%, MH^+).

1'-Methyl-5-((trimethylsilyl)methyl)-4,5-dihydro-*2H*-spiro[furan-3,3'-indolin]-2'-one (190)

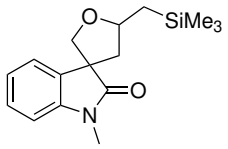

To compound **159** (1.00 g, 5.71 mmol), and allylsilane (1.81 mL, 11.4 mmol) in DCM (20 mL) at 0 °C was added BF_3OEt_2 (141 μL, 1.14 mmol) and the mixture was stirred at 0 °C for 30 min. The residue was purified by column chromatography on silica gel, eluting with EtOAc–petrol (1:2) to afford compound **190** (355 mg, 21%) as a yellow gum as a mixture of diastereoisomers (dr 1.2:1, M = major, m = minor); **R_f** 0.80 [EtOAc–petrol (1:1)]; **^{1}H NMR** (400 MHz, $CDCl_3$) δ 7.37–7.27 (2H, m, 2 × Ar-H), 7.12–7.06 (1H, m, ArH), 6.88–6.81 (1H, m, Ar-H), 4.48 (0.55H, tt, *J* = 9.0, 6.0 Hz, CH^M), 4.35 (0.45H, tt, *J* = 9.0, 6.0 Hz, CH^m), 4.21 (0.55H, d, *J* = 9.0 Hz, CH^M), 3.96 (0.9H, s, 2 × CH^m), 3.81 (0.55H, d, *J* = 9.0 Hz, CH^M), 3.23 (1.65H, s, $CH_3{}^M$), 3.22 (1.35H, s, $CH_3{}^m$), 2.56 (0.45H, dd, *J* = 12.5, 6.5 Hz, CH^m), 2.23–2.08 (0.9H, m, 2 × CH^m), 1.77–1.66 (0.55H, m, CH^M), 1.35–1.25 (1.1H, m, 2 × CH^M), 1.08 (0.55H, dd, *J* = 14.0, 9.0 Hz, CH^M), 1.00 (0.45H, dd, J = 14.0, 9.0 Hz, CH^m), 0.05 (9H, s, 3 × CH_3); **^{13}C NMR** (101 MHz, $CDCl_3$) δ 179.0 (C=O), 178.4 (C=O),143.1 (ArC), 143.0 (ArC), 135.4 (ArC), 134.2 (ArC), 128.2 (ArC–H), 128.0 (ArC–H), 123.2 (ArC–H), 123.1 (ArC–H), 122.9 (ArC–H), 122.8 (ArC–H), 108.2 (ArC–H), 108.0 (ArC–H), 79.2 (CH^{M+m}), 76.7 (CH_2), 75.6 (CH_2), 55.7 (C), 55.5 (C), 47.3 (CH_2), 47.1 (CH_2), 26.6 (CH_3), 26.5 (CH_3), 24.3 (CH_2), 24.2 (CH_2), –0.8 (Si-$CH_3{}^M$), –0.8 (Si-$CH_3{}^m$). Spectroscopic data in accordance with literature values.[171;170]

(3a*S*,7*S*,8a*R*,8b*R*)-1',2-Dimethyl-3a,8,8a,8b-tetrahydro-1H,6*H*-spiro[dipyrrolo [1,2-*b*:3',4'-*d*]isoxazole-7,3'-indoline]-1,2',3(2*H*)-trione (193)

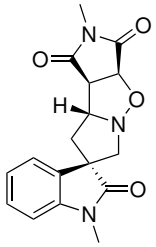

Aldehyde **123** (500 mg, 1.44 mmol) and hydroxylamine hydrochloride (160 mg, 2.30 mmol) were dissolved in PhMe (10 mL). $^{i}Pr_2NEt$ (481 μL, 2.76 mmol) was added and the mixture was heated to 60 °C and stirred for 2 h. *N*-methylmaleimide (**192**) (255 mg, 2.30 mmol) was added and the reaction mixture was heated to reflux and stirred for 3 h. When, by TLC, the reaction appeared to have still not gone to completion, further *N*-methylmaleimide **192** (128 mg, 1.84 mmol) was added, and the reaction mixture was stirred at reflux for a further 1 h. The mixture was cooled to RT and concentrated under reduced pressure. The residue was purified by column chromatography on silica gel, eluting with EtOAc–petrol (1:2.5) to give the oxindole **193** (293 mg, 62%) as a mixture of isomers (60:17:15:8).

A portion of the major isomer **A** was isolated (39 mg, 8%) as a yellow amorphous solid; **mpt** 175–180 °C; $\mathbf{R_f}$ 0.62 [MeOH–DCM 1:9]; **FT-IR** ν_{max} (film)/cm^{-1} 2941 (C–H), 1784 (C=O), 1694 (C=O), 1612, 1495, 1471, 1434, 1377, 1352, 1281, 1247, 1181, 1138, 1092, 1072, 1041, 993, 932, 870; **^{1}H NMR** (400 MHz, $CDCl_3$) δ 7.30 (1H, td, *J* = 7.5, 1.0 Hz, ArH), 7.21 (1H, d, *J* = 7.5 Hz, ArH), 7.07 (1H, td, *J* = 7.5, 1.0 Hz, ArH), 6.84 (1H, d, *J* = 7.5 Hz, ArH), 5.07 (1H, d, *J* = 7.5 Hz, CH), 4.25 (1H, ddd, *J* = 11.0, 6.5, 1.5 Hz, CH), 3.86 (1H, d, *J* = 15.0 Hz, CH) 3.70 (1H, dd, *J* = 7.5, 1.5 Hz, CH), 3.42 (1H, d, *J* = 15.0 Hz, CH), 3.22 (3H, s, CH_3), 3.08 (3H, s, CH_3), 2.55 (1H, dd, *J* = 13.0, 11.0 Hz, CH), 2.24 (1H, dd, *J* = 13.0, 6.5 Hz, CH); **^{13}C NMR** (101 MHz, $CDCl_3$) δ 178.4 (C=O), 175.2 (C=O), 174.8 (C=O), 142.9 (ArC), 134.2 (ArC), 128.8 (ArC–H), 123.4 (ArC–H), 122.3 (ArC–H), 108.5 (ArC–H), 76.2 (CH), 71.9 (CH), 65.3 (CH_2), 56.1 (C), 52.9 (CH), 42.8 (CH_2), 26.8 (CH_3), 25.3 (CH_3); **HRMS** m/z (ES) Found: MH^+, 328.1292. $C_{17}H_{17}N_3O_4$ requires MH^+ 328.1319; **LRMS** m/z (ES) 328 (100%, MH^+).

A mixture of diastereoisomers (189 mg, 40%, orange foam) was also isolated, composed of major isomer **A** (data as above) and isomer **B** (ratio 75:25). A second mixture of diastereoisomers was also isolated

as a mixture of diastereoisomers **C** and **D** (65 mg, 14%, ratio 66:34) as an orange foam.

The ratio was determined from the **^{1}H NMR** spectra by integrating the peaks for OC–H at 5.07 (0.60H, d, *J* = 7.5 Hz, isomer **A**), 5.00 (0.17H, d, *J* = 8.0 Hz, isomer **B**), 5.04 (0.08H, d, *J* = 8.0 Hz, isomer **D**), 5.03 (0.15H, d, *J* = 7.5 Hz, isomer **C**). Stereochemistry of major isomer determined by 2D NOESY NMR.

1'-Methyl-2-phenyl-3a,8,8a,8b-tetrahydro-*1H,6H*-spiro[dipyrrolo[1,2-b:3',4'-d]-isoxazole-7,3'-indoline]-1,2',3(*2H*)-trione (195)

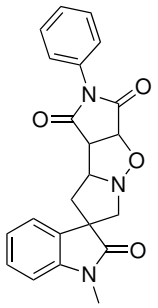

Compound **123** (192 mg, 0.552 mmol) and hydroxylamine hydrochloride (96.0 mg, 1.38 mmol) were dissolved in PhMe (3 mL). ^{i}Pr$_2$NEt (231 μL, 1.32 mmol) was added and the mixture was heated to 60 °C and stirred for 30 min. *N*-phenylmaleimide **194** (287 mg, 1.66 mmol) was added and the reaction mixture was refluxed for 3.5 h. The mixture was cooled to RT and concentrated under reduced pressure. The residue was purified by column chromatography on silica gel, eluting with EtOAc–hexane (1:2.5), then by column chromatography eluting with EtOAc–hexane (1:4 to 1:0) to afford compound **195** (140 mg, 78%) as an orange amorphous solid as a mixture of isomers (88:12); **mpt** 170–173 °C; **R$_f$** 0.16 [EtOAc–petrol (1:1)]; **FT-IR** ν_{max} (film)/cm^{-1} 2960 (C–H), 2874 (C–H), 1782 (C=O), 1711 (C=O), 1697 (C=O), 1610, 1493, 1468, 1376, 1350, 1266, 1247, 1187, 1086, 1070, 1019, 971, 869, 759; **^{1}H NMR** (400 MHz, $CDCl_3$) δ 7.47–7.30 (6H, m, 6 × ArH), 7.25–7.21 (1H, m, ArH), 7.07 (1H, td, *J* = 7.5, 1.0 Hz, ArH), 6.84 (1H, d, *J* = 7.5 Hz, ArH), 5.20 (0.88H, d, *J* = 7.5 Hz, CH^M), 5.13 (0.12H, d, *J* = 7.5 Hz, CH^m), 4.53 (0.12H, d, *J* = 7.5 Hz CH^m), 4.34 (0.88H, dd, *J* = 10.5, 6.5 Hz, CH^M), 3.88 (1H, d, *J* = 15.0 Hz, CH), 3.83 (1H, d, *J* = 7.5, CH), 3.45 (1H, d, *J* = 15.0 Hz, CH), 3.21 (2.68H, s, CH$_3{}^M$), 3.19 (0.36H, s, CH$_3{}^m$), 2.57 (1H, dd, *J* = 13.0, 10.5 Hz, CH) 2.25 (1H, dd, *J* = 13.0, 6.5 Hz, CH); **^{13}C NMR** (101 MHz, $CDCl_3$) δ 178.5 (C=O), 174.5 (C=O), 173.9 (C=O), 142.7 (ArC), 134.1 (ArC), 131.4 (ArC), 129.3 (ArC–H), 129.0 (ArC–H), 128.7 (Ar–CH) 126.5 (ArC–H), 123.4 (ArC–H), 122.3 (ArC–H), 108.8 (ArC–H), 76.1 (CH^M), 72.2 (CH^M), 70.2 (CH^m), 65.3 (CH$_2$), 62.6 (CH^m), 56.0

(C), 52.9 (CH), 42.70 (CH_2), 26.8 (CH_3); **HRMS** m/z (ES) Found: MH^+, 390.1448. $C_{22}H_{19}N_3O_4$ requires MH^+ 390.1452; **LRMS** m/z (ES) 390 (100%, MH^+).

Dimethyl 1-methyl-2-oxo-2',3',3a',4'-tetrahydro-6'*H*-spiro[indoline-3,5'-pyrrolo[1,2-*b*]-isoxazole]-2',3'-dicarboxylate (197)

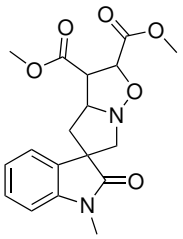

Compound **123** (220 mg, 0.632 mmol) and hydroxylamine hydrochloride (88 mg, 1.3 mmol) were dissolved in PhMe (5 mL). $^{i}Pr_2NEt$ (264 μL, 1.52 mmol) was added and the mixture was heated to 60 °C and stirred for 1 h. Dimethyl fumarate (**196**) (273 mg, 1.90 mmol) was added, and the reaction mixture was heated to reflux and stirred for 3.5 h. The mixture was cooled to RT and concentrated under reduced pressure, then purified by column chromatography on silica gel, eluting with EtOAc–Hexane (1:2) to afford compound **197** (213 mg, 93%) as an orange amorphous solid as a mixture of isomers (55:27:18) (**A:B:C**).

One mixture of isomers, containing isomers **A** and **B** (ratio 83:17), was isolated as an orange solid (47 mg, 21%) and characterised; **mpt** 82–84 °C; $\mathbf{R_f}$ 0.41, 0.50 [MeOH–DCM 1:9]; **FT-IR** ν_{max} (film)/cm^{-1} 2956 (C–H), 1737 (C=O), 1707 (C=O), 1612, 1493, 1474, 1437, 1376, 1352, 1260, 1205, 1129, 1085, 1020, 989; **^{1}H NMR** (400 MHz, $CDCl_3$) δ 7.45 (1H, dd, *J* = 7.5, 1.5 Hz, ArH), 7.30–7.22 (1H, m, ArH) 7.12–7.06 (1H, m, ArH), 6.80 (1H, d, *J* = 7.5 Hz, ArH), 5.22 (0.83 H, d, *J* = 5.0 Hz, CH^M), 5.09 (0.17H, d, *J* = 6.0 Hz, CH^m), 4.40 (1H, dt, *J* = 10.5, 7.0 Hz, CH), 4.23 (0.83H, dd, *J* = 7.0, 5.0 Hz, CH^M) 4.17–4.08 (0.17H, m, CH^m), 3.85 (3H, s, CH_3), 3.84 (1H, d, *J* = 18.5 Hz, CH), 3.71 (3H, s, CH_3), 3.70 (1H, d, *J* = 18.5 Hz, CH), 3.19 (3H, s, CH_3), 2.56 (0.17H, dd, *J* = 13.0, 7.0 Hz, CH^m), 2.33 (0.83H, dd, *J* = 13.0, 7.0 Hz, CH^M), 2.25 (0.17H, dd, *J* = 13.0, 10.5 Hz, CH^m), 2.09 (0.83H, dd, *J* = 13.0, 10.5 Hz, CH^M); **^{13}C NMR** (101 MHz, $CDCl_3$, 6 × quaternary C peaks could not be observed) δ 180.4 (C=O), 171.9 (C=O), 170.4 (C=O), 143.3 (ArC), 134.0 (ArC), 128.2(ArC–H), 124.5 (ArC–H), 123.5 (ArC–H), 108.0 (ArC–H), 77.9 (CH^m), 76.0 (CH^M), 72.2 (CH^m), 70.5 (CH^M), 66.0 (CH_2), 56.4 (C), 54.8 (CH), 53.1 ($CH_3{}^M$), 53.0 ($CH_3{}^m$), 52.9 ($CH_3{}^m$), 52.7 ($CH_3{}^M$), 41.6 (CH_2), 26.5 (CH_3); **HRMS** m/z (ES) Found: MH^+ 361.1394, $C_{18}H_{20}N_2O_6$ requires MH^+ 361.1405; **LRMS**

m/z (ES) 316 (100%, MH^+).

The second mixture of isomers, containing isomers **A**, **B** and **C** (12:23:65), was also isolated as a yellow amorphous solid (166 mg, 73%).

The ratio was determined from the ^{1}H NMR spectra by integrating the peaks for OC–H at 5.22 (0.55H, d, *J* = 5.0 Hz, isomer **A**), 5.09 (0.18H, d, *J* = 6.0 Hz, isomer **B**), 5.06 (0.27H, d, *J* = 8.0 Hz, isomer **C**) on the crude material.

Dimethyl (2'*S*,3*S*,3'*R*,3a'*R*)-1-methyl-2-oxo-2',3',3a',4'-tetrahydro-6'*H*-spiro[indoline-3,5'-pyrrolo [1,2-*b*]isoxazole] -2',3'-dicarboxylate (199)

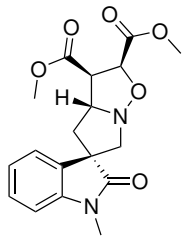

Compound **123** (500 mg, 1.44 mmol) and hydroxylamine hydrochloride (200 mg, 2.87 mmol) were dissolved in PhMe (7 mL). ^{i}Pr$_2$NEt (601 μL, 3.45 mmol) was added and the mixture was heated to 60 ℃ and stirred for 70 min. Dimethyl maleate (**198**) (539 μL, 1.90 mmol) was added and the reaction mixture was heated to reflux and stirred for 3.5 h. The mixture was cooled to RT and concentrated under reduced pressure, then purified by column chromatography on silica gel, eluting with EtOAc–Hexane (1:2) to afford compound **199** (353 mg, 63%) as an orange amorphous gum, as a mixture of isomers (95:5); $\mathbf{R_f}$ 0.28 [EtOAc–petrol (1:1)]; **FT-IR** ν_{max} (film)/cm^{-1} 2953 (C–H), 1738 (C=O), 1707 (C=O), 1612, 1493, 1470 1437, 1376, 1352, 1212, 1019; **^{1}H NMR** (400 MHz, $CDCl_3$) δ 7.43 (1H, br d, *J* = 7.5 Hz, ArH), 7.29 (1H, td, *J* = 7.5, 1.0 Hz, ArH), 7.10 (1H, td, *J* = 7.5, 1.0 Hz, ArH), 6.83 (1H, br d, *J* = 7.5 Hz, ArH), 5.14 (0.95H, d, *J* = 8.0 Hz, CH^M), 5.09 (0.05H, d, *J* = 6.0 Hz, CH^m), 4.48 (0.95H, td, *J* = 8.0, 5.0 Hz, CH^M), 4.25 (0.05H, t, *J* = 6.5 Hz, CH^m), 4.05 (0.95H, t, *J* = 8.0 Hz, CH^M), 3.91–3.65 (2H, m, CH_2), 3.79 (3H, s, CH_3), 3.74 (3H, s, CH_3), 3.22 (3H, s, CH_3), 2.45 (1H, dd, *J* = 13.5, 5.0 Hz, CH), 2.32 (1H, dd, *J* = 13.5, 8.0 Hz, CH); **^{13}C NMR** (101 MHz, $CDCl_3$, minor isomer present in small amounts by ^{1}H NMR but was not distinguishable here) δ 178.1 (C=O), 170.0 (C=O), 169.7 (C=O), 142.7 (ArC), 133.9 (ArC), 128.6 (ArC–H), 123.6 (ArC–H), 123.5 (ArC–H), 108.3 (ArC–H), 78.7 (CH), 67.9 (CH), 64.6 (CH_2), 55.4 (CH), 53.7 (C), 52.8 (CH_3), 52.7 (CH_3), 39.4 (CH_2), 26.8

(CH_3); **HRMS** m/z (ES) Found: MH^+, 361.1404. $C_{18}H_{21}N_2O_6$ requires MH^+ 361.1394; **LRMS** m/z (ES) 361 (100%, MH^+).

The ratio was determined from the ^{1}H NMR spectra by integrating the peaks for OC–H at 5.14 (0.95H, d, *J* = 8.5 Hz), 5.09 (0.05H, d, *J* = 6.0 Hz).

(4*R*,4'*R*,5*S*,5'*S*)-2,2'-Methylenebis[4,5-dihydro-4,5-diphenyloxazole] (202)

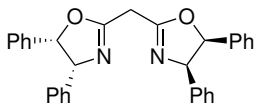

A mixture of (1*S*,2*R*)-**172** (3.71 g, 23.5 mmol) and diethyl malonimidate dihydrochloride **173** (10.0 g, 46.9 mmol) in DCM (100 mL) was stirred at reflux for 24 h. The reaction mixture was diluted with water (100 mL) and the organic layer was separated, dried ($MgSO_4$), filtered and concentrated under reduced pressure. The residue was purified by chromatography on silica gel, eluting with MeOH–DCM (1:49) to afford compound **202** (4.90 g, 36%) as an amorphous white solid; **mpt** 182–184 °C (lit.[183] 199–200 °C); $\mathbf{R_f}$ 0.63 [MeOH–DCM 1:9]; **^{1}H NMR** (400 MHz, $CDCl_3$) δ 7.13–6.90 (20H, m, 20 × ArH), 5.99 (2H, d, *J* = 10.5 Hz, 2 × CH), 5.65 (2H, d, *J* = 10.5 Hz, 2 × CH), 3.90 (2H, s, CH_2); **^{13}C NMR** (101 MHz, $CDCl_3$) δ 163.3 (C), 137.5 (ArC), 136.2 (ArC), 128.0 (ArC–H), 127.8 (ArC–H), 127.8 (ArC–H), 127.6 (ArC–H), 127.1 (ArC–H), 126.7 (ArC–H), 86.3 (CH), 74.3 (CH), 29.3 (CH_2); $[\alpha]^{19}_D$ = +147 (1.0, $CHCl_3$) (lit.[183] +240.5 (2.10, $CHCl_3$)). Spectroscopic data in accordance with literature values.[183]

Chapter 5: Appendix

HPLC Traces

(*S*)-3-Allyl-3-(hydroxymethyl)-1-methylindolin-2-one ((*S*)-179)

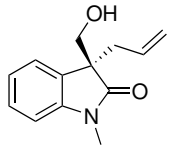

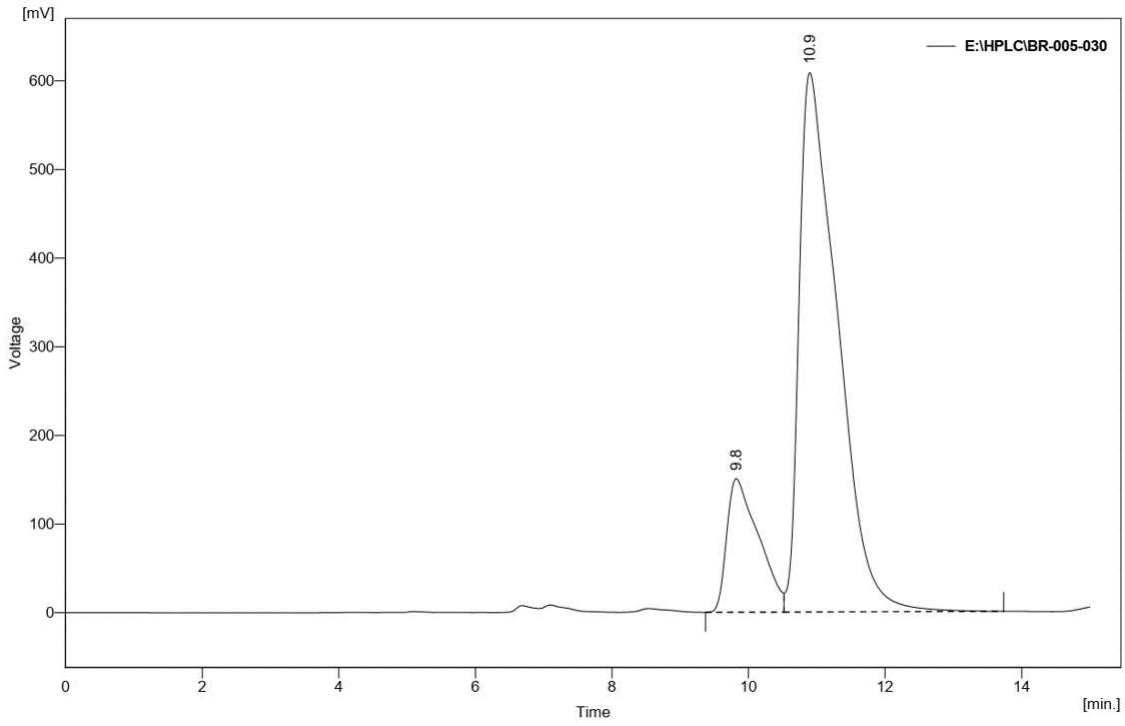

Entry	Retention time / min	Area / %
1	9.82	17.1
2	10.90	82.9

(*R*)-(3-Allyl-1-methyl-2-oxoindolin-3-yl)methyl *tert*-butyl carbonate ((*R*)-171)

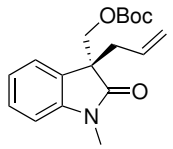

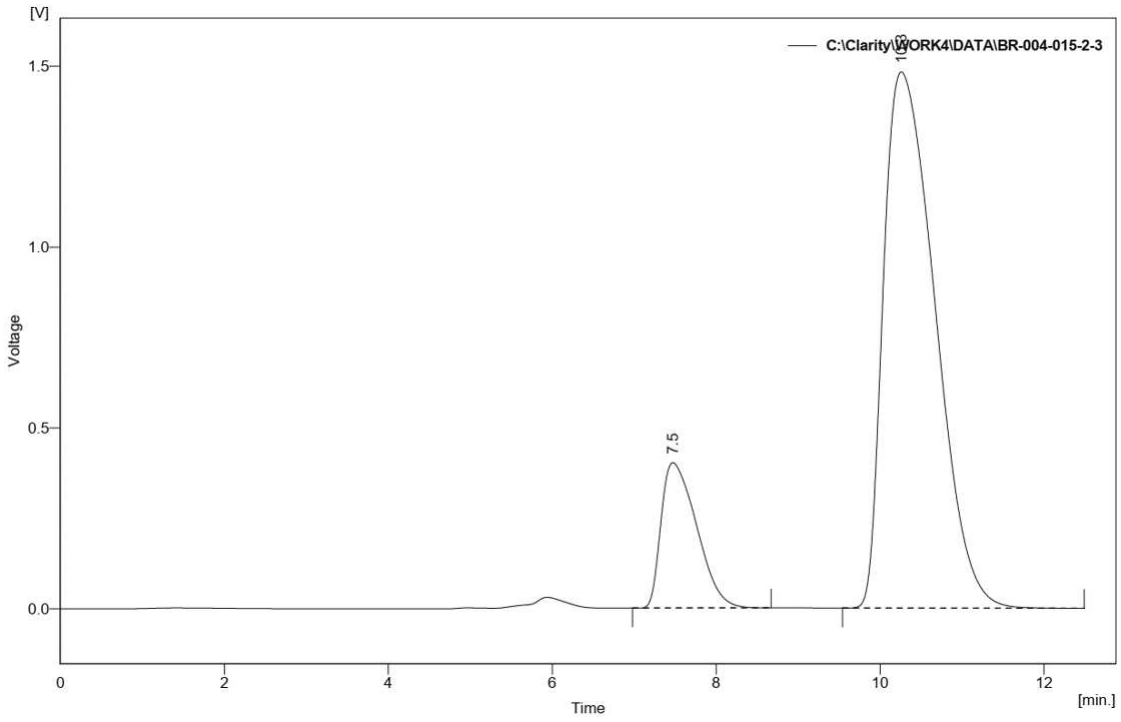

Entry	Retention time / min	Area / %
1	7.47	15.8
2	10.26	84.2

(*S*)-(3-Allyl-1-methyl-2-oxoindolin-3-yl)methyl *tert*-butyl carbonate ((*S*)-171)

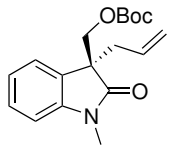

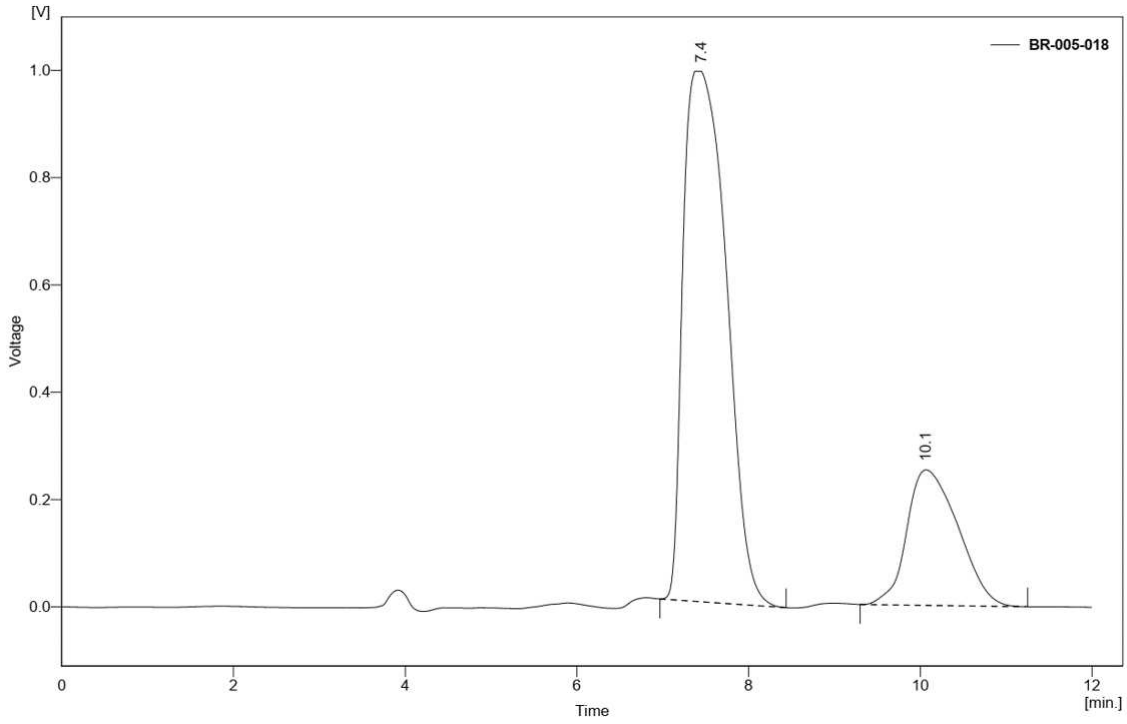

Entry	Retention time / min	Area / %
1	7.45	76.7
2	10.06	23.3

Bibliography

[1] K. V. Gothelf and K. A. Jørgensen, *Chem. Rev.*, 1998, **98**, 863–909.

[2] R. Huisgen, *Angew. Chem., Int. Ed. Engl.*, 1963, **2**, 565–598.

[3] E. Buchner, *Ber. Dtsch. Chem. Ges.*, 1888, **21**, 2637–2647.

[4] R. Huisgen, *Angew. Chem.*, 1963, **13**, 604–637.

[5] R. Huisgen, *J. Org. Chem.*, 1968, **33**, 2291–2297.

[6] R. A. Firestone, *J. Org. Chem.*, 1968, **33**, 2285–2290.

[7] K. N. Houk, J. Gonzalez and Y. Li, *Acc. Chem. Res.*, 1995, **28**, 81–90.

[8] J. Hamer and A. Macaluso, *Chem. Rev.*, 1964, **64**, 473–495.

[9] S. I. Murahashi and Y. Imada, *Chem. Rev.*, 2019, **119**, 4684–4716.

[10] H. Mitsui, S.-i. Zenki and T. Shiota, *J. Chem. Soc., Chem. Commun.*, 1984, 874–875.

[11] I. Coldham, A. J. Burrell, H. D. Guerrand and N. Oram, *Org. Lett.*, 2011, **13**, 1267–1269.

[12] R. Saruengkhanphasit, D. Collier and I. Coldham, *J. Org. Chem.*, 2017, **82**, 6489–6496.

[13] R. Hoffmann and R. B. Woodward, *J. Am. Chem. Soc.*, 1965, **87**, 4388–4389.

[14] J. I. García, J. A. Mayoral and L. Salvatella, *Acc. Chem. Res.*, 2000, **33**, 658–664.

[15] I. Oura, K. Shimizu, K. Ogata and S. I. Fukuzawa, *Org. Lett.*, 2010, **12**, 1752–1755.

[16] M. C. Tong, J. Li, H. Y. Tao, Y. X. Li and C. J. Wang, *Chem. Eur. J.*, 2011, **17**, 12922–12927.

[17] S. Peddibhotla and J. J. Tepe, *J. Am. Chem. Soc.*, 2004, **126**, 12776–12777.

[18] J. Liu, H. Sun, X. Liu, L. Ouyang, T. Kang, Y. Xie and X. Wang, *Tetrahedron Lett.*, 2012, **53**, 2336–2340.

[19] S. Kanemasa, T. Uemura and E. Wada, *Tetrahedron Lett.*, 1992, **33**, 7889–7892.

[20] S. Kanemasa, *Synlett*, 2002, 1371–1387.

[21] E. Vitaku, D. T. Smith and J. T. Njardarson, *J. Med. Chem.*, 2014, **57**, 10257–10274.

[22] K. C. Nicolaou, T. Montagnon and S. A. Snyder, *Chem. Commun.*, 2003, **3**, 551–564.

[23] L. F. Tietze and U. Beifuss, *Angew. Chem., Int. Ed.*, 1993, **32**, 131.

[24] R. Robinson, *J. Chem. Soc., Trans.*, 1917, **111**, 762–768.

[25] J. W. Medley and M. Movassaghi, *Chem. Commun.*, 2013, **49**, 10775–10777.

[26] American Chemical Society - 12 Principles of Green Chemistry, https://www.acs.org/greenchemistry/principles/12-principles-of-green-chemistry.html, (accessed July 2023).

[27] A. Behr, A. J. Vorholt, K. A. Ostrowski and T. Seidensticker, *Green Chem.*, 2014, **16**, 982–1006.

[28] M. Wink, in *Alkaloids: Biochemistry, Ecology, and Medicinal Applications*, ed. M. F. Roberts and M. Wink, Springer US, Boston, MA, 1998, ch. 2, pp. 11–44.

[29] A. M. Carroll, D. J. Kavanagh, F. P. McGovern, J. W. Reilly and J. J. Walsh, *J. Chem. Educ.*, 2012, **89**, 1578–1581.

[30] C. Krishnamurti and S. Rao, *Indian J. Anaesth.*, 2016, **60**, 861–862.

[31] M. Gates and G. Tschudi, *J. Am. Chem. Soc.*, 1952, **74**, 1109–1110.

[32] Y. Wang, A. Hennig, T. Küttler, C. Hahn, A. Jäger and P. Metz, *Org. Lett.*, 2020, **22**, 3145–3148.

[33] R. A. Stockman, *Tetrahedron Lett.*, 2000, **41**, 9163–9165.

[34] J. M. Macdonald, H. T. Horsley, J. H. Ryan, S. Saubern and A. B. Holmes, *Org. Lett.*, 2008, **10**, 4227–4229.

[35] H. Miyatake-Ondozabal, L. M. Bannwart and K. Gademann, *Chem. Commun.*, 2013, **49**, 1921–1923.

[36] H. Wei, C. Qiao, G. Liu, Z. Yang and C. C. Li, *Angew. Chem. Int. Ed.*, 2013, **52**, 620–624.

[37] J. M. Hughes and J. L. Gleason, *Angew. Chem. Int. Ed.*, 2017, **56**, 10830–10834.

[38] J. M. Hughes and J. L. Gleason, *Tetrahedron*, 2018, **74**, 759–768.

[39] I. Coldham, A. J. Burrell, L. E. White, H. Adams and N. Oram, *Angew. Chem. Int. Ed.*, 2007, **46**, 6159–6162.

[40] I. Coldham, S. Jana, L. Watson and N. G. Martin, *Org. Biomol. Chem.*, 2009, **7**, 1674–1679.

[41] Q. Zhang, G. Tu, Y. Zhao and T. Cheng, *Tetrahedron*, 2002, **58**, 6795–6798.

[42] A. J. Burrell, I. Coldham and N. Oram, *Org. Lett.*, 2009, **11**, 1515–1518.

[43] I. Coldham, L. Watson, H. Adams and N. G. Martin, *J. Org. Chem.*, 2011, **76**, 2360–2366.

[44] Z. T. Alkayar and I. Coldham, *Org. Biomol. Chem.*, 2019, **17**, 66–73.

[45] R. Hathway, MChem Project Thesis, University of Sheffield, 2019.

[46] N. Hennessey, MChem Project Thesis, University of Sheffield, 2020.

[47] G. P. Pollini, S. Benetti, C. De Risi and V. Zanirato, *Chem. Rev.*, 2006, **106**, 2434–2454.

[48] G. Fodor and R. Dharanipragada, *Nat. Prod. Rep.*, 1994, **11**, 443–450.

[49] K. L. Kohnen-Johannsen and O. Kayser, *Molecules*, 2019, **24**, 1–23.

[50] S. Scholtz, L. MacMorris, F. Krogmann and G. U. Auffarth, *J. Eye Stud. Treat.*, 2019, **2019**, 51–58.

[51] K. Fatur, *Econ. Bot.*, 2020, **74**, 140–158.

[52] Royal College of Physicians of Edinburgh, Deadly Nightshade - A Botanical Biography, https://www.rcpe.ac.uk/heritage/deadly-nightshade-botanical-biography, (accessed July 2023).

[53] The Woodland Trust - Deadly Nightshade, https://www.woodlandtrust.org.uk/trees-woods-and-wildlife/plants/wild-flowers/deadly-nightshade/, (accessed July 2023).

[54] G. Grynkiewicz and M. Gadzikowska, *Pharmacol. Rep.*, 2008, **60**, 439–463.

[55] K. L. Kohnen, S. Sezgin, M. Spiteller, H. Hagels and O. Kayser, *Plant Cell Physiol.*, 2018, **59**, 107–118.

[56] FDA Drug Shortages: Atropine Sulfate Injection, https://www.accessdata.fda.gov/scripts/drugshortages/dspActiveIngredientDetails.cfm?AI=Atropine%20Sulfate%20InjectionI&st=c, (accessed July 2023).

[57] FDA Drug Shortages: Scopolamine Transdermal System, https://www.accessdata.fda.gov/scripts/drugshortages/dspActiveIngredientDetails.cfm?AI=Scopolamine%20Transdermal%20SystemI&st=r, (accessed July 2023).

[58] P. Srinivasan and C. D. Smolke, *Nature*, 2020, **585**, 614–619.

[59] Home Office - Controlled drugs list, https://www.gov.uk/government/publications/controlled-drugs-list--2/list-of-most-commonly-encountered-drugs-currently-controlled-under-the-misuse-of-drugs-leg (accessed July 2023).

[60] A. Niemann, *Arch. Pharm.*, 1860, **153**, 129–155.

[61] Nobel Prize - Richard Willstätter - Biographical, https://www.nobelprize.org/prizes/chemistry/1915/willstatter/biographical/, (accessed July 2023).

[62] Y. J. Wang, J. P. Huang, T. Tian, Y. Yan, Y. Chen, J. Yang, J. Chen, Y. C. Gu and S. X. Huang, *J. Am. Chem. Soc.*, 2022, **144**, 22000–22007.

[63] J. Stratton, J. Clough, I. Leon, M. Sehlanova and S. MacDonald, *Monitoring of Tropane Alkaloids in Foods*, Fera Science Ltd. Technical Report FS102116, Food Standards Agency, 2017.

[64] M. Sienkiewicz, U. Wilkaniec and R. Lazny, *Tetrahedron Lett.*, 2009, **50**, 7196–7198.

[65] S. Lombardo and U. Maskos, *Neuropharmacology*, 2015, **96**, 255–262.

[66] I. Bick, J. Gillard and H. Leow, *Aust. J. Chem.*, 1979, **32**, 2523.

[67] F. Campbell and E. Edwards, *Can. J. Chem.*, 1977, **55**, 1372–1379.

[68] R. Lazny, M. Sienkiewicz, T. Olenski, Z. Urbanczyk-Lipkowska and P. Kalicki, *Tetrahedron*, 2012, **68**, 8236–8244.

[69] J. H. Rigby and F. C. Pigge, *J. Org. Chem.*, 1995, **60**, 7392–7393.

[70] H. M. L. Davies, E. Saikali and W. B. Young, *J. Org. Chem.*, 1991, **56**, 5696–5700.

[71] V. K. Aggarwal, C. J. Astle and M. Rogers-Evans, *Org. Lett.*, 2004, **6**, 1469–1471.

[72] T. Katoh, K. Kakiya, T. Nakai, S. Nakamura, K. Nishide and M. Node, *Tetrahedron: Asymmetry*, 2002, **13**, 2351–2358.

[73] S. Y. Jonsson, C. M. Löfström and J. E. Bäckvall, *J. Org. Chem.*, 2000, **65**, 8454–8457.

[74] I. Gauthier, J. Royer and H. P. Husson, *J. Org. Chem.*, 1997, **62**, 6704–6705.

[75] S. Ahmed, L. A. Baker, R. S. Grainger, P. Innocenti and C. E. Quevedo, *J. Org. Chem.*, 2008, **73**, 8116–8119.

[76] S. Rodriguez, U. Uria, E. Reyes, L. Prieto, P. Merino and J. L. Vicario, *Eur. J. Med. Chem.*, 2021, **2021**, 2855–2861.

[77] S. Rodriguez, U. Uria, E. Reyes, L. Carrillo, T. Tejero, P. Merino and J. L. Vicario, *Angew. Chem., Int. Ed.*, 2020, **59**, 6633–6935.

[78] A. Padwa and B. H. Norman, *Tetrahedron Lett.*, 1988, **29**, 2417–2419.

[79] M. S. Wilson and A. Padwa, *J. Org. Chem.*, 2008, **73**, 9601–9609.

[80] R. M. Coates and P. A. MacManus, *J. Org. Chem.*, 1982, **47**, 4822–4824.

[81] E. J. Corey, J. F. Arnett and G. N. Widiger, *J. Am. Chem. Soc.*, 1975, **97**, 430–431.

[82] S. A. Godleski, D. J. Heacock, J. D. Meinhart and S. Van Wallendael, *J. Org. Chem.*, 1983, **48**, 2101–2103.

[83] C. J. Stearman, M. Wilson and A. Padwa, *J. Org. Chem.*, 2009, **74**, 3491–3499.

[84] S. Takano, M. Sasaki, H. Kanno, K. Shishido and K. Ogasawara, *J. Org. Chem.*, 1978, **43**, 4169–4172.

[85] A. C. Flick, M. José, A. Caballero and A. Padwa, *Tetrahedron*, 2010, **66**, 3643–3650.

[86] A. C. Flick, M. José, A. Caballero, H. I. Lee and A. Padwa, *J. Org. Chem.*, 2010, **75**, 1992–1996.

[87] R. Cox, MChem Project Thesis, University of Sheffield, 2023.

[88] K. C. Nicolaou, P. G. Bulger and W. E. Brenzovich, *Org. Biomol. Chem.*, 2006, **4**, 2158–2183.

[89] G. Pattenden and S. Teague, *J. Chem. Soc. Perkin Trans.*, 1988, 1077–1083.

[90] R. F. De La Pradilla, C. Montero, M. Tortosa and A. Viso, *Chem. Eur. J.*, 2009, **15**, 697–709.

[91] P. O. Ellingsen and K. Undheim, *Acta Chem. Scand.*, 1979, **33**, 528–530.

[92] M. Vamos, K. Welsh, D. Finlay, P. S. Lee, P. D. Mace, S. J. Snipas, M. L. Gonzalez, S. R. Ganji, R. J. Ardecky, S. J. Riedl, G. S. Salvesen, K. Vuori, J. C. Reed and N. D. Cosford, *ACS Chem. Biol.*, 2013, **8**, 725–732.

[93] H. Le, A. Batten and J. P. Morken, *Org. Lett.*, 2014, **16**, 2096–2099.

[94] M. Ramos, A. F. Barrero, J. Altarejos and E. J. Alvarez-Manzaneda, *Tetrahedron*, 1993, **49**, 6251–6262.

[95] K. Takasu, S. Maiti, A. Katsumata and M. Ihara, *Tetrahedron Lett.*, 2001, **42**, 2157–2160.

[96] P. Verma, A. Chandra and G. Pandey, *J. Org. Chem.*, 2018, **83**, 9968–9977.

[97] J. Soika, C. McLaughlin, T. Neveselý, C. G. Daniliuc, J. J. Molloy and R. Gilmour, *ACS Catal.*, 2022, **12**, 10047–10056.

[98] C. Enkisch and C. Schneider, *Eur. J. Org. Chem.*, 2009, **2009**, 5549–5564.

[99] G. P. Black, F. Dinon, S. Fratucello, P. J. Murphy, M. Nielsen and H. L. Williams, *Tetrahedron Lett.*, 1997, **38**, 8561–8564.

[100] M. Zahel, Y. Wang, A. Jager and P. Metz, *Eur. J. Org. Chem.*, 2016, 5881–5886.

[101] K. Komine, Y. Urayama, T. Hosaka, Y. Yamashita, H. Fukuda and S. Hatakeyama, *Org. Lett.*, 2020, **22**, 5046–5050.

[102] F. C. Lightstone and T. C. Bruice, *Bioorg. Chem.*, 1998, **26**, 193–199.

[103] Z. Li, J. Zhao, B. Sun, T. Zhou, M. Liu, S. Liu, M. Zhang and Q. Zhang, *J. Am. Chem. Soc.*, 2017, **139**, 11702–11705.

[104] R. Grigg, M. J. R. Dorrity and J. F. Malone, *Tetrahedron Lett.*, 1990, **31**, 3075–3076.

[105] S. K. Taylor, D. Deyoung, L. J. Simons, J. R. Vyvyan, A. Wemple, N. K. Wood, S. K. Taylor, D. Deyoung, L. J. Simons, J. R. Vyvyan, M. A. Wemple and N. K. Wood, *Synth. Commun.*, 1998, **28**, 1691–1701.

[106] D. Y. Ong and S. Chiba, *Synthesis*, 2020, **52**, 1369–1378.

[107] M. Larchevěque and A. Debal, *Synth. Commun.*, 1980, **10**, 49–57.

[108] L. A. Paquette and R. A. Roberts, *Tetrahedron Lett.*, 1983, **24**, 3555–3558.

[109] L. Pan, C. Terrazas, U. M. Acuña, T. N. Ninh, H. Chai, E. J. Carcache De Blanco, D. D. Soejarto, A. R. Satoskar and A. D. Kinghorn, *Phytochem. Lett.*, 2014, **10**, liv–lix.

[110] P. Dey, A. Kundu, A. Kumar, M. Gupta, B. Mu Lee, T. Bhakta, S. Dash and H. Sik Kim, in *Recent Advances in Natural Product Analysis*, Elsevier Ltd, 2020, vol. 8, ch. 15, pp. 505–567.

[111] S. J. Tan, J. L. Lim, Y. Y. Low, K. S. Sim, S. H. Lim and T. S. Kam, *J. Nat. Prod.*, 2014, **77**, 2068–2080.

[112] M. R. Stephen, M. T. Rahman, V. V. B. Tiruveedhula, G. O. Fonseca, J. R. Deschamps and J. M. Cook, *Chem. Eur. J.*, 2017, **23**, 15805–15819.

[113] *World Health Organization Model List of Essential Medicines, 21st List*, World Health Organisation, Geneva, 2019.

[114] S. G. Davey, *Nat. Rev. Chem.*, 2020, 41570.

[115] A. Rahman, F. Nighat, A. Nelofer, K. Zaman, M. I. Choudhary and K. DeSilva, *Tetrahedron*, 1991, **47**, 3129–3136.

[116] S. Cheenpracha, T. Ritthiwigrom and S. Laphookhieo, *J. Nat. Prod.*, 2013, **76**, 723–726.

[117] A. Noor, *World Malaria Report 2022*, World Health Organisation, Geneva, 2022.

[118] *The potential impact of health service disruptions on the burden of malaria*, World Health Organisation, Geneva, 2020.

[119] NHS UK - Malaria, https://www.nhs.uk/conditions/malaria/causes/, (accessed July 2023).

[120] World Health Organisation - Overview of malaria treatment, https://www.who.int/malaria/areas/treatment/overview/en/, (accessed July 2023).

[121] K. Mugittu, B. Genton, H. Mshinda and H. P. Beck, *Malar. J.*, 2006, **5**, 3–5.

[122] E. A. Ashley, M. Dhorda, R. M. Fairhurst, C. Amaratunga, P. Lim, S. Suon, S. Sreng, J. M. Anderson, S. Mao, B. Sam, C. Sopha, C. M. Chuor, C. Nguon, S. Sovannaroth, S. Pukrittayakamee, P. Jittamala, K. Chotivanich, K. Chutasmit, C. Suchatsoonthorn, R. Runcharoen, T. T. Hien, N. T. Thuy-Nhien, N. V. Thanh, N. H. Phu, Y. Htut, K. T. Han, K. H. Aye, O. A. Mokuolu, R. R. Olaosebikan, O. O. Folaranmi, M. Mayxay, M. Khanthavong, B. Hongvanthong, P. N. Newton, M. A. Onyamboko, C. I. Fanello, A. K. Tshefu, N. Mishra, N. Valecha, A. P. Phyo, F. Nosten, P. Yi, R. Tripura, S. Borrmann, M. Bashraheil, J. Peshu, M. A. Faiz, A. Ghose, M. A. Hossain, R. Samad, M. R. Rahman, M. M. Hasan, A. Islam, O. Miotto, R. Amato, B. MacInnis, J. Stalker, D. P. Kwiatkowski, Z. Bozdech, A. Jeeyapant, P. Y. Cheah, T. Sakulthaew, J. Chalk, B. Intharabut, K. Silamut, S. J. Lee, B. Vihokhern, C. Kunasol, M. Imwong, J. Tarning, W. J. Taylor, S. Yeung, C. J. Woodrow, J. A. Flegg, D. Das, J. Smith, M. Venkatesan, C. V. Plowe, K. Stepniewska, P. J. Guerin, A. M. Dondorp, N. P. Day and N. J. White, *N. Engl. J. Med.*, 2014, **371**, 411–423.

[123] A. Jossang, P. Jossang, B. Bodo, H. A. Hadi and T. Sévenet, *J. Org. Chem.*, 1991, **56**, 6527–6530.

[124] K. Jones and J. Wilkinson, *J. Chem. Soc., Chem. Commun.*, 1992, 1767–1769.

[125] C. Pellegrini, C. Strässler, M. Weber and H.-J. Borschberg, *Tetrahedron: Asymmetry*, 1994, **5**, 1979–1992.

[126] G. Lakshmaiah, T. Kawabata, M. Shang and K. Fuji, *J. Org. Chem.*, 1999, **64**, 1699–1704.

[127] M. J. Wanner, S. Ingemann, J. H. Van Maarseveen and H. Hiemstra, *Eur. J. Org. Chem.*, 2013, 1100–1106.

[128] L. L. Chen, J. X. Song, J. H. Lu, Z. W. Yuan, L. F. Liu, S. S. K. Durairajan and M. Li, *J. Neuroimmune Pharmacol.*, 2014, **9**, 380–387.

[129] J. X. Song, J. H. Lu, L. F. Liu, L. L. Chen, S. S. K. Durairajan, Z. Yue, H. Q. Zhang and M. Li, *Autophagy*, 2014, **10**, 144–154.

[130] Z. Zhu, L. feng Liu, C. fu Su, J. Liu, B. C. K. Tong, A. Iyaswamy, S. Krishnamoorthi, S. G. Sreenivasmurthy, X. jie Guan, Y. xuan Kan, W. jian Xie, C. liang Zhao, K. ho Cheung, J. hong Lu, J. qiong Tan, H. jie Zhang, J. xian Song and M. Li, *Acta Pharmacologica Sinica*, 2022, **43**, 2511–2526.

[131] D. Yan, Z. Ma, C. Liu, C. Wang, Y. Deng, W. Liu and B. Xu, *Food Chem. Toxicol.*, 2019, **124**, 336–348.

[132] J. H. Lu, J. Q. Tan, S. S. K. Durairajan, L. F. Liu, Z. H. Zhang, L. Ma, H. M. Shen, H. Y. E. Chan and M. Li, *Autophagy*, 2012, **8**, 98–108.

[133] K. Koyama, Y. Hirasawa, A. E. Nugroho, T. Hosoya, T. C. Hoe, K. L. Chan and H. Morita, *Org. Lett.*, 2010, **12**, 4188–4191.

[134] A. Y. Hong and C. D. Vanderwal, *Tetrahedron*, 2017, **73**, 4160–4171.

[135] T. Mandal, G. Chakraborti, S. Karmakar and J. Dash, *Org. Lett.*, 2018, **20**, 4759–4763.

[136] A. A. Nagle, S. A. Reddy, H. Bertrand, H. Tajima, T.-M. Dang, S.-C. Wong, J. D. Hayes, G. Wells and E.-H. Chew, *ChemMedChem*, 2014, **9**, 1763–1774.

[137] D. Z. Chen, W. J. Xiao and J. R. Chen, *Org. Chem. Front.*, 2017, **4**, 1289–1293.

[138] L. Zhang, W. Ren, X. Wang, J. Zhang, J. Liu, L. Zhao and X. Zhang, *Eur. J. Med. Chem.*, 2017, **126**, 1071–1082.

[139] K. Holzschneider, F. Mohr and S. F. Kirsch, *Org. Lett.*, 2018, **20**, 7066–7070.

[140] *Eur. Pat.,* 0126 635 A2, 1984.

[141] Brand Tech - Solvent Boiling Points Chart, https://brandtech.com/solventboilingpointschart/, (accessed July 2023).

[142] A. T. Davies, A. M. Slawin and A. D. Smith, *Chem. Eur. J.*, 2015, **21**, 18944–18948.

[143] A. J. Mancuso, S. L. Huang and D. Swern, *J. Org. Chem.*, 1978, **43**, 2480–2482.

[144] E. Teoh, E. M. Campi, W. R. Jackson and A. J. Robinson, *New J. Chem.*, 2003, **27**, 387–394.

[145] F. Pesciaioli, P. Righi, A. Mazzanti, C. Gianelli, M. Mancinelli, G. Bartoli and G. Bencivenni, *Adv. Synth. Catal.*, 2011, **353**, 2953–2959.

[146] X. L. Liu, B. W. Pan, W. H. Zhang, C. Yang, J. Yang, Y. Shi, T. T. Feng, Y. Zhou and W. C. Yuan, *Org. Biomol. Chem.*, 2015, **13**, 601–611.

[147] S. Shimizu, T. Tsubogo, P. Xu and S. Kobayashi, *Org. Lett.*, 2015, **17**, 2006–2009.

[148] J. Bernauer, G. Wu and A. Von Wangelin, *RSC Adv.*, 2019, **9**, 31217–31223.

[149] A. Ortega-Martínez, C. Molina, C. Moreno-Cabrerizo, J. M. Sansano and C. Nájera, *Synthesis (Germany)*, 2017, **49**, 5203–5210.

[150] J. A. Dean, in *Lange's Handbook of Chemistry*, McGraw-Hill, 1992, ch. 4, pp. 4.41–4.53.

[151] S. A. McNelles, S. D. Knight, N. Janzen, J. F. Valliant and A. Adronov, *Biomacromolecules*, 2015, **16**, 3033–3041.

[152] D. T. Lewis, *J. Chem. Soc.*, 1940, 32–36.

[153] Sigma Aldrich Catalog - 4-Pentenoic anhydride, https://www.sigmaaldrich.com/catalog/product/aldrich/471801?lang=en&region=GB&gclid=EAIaIQobChMI3NigvcO65wIVA7DtCh015gxREAAYASAAEgKLq$_$D$_$BwE, (accessed July 2023).

[154] G. Bartoli, M. Bosco, E. Marcantoni, M. Massaccesi, S. Rinaldi and L. Sambri, *Synthesis*, 2004, 3092–3096.

[155] M. Fujita and T. Hiyama, *J. Org. Chem.*, 1988, **53**, 5415–5421.

[156] M. Chouhan, K. R. Senwar, R. Sharma, V. Grover and V. A. Nair, *Green Chem.*, 2011, **13**, 2553–2560.

[157] B. Parmar, P. Patel, R. S. Pillai, R. K. Tak, R. I. Kureshy, N. U. H. Khan and E. Suresh, *Inorg. Chem.*, 2019, **58**, 10084–10096.

[158] S. Hajra, S. Maity, S. Roy and R. Maity, *Eur. J. Org. Chem.*, 2019, **2019**, 269–287.

[159] L. Wu, Q. Shao, L. Kong, J. Chen, Q. Wei and W. Zhang, *Org. Chem. Front.*, 2020, **7**, 862–867.

[160] Sigma Aldrich, Sigma Aldrich Catalog - Dimethyl Sulfide, https://www.sigmaaldrich.com/GB/en/product/aldrich/516872, (accessed July 2023).

[161] Alfa Aesar, Alfa Aesar Catalog - Dimethyl Sulfoxide, https://www.alfa.com/en/catalog/A13280/, (accessed January 2023).

[162] X. Q. Mou, F. M. Rong, H. Zhang, G. Chen and G. He, *Org. Lett.*, 2019, **21**, 4657–4661.

[163] *Int. Pat.*,, WO 2005/123254, 2005.

[164] M. Quan, X. Wang, L. Wu, I. D. Gridnev, G. Yang and W. Zhang, *Nat. Commun.*, 2018, **9**, 1–11.

[165] S. Nicolai and J. Waser, *Angew. Chem., Int. Ed.*, 2022, **61**, 1–5.

[166] J. W. Clary, T. J. Rettenmaier, R. Snelling, W. Bryks, J. Banwell, W. T. Wipke and B. Singaram, *J. Org. Chem.*, 2011, **76**, 9602–9610.

[167] Z. Wu, S. N. Gockel and K. L. Hull, *Nat. Commun.*, 2021, **12**, 1–9.

[168] F. Yue, H. Ma, H. Song, Y. Liu, J. Dong and Q. Wang, *Chem. Sci.*, 2022, **13**, 13466–13474.

[169] H. B. Hepburn, N. Chotsaeng, Y. Luo and H. Lam, *Synthesis (Germany)*, 2013, **45**, 2649–2661.

[170] B. M. Sharma, M. Yadav, R. G. Gonnade and P. Kumar, *Eur. J. Org. Chem.*, 2017, **2017**, 2603–2609.

[171] S. Hajra, S. Roy and S. Maity, *Org. Lett.*, 2017, **19**, 1998–2001.

[172] R. C. Furnival, R. Saruengkhanphasit, H. E. Holberry, J. R. Shewring, H. D. Guerrand, H. Adams and I. Coldham, *Org. Biomol. Chem.*, 2016, **14**, 10953–10962.

[173] A. Pelšs, N. Gandhamsetty, J. R. Smith, D. Mailhol, M. Silvi, A. J. Watson, I. Perez-Powell, S. Prévost, N. Schützenmeister, P. R. Moore and V. K. Aggarwal, *Chem. Eur. J.*, 2018, **24**, 9542–9545.

[174] C. H. Heathcock, T. A. Blumenkopf and K. M. Smith, *J. Org. Chem.*, 1989, **54**, 1548–1562.

[175] Sigma Aldrich Catalog - 3-Bromopropionaldehyde dimethyl acetal, https://www.sigmaaldrich.com/GB/en/product/aldrich/272477, (accessed July 2023).

[176] Sigma Aldrich Catalog - 1-Methylisatin, https://www.sigmaaldrich.com/GB/en/product/aldrich/183075, (accessed July 2023).

[177] V. B. Brito, G. F. Santos, T. D. Silva, J. L. Souza, G. C. Militão, F. T. Martins, F. P. Silva, B. G. Oliveira, E. C. Araújo, M. L. Vasconcellos, C. G. Lima-Júnior and E. B. Alencar-Filho, *Mol. Divers.*, 2020, **24**, 265–281.

[178] Sigma Aldrich Catalog - 1-Methyl-2-oxindole, https://www.sigmaaldrich.com/GB/en/product/aldrich/466921, (accessed July 2023).

[179] N. Etkin, S. D. Babu, C. J. Fooks and T. Durst, *J. Org. Chem.*, 1990, **55**, 1093–1096.

[180] M. Jha, T. Y. Chou and B. Blunt, *Tetrahedron*, 2011, **67**, 982–989.

[181] U. Ellervik and G. Magnusson, *Acta Chem. Scand.*, 1993, **47**, 826–828.

[182] V. M. Breising, T. Gieshoff, A. Kehl, V. Kilian, D. Schollmeyer and S. R. Waldvogel, *Org. Lett.*, 2018, **20**, 6785–6788.

[183] *US Pat.,* US005298623A, 1994.